UNIVERSITY OF LEEDS

Characterising Diabetic Cardiomyopathy Using Cardiac MRI and Transcriptomics

Marilena Giannoudi

Submitted in Accordance with the Requirements for the Degree of

Doctor of Philosophy

The University of Leeds

Faculty of Medicine and Health

Leeds Institute of Cardiovascular and Metabolic Medicine

April 2025

Intellectual Property and Publications Statement

I confirm that the work submitted is my own and that appropriate credit has been given where reference has been made to the work of others.

This copy has been supplied on the understanding that it is copyright material and that no quotation from the thesis may be published without proper acknowledgement.

The following oral presentations have been made based on the findings presented in this thesis.

- Chapter 5: SCMR 2025 (The Global CMR Conference); Better Understanding the Disparity in Heart Failure Risk Between the Females and Males with Type 2 Diabetes, Washington USA, 29th Jan – 1st Feb 2025.
- Chapter 2: SCMR 2025 (The Global CMR Conference); The Progression of Myocardial Remodeling and Perfusion Changes in Patients with Moderate Aortic Stenosis, Washington USA, 29th Jan – 1st Feb 2025.
- Chapter 2: SCMR 2024 (The Global CMR Conference); Cardiac structural, functional remodelling and perfusion impairments across the spectrum of pressure afterload in patients with aortic stenosis, London UK, 25-27th Jan 2024.
- Chapter 2: Myocardial Remodelling Across the Spectrum of Aortic Stenosis. European Society of Cardiology Annual Congress, London 30th August – 2nd September 2024.

Declarations

This work is original and my own. Dr Henry Procter and Dr Sindhoora Kotha provided support with biopsy sample collection leading to the results in Chapter 3, as well as providing help with scanning and study visits leading to the results in this chapter. Mrs Melanie Spurr, Dr Patrick Thompson and Dr Wasim Javed provided help with scanning and study visits leading to the results in Chapters 4. Dr Amrit Chowdhary, Dr Nicholas Jex, Dr Sharmaine Thirunavukarasu, Dr Sindhoora Kotha and Dr Henry Procter provided help with scanning and study visits leading to the results in Chapters 5. Miss Caroline Smith and Miss Hollie-Marie North provided support with patient recruitment and study visits leading to the results in Chapters 2 and 3.

David Shelly, Lizette Cash, Julian Tongue, Margaret Saysell, Rebecca Robertson, Mitchell Denisa, and Gavin Bainbridge provided support with patient scanning leading to the results in Chapters 4 and 5. Dr David Broadbent provided physics support throughout. Mr Sotiris Papaspyros, Ms Betsy Evans, Mr Kalyana Javangula, Ms Mr Pankaj Kaul, and Mr Walid Elmahdy performed intra-operative myocardial biopsy sampling leading to the results in Chapter 3. Miss Marcella Conning-Rowland aided with myocardial and blood sample processing leading to the results in Chapter 3 and 4.

Acknowledgements

The culmination of this work would not have been possible without my supervisors, A. Professor Ric Cubbon and Professor Eylem Levelt. Their continued guidance and unwavering support have been invaluable on this journey. I will be forever grateful for everything they have taught me, both in the lab (imaging and wet work) and beyond. I hope this is only the start of a long collaboration. Additional thanks to my secondary supervisor Professor Mark Kearney for his support and advice during my thesis.

I would like to thank my wonderful colleagues Dr Amrit Chowdhary, Dr Sharmaine Thirunavukarasu, Dr Sindhoora Kotha, Dr Henry Procter, Dr Nicholas Jex, Dr Oliver Brown and Miss Marcella Conning-Rowland, whilst your friendship is what I will cherish most, I will be forever grateful for your help with the day to day running of my projects.

I am incredibly thankful to all the radiography team; David Shelly, Lizette Cash, Julian Tongue, Margaret Saysell, Rebecca Robertson, Mitchell Denisa, and Gavin Bainbridge for their support with scanning and to Dr David Broadbent for his technical support and troubleshooting.

I would also like to express my gratitude to the cardiac surgery team; Mr Sotiris Papaspyros, Ms Betsy Evans, Mr Kalyana Javangula, Mr Pankaj Kaul, and Mr Walid Elmahdy for their collaboration on the myocardial biopsy study.

My deepest thanks to the truly incredible cardiac research nurses, Miss Caroline Smith and Miss Hollie-Marie North. Your ability to always put the patient at ease is truly remarkable and I will be forever indebted to you for your organisation, kindness and patience.

Finally, this Phd is dedicated to my family. My parents have been my biggest role models in defining hard work and perseverance and I will never be able to thank them enough for supporting every dream of mine, believing in me and showing me that there are no limits to what I can achieve. To all my family and friends, especially my brother Vasilis, grandma, aunties, and Becky thank you for picking me up when I needed it most and cheering me on so that I could cross the finish line.

Thesis Abstract

Patients with type 2 diabetes mellitus (T2D) have an increased and premature risk of cardiovascular disease. In the presence of preceding myocardial pathologies, concomitant T2D results in a more exaggerated phenotype and worse prognosis.

Cardiac magnetic resonance (CMR) and phosphorus magnetic resonance spectroscopy (^{31}P-MRS) are advanced imaging modalities which allow for detailed characterisation of the myocardium in the presence of health and disease. Furthermore 'transcriptomics' offer an important unbiased approach to study the molecular phenotypes of disease, allowing for a deeper understanding of which genes (and at what level) are activated or suppressed, as well as their activity and expression, within a cell or tissue, in a detailed way.

The aim of this thesis was to combine imaging techniques with RNA sequencing to understand the changes to the myocardium in the presence of T2D. CMR and ^{31}P-MRS were used to define the impact of co-morbid T2D across the spectrum of aortic valve stenosis (AS), and heart failure with reduced ejection fraction (HFrEF), particularly with regards to the alterations in the myocardial energetic state, perfusion, structure and function. RNA extraction and sequencing was performed both on myocardial tissue samples taken at the time of valve replacement surgery and from bloods taken at the time of CMR for the diagnosis of causation of new HFrEF. Myocardial transcriptional differences between patients with severe AS with and without T2D, blood transcriptional differences between HFrEF patients with and without T2D, and transcriptomic correlates of CMR parameters with these concomitant cardiac diseases were sought.

Compared to controls, with increasing AS severity, there was progressive increase in left ventricular (LV) concentricity and a stepwise decline in cardiac function measured via global longitudinal shortening (GLS). Indices of cardiac perfusion (stress myocardial blood flow (MBF) and myocardial perfusion reserve (MPR) were only significantly reduced in patients with Severe-AS compared to controls, with significant differences also detected between patients with Moderate-AS and Severe-AS. Layer specific perfusion imaging revealed that stress MBF and MPR in the endocardial and epicardial myocardial layers were all significantly reduced in both Moderate-AS and Severe-AS. Myocardial energetics were reduced in both AS groups. In the presence of T2D these changes appeared to be more pronounced.

Principal components (PC) were used to represent RNA-seq results correlated with numerous CMR markers pre and post valve replacement. PC3 was negatively correlated with the pre-operative markers of myocardial contraction left atrial and left ventricular ejection fraction (LAEF and LVEF respectively), ($p< 0.001$), and positively with the perfusion parameters rest MBF (endo/epi) ratio and stress MBF (endo/epi) ratio respectively. Interestingly, the post-operative correlations in PC3 for LAEF and rest MBF (endo/epi) ratio were directionally opposite, and GLS correlated with PC1 and PC2. The reasons for these differential associations are unclear and require further exploration.

In another patient cohort of newly diagnosed patients with HFrEF, PC1 was correlated with LV mass, LV end-diastolic volume index and the visual presence or absence of inducible ischaemia in patients with Severe-AS going for valve replacement surgery. PC1 also correlated with gender, and four of the five genes most associated with PC1 in loading plots were found on sex chromosomes; XIST (on X), UTY, KDM5D, and RPS4Y1 (on chromosome Y); HLA-B, one

of the human leukocyte antigens involved in antigen recognition also substantially contributed to PC1. Correlations between PCs and CMR parameters were also noted.

Differences in the blood transcriptome of people with HFrEF with versus without T2D were observed, in addition to many blood transcriptomic correlates of cardiac function and disease. Further exploration of these may help to define the biological phenomena underpinning CMR traits.

The proof-of-concept work in this thesis showed that advanced imaging techniques can be used alongside transcriptomics to define the phenotypic characteristics of heart disease in different forms with concomitant T2D. Further work is needed to identify potential biomarkers from the differentially expressed genes (DEGs) that can be used for prognostication in this high-risk population.

Table of Contents

List of Tables

List of Figures

List of Abbreviations

ACS – Acute Coronary Syndrome

ADRA1B - α1B-adrenoreceptor

AGE - Advanced Glycation End-products

AHA - American Heart Association

ANGPTL4 - Angiopoietin-like-4

AR – Aortic Regurgitation

AS – Aortic Stenosis

ATP - Adenosine Triphosphate

AVR – Aortic Valve Replacement

BMI – Body Mass Index

BP – Blood Pressure

Bp – Base Pairs

BR1 - Resuspension Buffer

BR2 - Binding Buffer 2

BR3 - Buffer 3

BR4 - Wash Buffer 4

BR5 - Elution Buffer

BSA - Body Surface Area

β-MyHC - β-Myosin Heavy Chain

C3 - Complement Component 3

CACNA1A - Calcium Voltage-Gated Channel Subunit Alpha1 A

CAD - Coronary Artery Disease

CCND3 – Cyclin D3

CEPBD - CCAAT/Enhancer-Binding Protein Delta

CI – Confidence Interval

CMR – Cardiac Magnetic Resonance Imaging

CO - Cardiac Output

CRP - C-Reactive Protein

CSI - Chemical Shift Imaging

CTGF - Connective Tissue Growth Factor

DEGs - Differentially Expressed Genes

DKA – Diabetic Ketoacidosis

DM – Diabetes Mellitus

DNA – Deoxyribonucleic Acid

DPP-4 - Dipeptidyl Peptidase-4 Inhibitors

E - Early Transmitral Inflow Velocity

e’ - Doppler Velocity of the Medial Mitral Annulus

ECG - Electrocardiogram

ECs - Endothelial Cells

ECV - Extracellular Volume

EDV - End Diastolic Volume

EDVi – Indexed End Diastolic Volume

EF - Ejection Fraction

EIF2 - Eukaryotic Initiation Factor 2

ENO2 - Enolase 2

Endo - Subendocardial

Endo/Epi - Endo to Epi MBF Ratio

Epi - Subepicardial

ERBB3 - Erb-B2 Receptor Tyrosine Kinase 3

eGFR - Estimated Glomerular Filtration Rate

ESV - End Systolic Volume

FABP3 - Fatty Acid Binding Protein 3

FA – Fatty Acids

FDR - False Discovery Rate

FFA – Free Fatty Acids

FLASH - Fast Low Angle Shot

fMLP - N-Formyl-Methionyl-Leucyl-Phenylalanine

FOS - FOS Proto-oncogene

GADA – Glutamic Acid Decarboxylase Autoantibodies

GDM – Gestational Diabetes Mellitus

GLP-1 - Glucagon-Like Peptide-1

GLS - Global Longitudinal Shortening

GLUT4 - Glucose Transporter 4

GTEx - Genotype-Tissue Expression

31H-MRS - Proton Magnetic Resonance Spectroscopy

HbA1C - Glycated Haemoglobin

HBP - Hexosamine Biosynthetic Pathway

HCM – Hypertrophic Cardiomyopathy

HF – Heart Failure

HFpEF - Heart Failure with Preserved Ejection Fraction

HFrEF - Heart Failure with Reduced Ejection Fraction

HLA DR3-DQ2 - Human Leukocyte Antigen Alleles DR3-DQ2

HLA DR4-DQ8 - Human Leukocyte Antigen Alleles DR4-DQ8

HNF1- α - Hepatocyte Nuclear Factor 1- α

HNF1- β – Hepatocyte Nuclear Factor 1- β

HNF4- α - Hepatocyte Nuclear Factor 4- α

HOMA - Homoeostasis Model Assessment

HSPA2 - Heat Shock Protein A2

HR – Hazard Ratio

HV - Healthy Volunteers

IA-2A - Insulinoma-Associated-2 Autoantibodies

ICAM-1 - Inflammatory Cell Adhesion Molecule 1

IgA - Immunoglobulin A

IgG – Immunoglobulin G

IL-18 - Interleukin-18

IL-1β - Interleukin-1β

IL-6 - Interleukin-6

IR – Insulin Resistance

Kg – Kilograms

Klre1 - Killer Cell Lectin-Like Receptor Family E Member 1

LA – Left Atrium

LAEF – Left Atrial Ejection Fraction

LADA - Latent Autoimmune Diabetes in Adults

LDL - Low Density Lipoprotein (VLDL)

LGE - Late Gadolinium Enhancement

LGE – Late Gadolinium Enhancement

LGALS12 – Galectin 12

LIPE - Lipase E, Hormone Sensitive Type

LMNA - Lamin A/C

LOX-1 - Low-Density Lipoprotein Receptor-1

LOXL4 - Lysyl Oxidase-Like 4

LRRC19 - Leucine Rich Repeat Containing 19

LV – Left Ventricle

LVEDV – Left Ventricular End Diastolic Volume

LVEF – Left Ventricular Ejection Fraction

LVESV – Left Ventricular End Systolic Volume

LVH – Left Ventricular Hypertrophy

MAP2K5 - Mitogen-Activated Protein Kinase Kinase 5

MAPK - Mitogen-Activated Protein Kinase

MAPSE - Mitral Annular Plane Systolic Excursion

MBF - Myocardial Blood Flow

METTL9 - Methyltransferase 9

MHC - Major Histocompatibility Complex

MI – Myocardial Infarction

MIR30 – MicroRNA 30

MMPs - Matrix Metalloproteinases

MODY – Maturity Onset Diabetes of the Young

MOCO - Motion-Corrected

MPR - Myocardial Perfusion Reserve

MRI - Magnetic Resonance Imaging

MR – Mitral Regurgitation

mRNA - Messenger RNA

MRS - Magnetic Resonance Spectroscopy

MUSTN1 - Musculoskeletal, Embryonic Nuclear Protein 1

NADPH – Nicotinamide Adenine Dinucleotide Phosphate

NF-kB - Nuclear Factor κB

NFAT - Nuclear Factor of Activated T-Cells

New York Heart Assessment – NYHA Classification

NODM – No Diabetes

NPPA - Natriuretic Peptide Type A

NRXN3 - Neurexin 3

NSTEMI - Non-ST Elevation Myocardial Infarction

NT-proBNP - N-terminal Pro B-type Natriuretic Peptide

OGTT - Oral Glucose Tolerance Test

OMT – Optimal Medical Therapy

31P-MRS - Phosphorus Magnetic Resonance Spectroscopy

PCA - Principal Component Analysis

PC - Principal Component

PCr/ATP - Phosphocreatine to ATP Ratio

PCK1 - Phosphoenolpyruvate Carboxylase -1

PDK4 - Pyruvate Dehydrogenase Kinase 4

PET - Positron Emission Tomography

PGC1a - Peroxisome Proliferator-Activated Receptor-Gamma Coactivator

PKCβ2 - Protein Kinase C-β2

PPAR - Peroxisome Proliferator-Activated Receptors

PSC - PAXgene Shredder Spin Column

qPCR - Quantitative Polymerase Chain Reaction (qPCR)

RA - Right Atrium

RAA - Right Atrial Appendage

RAAS – Renin Angiotensin Aldosterone System

RAGE - Receptor for AGE

RIN - RNA Integrity Number

RNA - Ribonucleic Acid

RNA-seq - RNA-Sequencing

ROS - Reactive Oxygen Species

RPP – Rate Pressure Product

RV – Right Ventricle

SAVR - Surgical Aortic Valve Replacement

SERCA2a - Sarcoplasmic Reticulum Ca2+ ATPase (2a)

SGLT2 Inhibitors - Sodium-Glucose Cotransporter-2 Inhibitors

SLC25A6 - Solute Carrier Family 25 Member 6

sRAGE - Soluble RAGE

SPEC - Single-Photon Emission Computed Tomography

SSFP - Steady State Free Precession

STEMI - ST-Elevation Myocardial Infarction

STS – Society of Thoracic Surgeons

SV - Stroke Volume

T1D – Type 1 Diabetes

T2D – Type 2 Diabetes

TAVR - Transcatheter Aortic Valve Replacement

TGF-β1 - Transforming Growth Factor β1

TLR - Toll-Like Receptor

TNF-a - Tumour Necrosis Factor-a

TRPC4 - Transient Receptor Potential Channel 4

UCP3 - Uncoupling Protein 3

UK - United Kingdom

UTY - Ubiquitously Transcribed Tetratricopeptide

V1 – Visit 1

V2 – Visit 2

VAMP2 - Vesicle-Associated Membrane Protein 2

VCAM-1 - Vascular Cell Adhesion Molecule 1

VEGF - Vascular Endothelial Growth Factor

VENC – Velocity Encoding

VLDL - Very Low Density Lipoprotein

WHO - World Health Organisation

XIST - X-Inactive Specific Transcript

1. INTRODUCTION

1.1. Diabetes

Diabetes mellitus (DM) is a chronic multisystem disorder characterised by insufficient insulin production or insensitivity to insulin leading to hyperglycaemia. The insufficient production of insulin is due to the inflammatory and autoimmune β-cell destruction within the pancreatic islet cells, whereas insensitivity to insulin is a result of complex intracellular signalling perturbation, often linked to inflammation and metabolic stress (1-5).

The complex relationship between insulin and glucose homeostasis can be seen below, Figure 1.1

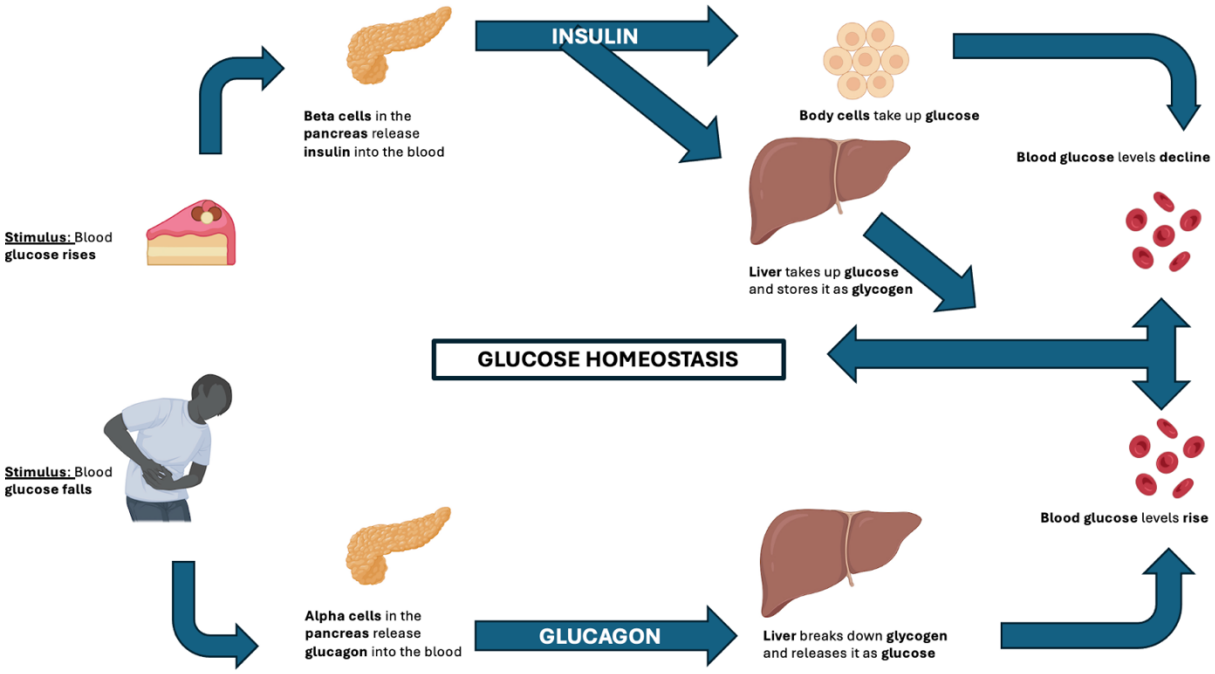

Figure 1.1: Glucose homeostasis feedback loop. Created using Biorender©

The latest statistics suggest that more than 5.8 million people are living with DM in the United Kingdom (UK), (6).

The typical symptoms are polyuria, polydipsia, and unintentional weight loss. However, depending on the subtype of diabetes other symptoms may also be present, or indeed it may be picked up as an incidental finding (7).

The diagnosis of this disease is determined by assessing blood glucose levels. According to the American Diabetes Association and Diabetes UK, diabetes can be diagnosed based on the criteria outlined in Table 1.1 (7, 8):

Table 1.1: Diagnostic criteria for diabetes and pre-diabetes according to Diabetes UK and the American Diabetes Association

Diagnosis	Fasting Plasma Glucose	HbA1C	Oral Glucose Tolerance Test	Random Plasma Glucose Test
Diabetes	>7.0mmol/L	≥6.5% (48mmol/mol)	≥11.1 mmol/L	≥11.1 mmol/L
Pre – Diabetes	5.6-6.9mmol/L	5.7-6.4% (39–47mmol/mol)	7.8-11.0mmol/L	-
Normal Glucose Control	<5.6mmmol/L	<5.7% (<39mmol/mol)	<7.8 mmol/L	-

In the presence of symptoms, patients can be diagnosed with any of the methods outlined in Table 1.1 at one time point only. In the absence of symptoms however, a diagnosis should not be based on a single glucose reading. Instead, confirmation is required from at least one additional result on another day being in the diabetic range. This can be from a fasting or random sample bood glucose sample, a glycated haemoglobin (HbA1C) test, or from an oral glucose tolerance test (OGTT), measuring the two-hour post glucose load (7-9).

Treatment of this chronic condition involves a multidisciplinary approach. Patient education on diet and lifestyle modifications as well as blood glucose monitoring is key. Medical therapy,

where needed, involves insulin replacement or oral anti-diabetic medications to normalise glycaemia and improve insulin sensitivity. A comprehensive list of oral diabetes medications and their mechanisms of action can be found in Table 1.2Table 1.2.

Table 1.2: Oral anti-diabetic medications and their mechanisms of action.

Oral Diabetes Medication	**Key Mechanism of Action**
Metformin	Lowers serum glucose levels by inhibiting hepatic gluconeogenesis and opposing the action of glucagon (10).
Sulfonylureas	Stimulate the pancreas to release more insulin (11).
Dipeptidyl Peptidase-4 Inhibitors (DPP-4 inhibitors)	Block the enzyme DPP-4 which is responsible for breaking down the incretin hormones. These hormones are vital for the inhibition of glucagon release and stimulation of insulin secretion (12).
Sodium-Glucose Cotransporter-2 Inhibitors (SGLT2 inhibitors)	Reduce renal reabsorption of glucose into the bloodstream, instead releasing more through the urine (13).
Thiazolidinediones	Increase insulin sensitivity in muscle and fat and reduce the production of glucose from the liver (14).
Glucagon-Like Peptide -1 (GLP-1) Receptor Agonists	Mimic the GLP-1 hormone to stimulate insulin release, reduce glucagon secretion and also slow gastric emptying (15).

The nuances of presentation, diagnosis and management depend on the subtype of diabetes a person is diagnosed with and will be discussed in more detail below.

1.1.1 Classification of Diabetes

Error! Reference source not found. depicts the different types of diabetes. Each will be briefly discussed in turn below. Other suggestions to classify diabetes have also been made. Ahlqvist et al performed data-driven cluster analysis from three different Scandinavian cohorts. Using the model variables of body mass index (BMI), diabetes onset age, presence or absence of Glutamic Acid Decarboxylase Autoantibodies (GADA) antibodies and homoeostasis model assessment (HOMA) based on insulin resistance using C-peptide concentrations, they

identified 5 distinct clusters; Cluster 1 – severe autoimmune disease: early-onset disease, relatively low BMI, poor metabolic control, insulin deficiency, and presence of GADA, Cluster 2 - severe insulin-deficient diabetes: early onset age, relatively low BMI, low insulin secretion (low HOMA2-B index), and poor metabolic control and GADA negative, Cluster 3 - severe insulin-resistant diabetes: insulin resistance (high HOMA2-IR index) and high BMI, Cluster 4 - mild obesity-related diabetes: characterised by obesity but not by insulin resistance, Cluster 5 - mild age-related diabetes: older than patients in other clusters and only modest metabolic derangements. Whilst this approach is effective at discriminating the different diagnostic and key demographic differences between the groups, it is currently not used in clinical practice (16).

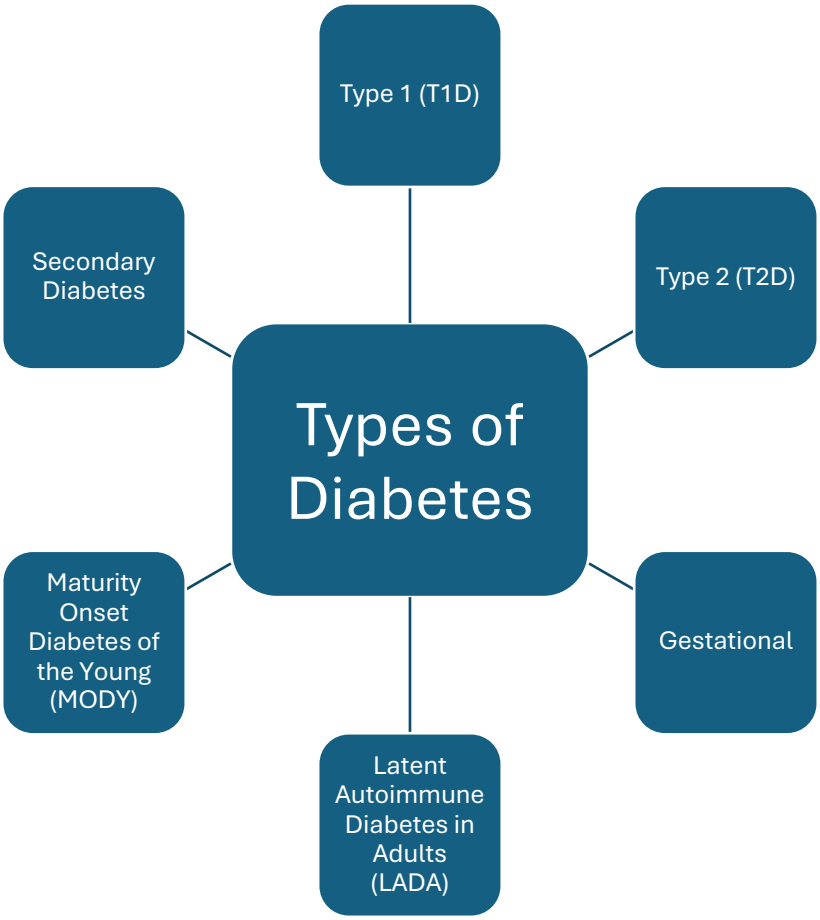

Figure 1.2: Radial cluster defining the types of diabetes

Type 1 Diabetes

It is estimated that approximately 400,000 people are living with Type 1 diabetes (T1D) in the UK. Of this cohort, 30,000 individuals are thought to be under 18 years of age (17).

T1D is a condition characterized by the immune-mediated destruction of pancreatic β-cells which are responsible for insulin-production. This leads to the absolute deficiency of insulin. T1D manifests in genetically susceptible individuals in whom the autoimmune process is triggered by one or more environmental factors. Whilst the precise aetiology remains unknown, genetic predisposition to the condition has been strongly associated with human leukocyte antigen alleles (HLA) DR and DQ. Specifically, HLA DR4-DQ8 and DR3-DQ2 have been reported to account for 90% of children's diagnosis with T1D. Postulated environmental factors include infections (coxsackie virus, rubella virus, mumps, influenza, COVID-19), childhood vaccinations, and dietary exposure to cow's milk and cereal (3-5, 18).

The loss of β-cell function progresses gradually, a process which may take years to finalise, during which time the affected individual remains asymptomatic. Symptomatic hyperglycaemia develops when a significant amount of β-cell dysfunction occurs (3-5, 18, 19). Childhood-onset T1D tends to present with more severe clinical presentations, including symptomatic severe hyperglycaemia or diabetic ketoacidosis (DKA). In adults, new-onset T1D may be misdiagnosed as type 2 diabetes (T2D), but youth-onset T1D is more common than adult-onset T1D (18, 20, 21).

DKA is characterized by marked hyperglycaemia associated with ketonuria, electrolyte disturbances and metabolic acidosis. In this state, patients typically present with a history of

polyuria, polydipsia, and unintentional weight loss. On clinical examination patients may have the characteristic acetone-like breath odour, lethargy, and, in severe cases, may present in a coma. The incidence of DKA in children has been quoted between 15% and 70%. Urgent treatment, usually in a high-dependency or intensive care unit, with intravenous fluids, insulin, potassium, and cardiac monitoring is essential (18, 20, 21).

T1D is one of the exceptions to the HbA1c diagnostic rules mentioned above. According to the world health organisation (WHO) and Diabetes UK children should not be diagnosed with diabetes according to the glycated haemoglobin marker. Instead, they should be diagnosed based on blood glucose levels as outlined above (7-9). Indeed, in the setting of T1D, most patients are initially diagnosed with DKA and then T1D. If there is any diagnostic uncertainty or further confirmation of an autoimmune process is required, GADA and Insulinoma-Associated-2 Autoantibodies (IA-2A) antibody (blood) tests can be undertaken (3).

Treatment, when not in the DKA state, is centred around a balanced diet, blood glucose monitoring and daily subcutaneous insulin administration (9, 20).

Type 2 Diabetes

Driven by the obesity epidemic, T2D is one of the most prevalent diseases within the adult population, both within the UK and worldwide (22). Latest figures suggest that more than 4.7 million people are living with this diagnosis in the UK, with an estimated 13.6 million individuals believed to be at high risk of developing the disease (23). This form of diabetes is caused by insufficient augmentation of insulin secretion by pancreatic β-cells to overcome the progressive inability of insulin-sensitive tissues to respond appropriately to insulin (24). This

has been particularly linked to obesity and the risk of T2D is known to increase linearly with an increase in BMI (25). The latest statistics released by Public Health England state that: 12.4% of people aged 18 years and over with obesity, also have a diabetes diagnosis. This is five times that of people with a healthy weight. Furthermore, men with a raised waist circumference are five times more likely to be diagnosed with diabetes than those without a raised waist circumference; and women are over three times more likely (26). The relationship between obesity and T2D is not just important because of its coexistence however. Importantly, whilst both have been found to be independently associated with a baseline adverse cardiovascular phenotype and incident major cardiovascular events; when combined, their risks are additive (27).

T1D primarily affects children and young adults, whereas T2D primarily affects adults over the age of 40. Patients may be diagnosed when asymptomatic as part of routine health checks. However, in those who have symptoms, these are typically polyuria (especially nocturia), polydipsia, fatigue, weight loss, poor wound healing and changes to eyesight (24). T2D is diagnosed as per the guidance outlined above, (**Error! Reference source not found.**) with fasting blood glucose measurements or HbA1c levels.

Management consists of diet and lifestyle modifications, glucose monitoring and anti-diabetic oral medications. Monotherapy with metformin or an SGLT2 inhibitor is the preferred first-line treatment option, but in the instances where this is not adequate to maintain glucose homeostasis, combination therapy is used. In cases where this fails to control glucose homeostasis, subcutaneous insulin is often commenced (24, 28, 29).

Gestational

Gestational diabetes mellitus (GDM) is hyperglycaemia that develops during pregnancy due to combination of β-cell dysfunction and insulin resistance (30). In the UK it is thought to complicate 1 in 20 pregnancies. Pregnant women considered to be at risk of GDM will receive testing for dysglycaemia typically between 24-28 weeks of gestation. At risk mothers are those with a BMI >30kg/m^2, age >40 years old, glycosuria, previous macrosomic baby (defined as >4kg), first degree relative with diabetes, or ethnicity associated with a high prevalence of diabetes (South Asia, black Caribbean or middle eastern). Women with a prior history of GDM will be tested for the condition at booking and if not diagnosed at this time, will be re-tested at 24-28 weeks (30, 31).

Typical symptoms associated with this form of diabetes include polyuria, polydipsia, lethargy and fatigue, genital thrush or blurred eyesight (32). Diagnosis is made with an oral glucose tolerance test. Importantly, any diagnosis of diabetes made prior to week 20 of gestation is considered pre-existing (undiagnosed) diabetes, with GDM being diagnosed only once the woman is in her second trimester (30, 33).

Treatment, once again, involves diet and lifestyle modifications. In the instances where this is inadequate, metformin and/or insulin may be required (30). GDM usually resolves within a few weeks of delivery of the baby. However, there is evidence to suggest that women are at an increased risk of developing T2D later in life (30).

Latent Autoimmune Diabetes in Adults

Latent autoimmune diabetes in adults (LADA) is considered an intermediate form of DM between T1D and T2D. Once again, this form of diabetes is characterised by the auto-immune destruction of the pancreatic islet cells. However, the phenotype tends to be less severe and presents later in life than T1D. Patients will typically have positive autoantibody blood tests, most commonly GADA, and present between the ages of 30-50 (whereas in T1D, most diagnoses occur in childhood and adolescence) (34, 35). One study has suggested that just under 10% of all adult-onset diabetic presentations across Europe are attributable to this cause (36).

The typical symptoms of diabetes remain present, with patients typically presenting with polyuria, polydipsia, fatigue and weight loss. However, the symptoms develop over a longer time frame than that seen in T1D (36). When compared to T2D these patients tend to be of a normal weight or underweight (in T2D most patients are overweight). Treatment begins with metformin, similar to T2D, but patients progress to requiring insulin much quicker (35, 36).

Maturity Onset Diabetes of the Young

Maturity onset diabetes of the young (MODY) has a genetic basis and is inherited in an autosomal dominant fashion. It is rare, with the current estimates suggesting it accounts for 1-2% of diabetes in the UK (approximately 20,000-40,000 people) (37).

The key features separating MODY from other forms of diabetes are the strong family history and a diagnosis of diabetes before the age of 25 years. The 4 most common genes affected are the hepatocyte nuclear factor genes; HNF1- α, HNF4- α, HNF1- β and glucokinase (37). To

diagnose MODY, a diagnosis of diabetes must first be made and then genetic testing must be undertaken, guided by clinical suspicion (37). The mainstay of treatment is subcutaneous insulin, alongside diet and lifestyle modifications and glucose monitoring (37).

Secondary Diabetes

This is a form of diabetes that results secondary to other medical conditions which may directly affect the pancreas or other endocrine organs, or reduce peripheral insulin sensitivity, disturbing glucose regulation. Such conditions can include cystic fibrosis, haemochromatosis, pancreatitis, Cushing's syndrome, glucagonoma, pancreatectomy or secondary to medications (such as corticosteroids and thiazide diuretics). Whilst the diagnosis remains the same as highlighted in **Error! Reference source not found.**, there is no set treatment route as this depends on the underlying cause. Secondary diabetes may be permanent or reversible (38).

Pre-diabetes

Impaired glucose tolerance and impaired fasting glucose are the intermediate stage in the natural history of DM, otherwise known as 'pre-diabetes' (39). Office for National Statistics data suggest that 1 in 9 people living in the UK (approximately 5.1 million in total) are affected by the condition (40).

Impaired glucose tolerance is defined as two-hour glucose levels of 7.8-11.0mmol/L on the 75-g OGTT, and impaired fasting glucose is defined as glucose levels of 5.6-6.9mmol/L in fasting patients. Both conditions are characterised by insulin resistance. Patients presenting in these categories are at high risk of developing T2D and should therefore be targeted for

primary prevention treatment, including strict diet and lifestyle modifications and consideration of control of other modifiable risk factors, such as hypertension and dyslipidaemia. Whilst anti-diabetic drug therapy with metformin has been shown to delay or prevent the onset of diabetes, medications are not as effective as lifestyle changes, and it is not known if treatment with these drugs is cost effective in the management of impaired glucose tolerance (41).

1.1.2 Complications of diabetes

Diabetes, and in particular T2D, is now considered a global emergency, affecting patients of all ethnic and social backgrounds due to the myriad of complications it promotes, including; amputation, stroke, myocardial infarction, heart failure, nephropathy and neuropathy (23, 42). Notably, hyperglycaemia is just one driver of such complications. The likelihood of these complications increases with the duration of the condition, especially when sub-optimally controlled. Figure 1.3 provides a schematic overview of the differing diabetic complications each of which will be briefly discussed below.

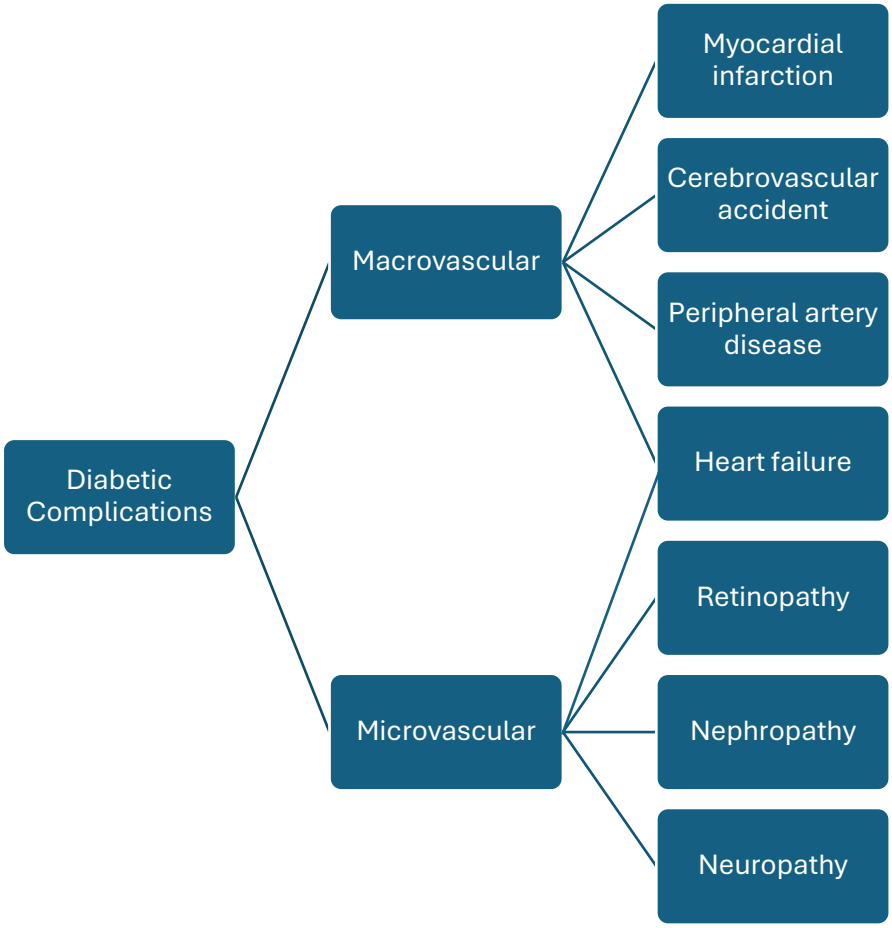

Figure 1.3: Overview of diabetic complications

Macrovascular complications

Macrovascular complications refer to arterial stiffening and atherosclerosis promoted by diabetes, particularly manifesting in coronary artery disease, cerebrovascular disease, and peripheral arterial disease (43, 44). Such complications occur in approximately 20% to 30% of all patients with diabetes, and significantly contribute to the morbidity and mortality rates, especially in those with T2D (45-47).

The central mechanism underlying macrovascular disease is atherosclerosis. This is caused by arterial chronic inflammation and endothelial dysfunction, with progressive accumulation of oxidised lipids from low density lipoprotein particles within the arterial wall. With time, infiltrating monocytes differentiate to macrophages and these, in turn, accumulate oxidized

lipids to form foam cells. A more complex inflammatory milieu develops and smooth muscle proliferation with collagen accumulation leads to a fibrous cap over a complex necrotic lipid-rich core. The cap is prone to rupture, leading to abrupt vascular occlusion by thrombus formation, with ischaemia or infarction of downstream tissues (48-50). Macrovascular complications can present as chronic or acute coronary syndromes, hypertension, strokes intermittent limb claudication and limb ischaemia, with the former examples contributing to the risk of developing heart failure.

Microvascular complications

Microvascular complications affect the capillaries and other small blood vessels. In one cohort study among patients with T2D, up to 20% experienced microvascular complications, the most prevalent being diabetic neuropathy, followed by diabetic retinopathy and the least common was diabetic nephropathy (48, 51).

There are multiple contributary mechanisms including activation of the polyol pathway (this is responsible for converting glucose to sorbitol, which accumulates and causes osmotic stress and ultimately leads to cellular damage), the protein kinase C pathway (once this pathway is activated this can lead vascular dysfunction), creation of advanced glycation-end products (these are formed when glucose reacts with proteins, alters their function, and promotes oxidative stress) and the hexosamine pathway (inducing glycosylation of transcription factors and many other molecules, perturbing their function) (52, 53). Another key mechanism is that of hyperglycaemia-induced mitochondrial superoxide production, leading to oxidative stress and endothelial dysfunction (52, 54, 55). The increased expression of pro-inflammatory cytokines, such as tumour necrosis factor-alpha (TNF-a) and interleukin-6 (IL-6), found in

patients with macrovascular complications is suggestive of an underlying inflammatory pathogenesis (53, 56-59). Many of the above mechanisms directly affect the endothelial cells, impairing their function and promoting apoptosis, leading to increased vascular permeability and altered blood flow (52, 53, 60).

Retinopathy

Hyperglycaemia leads to progressive damage of the retinal blood vessels resulting in abnormal permeability, capillary microaneurysms, capillary degeneration, and excessive formation of new blood vessels (neovascularization) (61). This can lead to haemorrhage, retinal detachment and eventually blindness. Depending on the severity, diabetic retinopathy can be subdivided into proliferative and non-proliferative. The most extreme form of the disease affects the macula (62).

Nephropathy

Hyperglycaemia leads to progressively reduced renal function and albuminuria via initial loss of the selective endothelial barrier properties in glomeruli, followed by progressive sclerosis of glomeruli. Over time this can lead to end stage renal failure, requiring dialysis and/or transplantation (62).

Neuropathy

Diabetic neuropathy can affect both the somatic and autonomic divisions of the nervous system (61). Damage to the nerves can present in multiple different forms including; peripheral neuropathy, autonomic neuropathies, atypical neuropathies, amongst others (63). The longer the nerve fibres, the earlier the loss of nerve conduction velocity at the nerve

terminal. The most common type is, peripheral neuropathy, which tends to occur in a glove and stocking distribution affecting toes and hands first before spreading towards the core (61).

Diabetic gastroparesis is a form of autonomic neuropathy which affects the vagus nerve. This results in delayed gastric emptying and symptoms of nausea and vomiting, bloating, acid reflux, abdominal pain, loss of appetite and weight loss (64, 65).

Diabetic foot complications occur as a combined result of macro- and microvascular complications, namely neuropathy both sensory and motor, and atherosclerosis. Patients have a reduced ability to feel pain and hence injuries can go unnoticed which in turn can lead to structural changes in the foot. Such changes combined with peripheral artery disease can lead to ulcers, infections, Charcot joints and even amputation (66, 67).

1.2. Diabetes and the Heart

Multiple observational studies have reported higher all-cause and cardiovascular mortality in patients with diabetes that in those without (68-71). Diabetic heart disease is an umbrella term to encompass factors including coronary artery disease (caused by the macrovascular complications of hyperglycaemia), cardiac autonomic neuropathy (the impairment of cardiovascular autonomic control in the absence of other causes in patients with diabetes which can present as ischaemia, arrythmias, orthostatic hypotension and in extreme cases sudden death syndrome) and diabetic cardiomyopathy (72, 73). This diagnosis can be applied to any patient with diabetes that develops cardiac disease as a direct consequence of their diabetes (72).

1.2.1 Diabetic heart disease

Heart failure (HF) is among the commonest initial presentation of cardiovascular disease (CVD) in patients with T2D (74, 75). In comparison to age-matched controls, the risk of developing HF increases 2-fold in men and 5-fold in women (76). The involvement of the heart in T2D is a complex process and the mechanisms underlying HF in patients with T2D are highly heterogeneous.

HF, which can be classified as reduced or preserved left ventricular ejection fraction, depending on the mechanism, and can be caused by multiple underlying pathologies including, ischaemic heart disease, hypertension, severe valvular dysfunction, and inherited cardiomyopathies. In the presence of such conditions and concomitant diabetes, the phenotype and outcomes may be more severe than the pathology without diabetes, as

discussed below. However, in the absence of such risk factors, the presence of cardiac dysfunction on a background of diabetes can be classified as diabetic cardiomyopathy (19, 77).

The proposed causal link between T2D and HF rests on several structural, functional, and metabolic observations. At the macroscopic level, the structural and functional changes in T2D include left ventricular (LV) hypertrophy, concentric LV remodelling, and impairment of LV systolic and diastolic performance (75, 78-81). Histological studies have demonstrated that at the microscopic level, T2D is associated with cardiomyocyte hypertrophy, perivascular fibrosis, increased collagen deposition and cellular triglyceride accumulation (82). Early studies on substrate metabolism of the human heart have revealed that myocardial glucose uptake is decreased in association with insulin resistance, whereas free fatty acid (FFA) uptake is increased in T2D (83, 84). These structural and functional changes may be related to the nonenzymatic glycation of vascular and membrane proteins, increased cellular fatty acid uptake and oxidative stress, which are characteristic of the T2D state (83, 84). Notably, these structural, functional and metabolic changes were shown to be predictors of mortality and related to contractile dysfunction (78, 79, 85, 86).

Table 1.3 provides an overview of the key changes in cardiac structure, function, metabolism and cell signalling pathways in diabetes as well as the current understanding of drivers of these changes. Such changes can be seen using cardiac imaging, cardiac magnetic resonance (CMR) in particular, on a macroscopic and functional level. Transcriptomics can also be used to assess such changes on a molecular level. Each will be reviewed in more detail below.

Table 1.3: Processes that are proposed to mediate changes in myocardial structure and function in diabetic heart disease

Process	Exemplar mechanisms	Consequences
Systemic hormonal dysregulation	• Leptin release from expanded adipose tissue depots, leads to activation of endothelin-1 mediated reactive oxygen series release. • Macrophage release of the adipokine resistin, induces cardiomyocyte hypertrophy. • Augmented insulin signalling may promote cardiomyocyte hypertrophy (87, 88).	• Left ventricular hypertrophy (LVH) • Increased LV mass
Myocardial lipotoxicity	• Cardiac lipotoxicity is the result of excess uptake of FFAs, which exceed the capacity for oxidation and storage. • Overexpression of proteins such as long-chain acyl Co-A synthetase, glycosylphosphatidylinositol (a membrane anchored form of lipoprotein lipase) or FA transport proteins, which are responsible in cardiac FA transport, have been shown to result in cardiac lipotoxicity in mice. This may lead to lipid-induced cell death. • Lipotoxic conditions cause the endoplasmic reticulum to swell and gradually breakdown (see further detail below). • Long chain FAs change the dynamics and function of plasma and mitochondrial membranes by altering the phospholipid composition. • The increase of FA oxidation, alongside the decrease of glucose oxidation, lead to the accumulation of toxic lipid metabolites such as diacyl glycerol (DAG) and ceramide as well as the increase of oxidative stress causing the release of reactive oxygen species (ROS) within cardiomyocytes. • Impaired systemic insulin production and/or insulin resistance results in elevated plasma FAs, uptake of which activates transcription pathways of PPARα/PGC1α that further increase the direct myocardial FFA uptake and oxidation. Decreased glucose transporter 4 (GLUT4) expression and translocation leads to reduced glucose uptake, glycolysis and glucose oxidation (19, 88, 89).	• Myocardial steatosis • Altered energetic substrate preference
Increased oxidative stress	• Oxidative stress is induced by excess reactive oxygen species (ROS) due to cardiac lipid accumulation and increased mitochondrial fatty acid oxidation. Excess fatty acids within the mitochondria are thought to promote mitochondrial superoxide generation and uncouple the respiratory chain impairing adenosine triphosphate (ATP) generation.	• LVH • Arrhythmias

	• ROS generated within the cytosol from NADPH oxidase can also interact with nitric oxide generated in some cells, forming peroxynitrite, leading to protein modification via nitrotyrosine formation. • Oxidative stress promotes a switch to alternative glucose metabolism pathways, resulting in the formation of other potentially toxic mediators and further cellular injury (as indicated by increased levels of protein kinase C activation, polyol and hexosamine (88).	
Altered Substrate Utilisation	• Reduced myocardial GLUT4 content and a defect in GLUT4 translocation leads to reduced rates of glycolysis and glucose oxidation. This ultimately leads to increased FA oxidation rates via the Randle cycle. The increased delivery of FA substrates activates PPARα signalling pathways. This leads to the induction of genes which are involved in lipid oxidation as well as an increased expression of pyruvate dehydrogenase kinase. • There is a loss of substrate flexibility. In particular, glucose uptake and utilisation decrease, whereas fatty acid utilisation and uptake increase. This results in triglyceride deposition and a decrease in ATP production (88).	• Changes to cardiac metabolism
Interstitial Fibrosis	• Increased collagen (in particular, type III) deposition around the intramural vessels and between myofibers. • Increase in the TGFβ1 receptor II density and expression of CTGF and PKCβ2 (88).	• Diastolic dysfunction
Mitochondrial Dysfunction	• Mitochondrial ROS leads to uncoupling of proteins within the mitochondria which results in increased oxygen consumption without a concomitant increase in ATP production. • Excess free fatty acid oxidation promotes oxidative stress via mitochondrial superoxide generation. In the presence of hyperglycaemia and insulin resistance, antioxidants are less abundant and so ROS accumulate. These can lead to mitochondrial fragmentation and hence further induce mitochondrial function. • Hyperglycaemia is also associated with mitochondrial swelling and a depletion in their number (19, 88, 89). • Mitochondrial permeability increases in the diabetic myocardium, which can induce apoptosis via release of immunogenic mitochondrial factors into the cytoplasm (90).	• Contractile dysfunction • Cardiac Fibrosis
Advanced Glycosylated End Products	• Advanced glycation end-products (AGEs) are generated by the non-enzymatic reaction between glucose (or other sugars) and lipids, proteins and nucleic acids. Their formation is increased in diabetes. They may cross link extracellular matrix proteins and connective tissues, hence decreasing collagen degradation, ultimately leading to fibrosis (88).	• Fibrosis

Altered Calcium haemostasis	• The formation of AGEs in the sarcoplasmic reticulum interferes with the dynamics of calcium homeostasis, reducing calcium content, by altering the expression of calcium channels (91). • Impaired calcium handling by its transporters leads to an increase in the action potential duration and ultimately prolonged diastolic time (88).	• Diastolic dysfunction • Contractile dysfunction
Increased activation of Renin – Angiotensin – Aldosterone System (RAAS)	• Hyperglycaemia and insulin resistance promote increased angiotensin II and aldosterone generation, which ultimately leads to fluid retention, vasoconstriction, myocardial fibrosis and inflammation.	• Fibrosis • Diastolic dysfunction • Heart failure
Chronic inflammation	• Myocardial biopsy evaluation has revealed increased abundance of many chemokines and cytokines including; IL-6, IL-1β, IL-18, TGF-β1 and TNF-α, immune cells, macrophage and leukocyte infiltration, vascular cell adhesion molecule 1 (VCAM-1) and inflammatory cell adhesion molecule 1 (ICAM-1). Amongst other effects, these activate fibroblasts which stiffens the cardiac wall (87, 88).	• Fibrosis
Increased use of the hexosamine biosynthetic pathway	• Under healthy conditions, the hexosamine biosynthetic pathway (HBP) pathway accounts for <5% of glucose metabolic flux. In the presence of hyperglycaemia, this increases, resulting in elevated UDP-N-acetylglucosamine which is essential in the post-translational modification (glycosylation) of the proteins with wide-ranging implications for cardiac structure and function (88).	• Diminished mitochondrial function • Reduced energy production • Impairment of insulin metabolic signalling • Cardiomyocyte apoptosis • Altered myocardial excitation-contraction coupling • Altered cardiac relaxation

Endoplasmic reticulum dysfunction	• The endoplasmic reticulum exhibits stress with damaged and misfolded proteins accumulate in the context of diabetes, potentially inducing cellular apoptosis. • Furthermore, endoplasmic reticulum stress directly affects calcium handling by contributing to the imbalance of calcium release from the sarcoplasmic reticulum (SR) into the cytosol alongside a decline in the action of calcium pumps in the SR (88).	• Diastolic dysfunction

PPAR: (peroxisome proliferator-activated receptor, -α/PGC: PPAR-γ coactivator-1α-,1DAG: diacylglycerols, ROS: reactive oxygen series, NOS: nitric oxide synthase, ATP: Adenosine triphosphate, TGFβ1: transforming growth factor β1, CTGF: connective tissue growth factor, PKCβ2: protein kinase C β2, IL-6: interleukin 6 , IL-1β: interleukin 1β, IL-18: interleukin 18 , TGF-β1: tumour growth factor -β1, TNF-α: tumour necrosis factor α

The term diabetic cardiomyopathy, however, has long been debated within the scientific community, as the chance of patients presenting with standalone cardiac dysfunction in the absence of other risk factors is relatively small. In particular, there are multiple studies highlighting that patients with diabetes, T2D in particular, have a high likelihood of exhibiting other co-morbidities. T2D is commonly associated with arterial hypertension, obesity and dyslipidemia, which makes elucidation of the specific role of diabetes difficult (19, 74, 75). The longer the presence of diabetes, the more likely it is associated with co-morbidities (92, 93). The prevalence of hypertension within this population has been quoted as high as 50% (92, 94-96). Other commonly associated conditions included hyperlipidaemia, arthritis and anxiety (92, 93). The most common combination of multi-morbidity in patients with T2D has been quoted as hypertension, hyperlipidaemia and obesity (93). In a large cohort study by Brown et al, the authors described that cardiovascular mortality and nonfatal events (myocardial infarction and ischaemic stroke) were more common in patients with T2D than their BMI matched non-diabetic counterparts, but as BMI increased within the T2D group, mortality and morbidity rates exponentially rose (27). As a result, the existence of a distinct diabetic cardiomyopathy has been questioned over the last 5 decades and remains controversial. However, regardless of this debate, what is most relevant to the affected patient population is that the 5-year survival rates of patients with T2D and HF are approximately 50%, which is a poorer prognosis than many cancers (97, 98). As a result, better understanding cardiac dysfunction mechanisms in T2D is vital to identify novel treatment targets.

1.2.2 Ischaemic heart disease

Myocardial infarction (MI) has been highlighted as the leading cause of death among patients with diabetes (99, 100). Atherogenesis progresses more rapidly in people with diabetes compared to their non-diabetic counterparts (101). Patients with diabetes have been shown to have worse outcomes than non-diabetic patients with ischaemic heart disease. Furthemore, diabetic patients have been shown to have more complex disease with diffuse, calcified multi-vessel disease initially thought to require coronary revascularisation and optimal medical treatment (OMT) (102-104).

When considering chronic coronary disease, a sub-analysis of the ISCHAEMIA trial (a prospective multicentre randomised control trial investigating invasive management with cardiac catheterisation and revascularisation in addition to OMT versus OMT alone) studied patients with diabetes. They exhibited higher rates of death or MI over the mean follow-up of 3.2 years, compared with participants without diabetes, with a 49% higher hazard of death or MI (hazard ratio (HR) 1.49; 95% confidence interval (CI): 1.31-1.70, $P<0.001$) (105). Moreover, participants with insulin-treated diabetes showed higher rates of death or MI relative to other subgroups (106). Importantly, of the patients randomised to OMT, a greater proportion of patients with diabetes went on to require invasive treatment than their non-diabetic counterparts. This was due to higher proportions of patients with diabetes experiencing a primary ischaemic event requiring intervention than in the non-diabetic cohort (106).

In the setting of acute coronary syndrome (ACS), encompassing unstable angina, non-ST elevation myocardial infarction (NSTEMI) and ST-elevation myocardial infarction (STEMI), mortality is significantly higher in patients with co-existing diabetes, across ACS subtypes, both at 30-days and at 1 year (107). Hyperglycaemia at presentation is also associated with worse outcomes (108). These unfavourable outcomes may not just be related to the diffuse atherosclerotic disease, but may also relate to the different biological make-up of the lesions. Intracoronary imaging studies have revealed that patients with diabetes have more 'vulnerable' lesion features including a lower minimal fibrous cap thickness and a higher percent area stenosis. Furthermore, these culprit lesions have been shown to have a higher prevalence of lipid-rich plaque and macrophage accumulation, which once again indicate plaque instability (109-111).

1.2.3 Valvular heart disease

The presence of concomitant diabetes in individuals with valve disease is also a rising issue within the ageing population. Of all the valve pathologies, diabetes appears to be most implicated with aortic stenosis (AS). In particular, it has been implicated with disease acceleration and negative outcomes (112-117). By contrast, however, some data suggest diabetes has a protective effect on left sided regurgitant lesions, aortic (AR) and mitral regurgitation (MR) (118). However, in one nationwide prospective observational cohort study, the presence of diabetes indicated poor prognosis (all-cause death) in the mitral and tricuspid regurgitation as well as multi-valve disease cohorts. Furthermore, the authors suggested that age, smoking, symptom severity (as measured by the New York Heart Association scale), LV systolic function and the need for valvular intervention were independent prognostic factors in patients with diabetes and valvular heart disease (118).

Another registry study confirmed the decreased incidence of regurgitant lesions in patients with diabetes, whilst highlighting that in the presence of adequate control of other cardiovascular risk factors such as blood pressure, lipid levels, BMI and kidney function, patients with diabetes were still at a higher risk of stenotic valvular lesions (119). It is postulated that this is likely due to the combination of inflammation and formation of AGEs contributing to valve calcification (120).

1.2.4. Hypertrophic cardiomyopathy

Hypertrophic cardiomyopathy (HCM) is the most common inherited cardiomyopathy. Its population prevalence is quoted at 1 in 200 to 1 in 500 (112, 121, 122). It is estimated that 9% of patients have concomitant diabetes, and this subgroup exhibit a worse clinical manifestation of the disease (112, 123, 124). Patients with co-existing HCM and diabetes have been shown to exhibit significantly higher wall thickness, LV ejection fraction, and LV concentricity (with a higher LV mass–to–LV end-diastolic volume ratio) as well as a higher burden of myocardial scar and worsened cardiac energetics compared to age and sex matched individuals with HCM alone (112, 125). Coinciding with this, patients with co-existing disease had lower global longitudinal strain, peak systolic circumferential strain, and diastolic strain rates (112). In a nationwide cohort study of almost 10,000 patients with HCM, those with co-existing diabetes had significantly higher risks of end stage renal disease, (HR 3.49, 95% CI 2.20–5.54) and left ventricular systolic dysfunction (HR 1.15, 95% CI 1.01–1.32) compared to non-diabetic subjects, independent of age, sex, ischemic heart disease, atrial fibrillation, and other comorbidities (126).

1.2.5 Gestational Diabetes

Diabetes is the most common metabolic disorder in pregnancy. The direct effects on the heart however, have not been defined in a lot of detail. In a recent study by Thirunavukarasu et al, CMR revealed that patients with GDM exhibit a higher LV mass, reduced GLS and impaired myocardial energetics (127). It is important to note that this is usually in the setting of obesity, as women with GDM had a higher BMI than age and sex matched women undergoing a normal pregnancy. GDM is an important condition to diagnose and treat, and most importantly to educate women on to ensure they develop habits which they will take into the post-partum period, as it has been estimated that women with GDM have a twofold higher risk of cardiovascular events post-partum, independent of their risk of developing T2D (128).

1.3. Cardiovascular Magnetic Resonance Imaging in Type 2 Diabetes Mellitus

CMR allows a comprehensive investigation of the structural and functional status of the heart. T2D affects myocardial mass, strain, systolic and diastolic function and perfusion, all of which can be accurately measured with cine CMR (129, 130). This form of cardiac imaging also allows for quantification of myocardial perfusion and perfusion reserve during pharmacological stress, offering insight into coronary arterial and microvascular integrity (131). The latest technology for myocardial perfusion CMR allows fully automated analysis with perfusion values that are in close correlation with the reference standards of positron emission tomography (PET) and microspheres (132). Combined with magnetic resonance spectroscopy (MRS), quantitative perfusion CMR has previously been used to describe the association between exercise energetics (defined by PCr/ATP – the ratio of phosphocreatine to ATP) and

myocardial perfusion reserve in T2D (133). CMR late gadolinium enhancement (LGE) imaging allows for the non-invasive visualisation of focal replacement fibrosis. Additionally, interstitial diffuse fibrosis can be detected and quantified by myocardial extracellular volume (ECV) from pre- and post-contrast T1 maps (134, 135). CMR T1 mapping for ECV quantification correlates closely with collagen area on histology (136). Importantly, multiparametric CMR imaging combining the MRS and CMR techniques allow for a more complete profiling of the metabolic sequelae and cardiovascular disease in patients with T2D. Further detail on the benefits of using CMR and the data that can be acquired will be presented in *2.2 METHODS - Cardiovascular magnetic resonance.*

1.3.1 T2D and cardiac structural changes

LV remodelling refers to LV structural adaptations in response to altered demand. Several alterations in LV geometry have been demonstrated in patients with T2D. A 1% rise in HbA1c level has been associated with a 3.0g increase in LV mass in elderly patients with T2D (137). Although increased LV mass is independently associated with T2D, often this increase has been shown to be modest (80, 138). LV concentric remodelling (a process defined by increased LV wall thickness altering myocardial geometry resulting in increased LV mass, reduced LV end-diastolic volume and stroke volume and normal LV mass indexed (129, 139)) represents the main structural characteristic of diabetic heart disease, and precedes the development of clinical HF. This may be associated with left ventricular systolic dysfunction, with an ejection fraction of <50% (140), which has been shown to be a strong predictor of adverse cardiovascular events (79). Importantly however, it must be noted that heart failure

with preserved ejection fraction (HFpEF - ejection fraction of >50%) is also common and associated with increased morbidity and mortality (141).

Interstitial fibrosis has been implicated in the pathogenesis of LV hypertrophy, and has been identified in the more advanced stages of diabetic heart disease (142). The role of interstitial fibrosis in the pathogenesis of LVH in stable/early diabetic cardiomyopathy is much less clear, as abnormal cardiomyocyte hypertrophy, rather than fibrosis, appears to predominate in the early stages (143). CMR imaging of native and post-contrast T1 mapping for ECV quantification allows for non-invasive quantification of myocardial extracellular matrix expansion. ECV has been shown to correlate closely with areas of collagen deposition on the histology of biopsies obtained from patients with HF (136). Using this technique, two studies demonstrated no significant abnormality in ECV and native T1 mapping in patients with well controlled T2D, suggesting the absence of significant extra cellular matrix expansion, even in the presence of LV concentric remodelling and diastolic dysfunction (129, 131). However, in another study of consecutive patients referred for CMR, investigators showed higher median ECV in patients with diabetes (*n*=231) than in those without diabetes (*n*=945) (144). They noted that such changes were not correlated with indices of glycaemic control, nor left ventricular ejection fraction. Finally, in an observational case control study following patients with T2D, with and without micro-albuminuria (and 30 controls), patients with diabetes had higher ECV values. These decreased after renin angiotensin aldosterone system (RAAS) blockade, suggesting that such changes may be partially reversible (145).

1.3.2 T2D and myocardial functional changes

Despite the link with HF on a population level, the majority of studies report that diabetes has little or no effect on LV ejection fraction (LVEF) (75, 80). However, diabetes traditionally has been linked to diastolic dysfunction, mainly based on echocardiography. Consequently, diastolic abnormalities have been suggested as the earliest functional effect of diabetic cardiomyopathy, with reported prevalence rates in asymptomatic, normotensive patients with T2D varying from 15% to as high as 75% (146).

The combination of pulsed tissue Doppler velocity of the medial mitral annulus (e') with early transmitral inflow velocity (E) has been validated as a reliable index of left ventricular filling pressure. E/e' ratio has been shown to be a useful prognostic biomarker in patients with T2D (147). Abnormality in E/e' was shown to be associated with insulin resistance (148). From et al., in large study of 1,760 patients with diabetes, showed that elevated E/e' was associated with the subsequent development of HF and increased mortality, independent of hypertension, coronary disease or other echocardiographic parameters (147).

The use of less load-dependent measures of myocardial function (i.e. strain imaging by echocardiography and CMR) has demonstrated subtle systolic dysfunction to be a frequent feature of subclinical heart disease in patients with T2D. Both reduced longitudinal contractility and impaired systolic circumferential strain have been shown in patients with T2D (133). Although these subclinical abnormalities in contractility are widely considered to be a precursor to the onset of clinical HF in diabetes, prognostic data on the use of strain

measures in diabetes is lacking, and large longitudinal studies will need to assess this, and better define the spectrum of diabetic heart disease.

1.3.3 T2D and myocardial metabolic changes

The myocardium is unique in its requirement to undergo uninterrupted cycles of contraction and relaxation, and hence has high energy demands. The average human heart beats approximately 100,000 times per day (90). For the effective production and utilisation of the cardiac energy, several key processes must occur. These are highlighted in Figure 1.4.

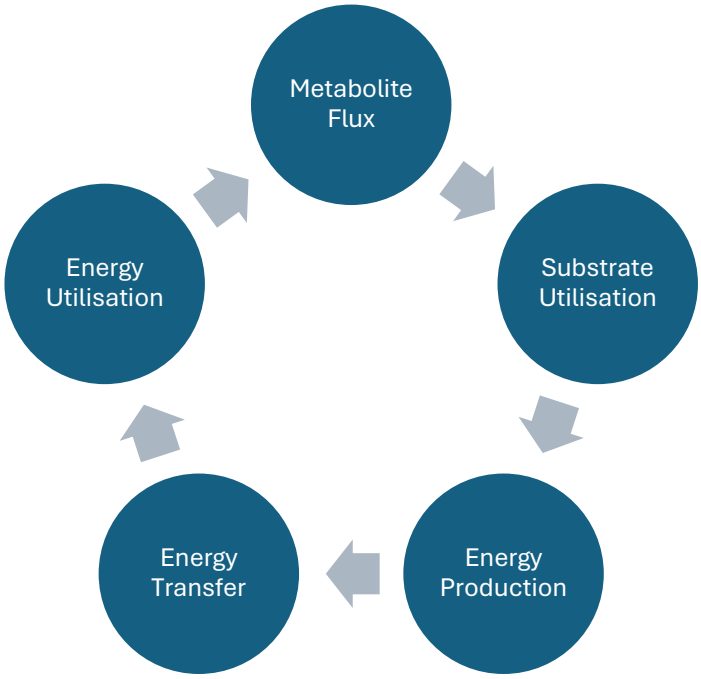

Figure 1.4: The key processes required for effective cardiac metabolism

Each of these processes will be considered in turn:

Metabolite Flux

A constant myocardial blood supply, matched to its fluctuating metabolic demands, is necessary for maintenance of appropriate metabolite flux during rest and stress. Metabolites are actively and selectively transported across the cardiac endothelial barrier to cardiomyocytes (149).

Substrate Utilisation

The heart utilises many substrates such as FFA, carbohydrates, amino acids and ketones. Under normal physiology 70% of ATP generation is through FA oxidation, and the remaining 30% through ketones, glucose and lactate. Substrate switching can occur rapidly and is essential to ensure continuous ATP generation (150).

Energy Production, Transfer and Utilisation

Normal cardiac function is dependent on the constant resynthesis of ATP through the process of oxidative phosphorylation in the mitochondria, as illustrated in Figure 1.5.

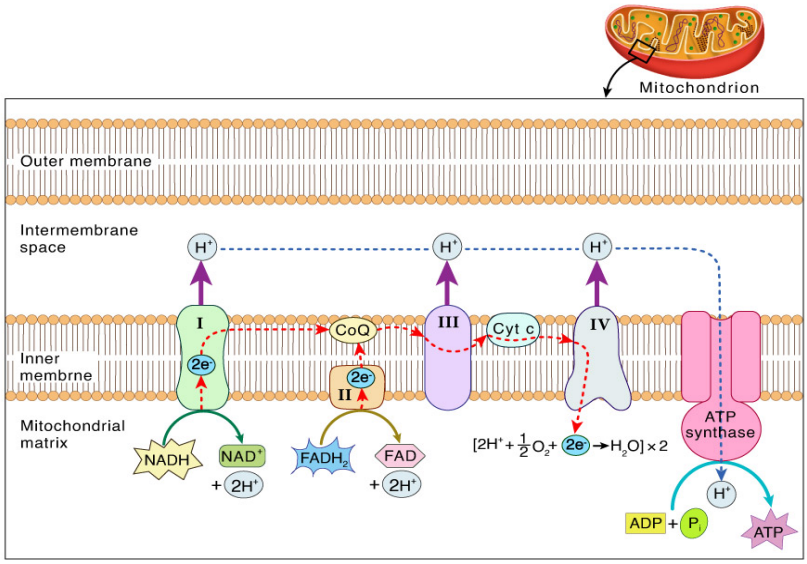

Figure 1.5: The process of oxidative phosphorylation within mitochondria. (Taken directly from ScienceFacts.net)(151)

The healthy heart is metabolically flexible and utilises various substrates for energy production, depending on oxygen availability, substrate concentration, hormone levels and workload. In the healthy state, the heart depends on the use of a wide array of metabolic substrates; the most predominant being FFAs, with glucose accounting for a small proportion. The heart has a limited ability to synthesise FA de novo and is therefore dependent on long-chain FA transported in the blood as albumin-bound FA, triglyceride-rich very low-density lipoprotein and dietary triglycerides in chylomicrons (150). In contrast, glucose is freely transported in the circulation. Both glucose and FA enter the cardiomyocyte using their corresponding transporters and are metabolised to produce ATP. Glucose is metabolised via glycolysis, whereas FA are metabolised via mitochondrial β-oxidation, prior to convergence of the two pathways at the Krebs cycle (90, 152, 153). Under healthy conditions, the rate of ATP hydrolysis is matched to that of ATP resynthesis (via oxidative phosphorylation, which is fuelled by reducing equivalents NADH and $FADH_2$ generated by beta-oxidation of fatty acids, the oxidation of pyruvate, and the Krebs cycle) (90).

Cardiac energy metabolism can be tracked non-invasively using phosphorus magnetic resonance spectroscopy (^{31}P-MRS). The relative concentration of phosphocreatine to ATP (PCr/ATP) is a sensitive index of the energetic state of the myocardium (Figure 1.6) (86). ^{31}P-MRS allows for the non-invasive assessment of myocardial PCr/ATP. Mitochondrial oxidative phosphorylation is responsible for the release of energy from fuels. The subsequent energy created by these fuels is transferred to the high energy phosphate bonds of ATP. Mitochondrial creatine kinase catalyses the transfer of the high energy phosphate bonds in ATP to creatine to form PCr. The smaller size of this molecule permits diffusion out of the

mitochondria into the cytoplasm, where it can facilitate energy-demanding processes such as sarcomere filament sliding (154, 155).

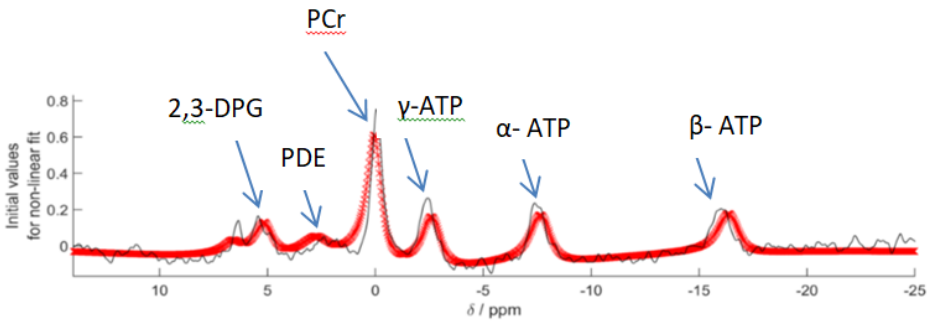

Figure 1.6: Typical result of a 31P-MRS spectrum.

The metabolic phenotype of diabetic heart disease is characterized by impaired myocardial energetics. As shown in Table 1.3, the primary consequence of altered metabolism as seen in T2D is mitochondrial dysfunction. This has been shown to lead to reduced ATP production and an increase in the production of ROS, when compared to non-diabetic counterparts. In the presence of diabetes FA utilisation and mitochondrial uncoupling is high, resulting in elevated rates of oxygen consumption. Within these dysfunctional mitochondria, uncoupling occurs, resulting in reduced efficiency of ATP synthesis and increasing oxygen use (which is different to the non-diabetic heart in which there is a balance of ATP production to oxygen consumption). The aforementioned mitochondrial dysfunction is aggravated by ROS causing mitochondrial DNA and cellular damage (90). These processes combine and are reflected by reductions in phosphocreatine (PCr) to adenosine triphosphate (ATP) (PCr/ATP) ratio assessed by ^{31}P MRS non-invasively (156, 157).

Decreased myocardial PCr/ATP is a predictor of mortality, linked to contractile dysfunction, and is a well-recognized complication of diabetes (86, 133, 158). This pre-existing energetic deficit in diabetic heart disease is exacerbated by exercise (133). Additionally, exercise PCr/ATP was shown to correlate with impaired myocardial perfusion and oxygenation, suggesting that, in diabetes, coronary microvascular dysfunction exacerbates derangement of cardiac energetics under conditions of increased workload (133).

Although significant correlations between myocardial systolic strain and PCr/ATP have been demonstrated (148), the causal role of altered energetics in contractile dysfunction in diabetic hearts remains unclear, and additional research is therefore necessary to delineate the role of myocardial energetics in the development of cardiac dysfunction in patients with T2D.

Myocardial steatosis in patients with T2D

Myocardial lipid overload, reflecting triglycerides in particular, has been associated with LV diastolic dysfunction and concentric LV remodelling (129, 159). It has been shown that in patients with diabetes, independent of BMI, there is increased myocardial and hepatic triglyceride content, which is associated with impaired myocardial energetics. Functionally, the consequence of this lipid overload is linked with reductions in peak systolic strain and diastolic strain (160). Proton MRS (^{1}H-MRS) is a non-invasive technique of choice to measure lipids, choline and creatinine. Single breath hold, cardiac gated sequences are essential for accurate results. However, this technique currently is only available for research and not clinical use (159).

1.3.4 T2D and myocardial perfusion

Coronary artery disease (CAD) is commonly found in people with T2D and has a well-established relationship to morbidity and mortality (161). The literature suggests a global prevalence of 20-40% in people with T2D (71, 102, 162). This is particularly pertinent as it is frequently unrecognised prior to complications arising (e.g. myocardial infarction, heart failure, sudden cardiac death). CMR LGE sequences can be used to detect prior myocardial infarction. A previously published study demonstrated that patients with diabetes without a history of CAD had approximately the same the risk of future MI as patients with prior MI but no diabetes (71). This gave rise to the concept of patients with diabetes being established as 'coronary risk-equivalent' (163).

A study comprising of 1123 asymptomatic patients with T2D and no known or suspected CAD found inducible myocardial ischaemia in 22% of the study population using single-photon emission computed tomography (SPECT) (164). Multiple studies using (pharmacological or exercise) stress echocardiography have demonstrated the modality to be a useful tool for risk stratification and prognostic evaluation in patients with T2D. Patients with T2D and positive ischaemia findings or with peak EF <40% were at high risk of cardiovascular mortality, and non-fatal MI (165-167).

Another study using stress perfusion CMR, showed the presence of inducible ischaemia was associated with an almost five-fold increased likelihood of cardiac death and non-fatal MI amongst patients with diabetes, compared to the annual rate of cardiac death and non-fatal MI of 1.4% per year in diabetes patients without inducible ischaemia (168).

Myocardial perfusion abnormalities can be detected in patients with T2D even in the absence of CAD (133). This is often linked to coronary microvascular dysfunction, which can occur due to structural or functional alterations. Structural abnormalities can include: luminal obstruction, infiltration of inflammatory cells, vascular remodelling and perivascular fibrosis. Functional dysfunction includes endothelial and smooth muscle cell dysfunction leading to abnormal vasomotor responses (77). Furthermore, CMR perfusion studies have also demonstrated that impairment in the myocardial perfusion reserve in patients with T2D is indicative of microvascular dysfunction (169, 170).

At present, the most common approach to perform stress CMR is to induce hyperaemia using vasodilators such as adenosine, regadenoson or dipyridamole (171). Whilst their mechanism of action is the same, their half life, dose and method of administration varies (172). The most commonly used agent of the three, which also has the shortest half life, is adenosine (173). The drug alternative to this, is the direct acting inotropic agent Dobutamine. In a head-to-head study comparing the differences of adenosine to dobutamine in which 79 consecutive patients were subjected to the administration of both stress agents, the results of which were corroborated by invasive angiography, dobutamine was deemed superior to adenosine stress for the induction of ischaemia induced regional wall motion abnormalities, whereas adenosine had superior specificity in identifying only high-grade (defined as >50% luminal stenosis) perfusion deficits. In particular, adenosine ischaemia induced wall motion abnormalities were seen only in segments of >70% stenosis (174). Whilst there is evidence to suggest that in the presence of HF, patients with severe left ventricular systolic dysfunction may be subject to a blunted stress response, requiring higher doses of adenosine to achieve the required haemodynamic response, both stress agents are considered comparable for

detecting coronary artery disease (173, 175). It must be noted that the two drugs have different relative contraindications which may affect their the choice in their administration. Adenosine (and all other vasodilators) should be avoided in: known hypersensitivity, 2nd and 3rd degree heart block, as well as severe reversible obstructive airway disease. Dobutamine however, should be avoided in the presence of narrow angle glaucoma, myasthenia gravis, obstructive uropathy and obstructive gastrointestinal disorders (172).

The non-pharmacological alternative for performing stress CMR is for the patient to undertake exercise. Different methods for performing exercise exist. One option is for the patient to run on a compatible treadmill next to the MRI machine, but the most common method is the use of a supine cycle ergometer. The main advantages of exercise CMR compared to the use of pharmacological agents is fewer adverse events, contraindications and side effects. Despite these benefits however, the main issues associated with this technique are the effect exercise has on image acquisition and consequently on quality. Exercise creates increased physical and respiratory motion which may lead to artefacts. Furthermore, heart rate variability may lead to ECG gating issues, in addition to problems with monitoring of potential ECG changes (given the absence of a 12-lead ECG monitoring system) (176). In the presence of diabetes (both type 1 and 2), exercise CMR has demonstrated that diabetic patients exhibit a smaller increase in their ejection fraction that non-diabetic controls as well as smaller end-systolic, end-diastolic and stroke volumes of the left ventricle both at rest and rest compared to non-diabetics and controls (176).

CMR assessment can therefore provide a holistic review of the changes to the myocardium that occur in the presence of diabetes, including assessment of myocardial ischaemia, viability and function.

1.4 Transcriptomics in exploring diabetic heart disease

'Transcriptomics' refers to the study of all the ribonucleic acid (RNA) molecules within a cell. This offers an important unbiased approach to study the molecular phenotypes of disease. The genetic code that is transcribed into RNA molecules has been estimated to be less than 5% of the whole genome of humans. Layers of complexity arise however, when non-protein coding sequences are transcribed and when different variants of messenger RNA (mRNA) are produced through the processes of splicing, RNA editing and alternative transcription. Transcriptomics therefore allows for a deeper understanding of which genes (and at what level) are turned on or off, as well as their activity and expression within a cell or tissue in a detailed way (177).

RNA sequencing is considered a method which allows 'an unbiased survey of the entire transcriptome in a high-throughput manner' (178). As such, it can take on multiple forms; including first generation, next (second) generation and third generation processing. The differences in the methods include their run time, read length and cost. Irrespective of the method, however, RNA sequencing allows for differential gene expression analysis hence providing clues to their function and potential molecular mechanisms and biomarkers. Another benefit of RNA sequencing is its ability to detect somatic mutations and undiscovered small RNAs, given base-by-base assessment of transcripts, in contrast to earlier array-based

methods. These data can therefore transform our understanding of disease at a molecular level (179).

In work I contributed to independent of my PhD project, RNA-sequencing data from the Genotype-Tissue Expression (GTEx) project was used to define differentially expressed genes (DEGs) in right atrium (RA) and LV myocardium from people with versus without DM (type 1 or 2). Within the 32 DEGs noted in RA, enrichment was seen within the immune system parameters, including immunoglobulin G and A (IgG & IgA) immunoglobulin complexes. Within the 32 DEGs noted in LV, IgG immunoglobulin complex was also altered, but differences were also seen related to neuronal activity such as neuroligin family binding protein and structural constituent of myelin sheath. Importantly, there was no overlap in the DEGs present in the LV compared to the RA. Exploration of these DEGs in the UK Biobank plasma proteomics cohort revealed three LV DEGs with a directionally concordant change in myocardial RNA expression and their plasma protein concentration; ERBB3, NRXN3 and HSPA2. Table 1.4 below depicts the function of each of these proteins and their relationship with diabetes (180).

Table 1.4: Proteins associated with the presence of DM from LV derived DEGs.

Name of Protein	Associations with myocardial function	Association with DM
ERBB3	• Impaired LV contractility (measured by both LVEF and GLS) • Higher LV mass • *The above phenotypic changes are evident when ERBB3 is expressed in low quantities (180).*	Lower expression in patients with DM (180).
NRXN3	• *Detected levels too low to draw valid conclusions (180, 181).*	Lower expression in patients with DM (180).
HSPA2	• Impaired LV contractility (measured by both LVEF and GLS) • Higher LV mass • *The above phenotypic changes are evident when HSPA2 is expressed in higher quantities (180).*	Higher expression in patients with DM (180).

Perhaps most importantly, the aforementioned plasma proteins were investigated for their association with future incident HF and cardiovascular mortality. When adjusting for confounding factors, low circulating ERBB3 and high circulating HSPA2 were associated with increased risk of future cardiovascular events (180).

Cherpaz et al, have also explored the myocardial transcriptomic profile of patients with and without T2D in the context of severe AS requiring valve intervention. They proposed that the LV remodelling seen in patients with concomitant T2D and severe AS is associated with mitochondrial calcium signalling alterations. Using LV septum samples taken at the time valve replacement surgery, they discovered downregulation of DEGs related to mitochondrial respiratory chain function, mitochondrial organisation, amino acid metabolism and regulation of muscle contraction in patients with T2D when compared to their counterparts without T2D. In particular, decreased gene expression of CACNA1A, an L-type calcium channel predicted the inhibition of sarco-endoplasmic reticulum calcium ATPase and the calmodulin gene expression. Furthermore, several genes were downregulated for complexes I, III and IV of the respiratory chain and from ATP synthase (182). By contrast, DEGs associated with regulation of inflammation, extracellular matrix organisation, endothelial function and

angiogenesis as well as development of cardiac hypertrophy were upregulated in the T2D patient group, in particular Endothelin-1 (182).

Finally in a paper by Liu et al, exploring the mechanisms of HF in T2D, the use of a gene profiling database to identify protein-protein interaction networks, revealed that the vascular endothelial growth factor (VEGF) and mitogen-activated protein kinase (MAPK) signalling pathways may be responsible for this pathology (183). VEGF in particular has been associated with diabetic microvasculopathy, retinopathy, nephropathy and neuropathy. VEGF is an angiogenic factor with endothelial cell-selective mitogenic activity that is responsible for vasculogenesis. In the disease state of diabetes, it is believed that the mechanisms responsible for disrupting the pathway include hypoxia, and pre-existing endothelial dysfunction which contribute to the formation of new vessels and microaneurysms (184). The MAPK pathway on the other hand is activated by ROS and is also associated with diabetic microvascular complications and myocardial remodelling via the overexpression of TGF-β (185, 186).

This chapter has explored the current literature on diabetes and the heart, exploring the different types of diabetes, its complications and how common cardiac pathologies can be affected by the presence of concomitant diabetes. Also presented above are different methods of investigating diabetic heart disease. However, there remain many gaps in the literature on how diabetes affects the myocardium in health and disease, with many studies not taking advantage of the full repertoire of CMR phenotyping, few using transcriptomics, and none linking the transcriptomics to CMR phenotypes. These gaps suggest the potential

for research to define better biomarkers of diabetic heart disease, which are underpinned by deeper mechanistic understanding.

1.5 Aims and Hypothesis

My hypothesis is that T2D distinctly impacts the myocardium depending on the context provided by factors such as sex or disease. Furthermore, I propose that comprehensive cardiac magnetic resonance, transcriptomics, and their integration, can help to better understand diabetic heart disease and suggest novel biomarkers.

The aims of this study, therefore, are to:

1. Investigate diabetic heart disease across the spectrum of AS using comprehensive CMR assessment.
2. Use myocardium acquired at the time of surgical aortic valve replacement to define transcriptomic features of T2D in the context of aortic stenosis.
3. Integrate CMR phenotypes with myocardial transcriptomics from people undergoing surgical aortic valve replacement to understand the molecular basis of CMR phenotypes.
4. Define the blood transcriptomic profile of people with heart failure versus heart failure with T2D and integrate this with their CMR data to explore if circulating inflammatory cells can inform about advanced diabetic heart disease.
5. Assess for subclinical heart disease using comprehensive CMR imaging in people with apparently uncomplicated T2D and explore whether this differs in men and women.

2. T2D across the spectrum of Aortic Stenosis

2.1 INTRODUCTION

Aortic stenosis (AS) is the most common valvular heart disease in the Western world (187), and hence large numbers of people undergo valve replacement intervention across the world every year. Transcatheter aortic valve replacement (TAVR) is now considered the gold standard for elderly patients globally, whilst less frail and comorbid patients will be offered surgical aortic valve replacement (SAVR) (188, 189). Importantly, there is a large overlap between the phenotype of the remodeled LV in patients with increasing severity of AS and that of patients with T2D. Table 2.1 below highlights the phenotypic appearance of the LV in both T2D and AS when a patient is subject to CMR.

Table 2.1: An overview of myocardial parameters measured at the time of CMR seen in both T2D and AS.

CMR Parameters	Appearance in DM	Appearance in severe AS
LV Mass	Increased; likely due to cardiac steatosis, hypertension and obesity. Increased LV mass to LV end diastolic volume ratio indicates concentric remodelling (129, 190).	Increased LV mass with concentric hypertrophy and remodelling due to pressure overload (191-194).
LV ejection fraction (EF)	There is no direct link between T2D causing a decreased LVEF as such, with the exception of cardiomyopathy which will be discussed in more detail in Chapter 4. However, heart failure in the presence of pre-existing T2D results in a more pronounced decline with time (particularly in the presence of co-existing ischaemia) (195).	As compensatory mechanisms become insufficient, LVEF decreases. Importantly this can decline before stenosis is severe (196, 197).
Left atrial (LA) volume and EF	Increased LA volume and reduced LAEF, associated with rising HbA1c and BMI (198, 199).	The LA dilates and develops fibrosis with reduced LAEF. The degree of dilatation is not correlated with valve stenosis severity (200, 201).
Myocardial T1	T1 values are significantly elevated in the T2D population (compared to age and sex matched healthy controls) and this correlates with the degree of remodelling as measured by the LV mass to volume ratio (202, 203).	T1 values are significantly elevated in patients with AS (compared to age and sex matched healthy controls) and this is associated with adverse clinical outcomes (204-206).
Extracellular volume (ECV)	Coinciding with the increased T1, some T2D studies have reported increased ECV values in T2D cohorts compared to healthy controls (203, 207). However, this finding is not universal and thought to be potentially related to coexisting hypertension or ischemic heart disease.	ECV is elevated in AS and has been shown to correlate with markers of LV decompensation (LV mass, LA volume and increasing breathlessness) and is independently associated with all-cause mortality (208-210).
Stress Perfusion	If there is established coronary artery disease there will be a stress perfusion defect in keeping with the artery affected. However in the absence of the above, patients with T2D are at risk of presenting with microvascular obstruction. Furthermore, there is evidence to suggest that diabetic patients may present with higher global myocardial blood flow (MBF) at rest and lower maximal MBF during vasodilator stress than control patients (211, 212).	Microvascular obstruction as evidenced by low MBF and myocardial perfusion reserve (MPR) is common in aortic stenosis due to the compensatory mechanism of microcirculatory autoregulation inducing vasodilation to minimise microvascular resistance and increase total MBF (213). These abnormalities can however improve, or fully reverse after aortic valve replacement (214, 215).
Late Gadolinium Enhancement (LGE)	T2D patients can present with both ischaemic and non-ischaemic scar.	Non-ischaemic LGE is common in severe AS, mostly in the mid-basal

	Around 10% have the latter, mostly in the basal-lateral or the basal-inferolateral LV.(159) The presence of such non-ischaemic scar is correlated with increased LV mass (216).	segments of the interventricular septum. It is associated with increased LV mass and volume, lower LVEF and global longitudinal strain (GLS). It has also been associated with an increased all-cause mortality (217-219).
Phosphocreatine to adenosine triphosphate ratio (PCr/ATP)	Reduced PCr/ATP (reflecting impaired cardiac energetics) on phosphorus spectroscopy is seen in both skeletal muscle and myocardium in patients with T2D (220-222).	PCr/ATP ratio is reduced in severe aortic stenosis and associated with reduced GLS, higher LV wall thickness and the presence of myocardial fibrosis (223-225).

AS most often represents a slowly progressive degenerative process, characterized by a long asymptomatic subclinical stage that can last for many years or decades (187), for which there is no effective medical therapy capable of slowing disease progression. The degree of valve restriction is currently classified as mild, moderate, and severe by clinical practice guidelines; however, these phenotypes fall within a continuous spectrum and so this categorization is likely to be oversimplistic. AS accounts for substantial global morbidity and premature mortality, even in patients with less than severe AS (226, 227). Epidemiological studies suggest reduced survival rates in patients with moderate AS, with 5-year mortality rates as high as 56%, which is nearly equivalent to severe AS (228, 229). Compared with no AS, the adjusted risk of all-cause mortality was shown to be 1.92-fold higher in moderate AS, and 2.27-fold higher in severe AS (230). However, the mechanisms for this adverse prognosis in moderate AS remain poorly understood.

Emerging evidence suggests that the myocardial remodeling response to AS is critical for the long-term prognosis, with the extent of cardiac damage shown to be linked to worse prognosis, independent of valvular obstruction severity (130, 231). During the asymptomatic period, the heart compensates for the pressure overload with increased wall thickness, which

maintains normal wall stress and contraction (232). However, with time this hypertrophic response decompensates, and patients transition to the development of symptoms, heart failure and adverse events (232). In this situation, the only effective treatment is aortic valve replacement (AVR), either surgically (SAVR) or using a transcatheter approach (TAVR). Indeed, current guidelines recommend AVR in patients with severe AS in the presence of symptoms or evidence of cardiac dysfunction i.e. LVEF <50% on cardiac imaging (187, 233). While not yet proven, it has been hypothesised that myocardial ischemia may be a precursor to fibrosis and therefore potentially linked to LV decompensation in AS. Moreover, in relation to myocardial ischemia, reduced capillary density has been demonstrated in patients with AS undergoing AVR (234). Interestingly, these perfusion defects are reversible early after AVR (234).

Cardiovascular magnetic resonance imaging (CMR) allows for interrogation of each of these myocardial processes, providing the reference standard for the assessment of the myocardial remodeling observed in AS (130). CMR also provides assessment of myocardial fibrosis using LGE and T1 mapping techniques, which provide powerful prognostic information in patients with AS (208, 235). CMR perfusion mapping allows pixel-wise quantification of global perfusion indices at rest and after pharmacological stress, using the indices of myocardial blood flow (MBF) in ml/g/min and myocardial perfusion reserve (MPR) (236). The perfusion dynamics of the epicardial and endocardial layers differ in severe AS, with preferential flow shifting from the endocardium to epicardium, which is probably driven by a relatively less pronounced reduction in MBF in the epicardial layer compared to the endocardial layer (237). Automated in-line myocardial perfusion quantification using CMR also provides a comprehensive assessment of the endocardium and epicardium perfusion (238). Moreover,

^{31}P-MRS allows non-invasive assessment of the myocardial energetic state (239). Using ^{31}P-MRS, multiple studies have shown myocardial energetic compromise as reflected by reductions in myocardial energetics index phosphocreatine to ATP (PCr/ATP) to be an important feature of the metabolic phenotype of the AS.

The cornerstone of routine clinical assessment of valve disease is transthoracic echocardiography. It is non-invasive and portable, cheap and can provide qualitative valve assessment including valve morphology, degree and positioning of calcification and involvement of commissures. Furthermore, its high spatial and temporal resolution can provide a detailed assessment of transvalvular blood flow. Such qualities make it effective for the long term follow-up of patients (240-242). However, there are certain challenges with this technique, including poor echo windows and variability in the quality of images acquired by sonographers and doctors which can impact diagnosis. CMR can overcome such issues. The lack of radiation exposure and the highly accurate and reproducible images obtained make this a desirable option for valve assessment. Furthermore, it can provide an accurate and in-depth assessment of the dimensions and appearance of both ventricles which may impact the diagnosis and management of any valve disease as well as provide detailed information about associated remodeling (including fibrosis and scarring). This cannot be done by other imaging techniques. For the aortic valve in particular, CMR is superior to echo as it can also provide information about the dimensions of the aorta. In the context of AS, however, it must be stated that CMR has inferior spatial and temporal resolution to echocardiography and therefore may underestimate stenosis severity (240-242). In light of this, the majority of patients will have assessments with both imaging modalities throughout their AS journey and follow up.

In the presence of T2D, the risk of developing AS is increased, with some studies reporting as many as 40% of people with diabetes developing aortic valve stenosis (225, 243, 244). Degenerative aortic stenosis is particularly associated with T2D due to the inflammatory processes that are associated with diabetes (as discussed in Chapter 1) (114, 244). In the presence of concomitant diabetes, patients are more likely to progress to severe valve stenosis and are at an increased risk of morbidity and mortality related to their valve disease (114, 225, 243). In a multivariate analysis conducted by Lu et al to investigate adverse outcomes in the presence of valve disease with coexistent T2D, increasing age, current smoking status, worse baseline functional class (as measured by the New York Heart Assessment – NYHA classification) and lower values of haemoglobin, albumin and ejection fraction were associated with death, heart failure hospitalisation and myocardial infarction (118).

To date only a few studies, and of small sample size, assessed and compared myocardial remodeling in patients with moderate and severe AS (245). Furthermore, little is known about the degree and rate of progression in patients with moderate towards severe AS (246-248).

This prospective study aimed to test the hypothesis that patients with moderate AS also exhibit significant myocardial remodeling which may underpin their previously described adverse prognosis compared to the general population, and that this is aggravated by T2D (249, 250). It aimed to use 2 consecutive CMR measurements to determine the changes in myocardial structure, function, perfusion and scarring over 1 year in patients with moderate AS with or without T2D, in comparison to patients with severe AS and healthy controls.

Therefore, using CMR and ^{31}P-MRS, cardiac phenotypic differences between patients with moderate AS and severe AS, in comparison to demographically matched volunteers with normal aortic valve function were assessed prospectively. Subgroup analysis was undertaken for patients with co-existing T2D and volunteers with T2D but no AS.

2.2 METHODS

2.2.1 Study design and oversight

This single-center prospective case-control study complied with the Declaration of Helsinki and was approved by National Research Ethics Committees (ref:18/YH/0168 for the severe AS cohort and ref:18/YH/0168 for the moderate AS cohort and healthy volunteers). The study was funded by the Wellcome Trust (Grant 207726/Z/17/Z), British Heart Foundation (RG/16/1/32092), NIHR Leeds BRC (NIHR203331) and the University of Leeds Erdheim Fellowship award. Our research team has previously reported changes in myocardial energetics and perfusion parameters and LV structure and function in patients with severe AS (30 with and 65 without T2D) before and after AVR, and also reported myocardial recovery differences after AVR between severe AS patients with and without T2D (225). All data presented here are newly collected for the purposes of my PhD and none of the results have been previously published.

2.2.2 Inclusion criteria

Adult patients with severe AS who had been referred for surgical or transcatheter AVR and patients with moderate AS who were under the routine clinical care of the valve clinic at the Leeds Teaching Hospitals NHS Trust were eligible for inclusion. The diagnosis of severe AS was based on peak aortic forward flow velocity of greater than 4m/s at valve clinic echocardiography according to current cardiovascular society guidelines (187, 233). The diagnosis of moderate AS was based on peak aortic velocity of 3.0–3.9m/s or mean gradient of 20–39mmHg and aortic valve area (AVA) >1 and <1.5cm^2 on valve echocardiography on a recent valve clinic assessment (within 1-3 months prior to CMR research visit) (251). Controls were prospectively recruited from adverts posted at regional leisure activity walking groups.

2.2.3 Exclusion criteria

Participants were excluded if they had previous myocardial infarction, coronary artery bypass grafting or angioplasty, chronic obstructive lung disease, more than mild bystander valve disease, significant kidney dysfunction (estimated glomerular filtration rate [eGFR]<30mL/min/1.73m^2), known heart failure or reduced LV ejection fraction (<55%), cardiomyopathy (based on infiltrative diseases [e.g., amyloidosis], accumulation diseases [e.g., haemochromatosis, Fabry disease], or hypertrophic cardiomyopathy), or any contraindication to CMR. As the research protocol included a 6-minute walk test, potential participants with mechanical or permanent mobility issues were excluded. All patients with severe AS were listed for AVR and had flow-limiting CAD excluded by clinically indicated invasive angiography. Controls and patients with moderate AS did not undergo coronary angiography. Prior myocardial infarction was excluded by LGE in all participants.

2.2.4 Study Protocol

Figure 2.1 is a graphical representation of the study protocol that all participants were subjected to. Each aspect of this will be described in turn below.

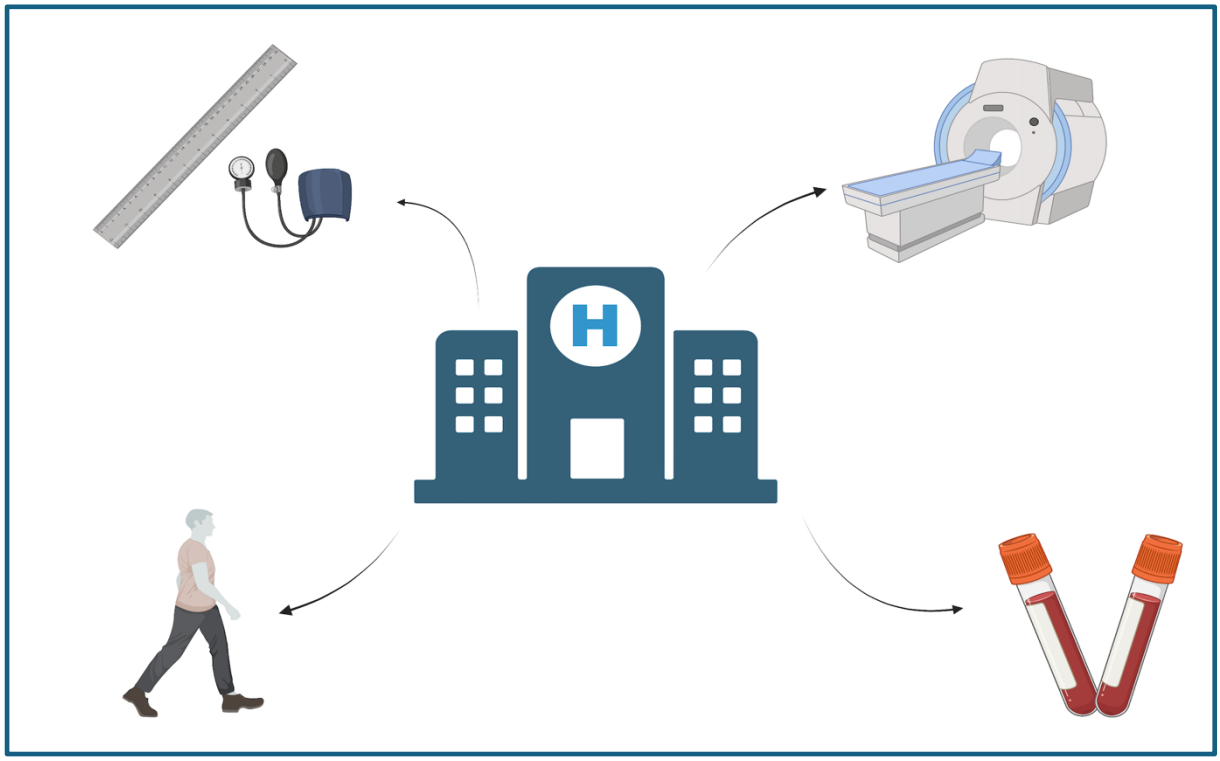

Figure 2.1: A schematic overview of the study protocol.

Anthropometric measurements

Height and weight were recorded, and BMI was calculated. The blood pressure was recorded after being seated for over 10 minutes. A 12-lead electrocardiogram was recorded. A fasting blood sample was taken for assessments of full blood count, eGFR, lipid profile, glycated HbA1c, renal function, glucose, and N-terminal pro B-type natriuretic peptide (NT-proBNP) concentrations.

Six-minute walk test

Functional exercise capacity was assessed using a 6-minute walk test according to established guidelines (252). Participants were instructed to walk along a 30-meter corridor and cover the maximum achievable distance in 6-minutes under the supervision of investigators trained in conducting the test. At the end of 6-minutes, participants were asked to stop, and the distance walked was measured in meters.

Cardiovascular magnetic resonance

All participants were subject to the CMR protocol displayed in Figure 2.2, consisting of phosphorus spectroscopy, cardiac volumes, mass and function, left atrial volumes and function, pre- and post- contrast T1 mapping of the 3 short axis slices of the heart (base, mid and apex), rest and stress adenosine quantitative perfusion and late gadolinium enhancement imaging. All scans were conducted on a Siemens 3 Tesla PRISMA MR system (Erlangen, Germany). The full protocol was completed within an average of 90 minutes which included the patient being removed from the magnet to facilitate a change of coil between the spectroscopy scan and the cardiac scan.

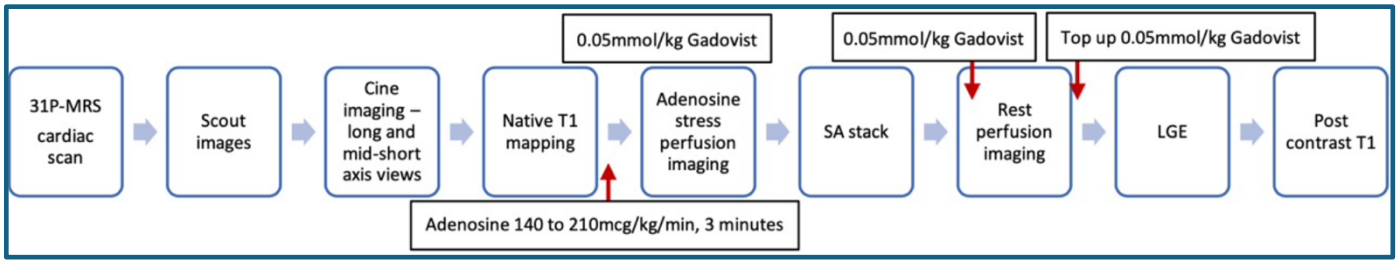

Figure 2.2: Multiparametric cardiac magnetic resonance imaging scan protocol.

^{31}Phosphorus magnetic resonance spectroscopy

CMR and ^{31}P-MRS were performed on a 3.0 Tesla MR system (Prisma, Siemens, Erlangen, Germany). ^{31}P-MRS was performed to assess myocardial PCr/ATP from a mid-ventricular septum voxel selected from a 3D MRS imaging matrix, with patients lying supine and a ^{31}P transmitter/receiver cardiac coil (Rapid Biomedical GmbH, Rimpar, Germany) placed over the heart as previously described (253). ^{31}P-MRS data were acquired with a non-gated 3D acquisition-weighted chemical shift imaging (CSI) sequence (254).

Ventricular volumes, function, mass, and strain rate assessment

CMR assessment provides an accurate and reproducible method for measuring left ventricular volumes and mass (255). Cardiac volumes were acquired using Steady State Free Precession (SSFP) imaging. Pilot, horizontal and vertical long axis, and short axis stack images were acquired with the patient in the supine position. Each slice was 8mm thick with a 3mm gap and was prospectively gated with echo time of 1.5ms; repetition time of 3ms; and flip angle of 50°. The slices were obtained whilst the participants were breath-holding at the end of normal expiration to minimize the effects of respiratory motion.

LV short axis epicardial and endocardial borders were manually contoured from base to apex at end diastole and end systole, to determine the end diastolic volume (EDV); end systolic volume (ESV) and stroke volume (SV) using Cvi42© (Circle Cardiovascular Imaging Inc., Calgary, Canada), as shown in Figure 2.3. Of note the basal slice was defined as the slice of LV in which at least 50% of the blood volume was surrounded by myocardium at end-systole and

end-diastole. By contrast the apical slice was defined as that showing intracavity blood pool at end diastole and end systole.

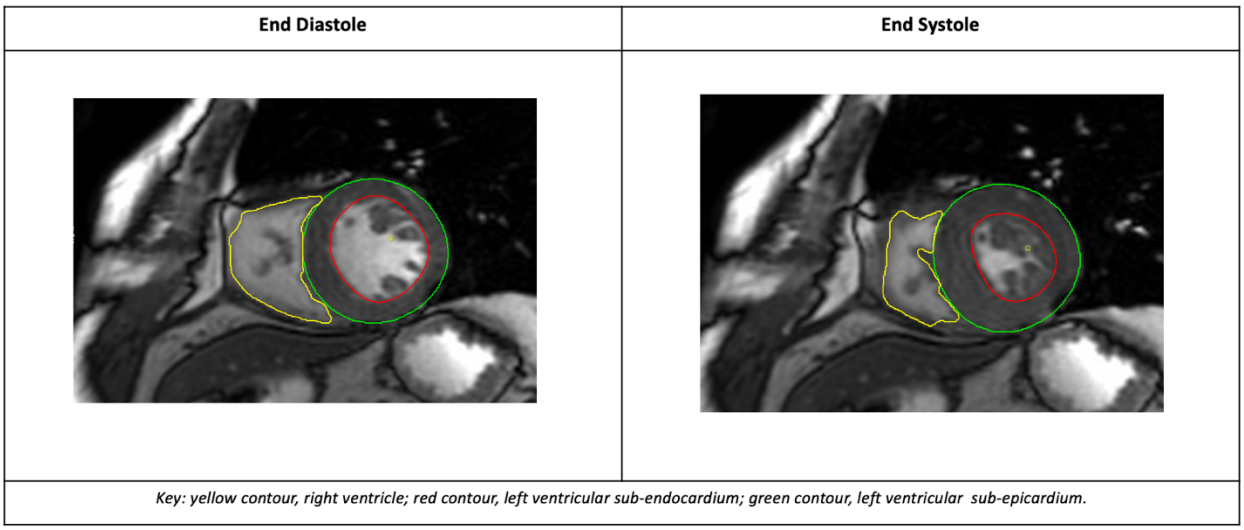

Figure 2.3: Example contouring of 1 slice of the left and right ventricle of a participant's short axis stack showing all contours at end-systole and end-diastole.

Ejection fraction (EF) was calculated using the formula: *EF = SV/EDV* and cardiac output (CO) via formula: *CO=SV x heart rate*. Myocardial mass was calculated by subtracting the endocardial volume from the epicardial volume. Left ventricular mass was calculated based on prior knowledge of myocardial specific gravity (1.05 g/cm^3).

Another method of measuring contractile function is by measuring longitudinal ventricular shortening between end diastole and end systole. Global longitudinal shortening (GLS) has been offered as a percentage ratio to quantify LV contraction; the larger the value acquired, the better the contractile ability (256). Just as with EF, a high GLS is suggestive of normal contractile function, whereas a low value represents contractile dysfunction. Perhaps more importantly, however, GLS has been shown to decline prior to ejection fraction in those

patients that go on to develop heart failure. Furthermore, there is evidence to suggest that GLS can predict prognosis in a range of cardiovascular pathologies in the presence of a normal ejection fraction (256-259). Automated software provided GLS measurements, through the Gadgetron open-source medical imaging reconstruction framework (260). The algorithm uses the 2-, 3- and 4-chamber cine images recognizing the anatomical landmarks of the anterior and inferior points, inferolateral and anteroseptal points and inferoseptal and anterolateral mitral annular hinge points respectively. Detection is performed for every cine phase covering the entire cardiac cycle. The GLS value is calculated using the following equation: GLS= 100 x [(LV EDV length – LV ESV length)/LV EDV length)] (256). An example of the automated analysis can be seen in Figure 2.4.

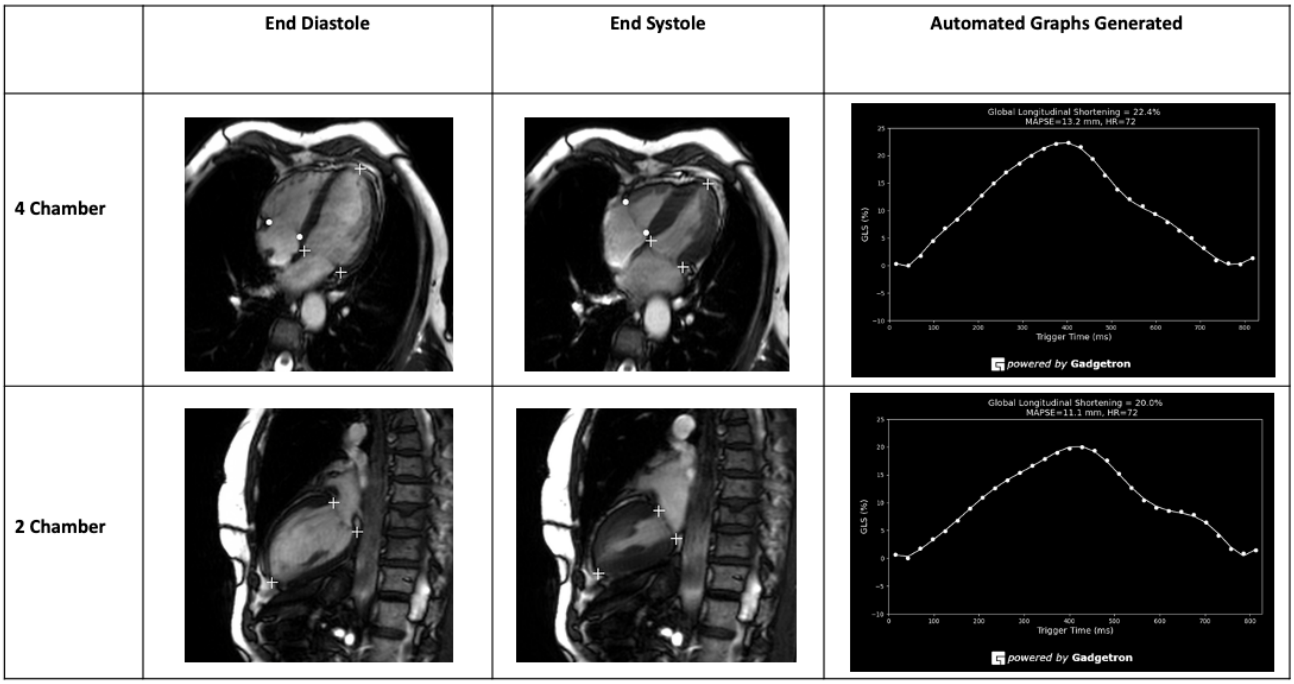

Figure 2.4: Example of automated GLS analysis.

LV Maximal Wall thickness

After completion of all contours at end diastole of the LV, a manual measurement of the maximal LV wall thickness was made from the edge of the sub-epicardial border to that of the sub-endocardial border in the septal wall across all LV slices. The largest measurement was recorded as the LV maximal wall thickness.

LV Diastolic function

Defining the ratio of the early diastolic (E) peak velocity to the atrial contraction (A) peak velocity – E/A ratio can be used as an indirect measure of LV diastolic function. Early diastolic peak velocity corresponds to early (rapid) filling of the LV, whereas the atrial contraction peak velocity represents atrial systole at LV end diastole. To calculate the E/A ratio the flow analysis module in Cvi42© (Circle Cardiovascular Imaging Inc., Calgary, Canada) was used. A contour was drawn around the mitral valve in the short axis cine view and this was propagated through the velocity – encoded phase contrast view. The software then created a mitral inflow velocity time curve (as shown in Figure 2.5) and the E wave and A wave were discerned by the reader (myself).

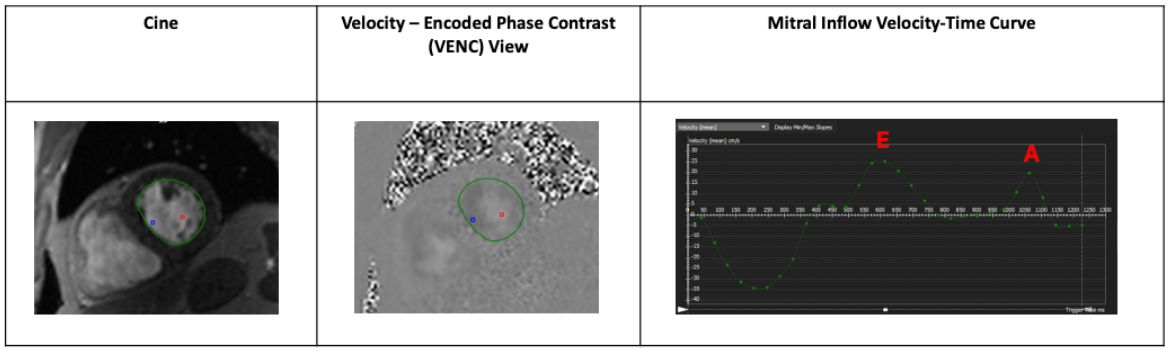

Figure 2.5: Example of diastolic function calculation

Left atrial volumes and function

The LAEF was calculated using the biplane area-length method in the horizontal and vertical long axes. The LA endocardial border was manually contoured in both the horizontal and vertical long axes views, as shown in Figure 2.6, with the mitral annulus serving as the division between the LA and LV. The maximum LA area was defined as the phase with the largest LA dimension and contoured in the frame immediately prior to mitral valve opening. The minimum LA area was defined as the phase with the smallest LA dimension and contoured in the frame immediately after mitral valve closure. Importantly, the LA appendage was included in LA volume whereas the pulmonary veins were excluded at their ostia. LAEF was derived via: *LAEF = [(LA EDV – LA ESV)/LA EDV] x 100*.

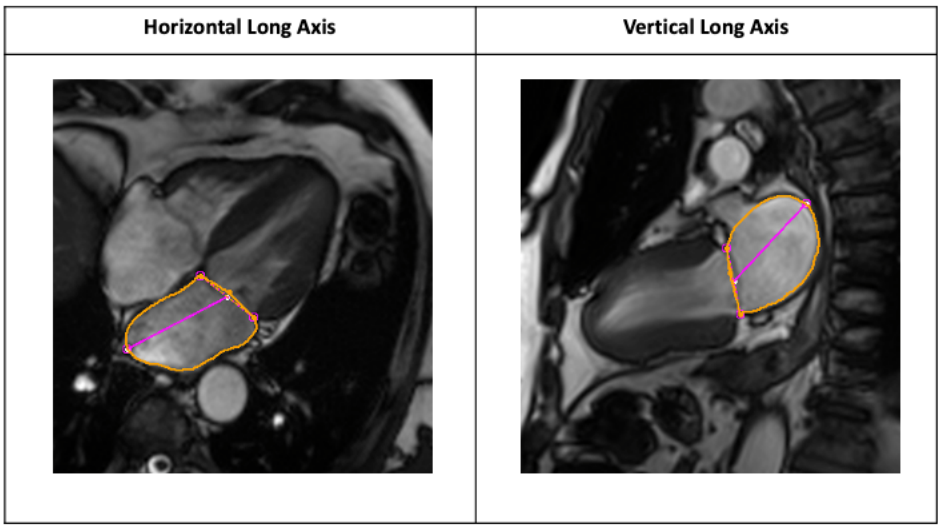

Figure 2.6: Bi-plane left atrial endocardial contours in the horizontal and vertical long axis views.

T1 mapping

Native T1 maps were acquired in 3 short-axis slices, using a breath-held modified look-locker inversion recovery acquisition, with the following parameters: ECG triggered 5s (3s;single shot, SENSE factor 3; pre-pulse delay 350ms, trigger delay set for end diastole, echo time (TE)/

repetition time (TR)= 1.09/774ms, flip angle 20^{o}, acquisition matrix 380x380mm, slice thickness 8mm, giving a re-constructed voxel size of 1.5x1.5x8mm). Shimming and centre frequency adjustments were performed as necessary to generate images free from off resonance artefacts. Post-contrast T1 mapping was performed using the same approach 15 minutes after the last contrast injection.

Adenosine Stress Perfusion

Perfusion imaging used free-breathing, fast low angle shot (FLASH) magnetic resonance protocol with motion-corrected (MOCO) automated in-line perfusion mapping using the Gadgetron streaming software image reconstruction framework as previously described (236). Adenosine was infused at a rate of 140µg/kg/min, with the option of increasing it to a maximum of 210 µg/kg/min for a minimum of 3 minutes according to hemodynamic and symptomatic response. A significant hemodynamic response was defined as an increase of heart rate >10 beats/min, or a blood pressure drop <10 mm Hg and >1 adenosine-related symptom, (e.g., chest tightness, breathlessness) (261). Adenosine stress was well tolerated by all study participants. A minimum 10-minute interval was kept between perfusion acquisitions to ensure equilibration of gadolinium kinetics and resolution of all hemodynamic effects of adenosine. For each perfusion acquisition, an intravenous bolus of 0.05mmol/kg gadobutrol (Gadovist, Leverkusen, Germany) was administered at 5ml/s followed by a 20ml saline flush using an automated injection pump (Medrad MRXperion Injection System, Bayer).

Late gadolinium enhancement

LGE imaging was performed with a top-up bolus of 0.06 mmol/kg of body weight of the gadolinium-based contrast agent gadobutrol (Gadovist, Leverkusen, Germany). This was

administered at 5ml/s followed by a 20ml saline flush, given through an intravenous cannula in the anti-cubital fossa, using an automated injection pump (Medrad MRXperion Injection System, Bayer). The scan parameters for these sequences were: slice thickness 8 mm, flip angle 20°, Repetition time/ Echo time =3ms/7.5ms. The LGE phase-sensitive inversion recovery sequences were performed, a minimum of 8 minutes after contrast administration.

Quantitative analysis of ^{31}P-MRS and CMR data

All ^{31}P-MRS and CMR post-processing analyses (with the exception of perfusion mapping, and global longitudinal shortening [GLS] data) were performed offline by myself.

The 31P-MRS was performed offline by using software within the MATLAB version R2021a (MathWorks) as previously described (253). Analysis was performed on two consecutive mid left ventricular slices in the short axis orientation and the average saturation and blood corrected PCr/ATP was reported. Of note, reproducibility testing was completed on a group of 15 patients with inter-observer variability measuring at <5% (between myself and members of the wider research team).

Cvi42© (Circle cardiovascular imaging, Calgary, Canada) was used to perform CMR analysis. The images for biventricular and atrial volumes, biventricular and atrial function, as well LV maximal wall thickness were analyzed as described above· Similarly, the automated software which provided GLS measurements has also been described above.

Perfusion mapping used artificial intelligence (Gadgetron Framework) for instant quantification of perfusion indices in addition to rest and stress MBF and myocardial

perfusion reserve (MPR). Segmental layer-specific perfusion metrics (subendocardial [Endo], subepicardial [Epi] MBF and MPR, and Endo to Epi MBF ratio [Endo/Epi]) values were automatically obtained as an average of all pixel values of each of the 16 segments (262). The 16 segments were further sub-divided transmurally to create endocardial and epicardial segments with corresponding rest and adenosine-stress MBF values and ratios to reflect transmural gradient. Global endocardial:epicardial (Endo/Epi) ratio was calculated by averaging the ratio across the 3 slices.

T1 mapping analysis was performed from a manually contoured region of interest in the mid-wall of the septum using the native pre-contrast and native post-contrast T1 times of myocardium, blood pool and hematocrit from basal and mid short axis T1 maps using Cvi42© (Circle cardiovascular imaging, Calgary, Canada). The average T1 value of the two slices was then calculated, as shown in Figure 2.7. The ECV was then defined as $ECV = (1-Hct) \times [\Delta R1myocardium]/[\Delta R1blood]$, based on the patient's haematocrit from the blood tests taken on the study visit. The partial voluming of blood was minimised by keeping the contours within the myocardial layers. Regions with a non-infarct LGE were excluded from ECV analysis.

	Basal LV Slice	Mid LV Slice	Value To Use
Pre-contrast T1 map	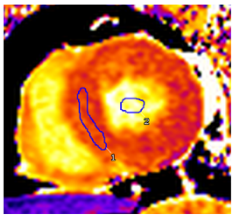	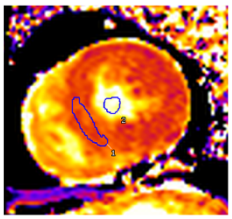	**Myocardium** = (contour 1 from basal slice + contour 1 from mid slice)/2 **Blood pool** = (contour 2 from basal slice + contour 2 from mid slice)/2
Post-contrast T1 map	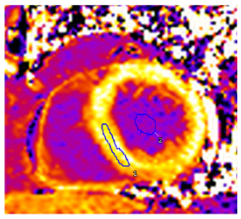	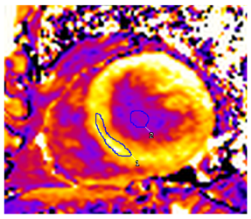	**Myocardium** = (contour 1 from basal slice + contour 1 from mid slice)/2 **Blood pool** = (contour 2 from basal slice + contour 2 from mid slice)/2

Figure 2.7: Method for pre and post contrast average myocardial and blood pool calculations for T1 mapping assessment.

The LGE pattern was first defined visually. The presence of non-ischemic LGE was considered present if seen in both long- and short-axis planes, in 2 phase-encoding directions, and extending beyond the localized ventricular insertion areas. The location was classified as septal, RV insertion point, LV free-wall, or as occurring in multiple locations, examples can be seen in Figure 2.8. The pattern was classified as linear mid-wall, sub-epicardial, focal, or as occurring in multiple patterns. Any participants with an infarct pattern of LGE were excluded to focus on non-ischaemic myocardial disease.

Location of LGE			
No LGE	**RV Insertion Point**	**Septal Wall**	**Lateral Wall**
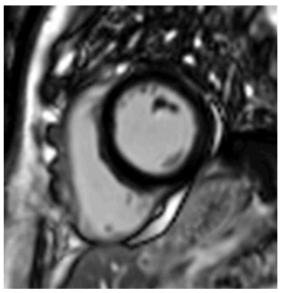	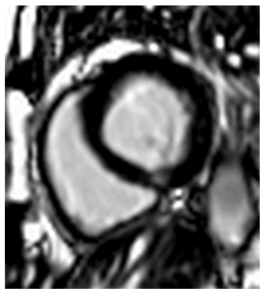	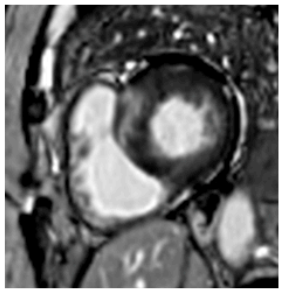	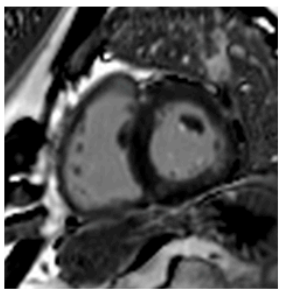

Figure 2.8: Different patterns of LGE seen in study participants

Quantification of LGE extent was performed in the short-axis slices by manually drawing endocardial and epicardial borders and selecting a region of interest in the remote healthy myocardium using the Cvi42 tissue characterization software (Cvi42© - Circle cardiovascular imaging, Calgary, Canada). Mean signal intensity and SD of the region of interest were then measured, and enhanced myocardium was defined as myocardium with a signal intensity ≥5 SDs above the mean of the region of interest. The extent of LGE was expressed as a percentage of the LV mass. Right ventricular (RV) insertion point LGE was not included in the quantitative analysis.

2.2.5 Sample size

Priori sample size calculations were performed based on pilot data (one for LV concentricity index: relative ratio of LV mass to LV EDV and another for the quantification of vasodilator-stress MBF) obtained from patients with moderate AS data (n=5) and healthy controls (n=15). These pilot study assessments showed mean LV mass to LVEDV ratio of 0.86±0.19 in patients

with moderate AS versus 0.70±0.20 in controls. Based on these pilot data for the two groups, a minimum of 18 patients were needed to be recruited per group to detect a difference in LV mass to LVEDV ratio between patients with moderate AS and controls with 80% power at a 5% significance level on a two-sided t-test (calculations were performed on ClinCalc.com software (263)). A second sample size calculation was performed for comparisons of vasodilator-stress MBF between the two groups (Moderate-AS:1.74±0.24 versus controls:2.11±0.25ml/min/g). Based on these pilot data for the two groups, a minimum of 18 patients needed to be recruited (9 per group) to detect a significant difference in vasodilator-stress MBF between patients with moderate AS with and controls with 90% power at a 5% significance level on a two-sample t-test (calculations performed on ClinCalc.com software (263)). These targets were achieved in this study. In addition to these pre-specified comparisons, other exploratory analyses were also performed but without power calculations due to their exploratory nature.

2.2.6 Statistical analysis

Statistical analysis was performed using GraphPad Prism software (version 10.0.3). All data were checked for normality using the D'Agostino-Pearson Test. Data are presented as mean ±95% confidence intervals when normally distributed, or median with interquartile range (IQR) for nonparametric continuous data. Categorical data are presented as numbers and percentages and compared using the Pearson χ^2 test. All comparisons between >2 groups were performed by 1-way ANOVA, or Kruskal-Wallis tests for nonparametric data, with post hoc Bonferroni corrections. Student's t-test, or Mann-Whitney U test for non-parametric data, were used when comparing 2 groups. Bivariate correlations were performed using

Pearson's or Spearman's method, as appropriate. A 2-sided *P* value of <0.05 was applied as indicating threshold of significance.

2.3 RESULTS

2.3.1 Participant demographics and clinical characteristics

Fifty-two patients with severe symptomatic AS awaiting AVR (18 with T2D), 25 patients with moderate AS under routine clinical monitoring (10 with T2D), and 23 controls with no valvular dysfunction or any other cardiovascular disease (5 with T2D), were prospectively recruited between September 2022 and October 2023, Figure 2.9.

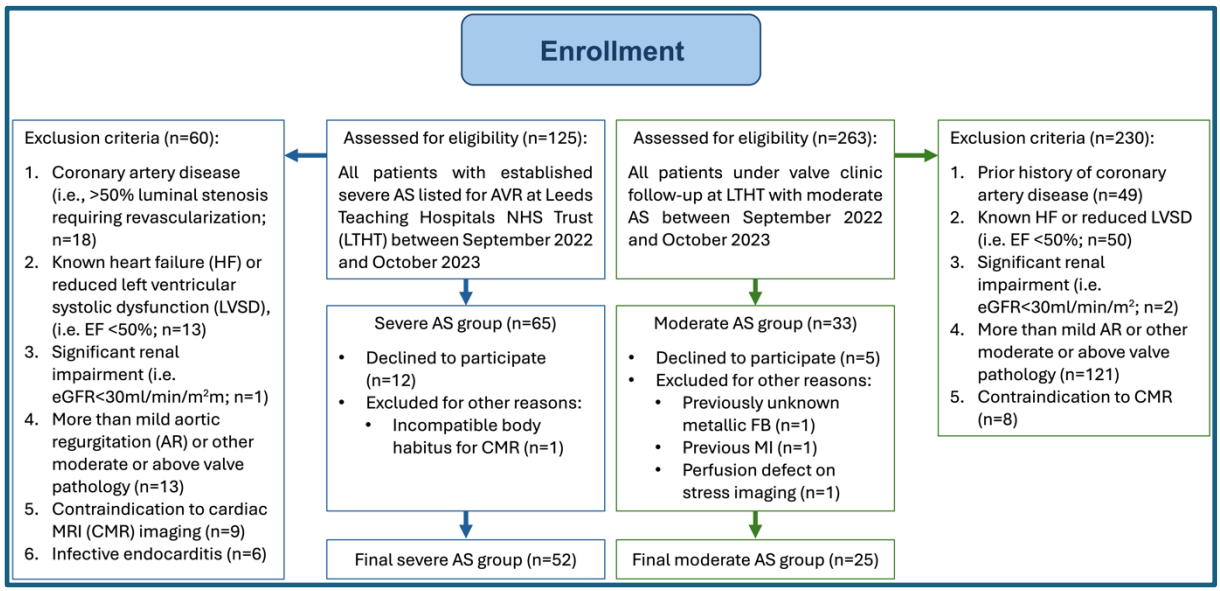

Figure 2.9: CONSORT diagram for patient recruitment into the study.

There were no significant differences in sex distributions or T2D prevalence across all study groups. The Moderate-AS and control groups were matched with respect to age; however, the Severe-AS group were older, Table 2.2. Patients with severe-AS were more symptomatic with 90% of the group classified NYHA Class II to IV (Table 2.2).

The 3 groups were matched for blood pressure, fasting glucose and HbA1c; but the resting heart rate was higher, and the haemoglobin was lower in the severe AS group (Table 2.2). Patients with Severe-AS had significantly higher NTproBNP levels than the Moderate-AS and the control groups (controls: 88 [61, 160], Moderate-AS: 124 [72, 218], Severe-AS: 499 [216, 1260]; P<0.0001). Despite the numerical difference in the NTproBNP between moderate and control groups, this was not statistically significant.

Table 2.2: Clinical characteristics, biochemistry and past medical history of all study group participants.

Variable	Controls n= 23	Moderate-AS n= 25	Severe-AS n= 52	P value
Age, y	66 (63,70)	68 (63, 72)	73 (70, 76)	**0.0273***
Female, n (%)	11 (48)	10 (42)	18 (35)	0.5395
BMI, kg/m²	25(24, 27)	30(28, 32)	30(28, 31)	**0.0019€***
Heart rate, bpm	60 (56, 64)	66 (61,71)	69 (66,73)	**0.0093***
Systolic BP, mmHg	131 (124, 138)	136 (129, 142)	134 (129, 140)	0.6469
Diastolic BP, mmHg	78 (75, 80)	76 (71, 80)	74 (71, 77)	0.4173
Creatinine, umol/L	68 (63, 73)	79 (71, 86)	81 (75, 86)	**0.0181***
Haemoglobin, g/L	144 (138, 150)	145 (141,149)	137 (133, 141)	**0.0213†**
TG, mmol/L	1.4 (1.1, 1.6)	2.0 (1.6, 2.5)	1.6 (1.3, 1.9)	0.0527
HbA1c, mmol/mol	40 (37, 44)	44 (40, 48)	42 (40, 45)	0.3596
Glucose, mmol/L	5.7 (4.9, 6.5)	6.5 (5.4, 7.5)	6.0 (5.6, 6.4)	0.3742
NT- proBNP, ng/L	88 [61, 160]	124 [72, 218]	499 [216, 1260]	**<0.0001***
Medications				
ACEi	1(4)	9(38)	10(19)	**0.0177**
ARB	1(4)	1(4)	12(23)	**0.0246**
Beta blocker	-	3(13)	17(33)	**0.0017**
CCB	2(9)	8(33)	12(23)	0.1242
Loop diuretic	1(4)	1(4)	8(15)	0.2079
Statin	5(22)	19(79)	36(69)	**<0.0001**
Antiplatelets	-	10(42)	21(40)	0.0011
DOAC	-	-	6(12)	0.0014
Metformin	4(17)	5(21)	12(23)	0.8559
Sulfonylurea	-	2(8)	5(10)	0.3134
GLP-1RA	-	-	1(2)	0.4941
SGLT2i	-	3(13)	1(2)	0.0549
AS Clinical Details				
TTE Vmax, m/s	-	3.3(3.2, 3.5)	4.6(4.4, 4.7)	**<0.0001†**
Bicuspid AV, n (%)	-	6 (25)	15 (29)	0.0650
NYHA Class, (%)				
I	23 (100)	22 (88)	5 (10)	**<0.0001**
II	-	3 (12)	30 (58)	**<0.0001**
III	-	-	16 (31)	**0.0004**
IV	-	-	1 (1)	-
6 min walk test, m	525[495, 555]	420[375, 465]	345[248, 420]	**<0.0001€***
Cardiovascular Past Medical History				
T2D, n (%)	5 (22)	9 (36)	19 (37)	0.4241
Stroke TIA, n (%)	-	2 (8)	6 (12)	0.2423
PAF, n (%)	-	-	6 (12)	0.0829
Hyperlipidemia, n (%)	5(22)	17 (71)	35 (67)	**0.0004**
STS Surgical Risk Score (%)	-	1.14 [0.8, 1.95]	1.31[0.80,2.72]	0.3547

*€ signifies p<0.05 between controls and Moderate -AS group, * signifies p<0.05 between controls and Severe-AS group, † signifies p≤0.05 between Moderate-AS and Severe -AS.*

Normally distributed continuous variables are expressed as mean (±95% confidence intervals); nonparametric continuous variables are expressed as median [IQR]; and categorical variables are expressed as counts (percent). P signifies p value for comparisons across the groups with ANOVA for normally distributed datasets and Kruskal-Wallis test for non-parametric tests.

AS, indicates aortic stenosis; BMI, body mass index; TG, triglycerides; HbA1c, glycemic hemoglobin; NT-proBNP, N-terminal-pro hormone b-type natriuretic peptide; ACEI, angiotensin converting enzyme inhibitor; ARB, angiotensin receptor blocker; CCB, calcium channel blocker; DOAC, direct oral anticoagulant; GLP-1RA, glucagon-like peptide-1 receptor agonist; SGLT2i, sodium glucose co-transporter-2 inhibitor; TTE, trans-thoracic echocardiogram; V max, peak aortic forward flow velocity; AV indicates aortic valve; T2D, type 2 diabetes; TIA, transient ischemic attack; PAF, paroxysmal atrial fibrillation; STS, society of thoracic surgeons.
y, indicates years; n, number; kg, kilograms; m2, meters squared; bpm, beats per minute; mmHg, millimeters of mercury; umol/L, micromoles per liter; g/L, grams per liter; mmol/L, *millimoles per liter; mmol/mol, millimoles per mole; ng/L, nanograms per liter; m/s, meters per second; m, meters.*

2.3.2 Cardiovascular magnetic resonance and ^{31}Phosphorus-magnetic resonance spectroscopy findings

Cardiac remodeling Moderate vs Severe-AS

Compared to controls, both AS groups showed LV concentric remodeling with a stepwise increase from the moderate to severe AS groups in the LV mass-index (controls: 46 [40, 51], Moderate-AS: 58 [51, 65], Severe-AS: 70 [65, 75]g/m^2; *P*<0.0001) and LV concentricity index (controls: 0.58 [0.54, 0.62], Moderate-AS: 0.74 [0.64, 0.84], Severe-AS: 0.89 [0.83, 0.95]g/mL; *P*<0.0001) with significant differences also between the Moderate-AS and Severe-AS (Figure 2.10).

Consistent with the recruitment criteria, LV ejection fraction was normal in all patients with moderate and severe AS (Table 2.3Table 2.5: CMR and 31P-MRS findings of the moderate-AS groups and healthy controls at baseline.). However, Severe-AS patients showed significantly impaired GLS (controls: 19.9 [17.6, 22.2], Moderate-AS: 17.7 [16.6, 18.8], Severe-AS: 13.4 [12.5, 14.4]%; *P*<0.0001;) and left atrial function compared to both the Moderate-AS group and the controls (Table 2.3). GLS was also significantly reduced in the Moderate-AS patients compared to controls (Figure 2.10).

Table 2.3: CMR and 31P-MRS findings of all groups

CMR Variable	Controls n= 23	Moderate-AS n= 25	Severe-AS n= 52	P value
LV end-diastolic volume indexed to BSA, mL/m²	79 (72, 85)	73 (65, 80)	79 (74, 84)	0.3283
LV end-systolic volume indexed to BSA, ml/m²	30 (27, 33)	28 (23, 33)	29 (26, 31)	0.7922
LV mass, g	87 (74, 100)	103 (86, 120)	133 (121, 145)	**<0.0001** *†
LV mass indexed to BSA, g/m²	46 (40, 51)	58 (51, 65)	70 (65, 75)	**<0.0001**€ *†
LV mass to LV end-diastolic volume, g/mL	0.58 (0.54, 0.62)	0.74 (0.64, 0.84)	0.89 (0.83, 0.95)	**<0.0001**€ *†
LV stroke volume indexed to BSA, ml/m²	49 (44, 53)	45 (40, 50)	48 (46, 51)	0.3637
LV ejection fraction, %	62 (60, 64)	65 (63, 66)	63 (61, 66)	0.3958
LV maximal wall thickness, mm	9.9 (9.2, 10.5)	12.3 (11.2, 13.3)	14.8 (14.1, 15.5)	**<0.0001**€ *†
LA biplane end-diastolic volumes, mL	73 (63, 83)	68 (55, 80)	88 (78, 97)	**0.0170**†
LA biplane end-systolic volumes, mL	34 (27, 42)	35 (25, 44)	58 (48, 67)	**0.0008***†
Biplane LA EF, %	57 (52, 63)	59 (52, 66)	40 (35, 44)	**<0.0001***†
GLS, %	19.9 (17.6, 22.2)	17.7 (16.6, 18.8)	13.4 (12.5, 14.4)	**<0.0001***†
Native T1, ms	1262 (1242, 1282)	1309 (1280, 1339)	1333 (1317, 1348)	**<0.0001**€ *
Native Blood Pool, ms	1891 (1856, 1925)	1873 (1831, 1915)	1947 (1919, 1975)	**0.0043**†
Extra cellular volume fraction, %	0.21 (0.20, 0.23)	0.22 (0.21, 0.26)	0.24 (0.23, 0.25)	0.1971
LGE, %	0.0 [0, 0]	0.0 [0, 4.8]	2.9 [0, 6.2)	**0.0006** *
PCr/ATP	2.2 (2.0, 2.3)	1.8 (1.6, 2.0)	1.7 (1.6, 1.8)	**<0.0001€***
Stress MBF, ml/min/g	2.1 (1.9, 2.3)	1.9 (1.6, 2.2)	1.3 (1.2, 1.5)	**<0.0001*†**
Endo MBF Stress, ml/min/g	2.0 (1.8, 2.3)	1.7 (1.5, 2.0)	1.2 (1.1, 1.3)	**<0.0001**€ *†
Epi MBF Stress, ml/min/g	2.1 (1.8, 2.3)	2.0 (1.7, 2.3)	1.5 (1.4, 1.6)	**<0.0001*†**
Endo/Epi MBF Stress Ratio	1.00 (0.93, 1.07)	0.87 (0.80, 0.94)	0.81 (0.75, 0.82)	**<0.0001**€ *†
Rest MBF, ml/min/g	0.6 [0.6, 0.7]	0.6 [0.6, 0.8]	0.7 [0.6, 0.8]	0.1673
Endo/Epi MBF Rest ratio	1.12 (1.10, 1.14)	1.06 (1.03, 1.09)	1.03(1.02, 1.06)	**<0.0001€***
MPR	3.3 (2.8, 3.6)	2.8 (2.4, 3.2)	1.9 (1.8, 2.1)	**<0.0001***†
Endo MPR	3.2 (2.7, 3.6)	2.5 (2.1, 2.9)	1.7 (1.5, 1.8)	**<0.0001**€ *†
Epi MPR	3.6 (3.1, 4.0)	3.0 (2.6, 3.4)	2.2 (2.0, 2.4)	**<0.0001**€ *†
Rest RPP	7884 (7223, 8545)	8853 (8069, 9638)	9128 (8416, 9840)	0.0803
Stress RPP	11233 (9465, 13001)	11181 (9999, 12363)	10095 (9475, 10714)	0.1677
Increase in RPP, %	28 (21, 34)	27 (19, 35)	24 (18, 29)	0.2211

*€ signifies p<0.05 between controls and Moderate-AS group, * signifies p<0.05 between controls and Severe-AS group, † signifies p≤0.05 between Moderate-AS and Severe -AS.*

Normally distributed continuous variables are expressed as mean (±95% confidence intervals); nonparametric continuous variables are expressed as median [IQR]; and categorical variables are expressed as counts (percent). P signifies p value for comparisons across the groups with ANOVA for normally distributed datasets and Kruskal-Wallis test for non-parametric tests.

LV indicates left ventricle; BSA, body surface area; SV, stroke volume; RV, right ventricle; LA EF, left atrial ejection fraction; GLS, global longitudinal shortening; LGE, late gadolinium enhancement; PCr/ATP ratio phosphocreatine to adenosine tri-phosphate ratio; Endo, endocardial; MBF, myocardial blood flow; Epi, epicardial; MPR, myocardial perfusion reserve; RPP, rate pressure product.
Ml/m², indicates milliliters per square meter; g, grams; g/m2, grams per square meter; g/ml, grams per milliliter; mm, millimeter; mL,milliliter; ms, millisecond; mil/min/g, milliliters per minute per gram.

The native T1 was higher in both AS groups compared to controls, with significant differences also between the Moderate-AS and Severe-AS (controls: 1262 [1242, 1282], Moderate-AS: 1309 [1280, 1339], Severe-AS: 1333 [1317, 1348]ms; *P*<0.0001; Figure 2.10). Patients with Severe-AS had higher ECV than the Moderate-AS and the control groups (controls: 0.21[0.20, 0.23], Moderate-AS: 0.22[0.21, 0.26], Severe-AS: 0.24[0.23, 0.25]%, *P*=0.006). There was significant correlation between global T1 and MPR; global MPR (r=-0.24, P=0.026), endo MPR (r=-0.26, P=0.016) and epi MPR (r=-0.27, P=0.015). There were no correlations with ECV and perfusion or energetics.

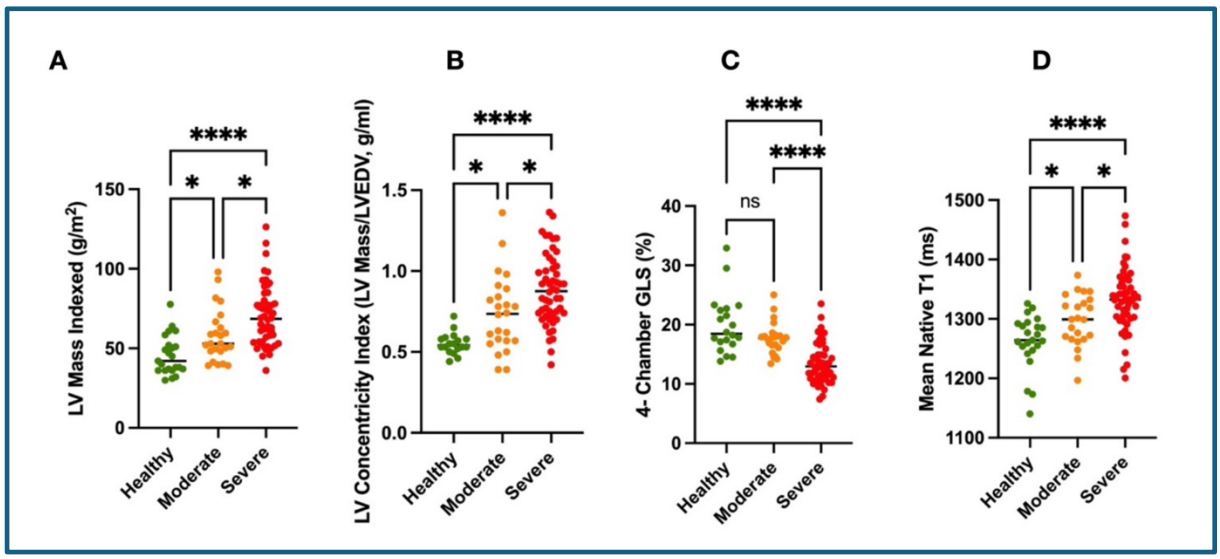

*Figure 2.10: Column scatter graphs with means showing differences in (A) Left ventricular (LV) mass indexed to the body surface area (g/m2), (B) LV concentricity index (LV mass over LV end-diastolic volume ratio, g/ml), (C) Global longitudinal shortening (%), (D) Mean native T1 (milliseconds) between the patients with moderate AS, severe AS and controls. Asterisks represent varying levels of significance with: * p ≤ 0.05 and **** p≤0.0001*

Non-infarct pattern myocardial scarring was detected using LGE in 65% (n=34) of patients with severe AS with a calculated median scar area of 2.9 [0, 6.2]%. This did not include signal related to isolated RV insertion point hyperenhancement, as this is considered a normal variant (264-266). No patients had subendocardial infarct pattern LGE requiring their exclusion. RV insertion point hyperenhancement was noted in 25 severe-AS patients, 6 moderate-AS patients and 2 controls. All other LGE was noted in the mid-wall of the LV, most

commonly in the lateral wall (37% severe-AS, 12% Moderate-AS, 9% HVs), followed by the septal (31% severe-AS, 20% Moderate-AS, 0% HVs), inferior (31% severe-AS, 20% Moderate-AS, 0% HVs), inferolateral wall (31% severe-AS, 8% Moderate-AS, 4% HVs) and the anterior wall (6% severe-AS, 0% Moderate-AS, 0% HVs).

The AS severity (peak aortic valve velocity [Vmax]) correlated with the LV-mass (r=0.42, *P*=0.0005) and GLS (r=-0.47, *P*=0.0001) as shown in Figure 2.11.

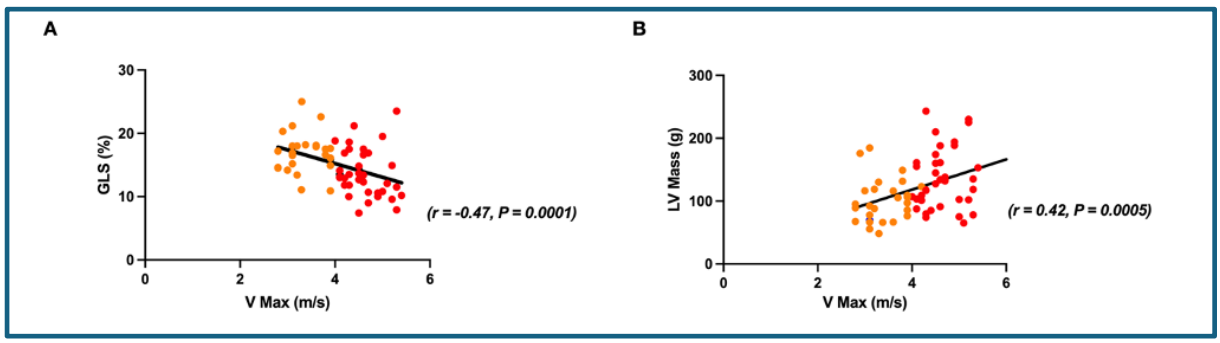

Figure 2.11: Scatterplots showing the correlations of the peak aortic valve velocity (Vmax, m/s) severity of aortic stenosis with: (A) Global longitudinal shortening (GLS, %), (B) Left ventricular mass (LV Mass, g). Orange dots represent patients with moderate AS and red dots represent patients with severe AS. P signifies p value for comparisons between each of the variables when measured against peak aortic valve velocity. The r value represents correlation coefficient as measured by linear regression analysis.

Cardiac energetics and perfusion and function, Moderate vs Severe AS

Compared to controls, both AS groups showed significantly lower myocardial PCr/ATP (controls: 2.2 [2.0, 2.5], Moderate-AS: 1.8 [1.6, 2.0], Severe-AS: 1.7 [1.6, 1.8]; *P*<0.0001) with no significant difference between the moderate and severe AS group (Figure 2.12). There was a negative correlation between the PCr/ATP and the LV mass (r=-0.30, *P*=0.008), but not LV mass-index.

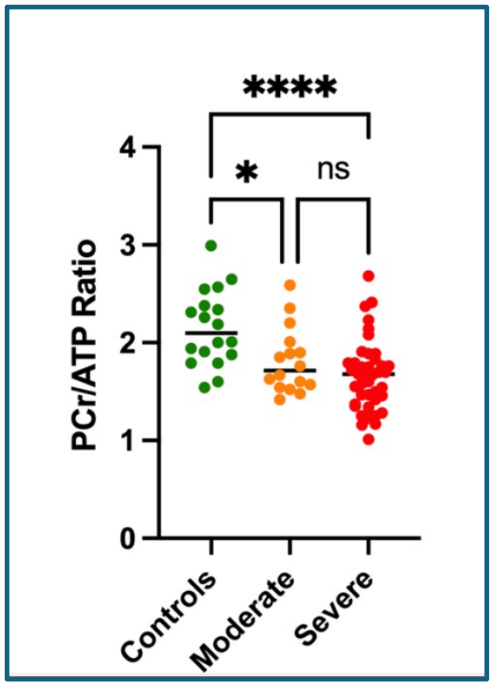

*Figure 2.12: Column scatter graphs with means and 95% confidence intervals showing differences in myocardial phosphocreatine to adenosine triphosphate ratio (PCr/ATP) between the patients with moderate aortic stenosis (AS), severe AS and controls. Asterisks represent varying levels of significance with: * $p \leq 0.05$ and **** $p \leq 0.0001$*

Relative to controls, only the Severe-AS group showed significant reductions in global adenosine-stress MBF (controls: 2.1 [1.9, 2.3], Moderate-AS: 1.9 [1.6, 2.2], Severe-AS: 1.3 [1.2, 1.5]ml/min/g; *P*<0.0001) and global MPR (controls: 3.3 [2.8, 3.6], Moderate-AS: 2.8 [2.4, 3.2], Severe-AS: 1.9 [1.8, 2.1]; *P*<0.0001), as shown in Figure 2.13. However, adenosine-stress Endo-MBF (controls: 2.0 [1.8, 2.3], Moderate-AS: 1.7 [1.5, 2.0], Severe-AS: 1.2 [1.1, 1.3]ml/min/g; *P*<0.0001), adenosine-stress Endo/Epi ratio (controls: 1.00[0.93,1.07], Moderate-AS: 0.87 [0.80, 0.94], Severe-AS: 0.81 [0.75, 0.82]; *P*<0.0001), Epi-MPR (controls: 3.6 [3.1, 4.0], Moderate-AS: 3.0 [2.6, 3.4], Severe-AS: 2.2 [2.0, 2.4]; *P*<0.0001), Endo-MPR (controls: 3.2 [2.7, 3.6], Moderate-AS: 2.5 [2.1, 2.9], Severe-AS: 1.7 [1.5, 1.8]; *P*<0.0001) and rest-Endo/Epi (controls: 1.12 [1.10, 1.14], Moderate-AS: 1.06 [1.03, 1.09], Severe-AS: 1.03 [1.02, 1.06]; *P*<0.0001) were all significantly reduced in both Moderate-AS and Severe-AS (Figure 2.13). While Epi-MBF was not significantly reduced in Moderate-AS,

this was significantly reduced in Severe-AS (controls: 2.1 [1.8, 2.3], Moderate-AS: 2.0 [1.7, 2.3], Severe-AS: 1.5 [1.4, 1.6]ml/min/g; P<0.0001, Figure 2.13).

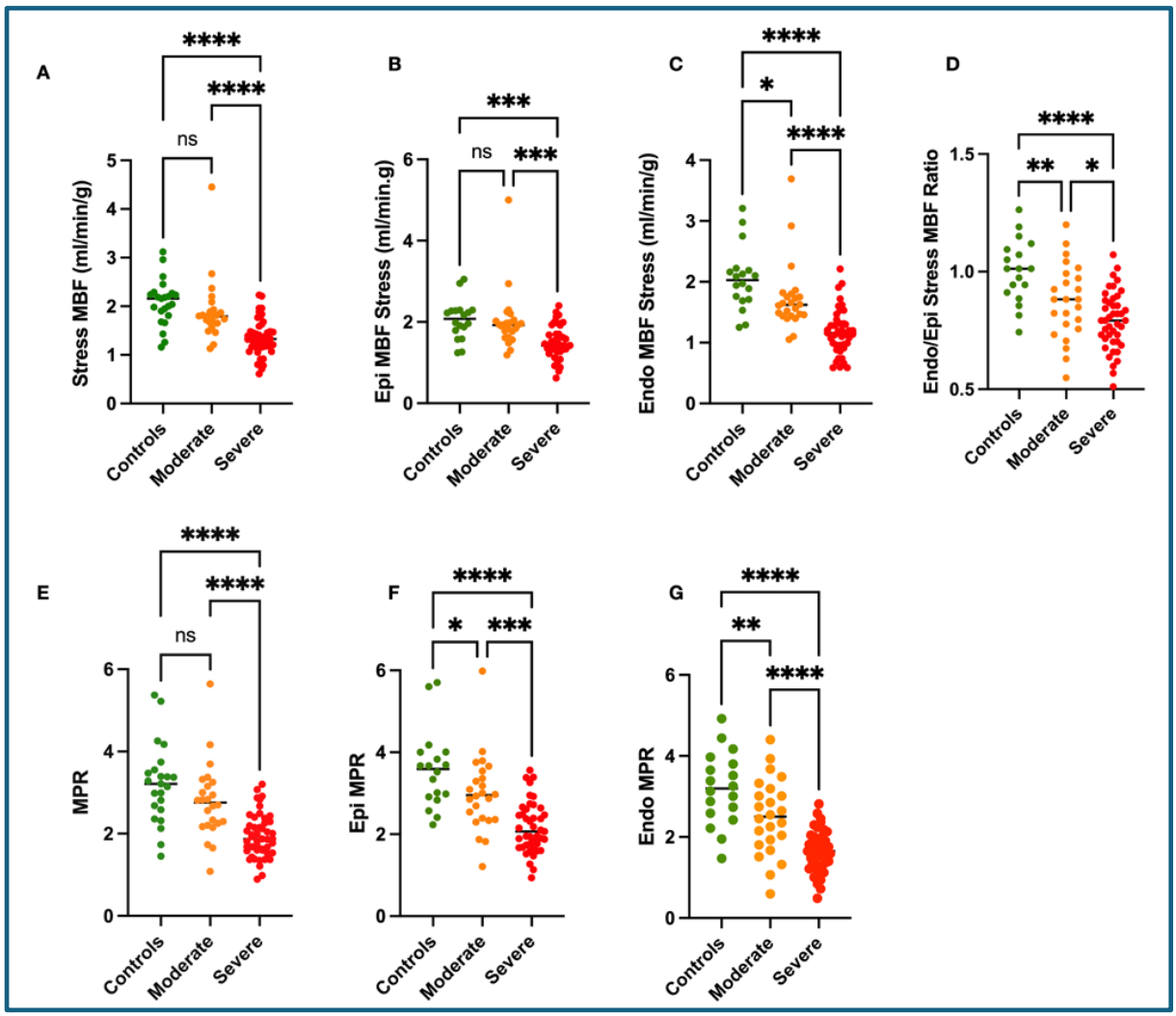

*Figure 2.13: Column scatter graphs with means and 95% confidence intervals showing differences in (A) phosphocreatine to ATP ratio (PCr/ATP), (B) Vasodilator stress myocardial blood flow (MBF, ml/min/g), (C) myocardial perfusion reserve (MPR) between the patients with moderate-AS, severe-AS and controls. Asterisks represent varying levels of significance with: * $p \leq 0.05$, ** $p \leq 0.01$, *** $p \leq 0.001$ and **** $p \leq 0.0001$.*

There were significant correlations between the AS severity (Vmax on TTE) and the global-MPR (r=-0.44; *P*=0.0005), Endo-MPR (r=0.19; *P*=0.0007), stress-MBF (r=-0.45; *P*=0.0003) and adenosine-stress Endo-MBF (r=0.27; P<0.0001), as shown in Figure 2.14.

There were also significant correlations between the markers of LV function and perfusion parameters including a negative correlation of GLS with global stress MBF (r=0.42, P<0.0001), with stress Endo-MBF (r=0.40, P=0.0001), stress Epi-MBF (r=0.11, P=0.0024), stress Endo/Epi MBF ratio (r=0.26, P=0.0030), as well as the global rest MPR (r=0.40, P=0.0001), Endo-MPR (r=0.43, P<0.0001), and Epi-MPR (r=0.39, P=0.0003). Similar results were seen for mitral annular plane systolic excursion (MAPSE), another marker of LV longitudinal contraction: global adenosine-stress MBF (r=0.32, P=0.0029), stress Endo-MBF (r=0.40, P=0.0002), stress Epi-MBF (r=0.25, P=0.0250), stress Endo/Epi MBF ratio (r=0.35, P=0.0014) as well as global rest MPR (r=0.40, P=0.0001), rest Endo-MPR (r=0.44, P<0.0001), and rest Epi-MPR (r=0.37, P=0.0008). There were no significant correlations of perfusion parameters with the LV ejection fraction.

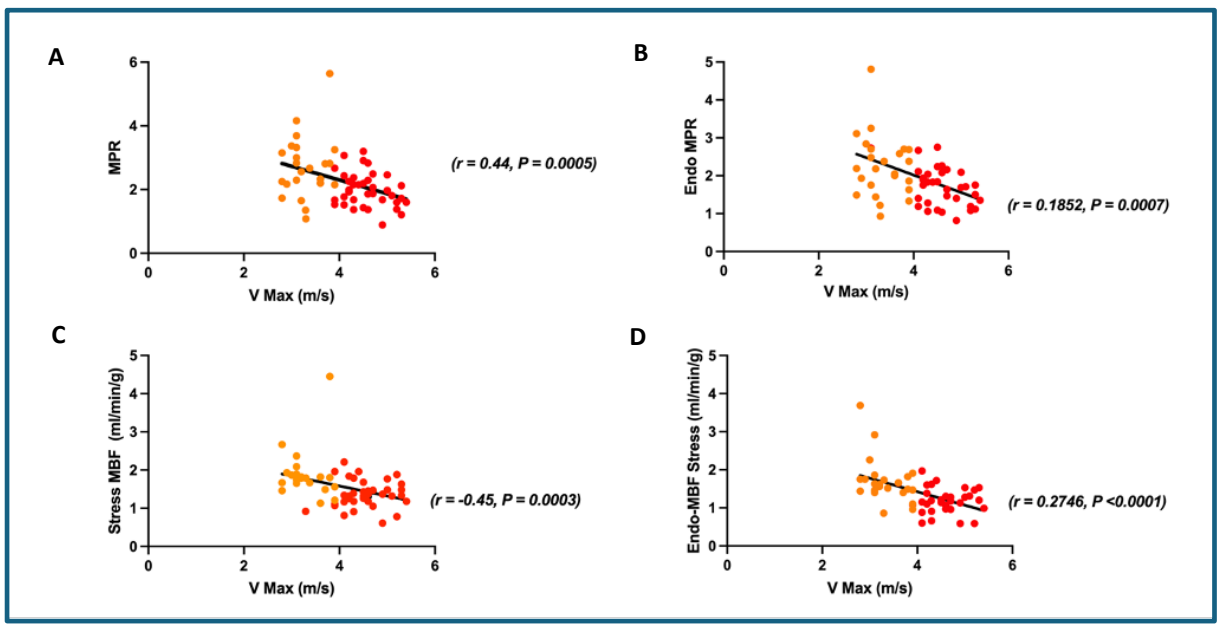

Figure 2.14: Scatterplots showing the correlations of the peak aortic valve velocity (Vmax, m/s) severity of aortic stenosis with: (A) Myocardial perfusion reserve (MPR), (B) Endocardial (endo) myocardial perfusion reserve (MPR), (C) Vasodilator stress myocardial blood flow (MBF, mls/min/g) and (D) vasodilator endocardial (Endo) stress myocardial blood flow (MBF, ml/min/g). Orange dots represent patients with moderate AS and red dots represent patients with severe AS. P signifies p value for comparisons between each of the variables when measured against peak aortic valve velocity. The r value represents correlation coefficient as measured by linear regression analysis.

2.3.4 The combination of DM with Moderate-AS - participant demographics and clinical characteristics.

The implications of DM in patients with severe aortic stenosis will be explored more in Chapter 3. Table 2.4 explores a subgroup analysis of patients with moderate AS, with and without co-existing T2D, against volunteers without AS, with and without co-existing T2D.

Table 2.4: Clinical characteristics and biochemistry of the moderate-AS groups and controls.

Variable	Controls DM n= 5	Moderate-AS DM V1 n= 10	P value Control DM vs Moderate-AS DM	Controls NODM n= 18	Moderate-AS NODM V1 n= 15	P value Control NODM vs Moderate-AS NODM	P value Control DM vs Control NODM	P value Moderate-AS DM vs Moderate-AS NODM
Age, y	62 [48, 74]	74 (68, 80)	0.0992	68 (65, 70)	64 (58, 69)	0.1396	0.3511	**0.0176**
Female, n (%)	2 (40)	2 (20)	0.6818	8 (44)	8 (53)	0.6109	0.8592	0.6056
BMI, kg/m²	23 [22,28]	29 (27, 32)	**0.0280**	26 (24, 24)	30 (27, 33)	**0.0093**	0.4033	0.7179
Heart rate, bpm	67 [63, 69]	70 (61, 79)	0.9678	59 (55, 63)	62 (57, 68)	0.2395	**0.0454**	0.1116
Systolic BP, mmHg	134 [129, 154]	140 (130,150)	0.9678	129(122, 137)	134(125, 144)	0.3919	0.1873	0.4098
Diastolic BP, mmHg	81 [70,90]	73 (61,85)	0.5762	77 (74,80)	78 (74, 82)	0.5564	0.3511	0.2760
Creatinine, umol/L	63 [57,71]	82 (67, 96)	0.0706	69 (64, 75)	77 (67, 86)	0.1436	0.3928	0.5939
Haemoglobin, g/L	140 [124,150]	146 (139,152)	0.2534	146 (139, 153)	144(139, 150)	0.7252	0.2333	0.7100
TG, mmol/L	1.1 [0.8, 1.9]	1.9 (1.3, 2.5)	0.1572	1.4 (1.2, 1.6)	2.1 (1.4, 2.9)	**0.0345**	0.2153	0.6254
HbA1c, mmol/mol	54 [44,58]	52 (44,59)	0.7899	37 (36, 38)	39 (36,41)	0.2615	**0.0264**	**0.0003**
Glucose, mmol/L	7.7 [6.7,10.9]	8.4 (5.8, 10.9)	0.7268	4.9 (4.7, 5.1)	5.3 (5.0, 5.6)	**0.0118**	**<0.0001**	**0.0021**
NT- proBNP, ng/L	73 [35, 162]	124 [47, 226]	0.3467	92 [65, 158]	129 [77, 241]	0.1926	0.4822	0.4191
Medications								
ACEi	-	5 (50)	0.0528	1(6)	5 (33)	**0.0394**	0.5900	0.4047
ARB	1(20)	1 (10)	0.5912	1(6)	-	0.3539	0.3106	0.2113
Beta blocker	-	2 (20)	0.2827	-	1 (7)	0.2660	-	0.3149
CCB	2 (40)	5 (50)	0.7144	-	4 (27)	**0.0194**	**0.0050**	0.2338
Loop diuretic	1(20)	-	0.1432	-	1(7)	0.2660	0.0524	0.4047
Statin	2 (40)	10 (100)	**0.0062**	3(17)	10 (67)	**0.0034**	0.2631	**0.0412**
Antiplatelets	-	3 (30)	0.1709	-	7 (47)	**0.0011**	-	0.4047
DOAC	-	-	-	-	-	-	-	-
Metformin	4 (80)	5 (50)	0.2636	-	-	-	**<0.0001**	**0.0022**
Sulfonylurea	-	2 (20)	0.2827	-	-	-	-	0.0710
GLP-1RA	-	-	-	-	-	-	-	-
SGLT2i	-	2 (20)	0.2827	-	1 (7)	0.2660	-	0.3149
AS Clinical Details								
Bicuspid AV, n (%)	-	1(10)	0.462	-	5 (33)	**0.0078**	-	0.7634
NYHA Class, (%)								
I	5 (100)	8(80)	0.2827	17(94)	18 (93)	0.3105	0.5900	**0.0490**
II	-	2(20)	0.2827	-	1(7)	0.5536	-	0.3149
III	-	-	-	-	-	-	-	-
IV	-	-	-	-	-	-	-	-
6 min walk test, m	-	392[288, 458]	-	525[495,555]	450[390,495]	**<0.0001**	-	0.5549
Cardiovascular Past Medical History								
Stroke / TIA, n(%)	-	-	-	-	2 (13)	0.1100	-	0.2286
PAF, n(%)	-	-	-	-	-	-	-	-
Hyperlipidemia, n (%)	1(20)	9 (90)	**0.0067**	4 (22)	7 (47)	0.1380	0.9151	**0.0270**

Normally distributed continuous variables are expressed as mean (±95% confidence intervals); nonparametric continuous variables are expressed as median [IQR]; and categorical variables are expressed as counts (percent). P signifies p value for comparisons across the groups with T-tests for normally distributed datasets and Mann-Whitney tests for non-parametric values.

AS, indicates aortic stenosis; BMI, body mass index; TG, triglycerides; HbA1c, glycemic hemoglobin; NT-proBNP, N-terminal-pro hormone b-type natriuretic peptide; ACEI, angiotensin converting enzyme inhibitor; ARB, angiotensin receptor blocker; CCB, calcium channel blocker; DOAC, direct oral anticoagulant; GLP-1RA, glucagon-like peptide-1 receptor agonist; SGLT2i, sodium glucose co-transporter-2 inhibitor; TTE, trans-thoracic echocardiogram; V max, peak aortic forward flow velocity; AV indicates aortic valve; T2D, type 2 diabetes; TIA, transient ischemic attack; PAF, paroxysmal atrial fibrillation; STS, society of thoracic surgeons.

y, indicates years; n, number; kg, kilograms; m2, meters squared; bpm, beats per minute; mmHg, millimeters of mercury; umol/L, micromoles per liter; g/L, grams per liter; mmol/L, millimoles per liter; mmol/mol, millimoles per mole; ng/L, nanograms per liter; m/s, meters per second; m, meters.

Participants in the Moderate-AS and T2D (Moderate-AS DM) group had a similar age and gender profile to the controls with T2D (Control-DM) subgroup. The same was noted for the cohorts without T2D (NODM). Interestingly, participants with AS exhibited higher BMI values than their DM counterparts, (Control-DM: 23 [22,28], Moderate-AS DM: 29 (27, 32), Control-NODM: 26 (24, 24), Moderate-AS NODM: 30 (27, 33); Control-DM vs Moderate-AS DM, P = 0.0280 and Control-NODM vs Moderate-AS NODM, P = 0.0093; Table 2.4).

As expected, the participants with T2D had higher fasting glucose and HbA1c, with statistical significance in the comparison of the DM vs NODM groups (Glucose (mmol/L); Moderate-AS DM: 8.4 (5.8, 10.9) vs Moderate-AS NODM: 5.3 (5.0, 5.6), P= 0.0021 and Control-DM: 7.7 [6.7,10.9] vs Control NODM: 4.9 (4.7, 5.1), P = <0.0001 and HbA1c (ng/l) Moderate-AS DM: 52 (44,59) vs Moderate-AS NODM: 39 (36,41), P= 0.0003 and Control-DM: 54 [44,58] vs Control NODM: 37 (36, 38), P = 0.0264), as shown in Table 2.4.

Numerical differences were seen in the NTproBNP values of the groups, with the presence of AS resulting in higher values irrelevant of diabetes status, but this did not reach statistical significance (Table 2.4).

2.3.5 The effect of T2D on Moderate-AS – CMR and ^{31}PMRS findings

Cardiac remodeling

The presence of co-existing T2D did not appear to contribute to more pronounced LV concentric remodeling in the context of Moderate-AS, defined by LV mass-indexed to BSA (Control-DM: 61 [44, 63], Moderate-AS DM: 52 [45, 71], Control-NODM: 40 [37, 50],

Moderate-AS NODM: 59 [48, 80]; Control-DM vs Moderate-AS DM; Table 2.5) nor LV concentricity index (Control-DM: 0.67 [0.57, 0.78], Moderate-AS DM: 0.61 [0.53, 0.81], Control-NODM: 0.55 [0.53, 0.59], Moderate-AS NODM: 0.78 [0.57, 0.91]; Table 2.5).

The native T1 value was higher in the AS cohorts irrespective of the DM status, and reached statistical significance within the NODM comparison; the lack of significance in the T2D comparison is likely due to the sample size of these groups (Control-DM: 1178 [1157, 1260] vs Moderate-AS DM: 1266 [1207, 1303], P= 0.1898, and Control-NODM: 1332 [1275, 1356] vs Moderate-AS NODM: 1285 [1257, 1297], P= 0.0102; Table 2.5). A similar result was not seen for measured extracellular volume. Within these small groups, LGE was uncommon, reflected in median values of zero (Table 2.5).

Cardiac energetics and perfusion and function

There were no statistically significant differences in the myocardial PCr/ATP ratios when comparing the DM and NODM groups separately. There was a statistically higher ratio in the participants with Moderate-AS and co-existing T2D compared to those without T2D, (PCr/ATP - Moderate-AS DM: 2.2 [2.0, 2.5] vs Moderate-AS NODM: 1.9 [1.6, 2.0], P= 0.0390; Table 2.5).

Unfortunately, due to a change in protocol, the control participants with co-existing T2D were not assessed using segmental layer-specific perfusion metrics like the other groups. Of the basic perfusion measures that were obtained for all groups however, the presence of aortic stenosis resulted in numerically worse global stress MBF (Control-DM: 2.2 [2.0, 2.3] vs Moderate-AS DM: 1.8 [1.3,1.9], P= 0.0060, and Control-NODM: 2.1 [1.8, 2.3] vs Moderate-AS NODM: 1.8 [1.7, 2.1], P= 0.1782) and MPR (Control-DM: 2.7 [2.1,3.3] vs Moderate-AS DM:

2.3 [2.2, 2.6], P= 0.1898, and Control-NODM: 3.2 [2.5, 3.5 vs Moderate-AS NODM: 3.0 [2.7, 3.4], P= 0.6855; Table 2.5) in DM and NODM groups; notably, MPR was lower in Moderate-AS DM vs Moderate-AS NODM (P= 0.0018), Figure 2.15.

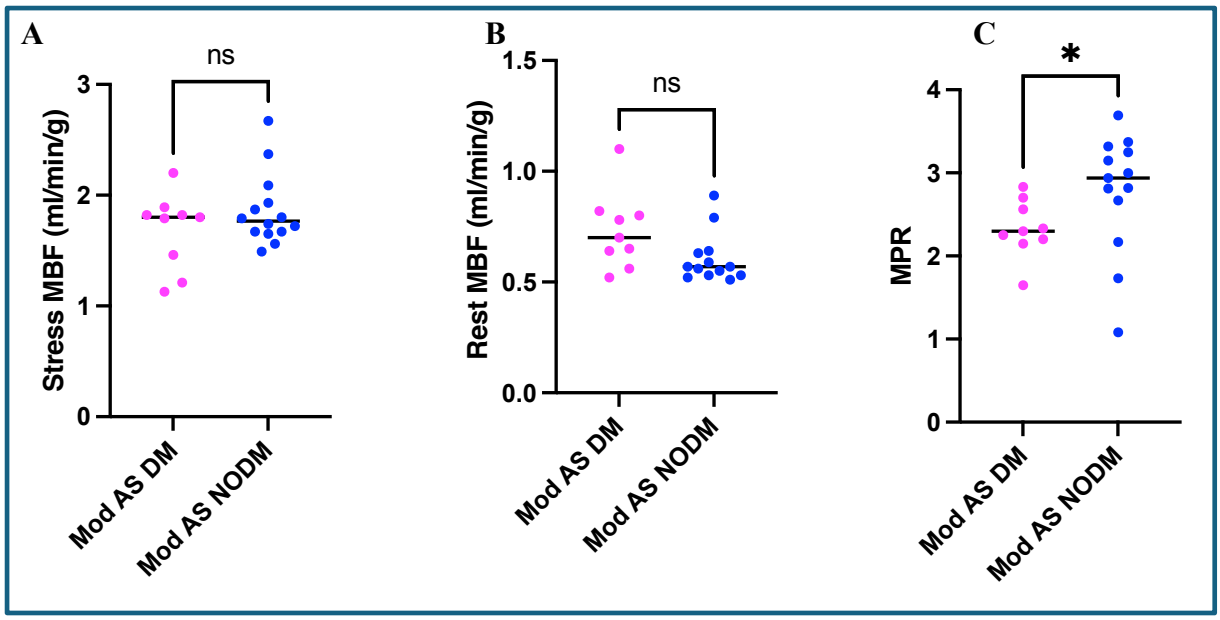

*Figure 2.15: Column scatter graphs with means and 95% confidence intervals showing differences in (A) Vasodilator stress myocardial blood flow (MBF, ml/min/g) (B) rest myocardial blood flow (MBF, ml/min/g), (C) myocardial perfusion reserve (MPR) between the patients with moderate-AS with and without concomitant T2D. Asterisks represent * $p \leq 0.05$, ns, represents no significance.*

Table 2.5: CMR and 31P-MRS findings of the moderate-AS groups and healthy controls at baseline.

Variable	Control DM n= 5	Moderate-AS DM n= 10	P value Control DM vs Moderate-AS DM	Controls NODM n= 18	Moderate-AS NODM n= 15	P value Control NODM vs Moderate-AS NODM	P value Control DM vs Control NODM	P value Moderate-AS DM vs Moderate-AS NODM
LV end-diastolic volume indexed to BSA, mL/m²	79 [69,93]	65 [60,76]	0.2398	79 [66,86]	76 [59,87]	0.8741	0.8087	0.4115
LV end-systolic volume indexed to BSA, ml/m²	34 [25,35]	23 [20,30]	0.2398	29 [23,34]	28 [19,32]	0.3849	0.4836	0.7702
LV mass, g	116 [74,130]	86 [67,106]	0.2398	73 [62,105]	105 [70,149]	**0.0392**	0.2105	0.1937
LV mass indexed to BSA, g/m²	61 [44,63]	52 [45,71]	0.2977	40 [37,50]	59 [48,80]	**0.0009**	0.0974	0.3472
LV mass to LV end-diastolic volume, g/mL	0.67 [0.57,0.78]	0.61 [0.53, 0.81]	0.7972	0.55 [0.53, 0.59]	0.78 [0.57, 0.91]	**0.0026**	**0.0489**	0.3101
LV stroke volume indexed to BSA, ml/m²	47 [44,59]	41 [40,48]	0.0599	46 [40,56]	46 [35,58]	0.7026	0.6342	0.3175
LV ejection fraction, %	62 [58,66]	65 [63,67]	0.1119	62 [59,66]	66 [60,68]	0.1985	0.8648	0.9070
LV maximal wall thickness, mm	9.5 [8.8,11.9]	12.1 [10.4,13.0]	0.1898	10.8 [9.2,13.7]	12.0 [10.6,14.5]	0.1480	0.3233	0.8264
LA biplane end-diastolic volumes, mL	82 [65,86]	70 [41,81]	0.1898	75 [54,91]	73 [40,102]	0.9627	0.5328	0.4460
LA biplane end-systolic volumes, mL	28 [19,42]	26 [16,47]	0.7972	37 [22,47]	29 [23,56]	0.9104	0.3865	0.3868
Biplane LA EF, %	64 [59,71]	58 [44,63]	0.1469	54 [46,68]	63 [53,67]	0.3409	0.1867	0.4460
GLS, %	19 [16,22]	18 [16,18]	0.3483	18 [17,23]	18 [17, 20]	0.3723	>0.9999	0.6293
Native T1, (ms)	1178 [1157,1260]	1266 [1207,1303]	0.1898	1285 [1257,1297]	1332 [1275,1356]	**0.0102**	**0.0114**	**0.0456**
Extra cellular volume fraction, (%)	0.23 [0.20, 0.28]	0.25 [0.24,0.27]	0.6853	0.22 [0.20,0.23]	0.27 [0.24, 0.29]	**<0.0001**	0.2615	0.1815
LGE, (%)	0 [0,0]	0 [0,4]	0.4872	0 [0,8.3]	0 [0,16]	0.1392	0.5584	0.4297
PCr/ATP	1.9 [1.6,2.3]	2.2 [2.0,2.5]	0.4127	1.9 [1.7,2.6]	1.9 [1.6,2.0]	0.3982	0.6180	**0.0390**
Stress MBF, ml/min/g	2.2 [2.0,2.3]	1.8 [1.3,1.9]	**0.0060**	2.1 [1.8,2.3]	1.8 [1.7, 2.1]	0.1782	0.6174	0.5099
Endo MBF Stress, ml/min/g	-	1.6 [1.3,1.6]	-	2.0 [1.7,2.2]	1.7 [1.5,1.9]	0.1398	-	0.0808
Epi MBF Stress, ml/min/g	-	1.9 [1.4,2.1]	-	2.0 [1.7,2.3]	1.9 [1.8,2.1]	0.5321	-	0.6502
Endo/Epi MBF Stress Ratio	-	0.9 [0.8,0.9]	-	1.0 [0.9,1.1]	0.9 [0.8, 1.0]	**0.0102**	-	0.6712
Rest MBF, ml/min/g	0.7 [0.6,1.1]	0.7 [0.6,0.8]	0.5185	0.6 [0.5,0.7]	0.6 [0.5,0.8]	0.5565	**0.0105**	0.2440
Endo/Epi MBF Rest ratio	-	1.0 [1.0,1.1]	-	1.1 [1.1,1.2]	1.1 [1.0,1.1]	**0.0246**	-	0.3381
MPR	2.7 [2.1,3.3]	2.3 [2.2,2.6]	0.1898	3.2 [2.5,3.5]	3.0 [2.7,3.4]	0.6855	0.3209	**0.0018**
Endo MPR	-	2.1 [1.8,2.2]	-	3.1 [2.4, 3.7]	2.7 [2.4, 3.1]	0.2571	-	**0.0079**
Epi MPR	-	2.5 [2.3,2.9]	-	3.5 [2.9,3.9]	3.3 [2.9, 3.8]	0.5198	-	**0.0212**
Increase in RPP, %	55 [51,59]	18 [14,19]	**0.0025**	28 [18,42]	26 [17,36]	0.8460	**0.0131**	0.1146

Normally distributed continuous variables are expressed as mean (±95% confidence intervals); nonparametric continuous variables are expressed as median [IQR]; and categorical variables are expressed as counts (percent). P signifies p value for comparisons across the groups with T -tests for normally distributed datasets and Mann-Whitney test for non-parametric values.

LV indicates left ventricle; BSA, body surface area; SV, stroke volume; RV, right ventricle; LA EF, left atrial ejection fraction; GLS, global longitudinal shortening; LGE, late gadolinium enhancement; PCr/ATP ratio phosphocreatine to adenosine tri-phosphate ratio; Endo, endocardial; MBF, myocardial blood flow; Epi, epicardial; MPR, myocardial perfusion reserve; RPP, rate pressure product.
Ml/m2, indicates milliliters per square meter; g, grams; g/m2, grams per square meter; g/ml, grams per milliliters; mm, millimeter; mL,milliiter; ms, millisecond; mil/min/g, milliliters per minute per gram.

Cardiac remodeling, perfusion and function of Moderate-AS cohort at baseline and at 12 months.

At the 12-month follow up assessment period, 18 of the original 25 patients returned for a follow up assessment identical to their baseline study visit. Whilst the number of patients that returned was too small to perform diabetes stratified analyses, paired t-tests were used to compare their original study visit CMR results to the measurements obtained at their follow up visit.

The CMR assessment revealed a progressive numerical increase in the mean LV concentricity index, which did not reach statistical significance (Visit-1: 0.74 [0.64, 0.84] vs Visit-2: 0.84 [0.73, 0.96]g/mL; *P*=0.156). An increasingly restrictive filling pattern of mitral inflow E/A ratio was detected (Visit-1: 1.3 [1.0, 1.5] vs Visit-2: 2.0 [1.5, 2.6]; *P*=0.042) along with a significant decline in left atrial function (Visit-1: 59 [52, 66] vs Visit-2: 47 [41, 53]%; *P*=0.016). There was no significant change in LV ejection fraction (Visit-1: 65 [63, 66]% vs Visit-2: 64 [60, 67]%; *P*=0.46) or GLS (Visit-1: 17.7 [16.6, 18.8]% vs Visit-2: 17.6 [15.5, 19.7]%; *P*=0.95). There was however a subtle numerical (non-significant) increase in non-ischemic pattern of myocardial scar on LGE (Visit-1: 0.0 [0, 4.8] vs Visit-2: 0.56 [0, 4.3]; P=0.58), as shown in Table 2.6.

Table 2.6: CMR and 31P-MRS findings of Moderate-AS patients at baseline (V1) and at 12 month follow up (V2).

Variable	Mod AS V1 n= 18	Mod AS V2 n= 18	P value
LV end-diastolic volume indexed to BSA, mL/m²	72 (63, 81)	73 (65, 81)	0.6707
LV end-systolic volume indexed to BSA, ml/m²	27 (22, 33)	28 (23, 32)	0.9959
LV mass, g	103 (82, 124)	119 (102, 136)	**0.0375**
LV mass indexed to BSA, g/m²	58 (50, 66)	65 (59, 70)	**0.0050**
LV mass to LV end-diastolic volume, g/mL	0.75 (0.62, 0.88)	0.84 (0.73, 0.96)	0.1714
LV stroke volume indexed to BSA, ml/m²	44 (38, 51)	46 (42, 50)	0.4998
LV ejection fraction, %	65 (63, 67)	64 (60, 67)	0.2858
LV maximal wall thickness, mm	12.2 (10.9, 13.6)	12.1 (11.4, 12.8)	0.7597
LA biplane end-diastolic volumes, mL	67 (52, 82)	69 (56, 82)	0.7550
LA biplane end-systolic volumes, mL	35 (23,46)	38 (27, 48)	0.6376
Biplane LA EF, %	61 (52, 69)	47 (41, 53)	**0.0024**
GLS, %	17.2 (16.0, 18.5)	17.6 (15.5, 19.7)	0.6972
Aortic Valve Area, mm²	1.5 (1.3, 1.6)	1.2 (1.1, 1.4)	**0.0278**
Aortic valve peak forward flow, m/s	3.2 (2.7, 3.6)	2.9 (2.7, 3.1)	0.1489
Native T1, ms	1306 (1279, 1333)	1334 (1297, 1371)	0.1572
Extra cellular volume fraction, %	0.23 (0.20, 0.25)	0.23 (0.21, 0.24)	0.9168
LGE, %	0.0 [0.0, 7.0]	0.56 [0, 4.3]	0.6250
PCr/ATP	1.9 [1.6, 2.2]	1.7 [1.7, 2.3]	0.9261
Stress MBF, ml/min/g	1.9 (1.6, 2.3)	1.4 (1.2, 1.6)	**0.0053**
Endo MBF Stress, ml/min/g	1.7 (1.4, 2.0)	1.2 (1.1, 1.4)	**0.0032**
Epi MBF Stress, ml/min/g	2.1 (1.6, 2.5)	1.5 (1.3, 1.7)	**0.0076**
Endo/Epi MBF Stress Ratio	0.85 (0.80, 0.91)	0.81 (0.74, 0.88)	0.1083
Rest MBF, ml/min/g	0.6 [0.5, 0.8]	0.6 [0.5, 0.7]	0.0133
Endo/Epi MBF Rest ratio	1.05 (1.01, 1.09)	1.02 (1.00, 1.06)	0.2992
MPR	2.8 (2.2, 3.3)	2.3 (1.9, 2.6)	**0.0292**
Endo MPR	2.4 (2.0, 2.9)	1.9 (1.7, 2.2)	**0.0412**
Epi MPR	3.0 (2.4, 3.5)	2.5 (2.1, 2.8)	**0.0275**
Increase in RPP, %	24 (16, 32)	25 (17, 32)	0.9521

Normally distributed continuous variables are expressed as mean (±95% confidence intervals); nonparametric continuous variables are expressed as median [IQR]; and categorical variables are expressed as counts (percent). P signifies p value for comparisons across the groups with paired T- tests for normally distributed datasets and Kruskal-Wallis test for non-parametric tests.

LV indicates left ventricle; BSA, body surface area; SV, stroke volume; RV, right ventricle; LA EF, left atrial ejection fraction; GLS, global longitudinal shortening; LGE, late gadolinium enhancement; PCr/ATP ratio phosphocreatine to adenosine tri-phosphate ratio; Endo, endocardial; MBF, myocardial blood flow; Epi, epicardial; MPR, myocardial perfusion reserve; RPP, rate pressure product.

Ml/m², indicates milliliters per square meter; g, grams; g/m², grams per square meter; g/ml, grams per milliliters; mm, millimeter; mL,milliiter; ms, millisecond; mil/min/g, milliliters per minute per gram.

Upon review of the perfusion parameters, there was significant deterioration in stress-MBF, compared to visit 1 (Visit-1: 1.9 [1.6, 2.2] vs Visit-2: 1.4 [1.2, 2.6]ml/min/g; P=0.006) and MPR (Visit-1: 2.8 [2.4, 3.2] vs Visit-2: 2.3 [1.9, 2.6]ml/min/g; P=0.04). In parallel with the global perfusion indices, the layer-specific perfusion parameters also showed significant reductions including the Endo-stress-MBF (Visit-1: 1.7 [1.5, 2.0] vs Visit-2: 1.2 [1.1, 1.4]ml/min/g; P=0.006) and Epi-stress-MBF (Visit-1: 2.0 [1.7,2.3] vs Visit-2: 1.5 [1.3, 1.7]ml/min/g; P=0.018), as shown in Figure 2.16. However, the numerical reductions in transmural Endo:Epi ratio for stress-MBF gradient (Visit-1:0.85 [0.78, 0.89] vs Visit-2: 0.80 [0.73, 0.88]; P=0.363) and rest-MBF gradient (Visit-1: 1.06 [1.02, 1.09] vs Visit-2: 1.03 [1.0, 1.1]; P=0.132) did not reach statistical significance (Table 2.6).

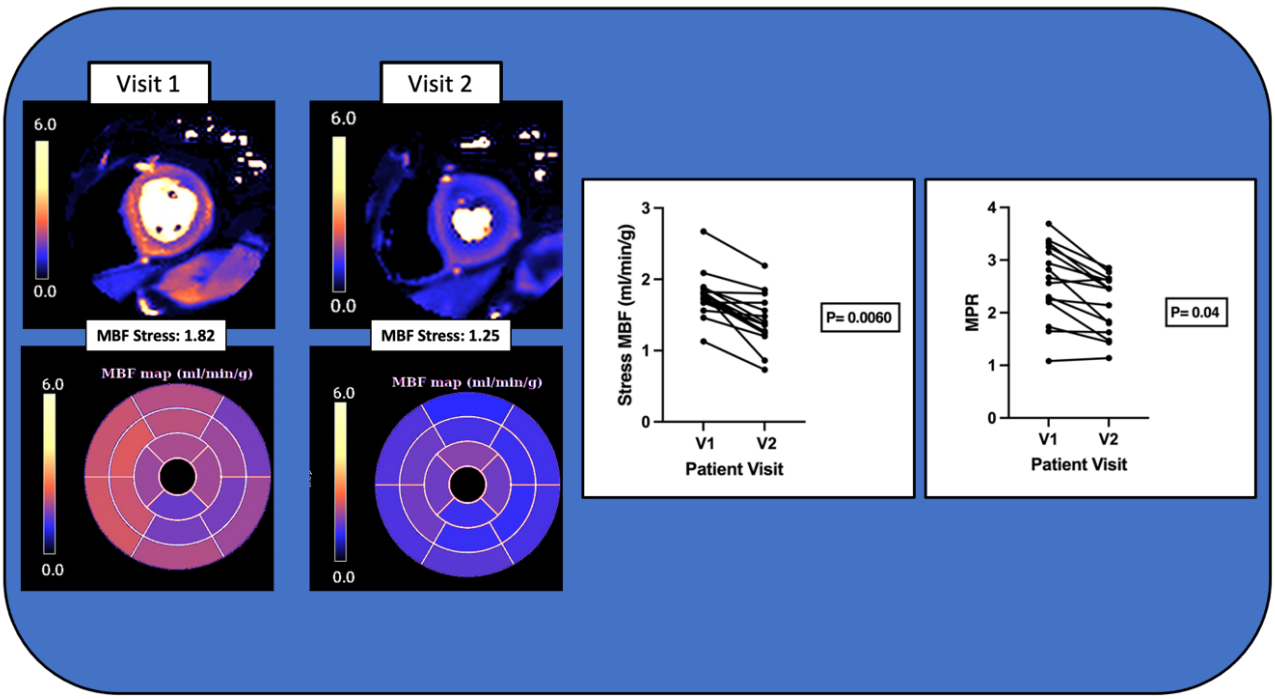

Figure 2.16: Representative images of myocardial perfusion changes in patients with moderate AS from baseline to 12 months follow up. Graphical depiction of stress myocardial blood flow at patient's visit 1 far left, and same patient's visit 2. Scatterplots comparing stress myocardial blood flow (MBF) on the left at visit 1 and visit 2, and myocardial perfusion reserve (MPR) on the right.

2.3.6 Clinical outcomes of the patient subgroups

Of the recruited patients with severe-AS, 39 (75%) proceeded to have surgical valve replacement, and 13 (25%) proceeded to have transcatheter aortic valve implantation.

Over the 12-month follow-up of the patients with Moderate-AS, 7 patients progressed to severe-AS, requiring referral for AVR. One was recruited as a participant in the 'Randomised Controlled Trial of Early valve replacement in severe ASYmptomatic Aortic Stenosis (EASY-AS)' (267) and is on the expectant management arm, two received SAVR and the rest underwent a TAVR procedure. These patients had significantly lower stress-MBF at baseline in comparison with those who did not progress to Severe-AS (1.6 [1.4, 1.8] vs 2.0 [1.7, 2.4]ml/min/g; *P*=0.038). No significant differences were seen between perfusion markers: global rest-MBF and MPR in the participants with stenosis progression to those that didn't.

2.4 DISCUSSION

Given the relevance of myocardial health in the prognosis of patients with AS, the first aspect of this study prospectively compared myocardial remodeling, energetics and perfusion parameters in patients with moderate and severe AS with preserved LV ejection fraction against controls without AS. The group of patients with moderate AS was then followed up at 12 months to define changes to the anatomy of the LV and aortic valve. Finally, subgroup analysis was performed to understand how co-existing T2D interacted with moderate AS.

Cardiac remodeling across the spectrum of AS

Moderate and severe AS were both associated with cardiac concentric hypertrophy, myocardial energetic deficit, and reduced exercise distance on 6-minute walk test. There was a progressive worsening of the hypertrophic remodeling of the LV as the severity of the valve stenosis increased. The patients with moderate AS exhibited significant reductions in LV contractile function, though this was less pronounced compared to the severe AS group.

While milder compared to that seen in severe AS, the degree of adverse myocardial remodeling associated with moderate AS in this study may be clinically important for the cardiovascular clinical outcomes in patients with moderate AS. There is consistent evidence linking concentric hypertrophic remodeling of the LV to adverse cardiovascular outcomes (268). It is therefore of clinical relevance to note that such remodeling is already evident in moderate AS. Indeed, an adverse association between greater LV mass-index and worse clinical outcomes has been shown among patients with severe and moderate AS (269).

The native T1 values were significantly elevated in both AS groups, and were shown to increase with rising stenosis severity. Native T1 represents a composite signal from both the intracellular and extracellular compartments and the reasons for elevated T1 in AS are likely multifactorial (270-272). Specifically, in this study the increased T1 may suggest increasing fibrosis, but the lower haemoglobin values in the severe AS cohort (while not being in the anaemic range) may also contribute. It is therefore plausible that elevated T1 may also be related to a blood component to the myocardial tissue composition as it is well established that patients with AS have higher resting blood flow to account for increasing myocardial oxygen demand (271).

In my study the surrogate markers of extracellular myocardial matrix expansion and replacement fibrosis were only significantly increased in the severe AS group and not in moderate AS. This may be of significant clinical relevance because among the imaging biomarkers of ventricular decompensation in AS, these CMR parameters have consistently been shown to be strong associates of all-cause and cardiovascular mortality after AVR (130, 208, 273, 274). In AS, myocardial fibrosis is a key pathological process driving the transition from hypertrophy to heart failure. In a study using invasive myocardial biopsy and CMR imaging, myocardial fibrosis in severe AS was shown to have three main alterations: endocardial thickening, subendocardial microscars, and diffuse interstitial fibrosis (270). However, this landmark study demonstrated that neither histological collagen volume fraction nor the CMR parameters ECV and LGE capture this fibrosis in its totality.

The ECV results in my study are on the lower spectrum of reported values in the literature on severe AS, likely reflecting that the severe AS cohort had a low surgical risk score, consistent with the eligibility criteria excluding major comorbidities and mandating normal LVEF. Supporting this hypothesis, a multicentre study which reported associations between ECV and clinical variables showed that there was a progressive increase in ECV with established coronary heart disease, society of thoracic surgeons (STS) and EuroSCORE II risk scores (208). In that study, there was also progressive evidence of LV decompensation with more patients classified as NYHA functional status III or IV, more patients demonstrating late gadolinium enhancement, and a progressive increase in indexed left atrial volumes, indexed LV volumes, and LV mass index in patients with higher ECV. Consistent with my results, patients with severe AS in the lowest tertile of ECV had ECV values less than 25.9%.

A study reported by Chin et al showed that myocardial extracellular volume expansion and replacement fibrosis are increased in AS, but were only weakly associated with the severity of stenosis (235). The dissociation between the valve severity and the extracellular expansion is consistent with my findings of no significant difference in either native T1 or ECV measurements between the moderate AS and the severe AS groups. However, patients with moderate AS did not demonstrate a similar degree of scarring on LGE compared to the severe AS group in my study. The discrepancy between the findings of our studies' LGE assessments may be due to the differences in comorbidities. While limiting generalizability, my study was stringent in excluding major comorbidities to reduce the possible confounding.

Cardiac energetics and perfusion across the AS spectrum

At a metabolic level, LV hypertrophy is associated with decreased myocardial high-energy phosphate pool (energetics) and reductions in the creatine kinase flux (275). These changes in turn cause myocardial energetic starvation in severe AS (245). The level of energetic deficit was similar between the moderate and severe AS groups and this correlated with the LV mass. This suggests that even a mild degree of hypertrophy is associated with a decreased myocardial high-energy phosphate pool.

It is known that coronary flow reserve is reduced in patients with AS, particularly severe AS, due to a multitude of factors including left ventricular hypertrophy, endothelial dysfunction, increased LV systolic pressure and reduced cardiac output (276). Furthermore, the degree of microvascular dysfunction is closely related to the degree of valve stenosis (276, 277). Liga et al, confirm this in their prospective perfusion study of patients with mild and moderate AS, which showed that inducible myocardial ischaemia is present even in mild and moderate

aortic valve stenosis (278). More severe forms of AS coincide with higher levels of LV hypertrophy and total LV mass. It is therefore considered that the rising intraventricular pressure in AS with time causes hypertrophy, which leads to an increased myocardial oxygen demand. To maintain equilibrium, coronary flow autoregulation induces vasodilation hence minimising coronary microvascular resistance in order to maintain a constant resting perfusion, ultimately leading to microvascular ischaemia (279, 280). The data presented in my study support this, with severe AS displaying associations with global, as well as endocardial and epicardial reductions in MBF and MPR, and reductions in the Endo/Epi-MBF gradient values. Furthermore, whilst moderate AS was not associated with reductions in the global myocardial perfusion metrics, the transmural perfusion dynamics were significantly affected, with reductions in stress Endo-MBF, Endo/Epi-MBF gradient, and Endo- and Epi-MPR compared to controls.

Follow-up of the moderate AS patients

Another objective of the current work was to increase insights into AS progression, given the lack of clarity surrounding this within the literature (187). Over the follow up period of 12 months, 28% of patients progressed to severe symptomatic AS and were referred for AVR. The patients who progressed to severe-AS showed worse myocardial perfusion at baseline, despite matching AS severity to those who did not progress to severe-AS.

The observed cohort of patients with moderate AS exhibited significant deterioration of global and layer-specific stress MBF and MPR, despite less pronounced changes in cardiac concentric hypertrophy and no significant change in LV systolic function on CMR. However,

LV diastolic function as measured by CMR mitral-inflow E/A ratio suggested a more restrictive filling pattern, along with worsened left atrial function.

To date, whilst microvascular ischaemia has been shown to predispose to an increased risk of valve replacement and death (278), no prior research group has investigated global and transmural myocardial perfusion parameters using automated, in-line pixel wise quantitative myocardial perfusion CMR in patients with moderate AS. Myocardial hypertrophy is accompanied by capillary density reduction, microcirculatory dysfunction and impaired stress MBF (281, 282). The results from my study confirm the previous studies showing significant reductions in global stress MBF in severe AS, whilst also highlighting that the extent of the impaired myocardial perfusion is subject to the severity of AS. In normal hearts, resting MBF is greatest in the endocardium (Endo/Epi ratio >1), but epicardial MBF is augmented during adenosine-induced hyperemia to a greater extent. Prior investigations have consistently reported that in AS, preferential coronary flow shifts from the endocardium to epicardium results in a significant decrease in endocardial MBF which may be the result of relatively less pronounced reduction in MBF in the epicardial layer compare to the endocardial layer (237). The reversal of normal Endo/Epi blood flow ratio may be important for the pathophysiology of AS, potentially resulting in subendocardial ischemia, apoptosis, and fibrosis even in patients without flow-limiting obstructive coronary artery disease. My data are therefore novel, showing for the first time that myocardial layer-specific perfusion parameters are already significantly affected in moderate AS.

Published literature suggests that the presence of T2D predicts faster AS progression in patients with moderate and severe stenosis (283, 284). In an observational study by Hwang

et al, the rate of AS progression was more pronounced in patients with T2D than their non-diabetic counterparts. Perhaps even more importantly however, the rate of progression depended on the degree of glycaemic control, with higher mean HbA1c percentage values being positively correlated with worsening valve stenosis (by both peak velocity and mean pressure gradient) (285). The cohort in my study was too small to conduct stratified analyses based on diabetes status. As a result, I am unable to assess the impact of diabetes on the progression of moderate aortic valve disease. However, this remains an important area for future investigation.

Investigating the effect of concomitant T2D on Moderate-AS

The presence of concomitant T2D in patients with severe AS has been previously described to be associated with more pronounced LV concentric remodeling (225). However, this wasn't replicated in my moderate AS cohort, nor were there statistically significant differences in markers of LV concentric remodeling. Similarly, a prospective study of over 200 patients with moderate and severe AS, with and without concomitant T2D, found no statistically significant differences in the makers of LV remodeling (LV mass), LV function or the presence of LGE. However, their DM cohort exhibited higher ECV compared to their non-diabetic controls, suggestive of diffuse interstitial fibrosis (284). In my analysis, whilst there are statistically significant differences between the T2D and non-diabetic groups' T1 values, these are in the opposite direction to what was expected, with higher values in the non-diabetic group. The most likely explanation for this is the small sample size of my study, but it is also possible that the more stringent exclusion criteria of my study contributed by excluding people most likely to have abnormal T1. Moreover, the lack of statistically significant differences in ECV in my study suggest that the T1 data may not imply important differences in interstitial fibrosis.

My data show a stepwise progression of LV concentric remodeling in the presence of worsening valve stenosis, highlighted at the start of the chapter. When considering the effects of T2D in patients with moderate AS it appears that changes in perfusion may be the first to affect the myocardium. Specifically, MPR has been shown to vary both globally and across different myocardial layers in patients with moderate AS, regardless of the presence of concomitant T2D, but appears to be more significant in the presence of concomitant disease. What cannot be explained from the current dataset however, is the mechanism of this change. In the absence of worsening concentric remodeling to mechanically contribute to microvascular dysfunction in the T2D cohort, it is unclear if such changes are due to endothelial dysfunction associated with diabetes or a primary consequence of the valve pathology. Furthermore, the literature suggests that stress perfusion is worse in the presence of concomitant T2D (284). Validation of the presented results is therefore needed to ensure their accuracy and reproducibility in a larger participant group. Once this has been performed, further analyses are required to establish the causation of the worsening perfusion seen in patient with T2D and moderate AS compared to those patients with valve disease without T2D.

Clinical perspectives

Current guidelines recommend AVR in patients with severe AS in the presence of symptoms or evidence of cardiac dysfunction (LV ejection fraction <50% on cardiac imaging) (187, 233). However, studies of early intervention strategies are currently proceeding to address the issue of excess cardiovascular death in patients with AS compared with the reference population even after undergoing AVR. These trials propose that early intervention can prevent irreversible myocardial pre-AVR damage and will therefore prevent adverse post-AVR

outcomes. The results so far however, are conflicting. In the RECOVERY (early surgery or conservative care for asymptomatic aortic stenosis) trial, 145 asymptomatic patients with very severe aortic stenosis (aortic-valve area of ≤0.75 cm^2) were also randomized to early (within 2 months of randomization) guideline-directed valve intervention. The primary end point was a composite of operative mortality or death from cardiovascular causes during the mean follow-up period of 4 years. The primary end point occurred in 1% of the early intervention group vs 15% of the conservative management group, hazard ratio, 0.09; 95% CI, 0.01 to 0.67; P=0.003. This provided striking evidence supporting early intervention (286). Furthermore, in the EARLY-TAVR (transcatheter aortic valve replacement for asymptomatic severe aortic stenosis), patients with asymptomatic severe AS and preserved EF were randomized to TAVR within 14 days after randomization or clinical surveillance in a 1:1 ratio. The primary end point was death, stroke, or unplanned hospitalization for cardiovascular causes. Of the 901 patients randomised, the primary end point occurred in 26.8% of the TAVR group and 45.3% in the clinical surveillance group, hazard ratio, 0.50; 95% CI, 0.40 to 0.63; P<0.001. Importantly over the mean follow up time of just under 4 years, 87% of the conservative management groups proceeded to require TAVR and there was no difference in the procedure related adverse events between the patients (287). The EVOLVED trial (early intervention in patient with asymptomatic severe aortic stenosis and myocardial fibrosis) was a randomized control trial in which patients with asymptomatic severe AS and concomitant myocardial fibrosis (diagnosed on CMR), were subjected to 'early' aortic valve intervention or conservative management. This is particularly pertinent as myocardial fibrosis is known to develop prior to LV dysfunction. Early intervention was defined as 'within two months' of an assessment confirming the coexistence of severe AS and myocardial fibrosis, allowing for constraints of local heart valve teams. Patients randomised to receive guideline-directed

conservative management received any appropriate and required medical treatment and were referred for aortic valve intervention at the discretion of their treating physician and local heart valve team. Patients were followed up for 12 months after randomisation to explore the primary end points of all-cause mortality or unplanned AS-related hospitalisation (defined as: any unplanned admission before or after aortic valve replacement with syncope, heart failure, chest pain, ventricular arrythmia, or second- or third-degree heart block attributed to the aortic valve disease). Patients in the early intervention group had a median time to intervention of 5 months, whereas in the conservative management group it was 20.2 months. Numerically fewer patients in the early intervention group experienced primary endpoints (18%, vs 23%), but this was not statistically significant, with a hazard ratio of 0.79 (95% confidence interval 0.44-1.43; P = 0.44). The authors proposed that further work is needed within this field as large confidence interval encompasses 'potential clinically meaningful benefits or harms from early intervention'. Furthermore, it is questionable whether the early intervention group did in fact receive early treatment, given that some patients waited as long as 8 months for their intervention procedure (288).

The literature is therefore conflicting as to the most appropriate time for valve intervention. RECOVERY and EARLY-TAVR support intervening prior to symptoms or a decline in LVEF. However, their results may not be generalizable to all populations. In RECOVERY, participants had critical AS and were young (mean age 62.6 years), fit (mean EuroSCORE II: 0.9%) and mostly had bicuspid valve disease (60% of the participants) (286). In contrast, EARLY-TAVR included older participants (mean age 76 years) with degenerative valve disease (289). Neither of these trials looked at the presence of fibrosis as a marker of severity of AS, as considered in EVOLVED (288), which one might have expected to augment the benefits of

early intervention by targeting those at greatest risk of adverse disease outcomes. More work is therefore required to investigate the effects of early valve intervention in patients with asymptomatic AS in the wider population and using surrogate markers of severity other than the degree of valve obstruction. My study contributes to the existing literature by showing that, while milder compared to that seen in severe AS, the degree of adverse myocardial remodeling associated with moderate AS may be clinically important for the cardiovascular clinical outcomes in patients with moderate AS. Furthermore, the overlap of CMR and clinical parameters displayed in the scatter plots across the different participant groups highlights the difficulty applying clinical cut-offs to disease management guidelines and choosing potential imaging biomarkers to aid such a decision as this is a spectrum of disease with no clear groupings.

Moderate AS is associated with high rates of morbidity and all-cause mortality (290-294). An Australian cohort study following up over 3,000 patients with moderate AS and a mean age of 74 years reported a 5 year all-cause mortality of 57%, and cardiovascular mortality of 26%, after adjusting for age, sex, pre-existing systolic or diastolic dysfunction (228). This is similar to another published report by Yechoor et al, in which they retrospectively reviewed the records of consecutive patients with moderate AS in a Veteran's Affairs hospital. Their cohort also consisted of participants with a mean age of 74 years, followed-up for just under two years, after which approximately 56% of participants died. Unfortunately, the authors could not provide details on the cause of death, but they do explain that the cohort had substantial co-morbidity, including: 89% with hypertension, 18% with chronic obstructive pulmonary disease, and 60% with coronary artery disease (292). Whilst my study specifically excluded major co-morbidities, other than T2D, the results are in keeping with those of the literature,

showing substantial progression to severe stenosis. Furthermore, the strict inclusion criteria and size of my cohort likely explains the lack of documented mortality events akin to the literature. This is pertinent when considering that in their retrospective analysis of a cohort of moderate aortic stenosis patients over a mean follow-up time of 5.6 years, Bae *at al* described that patients with concomitant T2D were more likely to suffer from adverse outcomes, including cardiovascular death, systolic dysfunction and need for aortic valve intervention. Indeed, the presence of T2D was independently associated with adverse outcomes (294). Another study has quoted diabetes as being independently associated with a 46% greater risk of major adverse cardiovascular events (MACE), (hazard ratio 1.46 [95% CI, 1.08–1.96]; P=0.012). Other risk factors associated for MACE were elevated NTPro-BNP, atrial fibrillation and LV diastolic dysfunction (293). However, other studies in the literature suggest T2D is not associated with increased mortality in people with moderate AS, highlighting that this adverse interaction is not uniformly supported and may relate to other characteristics of the study populations, such as age, comorbidity and the 'severity' of diabetes (284, 295).

Current guidelines suggest that intervention for moderate AS may be considered in the presence of LV systolic dysfunction (226, 296, 297). Larger prospective serial studies and randomized trials are needed to better understand the mechanisms of the high cardiovascular and all-cause mortality rates in patients with moderate AS. In the meantime, we await the results of the PROGRESS and EXPAND TAVR II trials reviewing the benefits of early TAVR in moderate AS (298). Should these trials find positive outcomes, the data from my work may support further trials using perfusion imaging to prioritise valve intervention.

Limitations

There are several limitations to my study which should be acknowledged. The cross-sectional nature of the study means that causality of the observed differences cannot be inferred, and the small sample recruited at a single site increases the risk of bias and type I error. This means that my major findings should be extrapolated to other populations with caution, and also that validation studies will be important.

While obstructive coronary artery stenosis was excluded using X-ray coronary angiography in all patients with severe AS, the control group and the moderate AS group did not undergo anatomical coronary imaging. However, it must be noted that significant coronary artery disease was deemed to be unlikely in these cohorts supported by the absence of both myocardial infarction and regional stress perfusion defects on their imaging studies. It is also important to note that my data cannot be generalised to people with AS and significant coronary disease.

A larger study with a longer follow-up duration will be required to confirm the clinical significance of the cardiac remodeling findings to the high cardiovascular and all-cause mortality rates in patients with moderate AS. As an important biomarker of adverse cardiovascular clinical outcomes, plasma troponin may have provided valuable insights into subclinical myocardial injury, complementing my NTproBNP measurements.

2.5 CONCLUSIONS

Moderate and severe AS are both associated with concentric LV hypertrophy, myocardial energetic deficit, subendocardial hypoperfusion, and limitations in exercise capacity. Patients

with Severe-AS exhibit a more pronounced phenotype with worse LV concentric hypertrophy and contractile dysfunction, compared to Moderate-AS.

The progression of moderate to symptomatic severe AS is presaged by myocardial perfusion alterations. These results suggest that changes in perfusion with increasing duration of AS could be among the most sensitive indicators of disease progression. Larger multicentre longitudinal studies are needed to evaluate this.

Finally, whilst the presence of concomitant T2D and moderate AS is associated with increased mortality and morbidity, their coexistence does not seem to predict a more severe concentrically remodelled LV phenotype. The earliest sign of co-existence of the two pathologies may be microvascular dysfunction, as measured by MPR. Larger observational studies are needed to confirm this, whilst mechanistic studies are needed to explore the molecular correlates of myocardial abnormalities in people with severe aortic stenosis with or without diabetes.

3. Assessing the impact of T2D on severe AS using CMR and transcriptomics

3.1 INTRODUCTION

Chapter 2 used CMR to explore the LV myocardial phenotypic changes associated with moderate to severe aortic stenosis, along with the similarities and interactions with T2D. As previously explained, the surgical treatment of this pathology also provides an opportunity to assess the myocardial transcriptomic profile of diabetic heart disease.

Whilst percutaneous biopsy is possible, the most straightforward way of routinely acquiring myocardial samples for transcriptomics is via cardiothoracic surgery. This can facilitate biopsy of the left ventricular myocardium, providing highly relevant tissue, but with potential risks, including transient conduction disturbances and ventricular or supraventricular arrhythmias, chest pain, intramyocardial hematoma and cardiac tamponade (299-301). Therefore, most studies assess the right atrial appendage (RAA) which has less of an important functional role, and some of which may be routinely discarded at the time of surgery as the venous portal for cardio-pulmonary bypass (302, 303).

It has already been outlined that AS is the most common valve disease affecting the western world. It is estimated that the prevalence of severe AS in those aged over 75 is 3.4% in Europe and the United States (304). Although this disease is usually considered to affect the older population, this is not always the case, with higher incidence seen in the young for bicuspid aortic valves (304, 305).

The treatment strategies for AVR consist of SAVR or TAVR. An exceedingly rare option is that of balloon valvuloplasty.

The European Society of Cardiology guidelines suggest that in the presence of symptoms, or an LVEF <50%, patients with severe AS should receive a heart team evaluation to guide further management. Patients under the age of 75 who are considered 'low risk' (defined as STS-PROM/EuroSCORE II <4%) and also those unsuitable for TAVR are recommended to be considered for SAVR (297).

In a recently published meta-analysis of 7 randomised trials (with >8,000 patients) comparing SAVR to TAVR for the treatment of patients with severe AS, all-cause mortality following the two techniques was reported as 'similar', with 32.6% being quoted for elective TAVR vs 29.6% for SAVR, over a varying time period of 1.5-10 years, between the different studies. Importantly, the surgical risk profile at the time of assessment, was not shown to affect these results (interaction P value = 0.48). Similar results were shown for cardiovascular mortality (22.1% vs 19.5% for TAVR and SAVR respectively). TAVR, however, carried a significantly increased risk of post procedure pacemaker implantation, and moderate-severe paravalvular leak at follow-up (306).

Other literature has suggested that performing TAVR in those who would have been eligible for surgery may be detrimental. Alabaddi et al recently published work showing that the rate of TAVR in those aged <60 years in the US is rising exponentially, and that within this population, there was a 2.5-fold higher risk of all-cause mortality after 5 years vs SAVR (307). Similarly, in a cohort study published by Handa et al, all-cause mortality in patients treated with TAVR was quoted to reach close to 20%, despite the study group consisting of low risk patients with STS score <4%, (308).

The myocardial transcriptome in the context of diabetes remains an area that has not been extensively explored, with relatively few studies providing comprehensive insights into the molecular mechanisms involved (309). Even more scarce are investigations specifically examining the diabetic myocardial transcriptome in the presence of concomitant aortic stenosis (182), a condition that may further complicate disease progression and treatment outcomes. Understanding these molecular alterations is crucial, as it could shed light on key regulatory pathways affected by both diabetes and aortic stenosis. New research in this field has the potential to uncover novel biomarkers that may aid in early diagnosis, risk stratification, and therapeutic targeting, ultimately contributing to improved clinical management and patient outcomes.

This prospective study aimed to test the hypothesis that patients with concomitant T2D in the context of severe-AS will have a pronounced concentrically remodeled phenotype, more prominent than in patients with standalone severe AS. Furthermore, patients with concomitant disease will exhibit more pronounced regression of their remodeled phenotype post SAVR. Finally, the use of RNA sequencing from tissue biopsy samples taken from the RAA at the time of surgery, will define differentially expressed genes (DEGs) associated with T2D and phenotypic characteristics of severe AS and T2D.

3.2 METHODS

3.2.1 Study design and oversight

This single-centre, prospective case-control study complied with the Declaration of Helsinki and was approved by National Research Ethics Committees (ref:18/YH/0168 for the severe AS cohort and ref:18/YH/0168 for the healthy volunteers). The study was funded by the Wellcome Trust (Grant 207726/Z/17/Z) British Heart Foundation (RG/16/1/32092), NIHR Leeds BRC (NIHR203331) and the University of Leeds Erdheim Fellowship award. From the severe AS cohort outlined in Chapter 2, patients were subject to both SAVR and TAVR. Of the patients undergoing SAVR, all were consented for right atrial appendage biopsy during surgery. In addition to this, a further 13 patients undergoing SAVR for severe AS were also recruited. It is important to highlight that all patients with severe AS undergoing AVR had a baseline assessment (V1), prior to their valve intervention and returned for a second study visit at 6-12 months post procedure (V2). The two study visits themselves were identical, comprising of anthropometric measurements, 6 minute walk tests, CMR and phosphorus spectroscopy assessments. The precise protocol details can be found in *2.2 METHODS*.

3.2.2 Inclusion and exclusion criteria

These are identical to those described in*, 2.2.2 Inclusion criteria and 2.2.3 Exclusion criteria*.

3.2.3 Right atrial appendage biopsy

At the time of the aortic valve replacement operation, the surgeon conducting the study took a biopsy of the RAA at the time of cannula insertion for the use of cardio-pulmonary bypass.

The size of the biopsy was at the individual surgeon's discretion. If there was any concern that taking a biopsy would endanger the patient or hinder the procedure the surgeon did not proceed with it (this occurred in 2 cases). Samples were immediately immersed in a biopsy preservation solution (BIOPS) and transported on ice to the laboratory within 10-minutes of excision. They were stored at -80°C to allow for batch processing.

3.2.4 RNA extraction

Preparation of samples

All benches and work surfaces were cleaned with 'Thermo Fisher Scientific, RNase Away surface decontaminant' (cat no 21-402-178) to remove any RNases, DNases and DNA contamination. Right atrial appendage biopsy samples were cut to ~40mg and kept on ice until use.

RNA extraction

RNA extraction was conducted on using the New England Biolabs Monarch Total RNA Miniprep Kit (NETB2010). The kit consists of the following equipment as outlined in Table 3.1.

Table 3.1: Items included in the New England Biolabs Monarch Total RNA Miniprep Kit (NETB2010).

Name of equipment/reagent found in the kit	**Product Code Number**
Monarch gDNA Removal Columns	T2017
Monarch RNA Purification Columns	T2007
Monarch Spin Collection Tubes	T2118
Monarch DNA/RNA Protection Reagent (2X)	T2011
Monarch RNA Lysis Buffer	T2012
Monarch Proteinase K	T2001
Monarch Proteinase K Resuspension Buffer	T2002
Monarch DNase I Reaction Buffer	T2003
Monarch DNase I 275 U	T2004
Monarch DNase I Reaction Buffer	T2005
Monarch RNA Priming Buffer	T2013
Monarch RNA Wash Buffer (5X)	T2014
Monarch Nuclease-free Water	T2006

The initial extraction process consisted of sample disruption and homogenisation. To undertake this, each RAA sample was placed into a round bottom Eppendorf. DNA/RNA protective solution was then added (having been diluted with nuclease-free water (1:1 ratio). As per the manufacturer's protocol, 600 µL of the combined solution was required for each 40mg RAA sample. A stainless-steel bead was placed into the Eppendorf before transfer to the tissue lyser, which was used at 30Hz for 1 minute on three occasions. The stainless-steel bead was then removed, and 60µL of Protein K Reaction buffer and 30µL of Protein K was added to each sample. After briefly vortexing, the samples were incubated on a heat block for 5 minutes at 55°C. Afterwards, the samples were once again briefly vortexed, prior to being spun in the centrifuge (16,000g) for 2 minutes to pellet debris. The supernatant was then transferred to an RNase-free microfuge tube (and the pellet was discarded). An equal volume of RNA Lysis Buffer, ~690µL, was added to the supernatant, prior to vortexing again.

Samples then underwent the RNA binding and elution process. 700µL of the sample was transferred into a gDNA removal column. The sample was spun for 30 seconds at 16,000g and the flow through discarded. The gDNA removal column was then removed and an equal volume of 100% ethanol (approximately 700µL) was added. The two solutions were mixed thoroughly by pipetting. 700µL of the combined solution was then placed in an RNA purification column. The sample was once again centrifuged for 30 seconds at 16,000g and the flow through discarded. This step was repeated for the remaining 700µL of solution.

The optional DNase treatment step was then performed to remove any residual gDNA. This was undertaken by adding 500µL RNA Wash buffer to all RNA purification columns. The samples were centrifuged for 30 seconds at 16,000g and the flow through discarded. A solution containing 5µL DNase I and 75µL DNase I reaction buffer was pipetted directly on top of the column matrix of each sample. All samples were then incubated for 15 minutes at room temperature, prior to adding 500µL RNA priming buffer. Samples were centrifuged for a further 30 seconds at 16,000g and flow through was discarded.

The RNA binding and elution step was then continued by adding 500µL RNA wash buffer and centrifuging for 30 seconds at 16,000 g. Flow through was discarded prior to adding another 500µL RNA wash buffer and spinning for 2 minutes at the same force. Flow-through was discarded and the RNA purification column was transferred to an autoclaved Eppendorf. Finally, 60µL nuclease-free water was directly added to the centre of the column matrix and the samples centrifuged at 16,000g for a final 30 seconds. The column matrix was removed and the final flow-through was kept.

3.2.5 RNA Clean Up

The extracted RNA samples were then subject to RNA clean up, using the Zymo Research 'RNA Clean & Concentrator-5' kit (DNase Included, Cat No. R1013), which included all the equipment outlined in Table 3.2.

Table 3.2: Contents of Zymo Research 'RNA Clean & Concentrator-5' kit

Solution	**Other Equipment**
RNA binding buffer	Zymo-Spin IICR spin column
RNA prep buffer	Collection tubes
RNA wash buffer	
DNase/RNase-Free Water	

At the start of the procedure, two solutions were made. The RNA buffer was prepared by adding 48ml of 100% ethanol to the 12 ml RNA Wash Buffer concentrate (R1017). The DNase I treatment was then made up in a 1:1 ratio of DNase I and DNA digestion buffer. 10µl of the DNase I treatment was added to each RNA sample and mixed well before incubation at room temperature for 15 minutes. 100µl of RNA binding buffer was then added to each sample and mixed well. This was followed by 150µl of 100% ethanol and mixed well prior to the sample being loaded onto the Zymo-Spin™ IC column. Centrifugation was then undertaken at 14,000g for 30 seconds and the flow through was discarded. 400µl of RNA Prep buffer was then added to each column prior to further centrifugation at 14,000g for 30 seconds. The flow-through was then once again discarded and 700µl of RNA wash buffer added to each column, followed by centrifugation at 14,000g for 2 minutes. The Zymo-Spin™ IC column was then transferred to a clean 1.5ml microcentrifuge tube. Finally, 15µl of DNase/RNase-free water was added to

each column. This was left to stand for 1 minute and then a final centrifugation was undertaken at 14,000g for 30 seconds. Samples were then stored at -80^{o}C.

3.2.6 Bulk RNA Sequencing Analysis

Sample Processing

Bulk total RNA-sequencing (RNA-seq) of 100 base pair single-end reads was performed by the University of Leeds Genomics Facility using Illumina NextSeq 2000 of rRNA depleted libraries. An RNA integrity number (RIN) of ≥5.8 was deemed acceptable for RNA sequencing analysis, in keeping with the threshold used in other previously published data (310). Within MobaXTerm of the University of Leeds' high performance computing cluster (ARC4). The raw counts were initial underwent quality control, using the software Fast QC (311, 312). Trimming to remove low quality bases (those <20base pairs (bp)) and adapter sequences was performed via Trim Galore (313). Any result comprising of <20 bp post trimming was also removed. This process was followed by alignment to the human reference genome, GRCh38, using STAR aligner (314). During this process the length of the overhang bases used when generating the splicing junction database from annotation files was set to 99. Finally, StringTie was used for transcript assembly and quantification of raw gene counts due to its ability to perform a reference guided assembly of transcriptomes and quantify transcripts' expression through read counts normalisation metrics and its capability to identify newly assembled transcripts in the genome (315).

Sample Analysis

Using R version 4.2.0, the package DESeq2 was used to define differentially expressed genes (DEGs) (316). For this analysis, count data was used with an associated RIN of ≥5.8 (as described above) and the aassociated clinical data used was that collected at the time of the patients' study visits. Genes with <10 counts were excluded prior to the DESeq2 analyses to reduce false positive signals likely to arise from these. Batch correction was undertaken and adjustments for the confounding variables of gender, RIN, batch number, BMI, age and T2D status was performed. It is important to note that all the previously mentioned variables were converted into categorical variables to ensure compatibility with the package. RIN categories were: "4-4.9", "5-5.9", "6-6.9", "7-7.9", labelled as: 4, 5, 6, 7, 8 respectively. The samples' batch number was 1,2 or 3, according to the order to processing. BMI data was categorised as per the WHO definitions for "Underweight", "Normal", "Overweight", "Obese", using the cut-offs: <18.5, 18.5-24.9, 25-29.9 or ≥30 (317). Age categories consisted of: "<50", "50s", "60s", "70s", "80+". Prior to further analysis, the counts obtained from the samples were normalised and transformed to variance stabilised expression levels. The PCAtools package was used for the creation of scree and volcano plots, principal component analysis (PCA) loading plots and Eigencor graphs (318).

Evaluation of the PCA loading and Eigencor plots allowed for a further evaluation of possible CMR markers which could be investigated further. Further DESeq2 analysis was therefore performed with the same covariates described above and with the patient cohort being subdivided into quartiles depending on their measurements of a specific CMR variable. Patients in top quartile were compared to those in the bottom quartile and a list of DEGs was extracted. Log fold-change shrinkage with Apeglm was applied to reduce false positive signals

from weakly expressed genes (319). Genes with a false discovery rate (FDR)-adjusted p value of <0.05 and a log2 fold change (lfc) of >0.5 or <-0.5 were selected as hits to minimise false positives and focus on important biological differences, respectively.

All DEGs were run through GProfiler, a bioinformatics tool used for functional enrichment analysis of gene lists (320). This allows for gene ID conversion and gene enrichment analysis. During the functional profiling of genes, a Benjamini-Hochberg FDR significance threshold of <0.05 was undertaken.

3.2.7 Statistical analysis

Statistical analysis of CMR data was performed using GraphPad Prism software (version 10.0.3). All data were checked for normality using the D'Agostino-Pearson Test. Data are presented as mean ±95% confidence intervals (when normally distributed) or medians with corresponding IQR (if nonparametric continuous variables). Categorical data are presented as numbers and percentages and compared with the Pearson χ^2 test. All comparisons between >2 groups were performed by 1-way ANOVA with post hoc Bonferroni corrections. Differences in nonparametric variables were assessed using a Kruskal-Wallis test. Student t-tests were used for comparison of normally distributed datasets and Mann-Whitney U tests were used for non-parametric tests where data were obtained for only two groups. Bivariate correlations were performed using Pearson's or Spearman's method, as appropriate. A 2-sided *P* value of <0.05 was applied as indicating threshold of significance.

3.3 RESULTS

3.3.1 Participant demographics and clinical characteristics

Of the original 52 patients with severe symptomatic AS awaiting AVR presented in Chapter 2, 39 underwent SAVR and were included in this sub-analysis (the remainder having TAVR). The full consort diagram of patient recruitment Figure 2.9.

There were no significant differences in the age or sex distributions in the patients with severe AS and the controls, participants without AS but with and without T2D for CMR comparisons (Table 3.3). As expected, the patients with severe AS, were more symptomatic than their age and sex matched controls, with no participants in that that group identifying themselves as NYHA Class I (Table 3.3).

The controls were matched to the Severe-AS groups with regards to baseline characteristics of systolic and diastolic blood pressure, heart rate, serum creatinine and hemoglobin concentration. There were no differences in the comparison of DM to NODM groups for the same variables, with the only exception being heart rate, where controls with T2D exhibited higher resting heart rates than controls without T2D (Table 3.3).

Patients with severe-AS but no T2D had significantly higher BMI measurements than controls without T2D (Severe-AS NODM: 28 (27,30) vs controls NODM: 25 (24, 27) kg/m^2, P= 0.01). A numerical difference was also seen for the T2D cohorts, once again with patients with concomitant severe-AS being heavier (Severe-AS DM: 29 [25, 33] vs controls DM: 23 [22, 29] kg/m^2, P= 0.06), but this did not reach statistical significance (Table 3.3).

Participants with T2D had significantly higher fasting glucose and HbA1c; there was no difference in the level of glycaemic control between patients with coexisting T2D and severe-AS and controls with T2D only (Table 3.3).

Finally, as seen in Table 3.3, patients with Severe-AS had significantly higher NTproBNP levels than the matched controls, irrespective of co-existent T2D (Severe AS DM: 499 [273, 2015] vs controls DM: 160 [35, 207] ng/L, P=0.0128; and Severe AS NODM: 193 [148, 945] vs controls NODM: 95 [71, 159] ng/L, P= 0.0005)

Table 3.3: Clinical characteristics and biochemistry of controls and patients with severe AS at baseline

Variable	Controls DM n= 5	Severe-AS DM V1 n= 12	Control DM vs Severe AS DM, P value	Controls NODM n= 18	Severe-AS NODM V1 n= 27	Control NODM vs Severe-AS NODM, P value	Control DM vs Control NODM, P value	Severe-AS DM vs Severe-AS NODM, P value
Age, years	62 [49, 74]	68 (62, 74)	0.4842	68 (65, 70)	69 (66, 72)	0.6753	0.3339	**0.0176**
Female, n (%)	2 (40)	4 (33)	0.7933	10 (56)	7 (26)	**0.0446**	0.5379	0.6352
BMI, kg/m²	23 [22,29]	29 [25, 33]	0.0603	25 [23, 28]	28 (27, 30)	**0.0146**	0.4033	0.7179
Heart rate, bpm	67 [63, 69]	71 (63, 78)	0.6857	59 (55, 63)	70 (65, 75)	**0.0016**	**0.0822**	0.1116
Systolic BP, mmHg	134 [129, 154]	137 (123,151)	0.9267	129 (122, 138)	130(123, 138)	0.8414	0.1873	0.4098
Diastolic BP, mmHg	81 [73,85]	75 (68,82)	0.2410	77 (74, 80)	79 (74, 83)	0.5572	0.3511	0.2760
Creatinine, umol/L	63 [57,70]	83 (71, 95)	0.0519	69 (64, 75)	75 (70, 80)	0.1485	0.3352	0.5146
Haemoglobin, g/L	139 [124,151]	139 (131,146)	0.9782	146 (139, 153)	146(140, 152)	0.9302	0.2804	0.7100
TG, mmol/L	1.1 [0.9, 2.5]	2.4 (1.3, 3.4)	0.5220	1.4 (1.2, 1.6)	1.2 (0.9, 1.5)	0.3886	0.9492	0.6254
HbA1c, mmol/mol	54 [47,55]	51 (47,54)	0.5572	37 (36, 38)	38 (36, 39)	0.6932	**0.0001**	**0.0003**
Glucose, mmol/L	7.7 [6.7,10.9]	8.4 (6.7, 10.1)	0.7617	4.9 (4.8, 5.1)	5.1 (4.9, 5.2)	0.2256	**<0.0001**	**0.0021**
NT- proBNP, ng/L	160 [35, 207]	499 [273, 2015]	**0.0128**	92 [65, 158]	193[148, 945]	**0.0003**	0.9604	0.5098
Medications								
ACEi	-	4 (33)	0.1399	-	6 (22)	**0.0317**	-	0.4633
ARB	-	2 (17)	0.3311	-	2 (7)	0.2375	-	0.5123
Beta blocker	-	8 (67)	**0.0121**	-	9 (33)	**0.0062**	-	0.0527
CCB	2 (40)	2 (17)	0.3014	-	4 (15)	0.0871	**0.0050**	0.8824
Loop diuretic	1 (20)	3 (25)	0.8247	-	-	-	**0.0524**	**0.0068**
Statin	2 (40)	6 (50)	0.7066	3 (17)	15 (56)	**0.0091**	0.2631	0.7481
Antiplatelets	-	2 (17)	0.3311	-	9 (33)	**0.0062**	-	0.2857
DOAC/VKA	-	4 (33)	0.1399	-	3 (11)	0.1147	-	0.0951
Metformin	4 (80)	6 (50)	0.2521	-	-	-	**<0.0001**	**<0.0001**
Sulfonylurea	-	2 (17)	0.3311	-	-	-	-	**0.0294**
GLP-1RA	-	-	-	-	-	-	-	-
SGLT2i	-	-	-	-	-	-	-	-
AS Clinical Details								
TTE Vmax, m/s	-	4.9 (4.1, 4.8)	-	-	4.5 (4.2, 4.7)	-	-	0.2228
Bicuspid AV, n (%)	-	6(50)	**0.0493**	-	11 (41)	**0.0018**	-	0.5904
NYHA Class, (%)								
I	5 (100)	2 (17)	**0.0015**	18 (100)	-	**<0.0001**	-	**0.0294**
II	-	5 (42)	0.0858	-	20 (74)	**<0.0001**	-	0.0515
III	-	5 (42)	0.1977	-	7 (26)	**0.0385**	-	0.3256
IV	-	-	-	-	-	-	-	-
6 min walk test, m	-	392[300, 450]	-	525[495,555]	428[358,495]	**<0.0001**	-	0.5549
Cardiovascular Past Medical History								
Stroke / TIA, n (%)	-	1(8)	0.5058	-	2 (7)	0.2375	-	0.9202
PAF, n (%)	-	2 (17)	0.3311	-	4 (15)	0.0871	-	0.8824
Hyperlipidemia, n (%)	1(20)	6 (50)	0.2521	3 (17)	11 (41)	0.0875	0.8619	0.5904

Normally distributed continuous variables are expressed as mean (±95% confidence intervals); nonparametric continuous variables are expressed as median [IQR]; and categorical variables are expressed as counts (percent). P signifies p value for comparisons across the groups with T-tests for normally distributed datasets and Mann-Whitney test for non-parametric values.

AS, indicates aortic stenosis; BMI, body mass index; TG, triglycerides; HbA1c, glycemic hemoglobin; NT-proBNP, N-terminal-pro hormone b-type natriuretic peptide; ACEI, angiotensin converting enzyme inhibitor; ARB, angiotensin receptor blocker; CCB, calcium channel blocker; DOAC, direct oral anticoagulant; GLP-1RA, glucagon-like peptide-1 receptor agonist; SGLT2i, sodium glucose co-transporter-2 inhibitor; TTE, trans-thoracic echocardiogram; V max, peak aortic forward flow velocity; AV indicates aortic valve; T2D, type 2 diabetes; TIA, transient ischemic attack; PAF, paroxysmal atrial fibrillation; STS, society of thoracic surgeons.

y, indicates years; n, number; kg, kilograms; m2, meters squared; bpm, beats per minute; mmHg, millimeters of mercury; umol/L, micromoles per liter; g/L, grams per liter; mmol/L, millimoles per liter; mmol/mol, millimoles per mole; ng/L, nanograms per liter; m/s, meters per second; m, meters.

3.3.2 Cardiovascular magnetic resonance and ^{31}Phosphorus-magnetic resonance spectroscopy findings

The differences in cardiac remodeling between patients with severe AS and controls have already been shown in *2.3.2 Cardiovascular magnetic resonance and 31Phosphorus-magnetic resonance spectroscopy findings*. In this chapter the focus will be on the combination of diabetes and severe-AS, including CMR assessment pre- and post-SAVR.

3.3.3 The effect of T2D on Severe-AS at baseline – CMR and 31P-MRS findings

Cardiac remodeling

Within the current cohort, patients with severe AS (with and without T2D) displayed more concentric LV remodeling than their age and sex matched controls. In the presence of concomitant T2D, this concentricity was more pronounced but did not reach statistical significance when compared to AS patients without T2D. In particular, such changes were seen in: LV mass indexed to BSA (Severe-AS NODM: 76 (69, 83), vs controls NODM: 39 [36,49] g/m^2, P= 0.0005) and LV concentricity index (Severe-AS NODM: 1.01 [0.77, 1.21] vs controls NODM: 0.55 (0.52, 0.58) g/mL, P= <0.0001). LV max wall thickness however was, statistically higher in both the T2D and NODM groups in the presence of severe-AS [(Severe-AS DM: 14.1 (12.2,16.0) vs controls DM: 9.5 [8.8,11.9]mm, P= 0.0127) and (Severe-AS NODM: 14.7 (13.5, 15.8) vs controls NODM: 9.9 (9.3, 10.5)mm, P= <0.0001)], Table 3.4.

Cardiac energetics and perfusion and function

The cardiac energetics index was numerically lower in patients with severe-AS irrelevant of T2D status, but these differences did not reach statistical significance, (Severe-AS DM: 1.6

[1.3, 1.8] vs controls DM: 1.9 [1.6,2.3], P= 0.1274; and Severe-AS NODM: 1.7 [1.3, 2.0] vs controls NODM: 2.1 [1.8, 2.5], P= 0.1373; Table 3.4).

Layer specific perfusion differences cannot be commented upon for the comparison of controls with T2D and patients with severe-AS and concomitant T2D, due to a change in protocol not permitting the acquisition of this data. However, global Stress MBF was significantly impaired in patients with both diseases (Severe-AS DM: 1.3 [1.0, 1.7] vs controls DM: 2.2 [2.0,2.3] ml/min/g, P= 0.0039) and rest MBF and MPR were also numerically worse, representing worse perfusion within this cohort (Table 3.4). Patients without T2D, but with severe AS exhibited significantly worse global and layer specific perfusion across stress MBF, rest MBF and MPR (Table 3.4).

Table 3.4: CMR and 31P-MRS findings of all patients with severe AS with and without concomitant T2D at baseline (V1).

Variable	Control DM n= 5	Severe-AS DM V1 n= 12	Control DM vs Severe-AS DM, P value	Controls NODM n= 18	Severe-AS NODM V1 n= 27	Control NODM vs Severe-AS NODM, P value	Control DM vs Control NODM, P value	Severe-AS DM vs Severe-AS NODM, P value
LV end-diastolic volume indexed to BSA, mL/m²	79 [69,93]	82 (70, 94)	0.6787	77 [66,85]	75 (70, 80)	0.6256	0.7352	0.1887
LV end-systolic volume indexed to BSA, ml/m²	34 [25,35]	34 (27, 40)	0.5728	29 [24,34]	26 (23, 30)	0.1671	0.4381	**0.0260**
LV mass, g	116 [74,130]	165 (124, 206)	0.0753	70 [61,104]	152 (135, 169)	**<0.0001**	0.1925	0.4538
LV mass indexed to BSA, g/m²	61 [44,63]	75 (55, 95)	0.2977	39 [36,49]	76 (69, 83)	**0.0005**	0.0914	0.9064
LV mass to LV end-diastolic volume, g/mL	0.67 [0.57,0.78]	0.93 (0.77, 1.09)	0.0400	0.55 (0.52, 0.58)	1.01 [0.77, 1.21]	**<0.0001**	**0.0389**	0.5272
LV stroke volume indexed to BSA, ml/m²	47 [44,59]	49 (41,56)	0.8385	46 (42,50)	48 [45, 51]	0.9863	0.3535	0.7426
LV ejection fraction, %	62 [58,66]	59 (54, 64)	0.3550	62 (60, 69)	65 (62, 69)	0.2242	0.7869	0.0545
LV maximal wall thickness, mm	9.5 [8.8,11.9]	14.1 (12.2,16.0)	**0.0127**	9.9 (9.3, 10.5)	14.7 (13.5, 15.8)	**<0.0001**	0.7185	0.5957
LA biplane end-diastolic volumes, mL	82 [65,86]	116 (82, 149)	**0.0280**	75 (63, 86)	73 [60, 117]	0.7250	0.5845	0.2306
LA biplane end-systolic volumes, mL	28 [19,42]	86 (48,123)	0.0080	38 (28,47)	41 [29, 87]	0.1930	0.3892	**0.0490**
Biplane LA EF, %	64 [59,71]	31 (19,43)	**0.0007**	52 (46, 58)	42 (36, 48)	**0.0294**	0.0186	0.0587
GLS, %	19 [16,22]	13 [12,14]	**0.0121**	20 [17,23)	15 (14, 17)	**0.0019**	0.9635	0.1472
Native T1, (ms)	1178 [1157,1260]	1303 (1269,1338)	**0.0027**	1278 (1264,1293)	1310 [1280, 1327]	**0.0102**	**0.0114**	0.9866
Extra cellular volume fraction, (%)	0.25 [0.20, 0.30]	0.23 (0.22, 0.25)	>0.9999	0.23 (0.22, 0.24)	0.22 (0.22, 0.23)	0.2280	0.4342	0.1668
LGE, (%)	0 [0,0]	3.2 [1.5, 13.7]	**0.0050**	0 [0,0]	1.8 [0.7, 6.2]	<0.0001	0.5680	0.2944
PCr/ATP	1.9 [1.6,2.3]	1.6 (1.3, 1.8)	0.1274	2.1 (1.8, 2.5)	1.7 [1.3, 2.0]	0.1373	0.4875	0.5116
Stress MBF, ml/min/g	2.2 [2.0,2.3]	1.3 (1.0, 1.7)	**0.0039**	2.0 (1.8, 2.2)	1.4 [1.2, 1.8]	**0.0055**	0.3670	0.2244
Endo MBF Stress, ml/min/g	-	1.2 [0.8,1.6]	-	2.0 (1.8, 2.3)	1.2 [0.9, 1.6]	**<0.0001**	-	0.6999
Epi MBF Stress, ml/min/g	-	1.4 [1.0, 1.9]	-	2.1 (1.8, 2.3)	1.6 [1.4, 2.0]	**0.0203**	-	0.1536
Endo/Epi MBF Stress Ratio	-	0.8 [0.8, 1.0]	-	1.0 [0.9,1.1]	0.8 (0.7, 0.8)	**<0.0001**	-	0.2259
Rest MBF, ml/min/g	0.7 [0.6,1.1]	0.6 (0.5, 0.7)	0.1094	0.6 [0.5,0.7]	0.6 [0.6, 0.8]	**0.0155**	0.0085	0.3816
Endo/Epi MBF Rest ratio	-	1.1 [1.0,1.1]	-	1.1 (1.1, 1.1)	1.0 (1.0, 1.0)	**<0.0001**	-	0.0561
MPR	2.7 [2.2, 3.3]	2.1 (1.7, 2.4)	0.0653	3.4 (2.9, 3.8)	2.3 [1.8, 2.7]	**<0.0001**	0.1296	0.2904
Endo MPR	-	1.7 [1.4, 2.1]	-	3.2 (2.8, 3.6)	1.9 [1.4, 2.1]	**<0.0001**	-	0.8823
Epi MPR	-	2.2 [1.8, 2.8]	-	3.6 (3.2, 4.0)	2.4 [2.0, 2.8]	**0.0002**	-	0.6565
Increase in RPP, %	84 [78,91]	19 [9, 75]	0.1143	28 (21, 34)	26 (20, 31)	0.6226	**0.0117**	0.8311

Normally distributed continuous variables are expressed as mean (±95% confidence intervals); nonparametric continuous variables are expressed as median [IQR]; and categorical variables are expressed as counts (percent). P signifies p value for comparisons across the groups with T-tests for normally distributed datasets and Mann-Whitney test for non-parametric values.

LV indicates left ventricle; BSA, body surface area; SV, stroke volume; RV, right ventricle; LA EF, left atrial ejection fraction; GLS, global longitudinal shortening; LGE, late gadolinium enhancement; PCr/ATP ratio phosphocreatine to adenosine tri-phosphate ratio; Endo, endocardial; MBF, myocardial blood flow; Epi, epicardial; MPR, myocardial perfusion reserve; RPP, rate pressure product.
Ml/m2, indicates milliliters per square meter; g, grams; g/m2, grams per square meter; g/ml, grams per milliliter; mm, millimeter; mL, milliliter; ms, millisecond; mil/min/g, milliliters per minute per gram.

Cardiac remodeling and function post AVR

There was a small dropout rate of patients that did not attend their 6-12 month post-operative study visit (V2) after having completed pre-operative visit (V1) and surgery. This comprised 3 patients (25%) in the T2D group and 3 patients (11%) in the NODM group. The reason for 'dropping out' in most cases was patient choice, with one patient not completing V2 as they were unable to fit into the scanner due to weight gain. To consider the effects of myocardial remodeling post AVR in more detail, the following section will focus on the patients who attended both for visit 1 and 2.

LV concentricity regressed after AVR in both the T2D and the NODM cohorts. Significant differences were seen in the NODM cohort for LV mass-indexed to BSA (Severe-AS NODM V1: 78 (71, 85) vs Severe-AS NODM V2: 62 (58, 66)g/m^2, P<0.0001) and LV max wall thickness (Severe-AS NODM V1: 15.0 (13.8, 16.2) vs Severe-AS NODM V2: 13.0 (12.0, 14.0)mm, P<0.0001) with additional numerical differences seen in the LV concentricity index (Severe-AS NODM V1: 1.05 (0.91, 1.19) vs Severe-AS NODM V2: 0.89 (0.78, 0.99)g/mL, P=0.0144) shown in Table 3.5. Numerical differences in keeping with regression of concentricity were also seen in the DM groups, but the same parameters did not reach statistical significance (Table 3.5).

LV function measured by ejection fraction did not change post AVR for either the DM or the NODM groups, (Severe-AS DM V1: 58 (52, 64) vs Severe-AS DM V2: 60 (48, 71)%, P= 0.77 and (Severe-AS NODM V1: 66 (62,69) vs Severe-AS NODM V2: 65 (60, 69)% , P= 0.64). Whilst GLS was impaired at baseline for all patients, and numerically was even lower in the patients with concomitant T2D, this improved post-intervention for both groups, though did not reach

statistical significance (Severe-AS DM V1: 13 [10,16] vs Severe-AS DM V2: 17 [13,22]%, P= 0.38 and (Severe-AS NODM V1: 15 (14, 17) vs Severe-AS NODM V2: 17 (15,19)%, P= 0.32), as shown in Table 3.5.

The markers of fibrosis, native T1 and ECV, decreased post-AVR in NODM patients (Severe-AS NODM V1: 1312 [1273, 1326] vs Severe-AS NODM V2: 1306 [1274, 1339]ms, P= 0.0034 and Severe-AS NODM V1: 0.22 (0.21, 0.23) vs Severe-AS NODM V2: 0.24 (0.23, 0.25)%, P<0.0001, respectively). By contrast, native T1 numerically decreased and ECV numerically increased in patients with Severe-AS and coexistent T2D post AVR, (Severe-AS DM V1: 1301 (1261, 1341) vs Severe-AS DM V2: 1295 (1250, 1340)]ms, P= 0.34; and Severe-AS DM V1: 0.23 (0.22, 0.25) vs Severe-AS DM V2: 0.25 (0.21, 0.29)%, P= 0.28 respectively), as shown in Table 3.5.

As per eligibility criteria, all patients with LV scar on LGE at baseline assessment had a non-infarct pattern. Moreover, as previously stated, this did not include isolated RV insertion point hyperenhancement, as this is considered a normal variant (264-266). Subendocardial scar suggesting the presence of a prior MI was an exclusion criterion, although this was not required in this study cohort. Irrelevant of coexisting diabetes status, there was regression of LGE scarring in both groups post AVR, though once again this did not reach statistical significance, (Severe-AS DM V1: 3.7 [1.5, 14.3] vs Severe-AS DM V2: 0.6 [0, 4.4]% , P= 0.2188 and Severe-AS NODM V1: 2.7 [1.0, 6.5] vs Severe-AS NODM V2: 1.2 [0, 4.1]% , P= 1.2 [0, 4.1]; Table 3.5).

Cardiac energetics and perfusion post AVR

With the loss of participants, in the serial analysis of PCr/ATP changes post AVR, the numerical improvement in cardiac energetics index was only evident in the DM group, and a small numerical decline was seen in the NODM group given the initially normal values within the AS group without DM, (Severe-AS DM V1: 1.6 (1.2, 1.7) vs Severe-AS DM V2: 1.9 [1.7, 2.0], P=0.25 and Severe-AS NODM V1: 1.6 [1.1, 2.1] vs Severe-AS NODM V2: 1.8 (1.5, 2.0), P= 0.3) Table 3.5).

Post AVR, patients showed improvements to all indices of perfusion irrelevant of co-existing T2D, although in most cases these were not statistically significant. Global adenosine-stress MBF (Severe-AS DM V1: 1.3 [1.1, 1.8] vs Severe-AS DM V2: 1.7 [1.4, 1.8]ml/min/g, P=0.22; and Severe-AS NODM V1: 1.5 [1.3, 1.8] vs Severe-AS NODM V2: 1.5 [1.1, 2.2]ml/min/g, P= 0.83), rest global MBF (Severe-AS DM V1: 0.6 (0.5, 0.7) vs Severe-AS DM V2: 0.7 (0.6, 0.8)ml/min/g, P=0.13; and Severe-AS NODM V1:0.6 [0.6,0.7] vs Severe-AS NODM V2: 0.6 [0.5, 0.7]ml/min/g, P= 0.004) and global MPR (Severe-AS DM V1: 2.1 [1.6, 2.4] vs Severe-AS DM V2: 2.4 [2.0, 3.2], P=0.3; and Severe-AS NODM V1: 2.4 [2.0, 2.7] vs Severe-AS NODM V2: 2.6 [2.1, 3.5], P= 0.33; Table 3.5).

Statistically significant layer-specific perfusion changes were also evident in the NODM subgroup when assessing the Endo/Epi MBF Stress Ratio (Severe-AS NODM V1: 0.8 [0.7, 0.9] vs Severe-AS NODM V2: 0.8 [0.8, 1.0], P <0.0001) and Endo/Epi MBF Rest ratio (Severe-AS NODM V1: 1.0 (1.0, 1.0) vs Severe-AS NODM V2: 1.1 (1.1, 1.1), P <0.0001; Table 3.5). Global changes to perfusion parameters are graphically depicted in Figure 3.1 and full numerical differences can be seen in Table 3.5.

Table 3.5: CMR and 31P-MRS findings of patients with severe AS with and without concomitant T2D at baseline (V1) who returned at 6-12 months post SAVR (V2).

Variable	Severe-AS DM V1 n= 9	Severe-AS DM V2 n= 9	Severe-AS DM V1 vs V2 P value	Severe-AS NODM V1 n= 24	Severe-AS NODM V2 n= 24	Severe AS NODM V1 vs V2 P value
LV end-diastolic volume indexed to BSA, mL/m²	78 (55, 101)	71 (50, 91)	0.3437	74 (70,79)	67 (62, 72)	**0.0031**
LV end-systolic volume indexed to BSA, ml/m²	34 (26, 43)	27 (19, 36)	0.1942	26 (22, 29)	24 (20, 27)	0.1383
LV mass, g	151 (106, 197)	122 (100, 145)	0.1834	157 (139,175)	124 (112, 138)	**<0.0001**
LV mass indexed to BSA, g/m²	69 (46, 91)	66 (42, 90)	0.7203	78 (71, 85)	62 (58, 66)	**<0.0001**
LV mass to LV end-diastolic volume, g/mL	0.87 (0.69, 1.05)	0.88 (0.78, 0.98)	0.8331	1.05 (0.91, 1.19)	0.89 (0.78, 0.99)	**0.0144**
LV stroke volume indexed to BSA, ml/m²	47 (37,56)	39 (30, 48)	0.1213	48 (45, 52)	44 (42, 47)	**0.0091**
LV ejection fraction, %	58 (52, 64)	60 (48, 71)	0.7670	66 (62,69)	65 (60, 69)	0.6415
LV maximal wall thickness, mm	14.4 (12.7,16.1)	13.9 (12.1, 15.8)	0.3949	15.0 (13.8, 16.2)	13.0 (12.0, 14.0)	**<0.0001**
LA biplane end-diastolic volumes, mL	122 (79, 165)	115 (81, 149)	0.4684	95 (72, 119)	86 (66, 106)	0.1918
LA biplane end-systolic volumes, mL	95 (48,141)	83 (47, 119)	0.3365	65 (41, 89)	60 (39, 81)	0.3975
Biplane LA EF, %	27 (13,41)	30 (18, 43)	0.6035	42 (35, 49)	37 (29, 46)	0.1246
GLS, %	13 [10,16]	17 [13,22]	0.3750	15 (14, 17)	17 (15,19)	0.3245
Native T1, (ms)	1301 (1261, 1341)	1295 (1250, 1340)	0.3437	1312 [1273, 1326]	1306 [1274, 1339]	**0.0034**
Extra cellular volume fraction, (%)	0.23 (0.22, 0.25)	0.25 (0.21, 0.29)	0.2753	0.22 (0.21, 0.23)	0.24 (0.23, 0.25)	**<0.0001**
LGE, (%)	3.7 [1.5, 14.3]	0.6 [0, 4.4]	0.2188	2.7 [1.0, 6.5]	1.2 [0, 4.1]	0.0224
PCr/ATP	1.6 [1.2, 1.7]	1.9 [1.7, 2.0]	0.2500	1.6 [1.1, 2.1]	1.8 (1.5, 2.0)	0.3125
Stress MBF, ml/min/g	1.3 [1.1, 1.8]	1.7 [1.4, 1.8]	0.2188	1.5 [1.3, 1.8]	1.5 [1.1, 2.2]	0.8288
Endo MBF Stress, ml/min/g	1.3 [1.0,1.7]	1.5 [1.1, 2.0]	0.1875	1.3 [1.0,1.7]	1.4 [1.0, 1.9]	0.4749
Epi MBF Stress, ml/min/g	1.4 [1.0, 2.0]	1.8 [1.4, 2.0]	0.4375	1.6 [1.4, 2.0]	1.6 [1.0, 2.3]	0.7750
Endo/Epi MBF Stress Ratio	0.8 [0.8, 1.0]	0.9 [0.8, 1.0]	0.4375	0.8 [0.7, 0.9]	0.8 [0.8, 1.0]	**<0.0001**
Rest MBF, ml/min/g	0.6 (0.5, 0.7)	0.7 (0.6, 0.8)	0.1263	0.6 [0.6,0.7]	0.6 [0.5, 0.7]	**0.0042**
Endo/Epi MBF Rest ratio	1.1 [1.0,1.2]	1.1 [1.0,1.2]	0.8750	1.0 (1.0, 1.0)	1.1 (1.1, 1.1)	**<0.0001**
MPR	2.1 [1.6, 2.4]	2.4 [2.0, 3.2]	0.2969	2.4 [2.0, 2.7]	2.6 [2.1, 3.5]	0.3300
Endo MPR	2.0 [1.3, 2.2]	2.4 [2.9, 3.1]	0.1250	2.0 [1.5, 2.2]	2.3 [1.9, 3.0]	0.1726
Epi MPR	2.4 [1.8, 3.0]	3.1 [2.4, 4.0]	0.1250	2.5 [2.1, 2.9]	2.9 [2.2, 3.9]	0.2958
Increase in RPP, %	25 [8, 92]	10 [10, 15]	0.5000	24 (18, 30)	21 (14, 28)	0.6279

Normally distributed continuous variables are expressed as mean (±95% confidence intervals); nonparametric continuous variables are expressed as median [IQR]; and categorical variables are expressed as counts (percent). P signifies p value for comparisons across the groups with T-tests for normally distributed datasets and Mann-Whitney test for non-parametric values.

LV indicates left ventricle; BSA, body surface area; SV, stroke volume; RV, right ventricle; LA EF, left atrial ejection fraction; GLS, global longitudinal shortening; LGE, late gadolinium enhancement; PCr/ATP ratio phosphocreatine to adenosine tri-phosphate ratio; Endo, endocardial; MBF, myocardial blood flow; Epi, epicardial; MPR, myocardial perfusion reserve; RPP, rate pressure product.
Ml/m2, indicates milliliters per square meter; g, grams; g/m2, grams per square meter; g/ml, grams per milliliter; mm, millimeter; mL, milliliter; ms, millisecond; mil/min/g, milliliters per minute per gram.

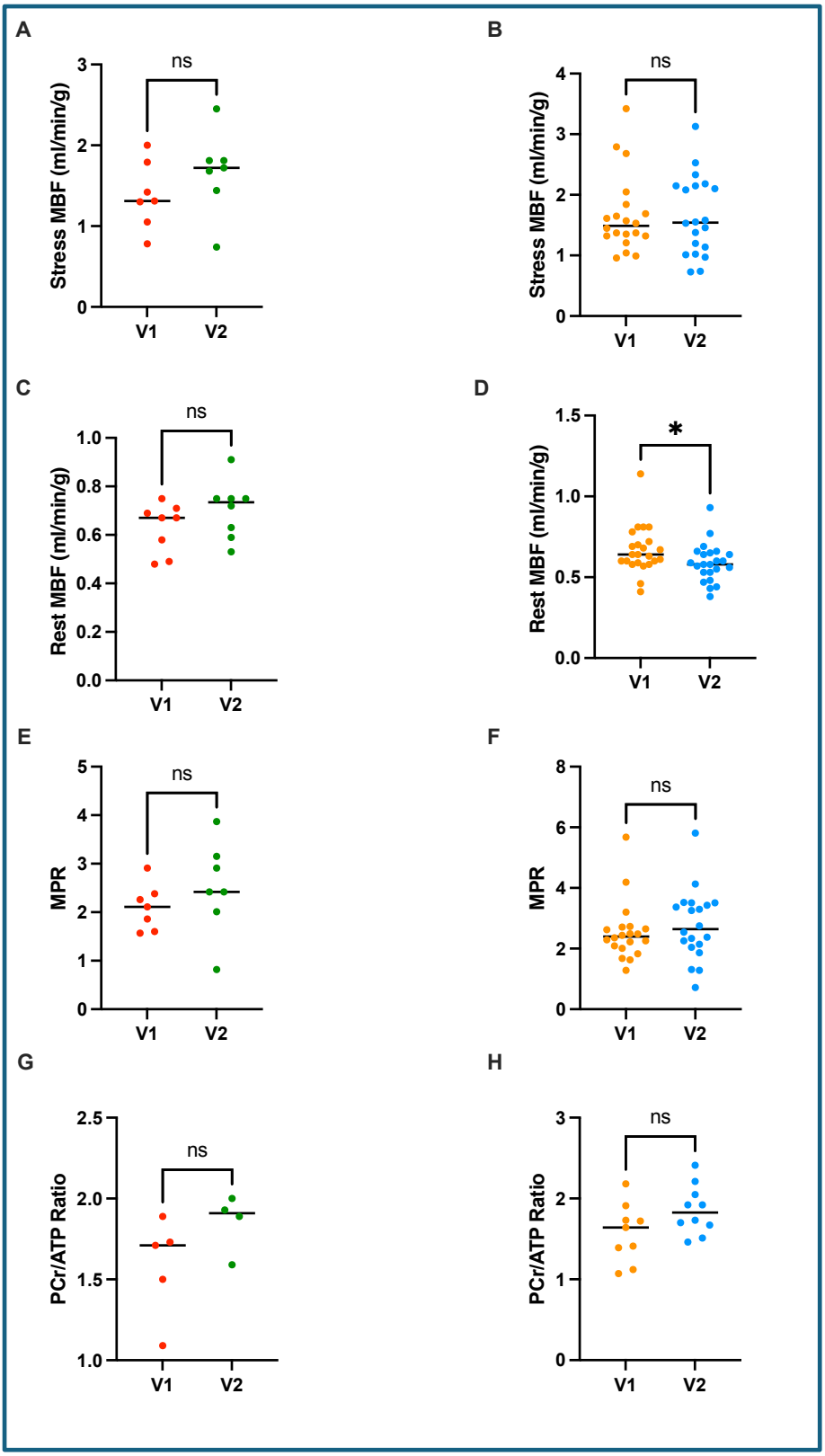

*Figure 3.1: Column scatter graphs with means showing differences in of the two groups pre (V1) and post (V2) AVR. A) Stress MBF between V1 and V2 in patients with T2D, B) Stress MBF between V1 and V2 in patients with NODM. C) Rest MBF between V1 and V2 in patients with T2D, D) Rest MBF between V1 and V2 in patients with NODM. E) MPR between V1 and V2 in patients with T2D, F) MPR between V1 and V2 in patients with NODM. G) PCr/ATP ratio between between V1 and V2 in patients with T2D, H) PCr/ATP ratio between between V1 and V2 in patients with NODM. Red dots are patients with T2D at V1, green dots are patients with T2D at V2, orange dots are patients with NODM on V1 and blue are patients with NODM at V2. NS represents no significance and * represents P <0.05.*

3.3.4 Clinical Outcomes

At a median follow-up of 11 months, only one death occurred (3% mortality when considering the cohort as a whole). This has been labelled a cardiovascular death in a patient with pre-existing T2D, but the precise cause of death is not known. The event occurred 1,350 days post operatively. There were no episodes of heart failure, myocardial infarction, endocarditis, requirement for a permanent pacemaker or stroke during the follow up period.

3.3.5 RNA-Seq correlates of T2D and their corresponding CMR phenotypes

To understand the myocardial molecular phenotypes associated with CMR phenotypes identified in people with severe AS and T2D, RNA-seq was performed. RNA extraction was attempted using myocardial samples from all 39 patients undergoing SAVR presented above. Of these, 34 of the samples had a RIN ≥5.8 and so were included in these analyses.

Figure 3.2 shows the distribution of transcriptional variance accounted for the first 10 principal components, with the first 5 accounting for almost half of the variance.

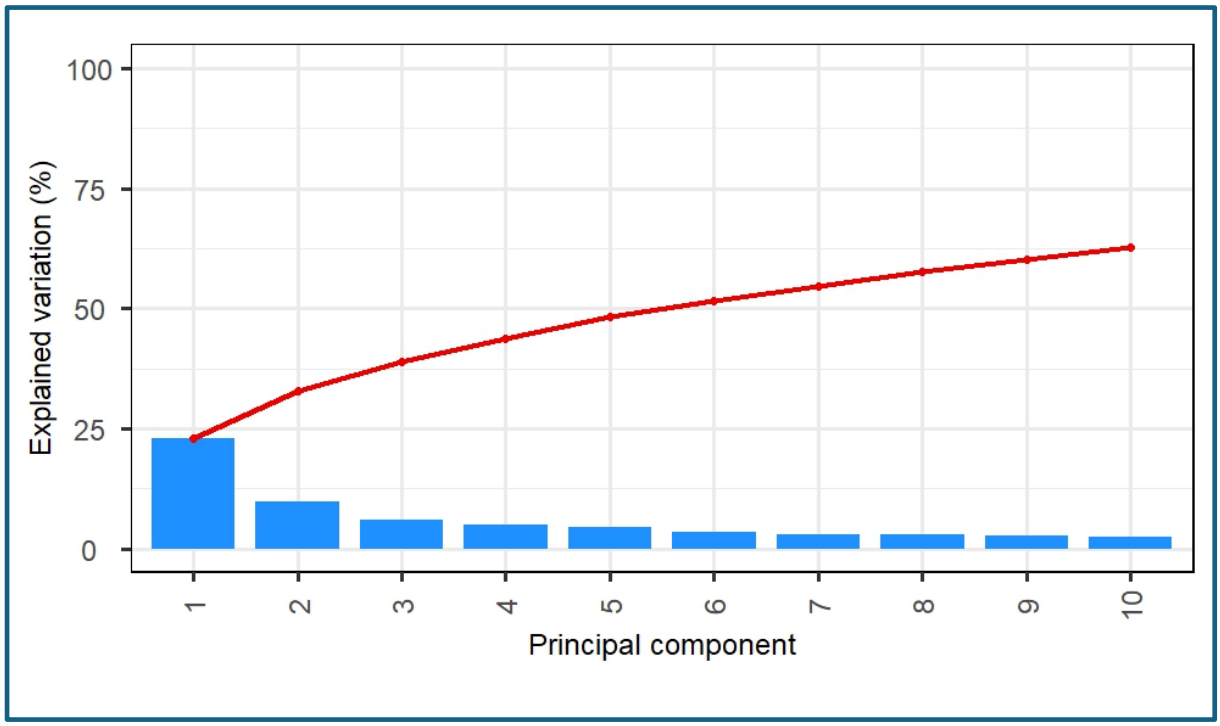

Figure 3.2: Scree plot of data highlighting variance of differentially expressed genes against principal components 1 to 10.

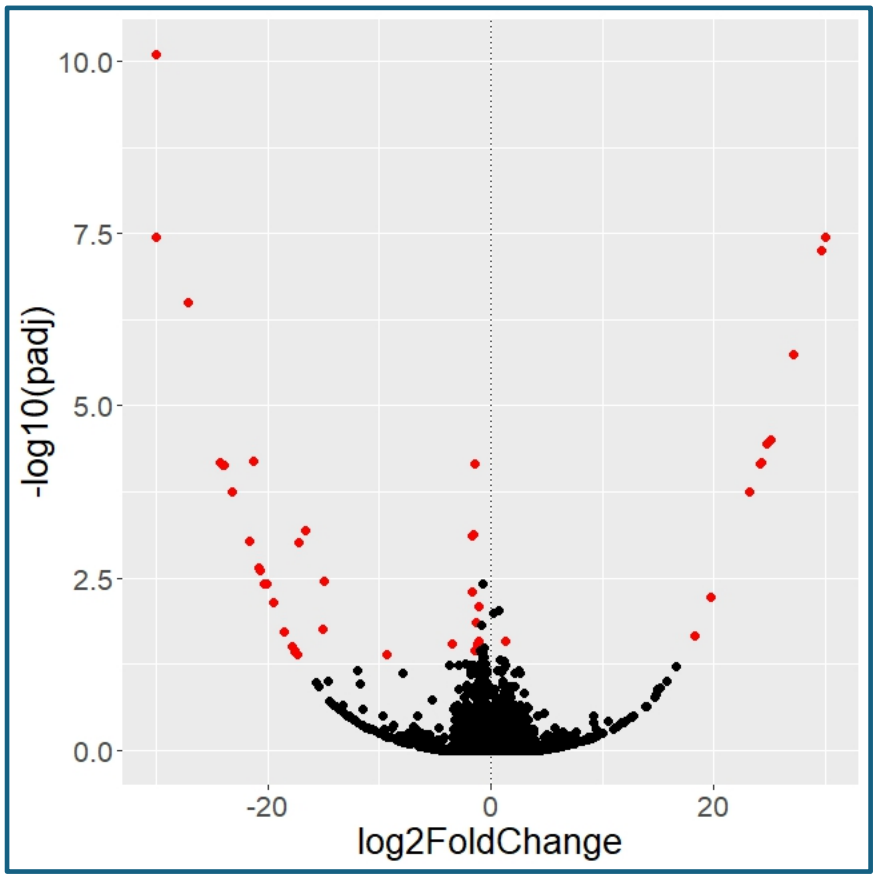

Figure 3.3: Volcano plot illustrating differential gene expression of DM vs NODM. Each dot represents a gene, with red colour denoting those that achieve Benjamini–Hochberg FDR-adjusted P < 0.05 and log2 fold change of <-0.5 or >0.5.

A total of 41,026 genes were quantified, with 284 showing differential expression between DM and NODM at an FDR adjusted p-value <0.05,

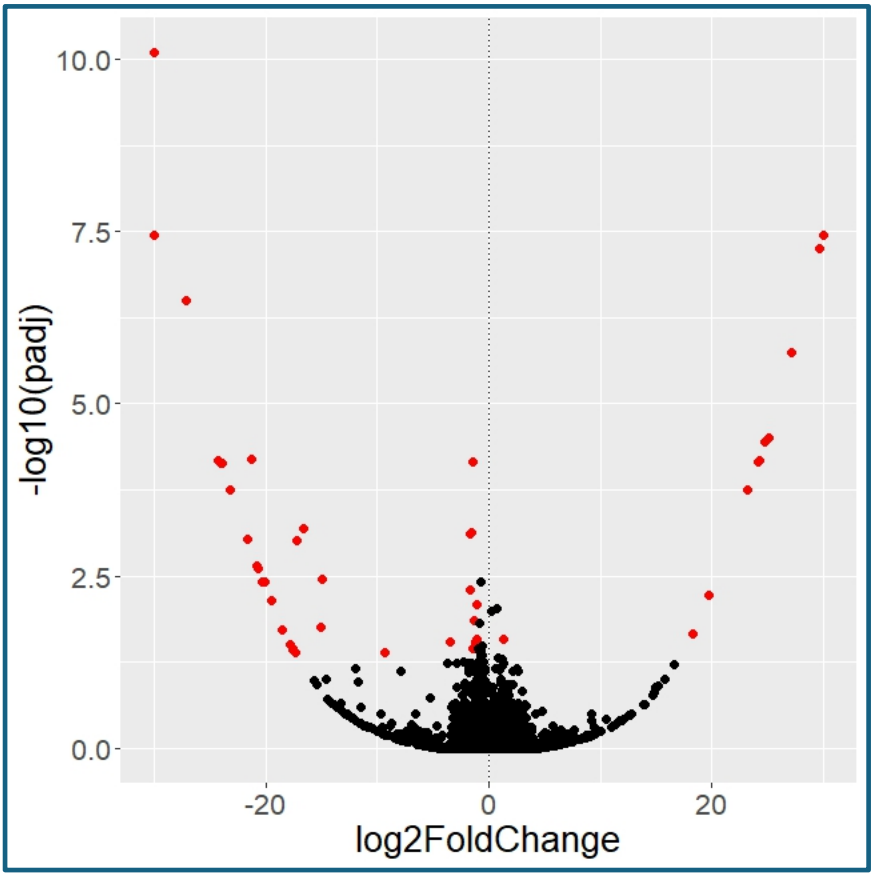

Figure 3.3. Further analysis focused on DEGs with log2 fold change greater than 0.5 or less than -0.5, in order to focus on larger biological effect sizes, and these are presented in Table 3.6.

Table 3.6: List of coding DEGs produced from undertaking differential gene expression analysis comparing samples of patients with T2D to those without. Log 2 fold change data presented to 3 decimal places and adjusted P value (FDR) presented to 5 decimal places.

Ensemble Gene ID	Gene Name	Log2 Fold Change	FDR P value	Description of function
ENSG00000200462	RNU6-727P	4.330	3.537E-08	RNA, U6 small nuclear 727, pseudogene
ENSG00000081800	SLC13A1	3.776	7.9251E-11	Solute carrier family 13 member 1
ENSG00000226794	MTND1P20	4.317	7.1085E-05	MT-ND1 pseudogene 20
ENSG00000243495	GMFBP1	4.337	0.00017	Glia maturation factor beta pseudogene 1
ENSG00000181617	FDCSP	4.334	0.00017	Follicular dendritic cell secreted protein
ENSG00000222222	RNU2-17P	4.331	0.00017	RNA, U2 small nuclear 17, pseudogene
ENSG00000243264	IGKV2D-29	4.327	0.00221	Immunoglobulin kappa variable 2D-29
ENSG00000211672	IGLV4-3	4.332	0.00250	Immunoglobulin lambda variable 4-3
ENSG00000223648	IGHV3-64	4.323	0.00385	Immunoglobulin heavy variable 3-64
ENSG00000236382	KRTAP10-13P	4.336	0.01879	Keratin associated protein 10-13, pseudogene
ENSG00000283547	MTATP6P8	4.320	0.03165	MT-ATP6 pseudogene 8
ENSG00000200379	RN7SKP45	4.319	0.03615	RN7SK pseudogene 45
ENSG00000230948	AURKBP1	4.336	0.03769	Aurora kinase B pseudogene 1
ENSG00000253236	LINC02143	4.329	0.03769	Long intergenic non-protein coding RNA 2143
ENSG00000207730	MIR200B	4.330	0.04052	MicroRNA 200b
ENSG00000211638	IGLV8-61	2.3089	0.04003	Immunoglobulin lambda variable 8-61
ENSG00000184811	TRARG1	0.828	0.02858	Trafficking regulator of GLUT4 (SLC2A4) 1
ENSG00000079277	MKNK1	0.057	0.01008	MAPK interacting serine/threonine kinase 1
ENSG00000254860	TMEM9B-AS1	0.151	0.00922	TMEM9B antisense RNA 1
ENSG00000226813	LINC01941	4.325	0.02201	Long intergenic non-protein coding RNA 194
ENSG00000256597	LINC02393	4.322	0.00612	Long intergenic non-protein coding RNA 2393
ENSG00000244043	RPS27P27	4.304	3.5261E-05	Ribosomal protein S27 pseudogene 27
ENSG00000151952	TMEM132D	4.320	3.0912E-05	Transmembrane protein 132D
ENSG00000136931	NR5A1	4.321	1.7787E-06	Nuclear receptor subfamily 5 group A member 1
ENSG00000249255	PGAM1P9	4.323	3.537E-08	Phosphoglycerate mutase 1 pseudogene 9
ENSG00000225984	HMGB1P26	4.331	3.537E-08	High mobility group box 1 pseudogene 26

Of the DEGs presented in Table 3.6 the majority are associated with the immune response. This is confirmed by Table 3.7, which presents a functional enrichment analysis using G:Profiler (320). Immune response and lipid metabolism regulation were the key biological processes involved.

Table 3.7: G profiler terms related to all DEGs arising from analysis of patients with vs without T2D. P values presented to 3 decimal places. (GO:BP represents biological process).

Source	Term name	Adjusted P value	Ensembl Gene ID (Gene Name) of contributory genes in DEGs
GO:MF	Interleukin-3 receptor activity	0.028	ENSG00000100368 (CSF2RB – Colony stimulating factor 2 receptor subunit beta)
GO:MF	[Acyl-carrier-protein] S-malonyltransferase activity	0.028	ENSG00000169710 (FASN – Fatty acid synthase)
GO:MF	3-oxoacyl-[acyl-carrier-protein] synthase activity	0.028	ENSG00000169710 (FASN – Fatty acid synthase)
GO:MF	3-oxoacyl-[acyl-carrier-protein] reductase (NADPH) activity	0.028	ENSG00000169710 (FASN – Fatty acid synthase)
GO:MF	Palmitoyl-CoA 9-desaturase activity	0.028	ENSG00000099194 (SCD – stearoyl-CoA desaturase)
GO:MF	Phosphopantetheine binding	0.028	ENSG00000169710 (FASN – Fatty acid synthase)
GO:MF	Immunoglobulin binding	0.028	ENSG00000239998 (non-coding), ENSG00000179639 (FCER1A – Fc epsilon receptor Ia)
GO:MF	High-affinity IgE receptor activity	0.028	ENSG00000179639 (FCER1A – Fc epsilon receptor Ia)
GO:MF	Amyloid-beta binding	0.028	ENSG00000130203 (non-coding), ENSG00000169896 (non-coding), ENSG00000133216 (EPHB2 – EPH receptor B2)
GO:MF	(3R)-hydroxyacyl-[acyl-carrier-protein] dehydratase activity	0.028	ENSG00000169710 (FASN – Fatty acid synthase)
GO:MF	Fatty acyl-[ACP] hydrolase activity	0.028	ENSG00000169710 (FASN – Fatty acid synthase)
GO:MF	Sodium:sulfate symporter activity	0.028	ENSG00000081800 (SLC13A1 – Solute carrier family member 1)
GO:MF	Interleukin-5 receptor activity	0.028	ENSG00000100368 (CSF2RB – Colony stimulating factor 2 receptor subunit beta)
GO:MF	[Acyl-carrier-protein] S-acetyltransferase activity	0.028	ENSG00000169710 (FASN – Fatty acid synthase)
GO:MF	Immune receptor activity	0.028	ENSG00000239998 (non-coding), ENSG00000179639 (non-coding), ENSG00000100368 (CSF2RB – Colony stimulating factor 2 receptor subunit beta)
GO:MF	Fatty acid synthase activity	0.028	ENSG00000169710 (FASN – Fatty acid synthase)
GO:MF	Metal chelating activity	0.028	ENSG00000130203 (APOE – Apolipoprotein E)
GO:MF	Nuclear receptor activity	0.030	ENSG00000072310 (non-coding), ENSG00000136931 (NR5A1 – nuclear receptor subfamily 5 group A member 1)

GO:MF	Sterol response element binding	0.032	ENSG00000072310 (SREBF1 – Sterol regulatory element binding transcription factor 1)
GO:MF	Very-low-density lipoprotein particle receptor binding	0.038	ENSG00000130203 (APOE – Apolipoprotein E)
GO:MF	Lipoteichoic acid binding	0.042	ENSG00000170458 (CD14 – Cluster differentiation 14 molecule)
GO:MF	Peptidoglycan immune receptor activity	0.042	ENSG00000170458 (CD14 – Cluster differentiation 14 molecule)
GO:MF	Opsonin receptor activity	0.04	ENSG00000170458 (CD14 – Cluster differentiation 14 molecule)
GO:MF	Phosphatidylcholine-sterol O-acyltransferase activator activity	0.048	ENSG00000130203 (APOE – Apolipoprotein E)
GO:MF	Lipopolysaccharide immune receptor activity	0.048	ENSG00000170458 (CD14 – Cluster differentiation 14 molecule)
GO:BP	Immune response	3.214e-7	ENSG00000243264 (non-coding), ENSG00000211672 (non-coding), ENSG00000223648 (non-coding), ENSG00000211638 (non-coding), ENSG00000179344 (HLA-DQB1 – Major histocompatibility complex, class II, DQ beta 1) ENSG00000239998 (non-coding), ENSG00000179639 (non-coding), ENSG00000171223 (non-coding), ENSG00000204472 (non-coding), ENSG00000170458 (non-coding), ENSG00000130203 (non-coding), ENSG00000100368 (non-coding), ENSG00000169896 (non-coding), ENSG00000106538 (non-coding), ENSG00000133216 (non-coding), ENSG00000086730 (non-coding), ENSG00000110057 (non-coding), ENSG00000112149 (CD 83 – Cluster of differentiation 83)
GO:BP	Regulation of steroid biosynthetic process	0.012	ENSG00000130203 (non-coding), ENSG00000072310 (non-coding), ENSG00000136931 (NR5A1 – Nuclear receptor subfamily 5 group member 1)
GO:BP	Regulation of toll-like receptor 4 signalling pathway	0.027	ENSG00000239998 (non-coding), ENSG00000170458 (CD14 – Cluster differentiation 14 molecule)
GO:BP	Antigen processing and presentation of peptide or polysaccharide antigen via MHC class II	0.033	ENSG00000179344 (non-coding), ENSG00000110057 (Unc-93 homolog B1, TLR signalling receptor)
GO:BP	Intermediate-density lipoprotein particle clearance	0.033	ENSG00000130203 (APOE – Apolipoprotein E)
GO:BP	Regulation of cellular response to very-low-density lipoprotein particle stimulus	0.033	ENSG00000130203 (APOE – Apolipoprotein E)
GO:BP	Positive regulation of heparan sulfate proteoglycan binding	0.033	ENSG00000130203 (APOE – Apolipoprotein E)
GO:BP	Monounsaturated fatty acid biosynthetic process	0.033	ENSG00000099194 (SCD – Stearoyl-CoA desaturase)

GO:BP	Negative regulation of neuron projection development	0.033	ENSG00000130203 (APOE – Apolipoprotein E), ENSG0000013321 (non-coding), ENSG00000012171 (SEMA3B – Semaphorin 3B)
GO:BP	Response to curcumin	0.033	ENSG00000169896 (ITGAM – Integrin subunit alpha M)
GO:BP	Positive regulation of dendritic spine development	0.036	ENSG00000130203 (APOE – Apolipoprotein E) ENSG00000133216 (EPHB2 – EPH receptor B2)
GO:BP	Secretion by cell	0.03	ENSG00000184811 (non-coding), ENSG00000179639 (non-coding), ENSG00000130203 (non-coding), ENSG00000169896 (non-coding), ENSG00000086730 (non-coding), ENSG00000072310 (SREBF1 – Sterol regulatory element binding transcription factor 1)
GO:BP	Postsynaptic membrane organization	0.036	ENSG00000130203 (non-coding), ENSG00000133216 (EPHB2 – EPH receptor B2)
GO:BP	Negative regulation of MAPK cascade	0.036	ENSG00000158050 (non-coding), ENSG00000130203 (non-coding), ENSG00000133216 (EPHB2 – EPH receptor B2)
GO:BP	Positive regulation of leukocyte proliferation	0.03	ENSG00000204472 (non-coding), ENSG00000100368 (non-coding), ENSG00000133216 (EPHB2 – EPH receptor B2)
GO:BP	Regulation of long-term synaptic potentiation	0.039	ENSG00000130203 (non-coding), ENSG00000133216 (EPHB2 – EPH receptor B2)
GO:BP	Integrated stress response signalling	0.039	ENSG00000171223 (non-coding), ENSG00000178573 (MAF – MAF bZIP transcription factor)
GO:BP	Negative regulation of dopamine metabolic process	0.039	ENSG00000169896 (ITGAM – Integrin subunit alpha M)
GO:BP	Negative regulation of NMDA glutamate receptor activity	0.039	ENSG00000133216 (EPHB2 – EPH receptor B2)
GO:BP	Lipid transport involved in lipid storage	0.039	ENSG00000130203 (APOE – Apolipoprotein E)
GO:BP	Phagocytosis, engulfment	0.039	ENSG00000204472 (non-coding), ENSG00000169896 (ITGAM – Integrin subunit alpha M)
GO:BP	Neuron projection retraction	0.039	ENSG00000133216 (EPHB2 – EPH receptor B2)
GO:BP	Positive regulation of prostaglandin-E synthase activity	0.039	ENSG00000169896 (ITGAM – Integrin subunit alpha M)
GO:BP	Negative regulation of smooth muscle cell proliferation	0.039	ENSG00000204472 (non-coding), ENSG00000130203 (APOE – Apolipoprotein E)
GO:BP	Modulation by host of viral process	0.039	ENSG00000130203 (non-coding), ENSG00000169710 (FASN – Fatty acid synthase)
GO:BP	Trans-synaptic signalling by trans-synaptic complex, modulating synaptic transmission	0.039	ENSG00000133216 (EPHB2 – EPH receptor B2)
GO:BP	Regulation of neuronal synaptic plasticity	0.042	ENSG00000130203 (non-coding), ENSG00000133216 (EPHB2 – EPH receptor B2)
GO:BP	Regulation of CD4-positive, alpha-beta T cell differentiation	0.042	ENSG00000171223 (non-coding), ENSG00000112149 (CD 83 – Cluster of differentiation 83)
GO:BP	Response to fatty acid	0.043	ENSG00000099194 (non-coding), ENSG00000072310 (SREBF1 – Sterol regulatory element binding transcription factor 1)
GO:BP	Cellular response to insulin stimulus	0.044	ENSG00000184811 (non-coding), ENSG00000106538 (non-coding),

			ENSG00000072310 (SREBF1 – Sterol regulatory element binding transcription factor 1)
GO:BP	Negative regulation of female gonad development	0.046	ENSG00000136931 (NR5A1 – Nuclear receptor subfamily 5 group A member 1)
GO:BP	Cellular response to triacyl bacterial lipopeptide	0.046	ENSG00000170458 (CD 14 - Cluster of differentiation 14)
GO:BP	Positive regulation of low-density lipoprotein particle receptor catabolic process	0.046	ENSG00000130203 (APOE – Apolipoprotein E)
GO:BP	Vesicle-mediated intercellular transport	0.046	ENSG00000133216 (EPHB2 – EPH receptor B2)
GO:BP	Vertebrate eye-specific patterning	0.04	ENSG00000169896 (ITGAM – Integrin subunit alpha M)
GO:BP	Primary sex determination	0.046	ENSG00000136931 (NR5A1 – Nuclear receptor subfamily 5 group A member 1)

To understand the associations between high-level global transcriptional variation (i.e. principal components) and clinical phenotype, an Eigencor plot was produced (Figure 3.4). Principal component (PC) 1, which by definition accounts for the greatest amount of transcriptional variance, showed no statistically significant correlations with any demographic parameters, whilst PC2 demonstrated modest positive correlation with T2D. Principal components 3 and 4 exhibited modest correlation with BNP, being positive in PC3 and negative in PC4. Gender also demonstrated negative association with PC4 and PC5.

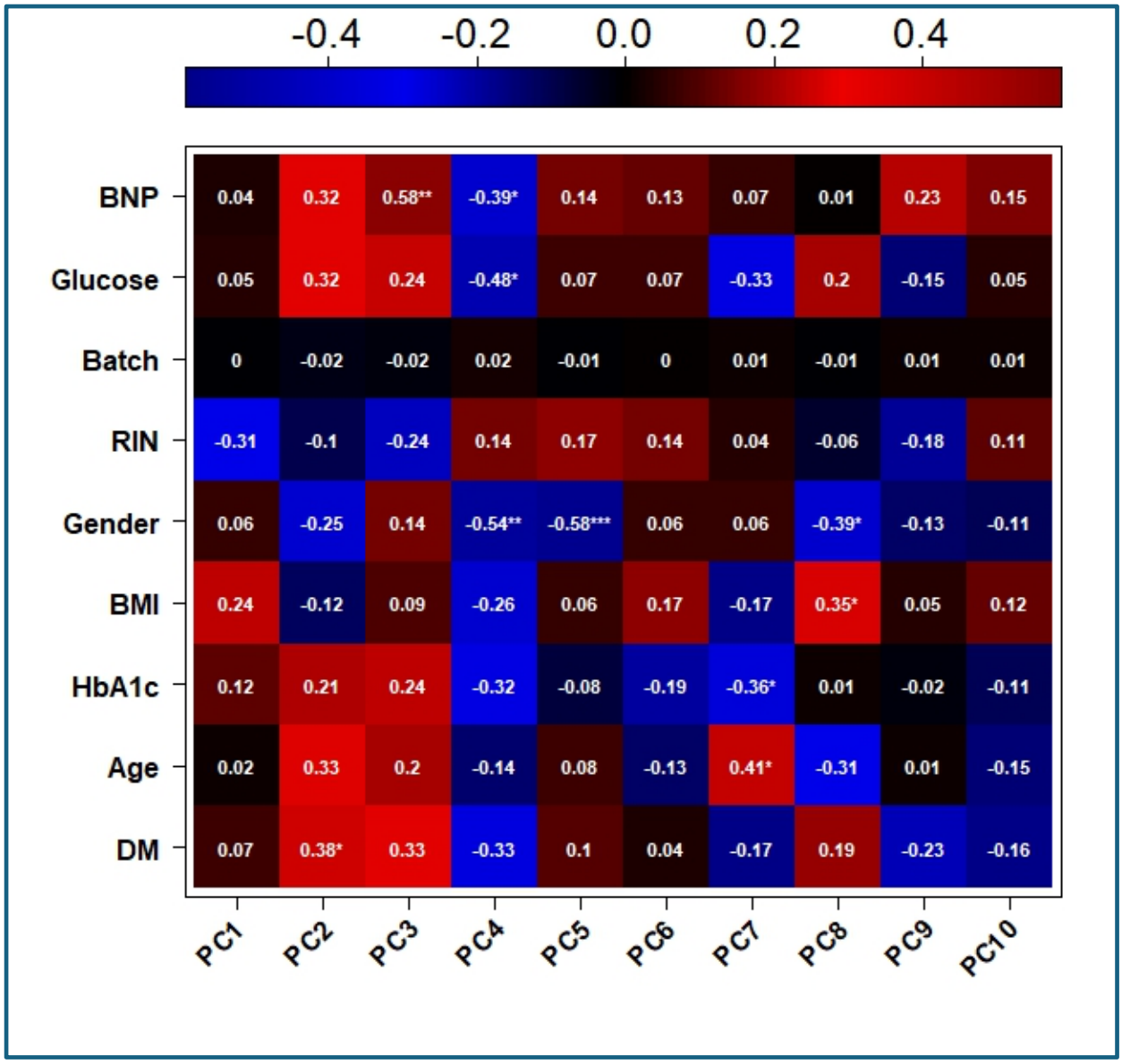

*Figure 3.4: Eigencor plot showing the correlation between principal components (1-10) on the x axis and baseline demographic traits on the y axis. Colours indicate the strength and direction of the correlation, with red representing positive correlations and blue representing negative correlations. The scaled bar on the right represents correlation coefficients, and significance levels are denoted by asterisks (*p < 0.05, **p < 0.01, ***p < 0.001). PC, principal component; DM, Type 2 Diabetes; HbA1c, glycated haemoglobin; BMI, body mass index; RIN, RNA integrity number; SBP, systolic blood pressure; BNP, b-natriuretic peptide.*

An Eigencor plot was then generated to explore transcriptional correlates of CMR phenotypes from the patients' baseline study visit, V1 (Figure 3.5). PC1 and PC2 showed no statistically significant correlations with any CMR parameters. However, PC3 exhibited strong negative correlations with LAEF and LVEF and strong positive correlations with global rest MBF ratio and left ventricular end systolic volume indexed to BSA.

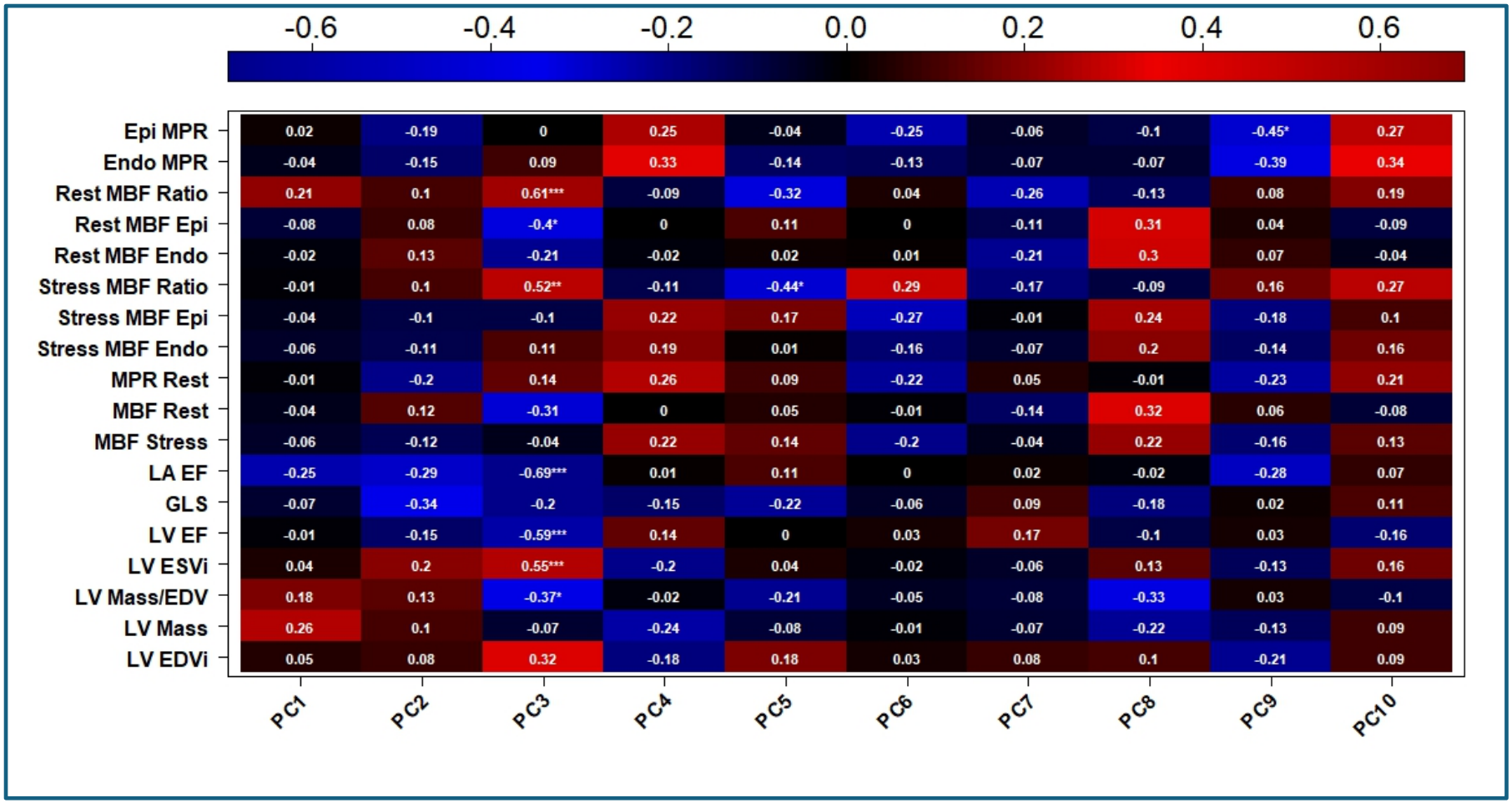

*Figure 3.5: Eigencor plot showing the correlation between principal components (1-10) on the x axis and cardiac MRI parameters from patients' baseline study visit (V1) on the y axis. Colours indicate the strength and direction of the correlation, with red representing positive correlations and blue representing negative correlations. The scaled bar on the right represents correlation coefficients, and significance levels are denoted by asterisks (*p < 0.05, **p < 0.01, ***p < 0.001). PC, principal component; LVEDVi, indexed left ventricular end diastolic volume; LV Mass EDV, left ventricular mass to end diastolic volume ratio; LVESVi, left ventricular end systolic volume indexed; LVEF, left ventricular ejection fraction; GLS, global longitudinal strain; Atrial EF, atrial ejection fraction; MBF Stress, stress myocardial blood flow; MBF Rest, rest myocardial blood flow; MPR rest global, global myocardial perfusion reserve; Stress MBF Endo, endocardial stress myocardial blood flow; Stress MBF Epi, epicardial stress myocardial blood flow; Stress MBF Ratio, stress myocardial blood flow ratio; Rest MBF Endo, endocardial rest myocardial blood flow; Rest MBF epi, epicardial rest myocardial blood flow; Rest MBF ratio, rest myocardial blood flow ratio; Endo MPR, endocardial myocardial perfusion reserve; Epi MPR, epicardial myocardial perfusion reserve.*

A further Eigencor plot was generated to explore transcriptional correlates of CMR phenotypes from the patients' follow up study visit, V2 (Figure 3.6).

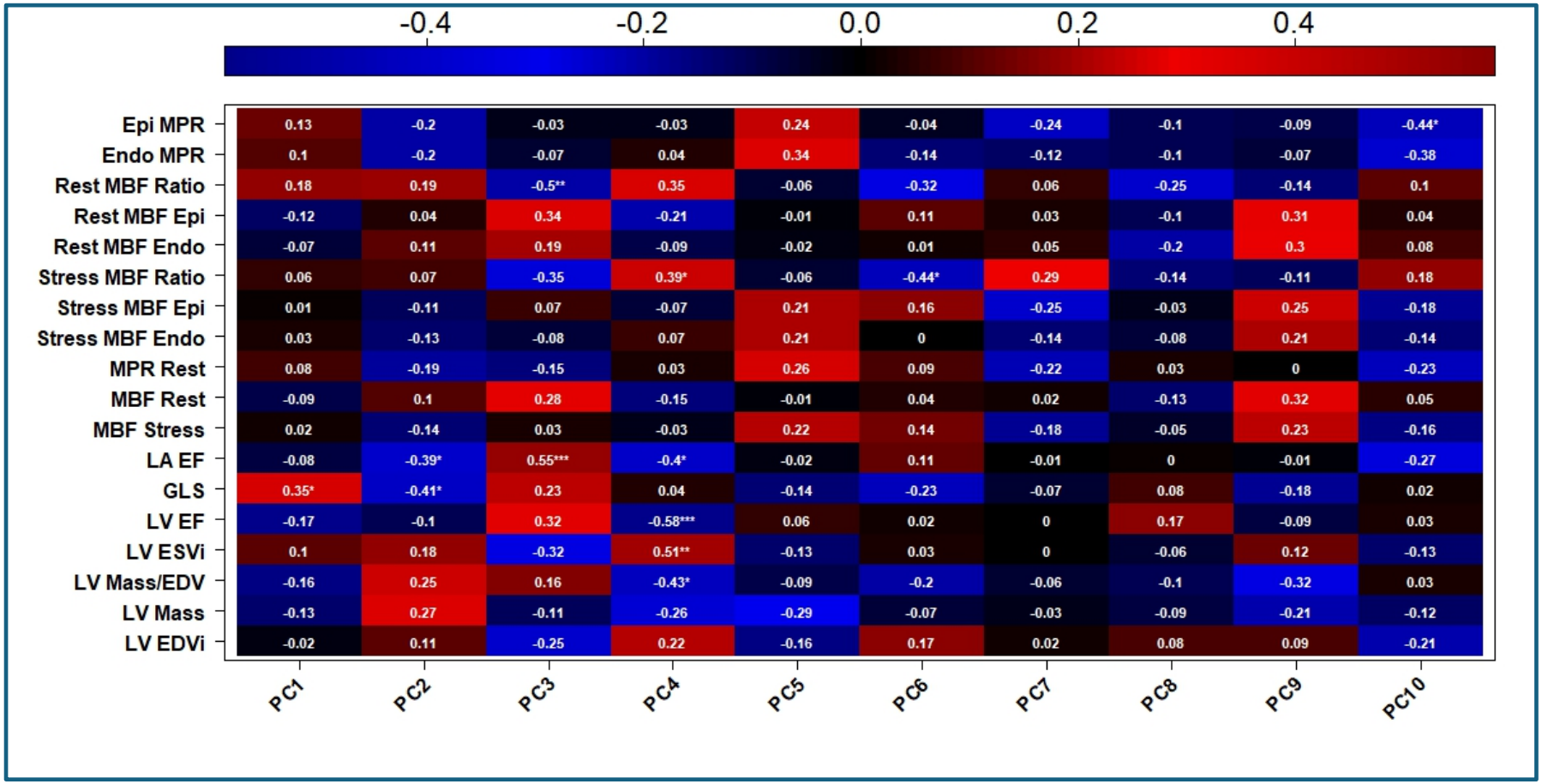

*Figure 3.6: Eigencor plot showing the correlation between principal components (1-10) on the x axis and cardiac MRI parameters from patients' follow up study visit (V2) on the y axis. Colours indicate the strength and direction of the correlation, with red representing positive correlations and blue representing negative correlations. The scaled bar on the right represents correlation coefficients, and significance levels are denoted by asterisks (*p < 0.05, **p < 0.01, ***p < 0.001). PC, principal component; LVEDVi, indexed left ventricular end diastolic volume; LV Mass EDV, left ventricular mass to end diastolic volume ratio; LVESVi, left ventricular end systolic volume indexed; LVEF, left ventricular ejection fraction; GLS, global longitudinal strain; Atrial EF, atrial ejection fraction; MBF Stress, stress myocardial blood flow; MBF Rest, rest myocardial blood flow; MPR rest global, global myocardial perfusion reserve; Stress MBF Endo, endocardial stress myocardial blood flow; Stress MBF Epi, epicardial stress myocardial blood flow; Stress MBF Ratio, stress myocardial blood flow ratio; Rest MBF Endo, endocardial rest myocardial blood flow; Rest MBF epi, epicardial rest myocardial blood flow; Rest MBF ratio, rest myocardial blood flow ratio; Endo MPR, endocardial myocardial perfusion reserve; Epi MPR, epicardial myocardial perfusion reserve.*

PC1 showed a mild positive correlation with GLS. PC2 exhibited a mild negative correlation with LAEF and GLS, whilst PC3 exhibited strong positive correlation with LAEF and mild negative correlation with global rest MBF ratio.

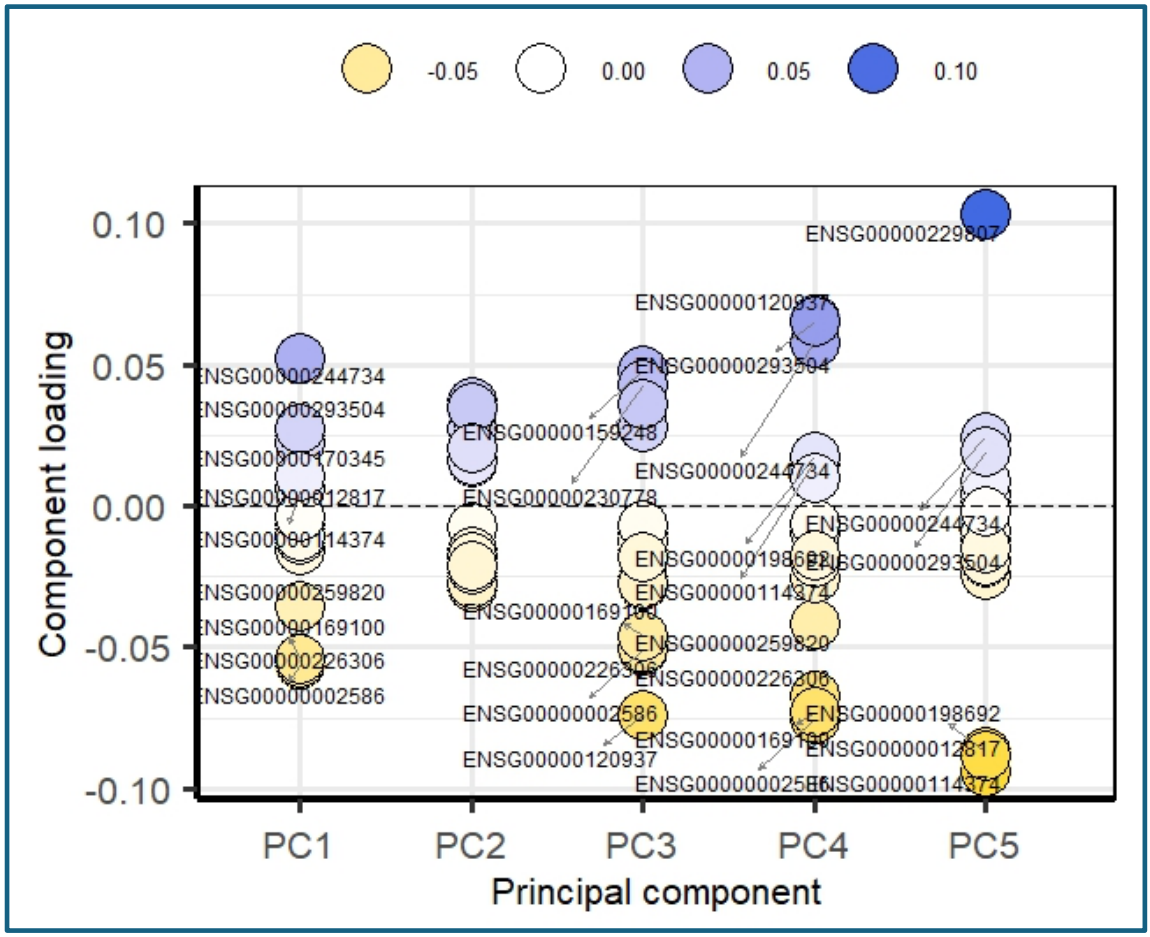

Figure 3.7: Loading plot depicting the contribution of differentially expressed genes to principal components 1-5. Each point represents a differentially expressed gene, with its position indicating the strength and direction of its contribution to each principal component. Variables farther from the origin have a stronger influence on the respective principal components.

To understand the genes that most strongly contributed to variance in PCs 1-5 of the V1 Eigencor plot seen in Figure 3.5 (noting that PC3 was associated with most CMR phenotypes), a loading plot was generated (Figure 3.7). Each of the identified genes are set out in Table 3.8.

Table 3.8: Details of the differentially expressed genes extracted from all principal components of the loading plot displayed in Figure 3.7.

PC	Ensembl ID	Gene Name	Gene Name Explained	Gene Type	Chromosome Location
1,4,5	ENSG00000244734	HBB	Haemoglobin subunit beta	coding	11
1,4,5	ENSG00000293504	-	-	-	-
1	ENSG00000170345	FOS	Fos proto-oncogene, AP-1 transcription factor subunit	coding	14
1,5	ENSG00000012817	KDM5D	Lysine demethylase 5D	coding	Y
1,4,5	ENSG00000114374	USP9Y	Ubiquitin specific peptidase 9 Y-linked	coding	Y
1,3	ENSG00000259820	MIR30DHG	MIR30D and MIR30B host gene	lncRNA	8
1,2,4	ENSG00000169100	SLC25A6	Solute carrier family 25, member 6	coding	X
1,2,3,4	ENSG00000226306	NPY6R	Neuropeptide Y receptor Y6	pseudo	5
1,3,4	ENSG00000002586	CD99	CD99 molecule (Xg blood group)	coding	X
3	ENSG00000159248	-	-	-	-
3	ENSG00000230778	HBB	Haemoglobin subunit beta	coding	11
3,4	ENSG00000120937	XIST	X inactive specific transcript	lncRNA	X
4	ENSG00000198622	EIF1AY	Eukaryotic translation initiation factor 1A Y-linked	coding	Y
4,5	ENSG00000198692	EIF1AY	Eukaryotic translation initiation factor 1A Y-linked	coding	Y

As shown in Table 3.8, the majority of the genes are coding and located on the sex chromosomes (321). Specifically relating to cardiac function, MIR30DHG has been associated with regulation of the MIR30 microRNAs which have been associated with fibrosis. The protein associated with SLC25A6 is implicated in the function of the permeability transition

pore complex, which regulates the release of mitochondrial products that induce apoptosis (322).

However, the small number of genes highlighted using this approach, along with their contribution to multiple PCs, makes it difficult to gain biological insights. Given the strong negative correlation of LAEF with the myocardial transcriptome (i.e. PC3), a further differential gene expression analysis was undertaken to attempt to identify DEGs that are associated with quartile 4 (Q4), with the lowest LAEF values, versus quartile 1 (Q1) of LAEF, with the highest values, in order to dissect potential molecular pathways linked to left atrial dysfunction or remodelling. This is intended as a proof-of-principle, which could be extended in future to other CMR phenotypes associated with RNA-seq PCs.

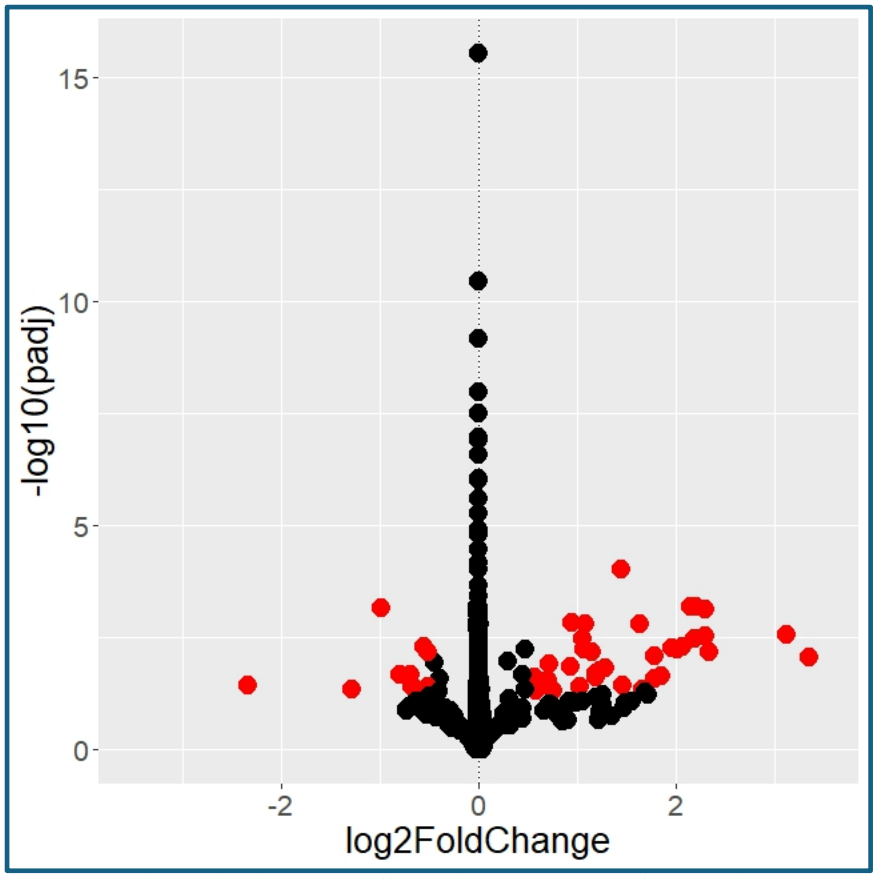

Figure 3.8: Volcano plot illustrating differential gene expression of upper vs lower quartiles of LAEF. Volcano plot illustrating differential gene expression. Each dot represents a gene, with red colour denoting those that achieve Benjamini–Hochberg FDR-adjusted P < 0.05 and log2 fold change <-0.5 or >0.5.

A total of 41,026 genes were quantified, with 284 showing an FDR adjusted p-value <0.05, Figure 3.8. Further analysis focused on DEGs that with log2 fold change greater than 0.5 or less than -0.5, in order to focus on larger biological effect sizes (Table 7). These DEGs were analysed using G:Profiler (320) for further functional enrichment characterisation and the resulting outputs can be found in Table 3.9.

Table 3.9: List of DEGs produced from undertaking differential gene expression analysis comparing LAEF quartile 1 to 4.

Ensemble Gene ID	Gene Name	Log2 FoldChange	FDR P value	Description of function
ENSG00000287838	None	3.34347	0.00883	Novel transcript
ENSG00000075035	WSCD2	3.11726	0.00281	WSC domain containing 2
ENSG00000167311	ART5	2.33764	0.00703	ADP-ribosyltransferase 5
ENSG00000181656	GPR88	2.29825	0.00075	G protein-coupled receptor 88
ENSG00000118298	CA14	2.28830	0.00290	Carbonic anhydrase 14
ENSG00000054938	CHRDL2	2.20001	0.00068	Chordin like 2
ENSG00000185760	KCNQ5	2.19257	0.00336	Potassium voltage-gated channel subfamily Q member 5
ENSG00000277734	TRAC	2.15215	0.00068	T cell receptor alpha constant
ENSG00000236714	LINC01844	2.06031	0.00507	Long intergenic non-protein coding RNA 1844
ENSG00000116983	HPCAL4	2.01583	0.00613	Hippocalcin like 4
ENSG00000133107	TRPC4	1.96125	0.00559	Transient receptor potential cation channel subfamily C member 4
ENSG00000230746	None	1.85383	0.02367	Novel transcript
ENSG00000282917	None	1.78139	0.00814	Novel transcript, antisense to CORIN and NFXL1
ENSG00000280670	CCDC163	1.77676	0.02754	CCDC163 homolog
ENSG00000111254	AKAP3	1.66051	0.04784	A-kinase anchoring protein 3
ENSG00000080224	EPHA6	1.63612	0.00157	EPH receptor A6
ENSG00000274317	LINC02334	1.45254	0.03782	Long intergenic non-protein coding RNA 2334
ENSG00000197728	RPS26	1.44838	0.0001	Ribosomal protein S26
ENSG00000173114	LRRN3	1.28557	0.01544	Leucine rich repeat neuronal 3
ENSG00000185565	LSAMP	1.23083	0.01808	Limbic system associated membrane protein
ENSG00000188488	SERPINA5	1.18391	0.02475	Serpin family A member 5
ENSG00000115194	SLC30A3	1.18367	0.02055	Solute carrier family 30 member 3
ENSG00000184261	KCNK12	1.14721	0.00673	Potassium two pore domain channel subfamily K member 12
ENSG00000150510	FAM124A	1.08297	0.00159	Family with sequence similarity 124 member A
ENSG00000169918	OTUD7A	1.06128	0.00585	OTU deubiquitinase 7A

ENSG00000169508	GPR183	1.05040	0.00340	G protein-coupled receptor 183
ENSG00000175564	UCP3	1.02074	0.04135	Nncoupling protein 3
ENSG00000170214	ADRA1B	0.94511	0.00154	Adrenoceptor alpha 1B
ENSG00000106538	RARRES2	0.93189	0.01443	Retinoic acid receptor responder 2
ENSG00000090975	PITPNM2	0.74848	0.04836	Phosphatidylinositol transfer protein membrane associated 2
ENSG00000124429	POF1B	0.71228	0.01299	POF1B actin binding protein
ENSG00000122986	HVCN1	0.70343	0.02783	Hydrogen voltage gated channel 1
ENSG00000162817	C1orf115	0.58187	0.04985	Chromosome 1 open reading frame 115
ENSG00000138411	HECW2	0.57156	0.02436	HECT, C2 and WW domain containing E3 ubiquitin protein ligase 2
ENSG00000198380	GFPT1	-0.51567	0.00662	Glutamine--fructose-6-phosphate transaminase 1
ENSG00000115977	AAK1	-0.52013	0.03961	AP2 associated kinase 1
ENSG00000136026	CKAP4	-0.55289	0.00512	Cytoskeleton associated protein 4
ENSG00000112357	PEX7	-0.67860	0.03782	Peroxisomal biogenesis factor 7
ENSG00000138131	LOXL4	-0.68162	0.04136	Lysyl oxidase like 4
ENSG00000176273	SLC35G1	-0.69392	0.02190	Solute carrier family 35 member G1
ENSG00000239388	ASB14	-0.79316	0.02171	Ankyrin repeat and SOCS box containing 14
ENSG00000151746	BICD1	-0.98924	0.00072	BICD cargo adaptor 1
ENSG00000131389	SLC6A6	-1.28690	0.04760	Solute carrier family 6 member 6
ENSG00000287702	None	-2.33525	0.03736	Novel transcript, antisense to GRM8

Of the DEGs listed in Table 3.9, their main functions related to the heart can be grouped into; cardiac function and remodelling, signal transduction and metabolism regulators. More specifically TRPC4 is associated with calcium signalling contributing to cardiomyocyte contraction and vascular tone regulation (323), UCP3 is known to regulate mitochondrial function (324), ADRA1B has been implicated with cardiac hypertrophy (325) and finally LOXL4 has been shown to be involved in extracellular matrix remodelling and fibrosis (326) which are contributing mechanisms of hypertrophy and cardiac dysfunction. Table 10 below contains the functional enrichment terms associated with the DEGs listed in Table 3.9. Attention to molecular function and biological process reveal that important pathways include adrenergic receptor signalling, cation transmembrane transporter activity and transport.

Table 10: G profiler terms related to differential gene expression analysis comparing LAEF quartile 1 to 4. P values presented to 3 decimal places. (GO:MF represents, molecular function and GO:BP represents biological process).

Source	Term name	Adjusted P value	Ensembl Gene ID (Gene Name) of contributory genes in DEGs
GO:MF	Adrenergic Receptor Signalling	0.013	ENSG00000181656 (non-coding), ENSG00000170214 (ADRA1B – adrenoreceptor alpha 1B)
GO:MF	Monoatomic cation transmembrane transporter activity	0.013	ENSG00000185760 (non-coding), ENSG00000133107 (non-coding), ENSG00000115194 (non-coding), ENSG00000184261 (non-coding), ENSG00000175564 (non-coding), ENSG00000122986 (non-coding), ENSG00000131389 (SLC6A6 –Solute carrier family 6 member 6)
GO:MF	Phosphatidylcholine binding	0.036	ENSG00000188488 (non-coding), ENSG00000090975 (PITPNM2 – Phosphatidylinositol transfer protein membrane associated 2)
GO:MF	Peroxisome matrix targeting signal-2 binding	0.045	ENSG00000112357 (PEX 7 – Peroxisomal biogenesis factor 7)
GO:MF	Beta2-adrenergic receptor activity	0.048	ENSG00000181656 (GPR88 – G protein coupled receptor 88)
GO:MF	Glutamine-fructose-6-phosphate transaminase (isomerizing) activity	0.048	ENSG00000198380 (GFPT1 - Glutamine-fructose-6-phosphate transaminase 1)
GO:BP	Monoatomic cation transmembrane transport	0.010	ENSG00000185760 (non-coding), ENSG00000133107 (non-coding), ENSG00000115194 (non-coding), ENSG00000184261 (non-coding), ENSG00000175564 (non-coding), ENSG00000122986 (non-coding), ENSG00000176273 (non-coding), ENSG00000131389 (SLC6A6 – solute carrier family 6 member 6)
GO:BP	Gamma-aminobutyric acid transport	0.045	ENSG00000133107 (non-coding), ENSG00000131389 (SLC6A6 – solute carrier family 6 member 6)

3.4 DISCUSSION

This chapter has characterised patients with sever-AS with and without concomitant T2D who have undergone SAVR. It presents characteristics of these patients pre-operatively compared to age and sex matched controls and defines changes in CMR measures of cardiac structure and function pre- to post-operatively. Furthermore, myocardial RNA sequencing has highlighted DEGs associated with T2D and CMR phenotypes that can be investigated further in the future.

3.4.1 Severe AS and T2D at baseline

With regards to baseline demographics, there were no significant differences in the T2D severe-AS patient group compared to the NODM severe-AS group other than the markers of diabetes themselves, glucose and HbA1c - an expected finding. Whilst the biomarker of cardiac dysfunction, NT-ProBNP, was raised in patients with severe-AS compared to the controls without AS, there was no difference between the patients with valve disease when comparing presence of concomitant T2D status. This is similar to the results seen in the moderate-AS cohort and may suggest that T2D has a lesser impact on myocardial stress than AS.

Similar to the results shown in Chapter 2, there was no exaggeration of concentric LV remodeling in the presence of both T2D and severe-AS, particularly considering the markers of LV mass, LV mass indexed to body surface area (BSA), LV max wall thickness, and LV mass to LV end-diastolic volume. Previously published work has suggested that in the presence of T2D there is a significantly more pronounced concentric remodeling of the LV even in the

absence of the significant LVH (129, 327). However, my data do not support this possibly due to limited number of 5 T2D control patients (n=5) (without AS) being included.

Compared to healthy controls, patients with severe-AS exhibited worse cardiac perfusion irrespective of their co-existing T2D status. Statistically significant differences were seen across all perfusion parameters of the NODM cohort but only for stress MBF of the T2D cohort. Prior studies have shown that such changes are also present in a statistically significant manner for patients with co-existing T2D (225). Such evidence, coupled with the numerical trends seen in my data, suggest that my cohort was underpowered.

Cardiac remodeling post-AVR

The cardiac remodelling in my cohort reflects what has already been described in the published literature, with a regression of LV hypertrophy and mass post SAVR (194, 225, 328, 329). In a meta-analysis performed by Nunes et al, including 27 studies investigating patients pre- and post-SAVR, they concluded that structural changes, such as LV mass regression, decrease in LVEDV and LVED diameter was evident as early as 1 month post operatively (330). Notably, the degree of regression is not affected by the method of intervention, with both SAVR and TAVR having been shown to reduce LV mass, and LV end diastolic volumes to a similar extent in a single centre study head-to-head study (331).

Regarding the effect of T2D on the remodeling process, Jex et al have reported that post SAVR reverse remodeling is present in patients without T2D, but similar regression of LV indexed mass is not seen in patients with T2D (225). With regards to myocardial function pre- and

post-SAVR, they found that LVEF did not change irrespective of T2D status, but in those without T2D, GLS improved post-SAVR, in contrast to patients with coexistent T2D (225).

ECV, as a marker for diffuse interstitial fibrosis has been shown to be higher in patients with T2D compared with age and sex matched controls. Furthermore, the higher ECV values seen in patients with T2D have been associated with heart failure hospitalisation and mortality (144). Similarly, in patients with severe-AS awaiting valve intervention, high ECV values have been associated with increased risk of both cardiovascular and all-cause mortality post-SAVR (208, 332). It has been postulated that T2D patients exhibit increased ECV due changes in fibroinflammatory markers (including stimulation of cytokines interleukin (IL)1β and TGF-β1 and a dysregulation of collagen degrading matrix metalloproteinases (MMPs)) (333). By contrast, the high ECV associated with severe AS is understood to be secondary to the chronic pressure overload, which is associated with myocyte hypertrophy to maintain left ventricular (LV) systolic function, along with diffuse fibrosis, perhaps from fibroblast activation (334, 335).

The results presented in this chapter reveal a numerical increase in ECV values post AVR in both the diabetic (non-significant) and the non-diabetic (significant) AS patients, with no significant differences in the T2D vs NODM groups in patients with severe AS who have undergone SAVR. This is in keeping with existing AS literature, reporting substantial regression of LV hypertrophy after AVR. Certainly, Bennet et al, have reported their findings of cellular and extracellular compartment regression due to afterload relief as early as 8 weeks post-operatively. They suggest that the increase in ECV that is seen in both the data presented here, and within their own cohort, is due to greater regression in the cellular

compartment than the extracellular compartment (194). It would perhaps have been expected for significant pre-operative differences to be seen in the surrogate imaging marker of fibrosis (ECV values) of patients with T2D (81, 144, 284), which was not case, perhaps due to the small sample size in my study.

Perfusion changes post-AVR

Within the cohort of patients described in this chapter, a numerical improvement in perfusion parameters post-SAVR was observed. In the previously mentioned study by Jex et al, the authors present similar results, showing improvements in perfusion after surgical or transcatheter AVR. When considering these improvements in the context of existing T2D, they report lower baseline vasodilator stress MBF and MPR are present in T2D with or without co-existing severe-AS, but in the presence of both there is a more severe phenotype. Post-AVR they found no significant difference in vasodilator stress-MBF in patients with T2D vs T2D controls, suggesting that transcatheter or surgical AVR can only reverse perfusion abnormalities related to AS (225). It is important to highlight that these changes were seen at 6 months post-SAVR. Importantly, similar findings were reported by Gallinoro et al. In their study of consecutive patients with unobstructed coronaries undergoing TAVR, whilst no changes in global coronary flow or coronary flow reserve were present immediately post-TAVR, compared to the pre-TAVR work up, significant improvements in perfusion were seen 6 months post-TAVR. This was likely due to the LV having time to remodel, with subsequently improved perfusion (336).

It has been postulated that changes in microcirculatory function are not directly dependent on LV mass regression, but may in fact be the result of reduced extravascular compression

and an increased diastolic perfusion time, which may work synergistically improve the hyperaemic myocardial blood flow and restore coronary vasodilatation reserve after AVR (337, 338). Indeed, Thornton et al have shown that changes in perfusion can occur as early as 8 weeks post operatively in their study of 23 patients with severe-AS versus 23 age and sex matched controls. Whilst MPR was reduced in patients with severe-AS compared to controls pre-SAVR, by 8 weeks post-operatively it was similar to that of controls (P>0.90 post-AVR to controls). In particular, the authors report that most of the abnormal perfusion arises from the subendocardial layer. The results presented in this chapter are in keeping with those published, with the largest numerical improvement in adenosine stress MBF post-SAVR arising from the endocardial layer (328). It would be interesting to see if the effect of coexisting T2D affects this finding, but given the small numbers within the diabetes cohort, such an analysis is insufficiently powered.

Clinical outcomes post AVR

When considering outcomes in people undergoing AVR, two key factors must be reviewed. The first, is the method of intervention and the second is co-existing comorbidities, such as T2D. These have an important bearing on the nature of people included in my study and so warrant further consideration to understand the generalisability of my findings.

The low adverse event rate within my cohort may simply reflect chance, due to the small sample size, but may also be because of this was an exclusively surgical cohort, which tends to exclude higher risk cases. Indeed, when comparing outcomes of TAVR vs SAVR at four years in a single center in Italy, overall survival was approximately 14% higher in the surgical cohort (339). The literature is now reporting increasing rates of TAVR in the 'young', which was

traditionally reserved for patients who were considered a high surgical risk, i.e. the old and frail (340, 341). Khan et al have reported that between 2012 and 2017 in the US, the numbers of patients aged >85 who had TAVR decreased, whereas those aged 55-74 increased. When comparing the rates of SAVR in the same study, rates of SAVR increased in patients younger than 55 years of age, whilst a decreasing trend was seen in those aged over 75 years (342). How this will translate in terms of long-term outcomes of younger TAVR recipients remains unclear.

In a retrospective cohort study assessing the effect of concomitant T2D in patients undergoing TAVR for severe-AS, Khadija et al report that whilst 30-day mortality was identical in patients with and without T2D, the diabetic cohort had higher mortality rates after one-year (10.4% vs 5.8%, P=0.036). Furthermore, at 30 days there was no difference in the rates of stroke, major bleeding, myocardial infarction or arrythmias, between the two groups (343). Perhaps more importantly, in a subgroup analysis of the T2D patients, those with worse glycaemic control had a numerically higher incidence of mortality (though this did not reach statistical significance). Furthermore, higher HbA1c levels were associated with an increased risk of acute kidney injury post TAVR (odds ratio = 2.3, P= 0.02) and higher fasting blood glucose levels were associated with increased incidence of stroke (odds ratio = 1.02, P= 0.013) (343).

In another large retrospective cohort study spanning data acquired from 2012 to 2017 in the US, data of patients with and without T2D were gathered after TAVR or SAVR. T2D patients undergoing TAVR had higher rates of hospitalisations post-procedure (from 0.97 to 7.68/100,000 US adults, P<0.001, between 2012 and 2017). Amongst the patients undergoing TAVR, those with co-existent T2D were younger, and had increasing prevalence of the other

associated conditions including: obesity, hypertension, dyslipidaemia, renal failure and coronary artery disease (342). Interestingly this was not the case in patients with severe-AS and T2D who underwent SAVR. Similarly to Khadija et al, the authors reported longer mean length of hospitalisation within the T2D group (342, 343), but no significant difference in the mortality rates of patients with and without T2D post-SAVR. However, the mean age of patients with T2D who underwent SAVR was older than those without T2D. Over the 5-year study period, age adjusted mortality in patients with coexistent T2D undergoing SAVR significantly decreased, but the diagnosis of T2D remained associated with higher age-adjusted mortality, stroke and acute renal failure incidence, as well as an increased risk of pacemaker requirement. The authors concluded that whilst with time mortality rates are decreasing with both techniques, SAVR was associated with higher in-hospital mortality and the use of TAVR is increasing in patients with co-existing T2D (342).

There remains a gap in the literature directly comparing treatment options of TAVR to SAVR in patients with T2D. However, in post-hoc analysis of the PARTNER study, a randomized controlled trial of TAVR to SAVR in high-risk patients with severe AS, TAVR reduced 1-year mortality in patients with T2D compared to SAVR (344).

Transcriptomic profile: T2D

The use of RAA biopsies taken at the time of SAVR has allowed for the undertaking of bulk RNA-sequencing (RNA-seq), consequently providing data on averaged gene expression from all cells in these samples. In previously published work by Conning-Rowland et al, bulk RNA-sequencing data was used to define DEGs in the right atrium (RA) and LV myocardium from patients with and without diabetes (both type 1 and 2). The authors reported that there was

no overlap in the DEGs present in the two different sites of the myocardium (180). The results presented in this chapter bring a novel perspective, showing for the first time that gene expression in the RAA correlates with CMR markers of LV function.

The results presented within this chapter reveal that RNA-seq PC2 was correlated with the presence of T2D (Figure 3.4). The DEG outputs and their associated gene ontology hits highlight the multiple pathways that contribute to the effects of T2D on the myocardium. The list of DEGs and the associated list of gene ontology molecular function and biological processes highlight several key themes:

- Immune function (based on the terms: immune receptor activity, immunoglobulin binding, high affinity IgE receptor activity, interleukin 3- and 5- activity, antigen processing and presentation via major histocompatibility complex (MHC) II as well as phagocytosis, immune response and CD4+ T cell differentiation).
- Lipid metabolism (based on the terms: fatty acid synthase activity, palmitoyl-CoA 9-desaturase activity, very low-density lipoprotein (VLDL) receptor binding lipid transport & LDL regulation)
- Synaptic and neuronal processes (based on the terms: Synaptic plasticity, dendritic spine development, Postsynaptic membrane organization and Neuron projection retraction).
- Steroid and hormonal regulation (based on the terms: Regulation of steroid biosynthesis and Nuclear receptor activity)
- Toll-like receptor (TLR) signalling.

This reflects a complex multi-system response featuring immune activation, dysregulated lipid metabolism inflammatory and hormonal signalling and several signalling pathways. It is also in-keeping with the literature, in which transcriptomic studies have highlighted the key genes associated with cardiac dysfunction in the presence of T2D are associated with inflammation, immune dysregulation and altered fatty acid oxidation (345).

Studies with examples highlighting the relationship the immune system plays with T2D through the use of transcriptomics include Lv et al, exploring the differences in transcriptome expression profiles of patients with T2D compared to healthy subjects through RNA sequencing of peripheral blood, the authors quote hundreds of coding and non-coding RNAs to be differentially expressed between the groups. Whilst there was no overlap between the DEGs in their analysis to that of mine, the top 10 enriched biological process terms for the genes involved in the protein–protein interaction network consisted of immune response processes. Furthermore, the gene LRRC19, was identified as being upregulated and possibly contributing to the activating nuclear factor κB (NF-kB) which in turn is associated with stimulating pro-inflammatory cytokines synthesis. This is particularly important as NF-κB and its target inflammatory factor genes, IL-1 and IL-6 are known to play a key role in the development of insulin resistance and T2D (346). Lin et al took this one step further and performed RNA sequencing in neutrophils of blood from patients with T2D and healthy controls. They reported over 1000 upregulated DEGs and 1000 downregulated DEGs in the neutrophils of the patients with T2D. GO analysis suggested that the involved DEGs were associated with myeloid leukocyte activation, T cell activation, adaptive immunity, and cytokine production (347). When investigating the transcriptomic alterations in the hearts of non-obese mice with T2D, also reported immune system processes as one of their key outputs

in the gene ontology analysis. Their associated genes included complement component 3 (C3), killer cell lectin-like receptor family E member 1 (Klre1) (348). Whilst the genes presented in these studies may not directly align with those of my data this is likely due to the differences in tissue investigated (blood in the two first studies mentioned vs RAA in mine). Furthermore in the study by Sárközy et al, this would not only have been affected by the use of mouse model, but also a different type of analysis in the form of micro-array compared to RNA sequencing. However, some of the genes connected to immue response in my cohort have also been found in previously published data too. Specifically HLA-DQA1 and HLA-DGB1 genes were found to be upregulated in the blood samples of patients with T2D and this also correlated to the extent of their glucose control, in particular this was overexpressed in well-controlled diabetics and led the authors to suggest that adequate glycaemic control may be responsible for reducing the inflammatory response of diabetic patients (349). Finally, Kesherwani et al who demonstrated altered expression of 351 genes in the heart of diabetic Akita versus control mice using RNA-seq. In particular they, portrayed increased expression of Angiopoietin-like-4 (ANGPTL4), phosphoenolpyruvate carboxylase -1 (PCK1), natriuretic peptide type A (NPPA) and pyruvate dehydrogenase kinase 4 (PDK4), with ANGPTL4 showing the greatest change in RNA expression. The ANGPTL family of proteins interact with Tie receptors, a family of tyrosine kinase receptors mostly expressed on endothelial cells (ECs) (225). This relationship is altered in inflammatory states, of which T2D is considered as one.

It is unsurprising that DEGs associated with key process of lipid metabolism are upregulated in the myocardial samples of the current patient cohort given that that adipose tissue plays a vital role in the development of insulin resistance in T2D (350-352). Whilst the precise mechanism of this remains unknown it is speculated to be secondary to a variety of processes

including impaired adipose tissue characteristics. This consists of: the visceral fat secreting adipokines that impair insulin sensitivity in the liver and muscle, which increase upon expansion of this depot, or that accumulation of visceral fat is a surrogate indicator of ectopic lipid accumulation and lipotoxicity in the liver and muscles which leads to insulin resistance. Another possibility is that excess lipid accumulation in visceral adipose tissue changes the properties of these tissues to accumulate macrophages that will in turn release inflammatory cytokines which can impair insulin sensitivity. Finally, another possibility is that of lipotoxicity in peripheral tissues and visceral adipose tissue cytokine production, contributing to systemic insulin resistance (350, 352). Mechanisms underpinning this lipotoxicity are likely mitochondrial dysfunction, lyosomal dysfunction, and the creation of ROS (352). Differences in the expression of DEGs related to lipid metabolism have been shown in transcriptomic studies both in humans and animals. The use of muscle and fat biopsies from the thighs of patients with T2D compared to healthy controls, revealed altered expression for over 2700 DEGs. These genes were then validated by quantitative polymerase chain reaction (qPCR) processing and revealed 10 genes; AKT2, BCL6, LIPE, METTL9, CD59, LMNA, FOS, CCL2, MUSTN1 and ZNF638. These same genes underwent pathway enrichment analysis to reveal the activation of pathways involved in glucose and lipid metabolism, such as the PPAR signaling pathway, and related to cholesterol metabolism, glycolysis and gluconeogenesis and fatty acid degradation (353). The DEG FOS has also been presented as a significant gene accounting for the variance of PC results from the RAA biopsy samples of the patient cohort and is transcription factor associated with cell growth, differentiation and stress response (354). Furthermore, it has been shown to play a role in cardiac hypertrophy and fibrosis and hence supporting the notion that inflammatory processes contribute to myocardial disease

in patients with T2D and concomitant severe-AS (355, 356) and highlighting the complex interplay of the differing mechanisms.

In the aforementioned mouse study by Sárközy et al myocardial RNA coded for genes representative of functional clusters of metabolism (348). Whilst these genes may not be exactly the same as those presented in my data, this could be due to the 'lean T2D' characteristics of the mice. The average BMI in my cohort was overweight at 29 kg/m^2 and given the evidence to suggest that DEGs may differ based on the intensity of insulin resistance, this may also be true for different weights. Furthermore, when investigating the effects of SGLT on the diabetic heart, RNA extraction from mouse myocardial samples fed high fat, high sucrose diets revealed high levels of metabolic gene expression, particularly for fatty acid metabolism. Importantly the administration of SGLT2 with consequent inhibition of this pathway resulted in an upregulation of oxidative phosphorylation (357). This is an essential process to minimise the development of heart failure (358).

As already alluded to, data from mouse models is of uncertain relevance to human heart disease associated with diabetes, emphasised by the discrepancies with human studies, such as that of Conning-Rowland et al (345). However, given the limited literature available in human studies they must be considered until further work is available.

Transcriptomic profile: Severe AS

The Eigencor plot associating RNA-seq PCs with the pre-operative (V1) CMR assessment was associated with no significant correlations until PC3 (Figure 3.5). By contrast, the Eigencor plot including post-operative (V2) CMR results exhibited significant correlation in PC1, 2 and 3 (Figure 3.6). This implies that myocardial biology is more informative of post-operative

myocardial function and may help to find biomarkers predictive of outcomes after surgery. However, both of these hypotheses require formal assessment in future research.

The DEG FOS presented in the initial list of genes associated with T2D and severe-AS has already been discussed. Other proteins identified in the literature associated with inflammatory processes and the development of calcific AS include: IL6, a pro-inflammatory cytokine, and the activation of Toll-like receptors - TLR2, TLR3 and TLR4(359). Interestingly it appears that DEGs differ in the pathogenesis of the disease between men and women, with females showing an upregulation in the DEGs driving pro-fibrotic processes, whereas in males the upregulation is in those associated with inflammation (355, 356, 360). This is further supported by the results presented in this chapter which show that a large number of DEGs associated with T2D and severe-AS are present on the sex chromosomes. Interestingly my results show hits of the TLR related genes in the gene ontology analysis of the biopsy samples when considering the DEGs upregulated in T2D. This may represent the overlap in phenotype seen in patients with T2D and severe-AS may be driven by some of the same underlying genes.

Transcriptomic profile: Severe AS & T2D

Cherpaz et al have performed similar work to that presented in this chapter in which they combined clinical, biological and echocardiography phenotype of patients with severe AS, with and without T2D, referred for SAVR, with transcriptomic and histological analyses of an intra-operative myocardial LV septal biopsy. Whilst the T2D patient group they present is slightly different from that of this cohort, in that some of their patients required insulin treatment suggestive of worse glycaemic control, the differences in the phenotypic cardiac changes between the diabetic and non-diabetic patients seen in CMR are similar. Concentric

remodelling was more pronounced in patients with T2D. In keeping with this, the extremity of the remodelling appears to be worse within their T2D cohort, which is likely a combination of a larger sample size and worse glycaemic control. The markers of plasma leptin (associated with energy and food balance), FABP3 (associated with lipid metabolism) and Endothelin (as vasoconstrictor peptide) were all significantly increased in the T2D group. Interestingly, inflammatory and fibrotic circulating markers were not different between the two groups, suggesting that the processes affecting T2D and AS may not be synergistic on this level. However, RNA sequencing performed from the myocardial biopsy samples taken at the time of SAVR revealed over 1000 DEGs between the T2D and no-T2D cohorts. Enrichment analysis performed to identify biological themes amongst upregulated DEGs identified extracellular matrix organisation, endothelial function and angiogenesis, regulation of inflammation and adaptation to cardiac hypertrophy. In contrast, analysis of themes amongst downregulated DEGs yielded amino acid metabolism, regulation of muscle contraction and mitochondrial electron processes and organisation. Importantly, regulation of cardiac muscle contraction, the amino acid metabolism, and mitochondrial transport were no longer significantly associated with T2D after adjusting for covariates, mostly after adjustment with hypertension and age (182). SLC25A6 was the only differentially expressed gene that was present both within my cohort's data (Table 3.8) and Cherpaz's DEGs. This could be due to the differences of biopsy tissue type or due to the differences in cohort characteristics (e.g. glycaemic control) between the two studies.

Correlations between PCs and CMR parameters were also noted. PC3 was negatively correlated with the pre-operative markers of myocardial contraction LAEF and LVEF ($p< 0.001$), and positively with the perfusion parameters rest MBF (endo/epi) ratio and stress

MBF(endo/epi) ratio respectively. Interestingly, the post-operative correlations in PC3 for LAEF and rest MBF (endo/epi) ratio were directionally opposite, and GLS correlated with PC1 and PC2. The reasons for these differential associations are unclear and require further exploration. Comparisons of my data to that of Cherpaz et al cannot be made as only echocardiography was performed and not under stress conditions. My findings are therefore novel and more work will be required to understand the molecular associates of the perfusion I identified.

Transcriptomic profile: LAEF

The analysis of DEGs between patients in the upper and lower quartiles of LAEF has identified numerous novel transcripts, emphasizing the gaps in our current understanding of the myocardial transcriptome. However, their associated gene ontology hits highlight multiple relevant and interesting pathways:

- Adrenergic receptor signalling (based on the terms: Beta2-adrenergic receptor activity and Adrenergic Receptor Signalling).
- Ion transport (based on the term: Monoatomic cation transmembrane transport)
- Lipid handling (based on the term: Phosphatidylcholine binding)
- Metabolic enzymal processes (based on the terms: Peroxisome matrix targeting signal-2 binding and Glutamine-fructose-6-phosphate transaminase (isomerizing) activity)

To my knowledge the literature does not have any transcriptomic data related to LA function in the presence of severe-AS. However, imaging studies have reported an increased LA

volume due to the chronically increased left ventricular overload which has been associated with impaired function, and as a possible marker for adverse prognosis in patients with severe-AS (201, 361, 362). The genes ontology hits identified which include the regulation of beta-adrenoreceptor signalling and ion channels, are both credible under such circumstances and warrant exploration in future studies.

Limitations

The literature and imaging results presented in this chapter highlight that T2D predominantly affects the myocardium of the LV. In light of this, how transferrable the bulk RNA sequencing data of the right atrial appendage to the LV can be questioned. Indeed, the recent work of Conning-Rowland et al showed no overlap in diabetes-associated DEGs in the RAA and LV myocardium (180). It must be acknowledged that my biopsy samples were taken from the RAA for patient safety and clinical ease during the procedure. However, the correlation of RAA transcriptome with some LV parameters in Eigencor plots suggests that it may still be possible to gain useful insights from this tissue.

The single centre and small T2D sample size nature of the current work, reduced the generalisability of the results. Future studies with larger sample sizes are needed to rigorously examine the cause–effect relationship between T2D and adverse outcomes in patients with AS.

Future Directions

I hope that some of my current list of LAEF DEGs will soon be explored at the plasma protein level using UK Biobank plasma proteomics data, potentially leading to circulating biomarkers of LAEF. The same approach may be applicable to other CMR phenotypes, although perfusion data is not available in UK Biobank. Furthermore, this approach will allow me to explore wider data, such as future clinical outcomes.

Next, I hope to validate DEGs in publicly available RNA-seq data, including emerging single cell/nucleus RNA-seq data from people with AS (363). Reproduced findings can be further validated by alternate approaches such as immunohistochemistry, and could also be explored in studies where genes are manipulated in cultured cells, such as cardiac fibroblasts.

I also hope to further explore my RNA-seq data using a deconvolution pipeline my group has developed using CIBERSORTx (364). This leverages signature matrices derived from single nucleus RNA-seq data from the Heart Cell Atlas to estimate the cellular composition of each participant's right atrial appendage (RAA). These data can be used to perform regression analyses, correlating my CMR parameters with myocardial cell lineage abundances.
Ultimately, these approaches could lead to the identification of potential biomarkers that can be targeted for further investigation, and possibly also to lead to the creation of therapies that can target cardiac dysfunction associated with AS and T2D.

3.5 CONCLUSIONS

Among patients with severe AS, those with T2D demonstrate persistent abnormalities in perfusion post SAVR compared to their non-diabetic counterparts. At the time of SAVR, RAA biopsies can be taken to examine the transcriptomic profile of patients with T2D and severe AS and draw inferences about myocardial remodelling. Whilst interesting transcriptomic insights have emerged from this work, further research is required to validate these and assess their role as clinical biomarkers to routes to novel therapies.

4. Transcriptomics and HF in the presence of T2D

4.1 INTRODUCTION

The prevalence of HF increases with advancing age and in the United Kingdom 1 in 15 people aged over 75 have the condition (365). In 2018, it was estimated that over 190,000 new cases of HF developed, with over 920,000 prevalent cases (1.6% of the UK population) (366). Patients can present to health care professionals with a variety of symptoms. Most typically, these include dyspnoea on exertion or at rest, paroxysmal nocturnal dyspnoea, leg oedema and fatigue. The symptoms can vary between men and women and in the context of co-existing comorbidities such as diabetes.

When HF is suspected based on symptoms, signs and elevated serum natriuretic peptides the first line imaging assessment is echocardiography. Beyond providing essential data to support the diagnosis of HF, this can stratify cases as heart failure with reduced ejection fraction (HFrEF), heart failure with preserved ejection fraction (HFpEF) or other types of heart failure (e.g. cor pulmonale). However, echocardiography does not provide robust aetiological data, which is more readily offered by CMR. CMR is a valuable tool in the multimodality assessment of HF, not only due to its high accuracy, reproducibility and lack of radiation, but perhaps most importantly due to its ability to characterise myocardial tissue. This assessment can help diagnose thrombus and scar, and the use of myocardial mapping of T1, T2 and T2* can provide evidence into specific pathologies, such as cardiac amyloid, oedema, as well as iron overload (367). Stress testing can also help in the diagnosis of ischaemic heart disease, which can not only contribute to the HF, but is the leading cause of death in males, and third most common cause of death in females in the UK (368). However, the molecular basis of many CMR phenotypes is poorly understood, and one route to addressing this is via correlation with

unbiased molecular phenotyping (or 'omics) methods. RNA-seq can provide transcriptomic information about gene expression patterns, which may help in understanding disease processes and CMR phenotypes.

The aim of this study, therefore, was to phenotypically characterise patients that attended for a 'real world CMR' to assess their newly diagnosed HFrEF. In particular, I set out to: 1) investigate how the blood transcriptome differed in patients with and without concomitant T2D; and 2) define transcriptomic correlates to CMR phenotypes.

4.2 METHODS

4.2.1 Study design and oversight

This single-center, prospective case-control study complied with the Declaration of Helsinki and was approved by National Research Ethics Committees (ref: 20/NW/0326). The study was funded by the British Heart Foundation (RG/16/1/32092), and the University of Leeds Erdheim Fellowship award.

4.2.2 Inclusion criteria

Adult patients with HFrEF with baseline LVEF ≤40% on echocardiography at the time of diagnosis.

4.2.3 Exclusion criteria

Participants were excluded if they had baseline LVEF >40%, known history of coronary artery disease (>70% on invasive coronary angiography), previous myocardial infarction, coronary

artery bypass grafting or angioplasty, chronic obstructive lung disease, significant kidney dysfunction (eGFR <30mL/min/1.73m2), known cardiomyopathy (based on infiltrative diseases [e.g., amyloidosis], accumulation diseases [e.g., haemochromatosis, Fabry disease], or hypertrophic cardiomyopathy), or any contraindication to CMR.

4.2.3 Anthropometric measurements

Height and weight were recorded, and BMI was calculated. A fasting blood sample was taken for assessments of full blood count, HbA1c, and for storage to aid subsequent RNA extraction.

4.2.4 Cardiovascular magnetic resonance

The CMR protocol, shown in Figure 9, consisted of cine imaging using a steady-state free precession sequence, pre- and post-contrast T1 mapping, T2 mapping, stress and rest perfusion LGE imaging. The details of the protocol are the same as mentioned in *2.2.4 Study Protocol, Cardiovascular magnetic resonance*. In brief:

Native T1 maps were acquired in 3 short-axis slices, using a breath-held modified look-locker inversion recovery acquisition (369). Post-contrast T1 mapping was performed using the same approach 15 minutes after the last contrast injection.

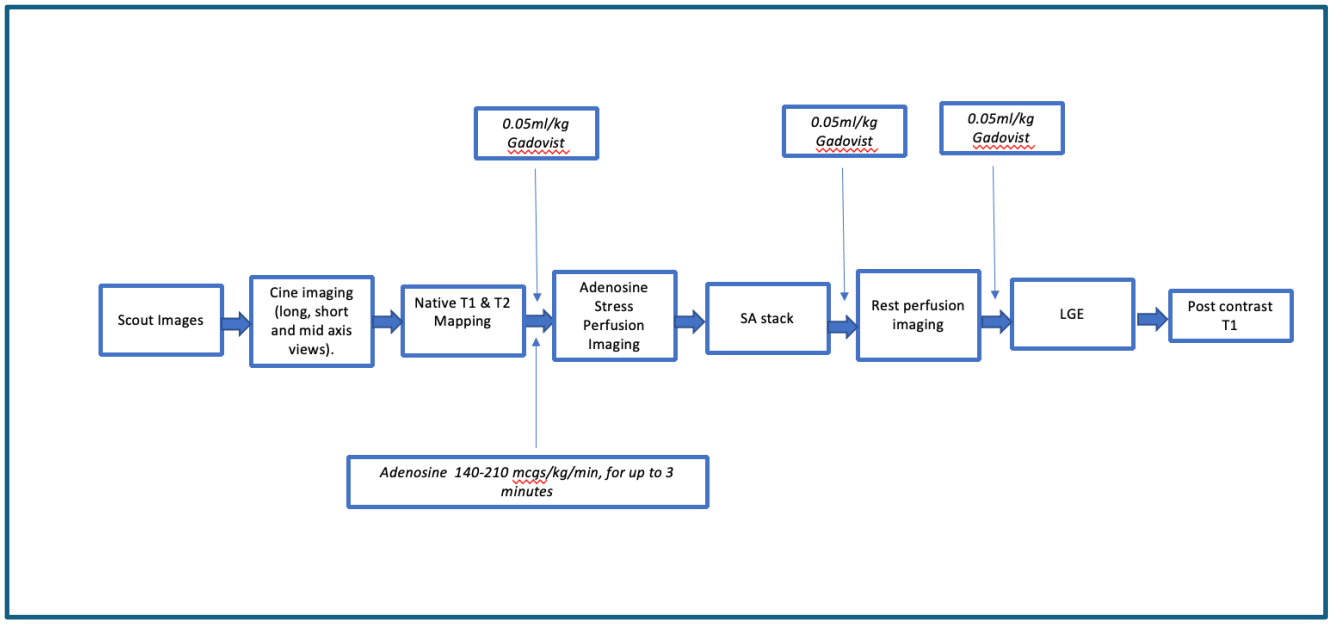

Figure 9: CMR protocol for patients presenting with a new diagnosis of HFrEF

Perfusion imaging used free-breathing, motion-corrected automated in-line perfusion mapping. Adenosine was infused at a rate of 140µg/kg/min, for a minimum of 3 minutes according to hemodynamic and symptomatic response as previously described (369). Adenosine stress was tolerated well by all patients during the stress perfusion studies. LGE was performed using a phase-sensitive inversion recovery sequence >8 minutes after contrast administration.

4.2.5 RNA extraction

Venous blood samples were collected directly into Qiagen PAXgene Blood RNA tubes (370), which immediately stabilise RNA molecules to provide high quality material for sequencing. These were initially stored at room temperature for 2-6 hours (to ensure complete lysis of blood cells), prior to storage at -80°C until batches of RNA extraction could be performed.

RNA extraction was conducted by using the PreAnalytix (A Qiagen Company) PAXgene Blood RNA Kit (Cat No 762164). The kit consists of the following equipment as outlined in Table 11

Table 11: Components of the PreAnalytix kit

Name of component found in the kit	**Description of component found in kit**
Buffer BR1	Resuspension Buffer
Buffer BR2	Binding Buffer
Buffer BR3	Wash Buffer
Buffer BR4	Wash Buffer
Buffer BR5	Elution Buffer
RNase-Free Water	
Proteinase K	
PAXgene RNA Spin Columns	
Processing Tubes	
Microcentrifuge Tubes	
DNase I, RNase-free	
Buffer RDD	
RNase-Free Water	
PAXgene Shredder Spin Columns	

Prior to first use, solid DNase was dissolved in 550 µL of RNase-Free Water provided with the set, as per manufacturer's instructions. Furthermore, four volumes of 100% ethanol was added to BR4 to prepare it for use. RNA extraction was performed as shown in Figure 10.

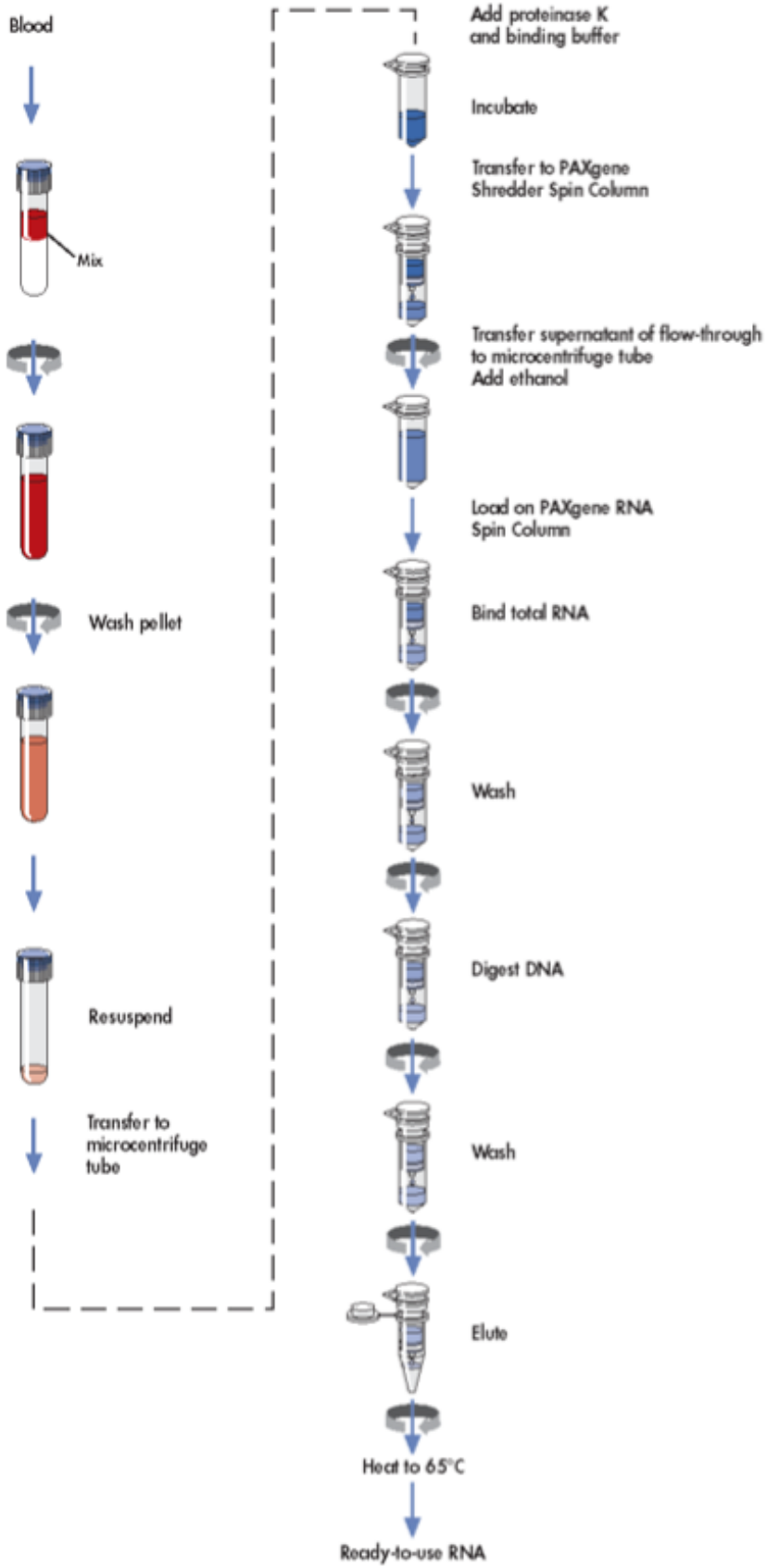

Figure 10: Manual RNA extraction protocol. The diagram is taken directly from the manufacturers protocol (371).

Prior to commencing, blood tubes were thawed at room temperature for 2 hours. Once the sample was thawed completely, the PAX RNA tube was placed in the centrifuge for 10mins at 5000 x g using a swing bucket rotor. The resulting supernatant was removed by decanting. RNAase-free water (4mls) was then added to the pellet, and the PAX RNA blood tube was then closed using a fresh secondary BD Hemogard closure device (supplied in the kit). The samples were vortexed until the pellet was visibly dissolved and subsequently centrifuged for 10 minutes at 5000 x g using a swing-bucket rotor. The resulting supernatant was then discarded. 350μL of the resuspension buffer (BR1) was then added to the pellet and each sample was once again vortexed until the pellets were visibly dissolved.

The samples were then transferred to a microcentrifuge tube, by transferring 1.5mL of the solution via pipette. 300μL of binding buffer 2 (BR2) and 40μL proteinase K (PK) were added to each sample. Each sample was mixed via vortex for 5 seconds and then placed in a shaker incubator for 10 minutes at 55°C at 400-1400 rpm.

Once incubation was complete, the lysate was directly placed into a PAXgene Shredder spin column (PSC) placed in 2mL processing tube, and underwent further centrifugation for 3 minutes at 20,000 x g. The entire supernatant of the flow-through fraction was then transferred to a fresh 1.5mL microcentrifuge tube without disturbing the pellet in processing tube. 350μL of 100% ethanol was added to each sample, and mixing was undertaken by briefly placing on the vortex. Centrifugation was then undertaken for 2 seconds at 1000 x g. 700μL of the resulting sample was pipetted into a PAXgene RNA spin column which was placed in a 2mL processing tube. This was subsequently centrifuged for 1 min at 20,000 x g.

The spin column was then placed in a new 2mL processing tube and the old processing tube was discarded along with its containing flow through.

The remaining sample was pipetted into a PAXgene RNA spin column and centrifuged for 1 minute at 20000 x g. The spin column was once again placed in a new 2mL processing tube and the old processing tube with the associated flow through contents were discarded.

With a pipette, 350μL of buffer 3 (BR3) was placed into a PAXgene RNA spin column. Centrifugation was once again undertaken for 1 min at 20000 x g. Again, the spin column was placed in a new 2mL processing tube and the old processing tube with the associated flow through contents were discarded.

10μL DNAase I (RNFD) stock solution was added to 70μL DNA digestion buffer in a 1.5mL microcentrifuge tube. The two solutions were mixed by gently flicking the tube and centrifuge briefly to collect the residual liquid from the sides of the tube. The resulting mixed solution, DNase I incubation mix (80μL), was pipetted directly onto the PAXgene RNA spin column membrane and placed on a benchtop at room temperature for 15minutes. 350μL wash buffer (BR3) was subsequently pipetted onto the PAXgene RNA spin column membrane and the sample was centrifuged for 1 minute at 20000 x g. The spin column was then placed into a new 2mL processing tube and the old tube with its associated flow -through were discarded. Wash buffer 4 (BR4) was added again to the PAXgene RNA spin column by pipetting 500μL of the solution and centrifuging for 1 minute at 20000 x g. The spin column was then placed into a new 2mL processing tube and the old tube and its containing flow -through were discarded. This step was repeated for a second time with a further 500μL of wash buffer 4 (BR4).

However, centrifugation at 20000 x g was now undertaken for 3 minutes. The processing tube containing the flow-through was discarded and the PAXgene RNA spin column was placed in a new 2mL processing tube. Further centrifugation was undertaken for 1 minute at 20000 x g. As, with the prior steps, the processing tube and its flow through were discarded at the PAXgene RNA spin column was placed in 1.5mL microcentrifuge tube. Subsequently 40 µL of elution buffer (BR5) was pipetted directly onto the PAXgene RNA spin column membrane. The samples were then centrifuged for 1 min at 20000 x g to elute the RNA. This step was repeat using 40µL elution buffer (BR5) and the same microcentrifuge tube.

Finally, the eluate was incubated for 5 minutes at 65°C. Once complete they were immediately chilled on ice. The extracted RNA samples were then stored at -80°C until further processing.

4.2.6 Bulk RNA Sequencing Analysis

Sample Processing

Just as in *3.2.6 Bulk RNA Sequencing Analysis,* bulk total RNA-seq of 100 base pair single-end reads was performed by the University of Leeds Genomics Facility using Illumina NextSeq 2000 of rRNA and globin depleted libraries (prepared with the Illumina TruSeq Stranded Total RNA with Ribo-Zero Globin kit). A RIN of ≥5.8 was deemed acceptable for RNA sequencing analysis, in keeping with the threshold used in other previously published data (310). Within MobaXTerm of the University of Leeds' high performance computing cluster (ARC4). The raw counts were initial underwent quality control, using the software Fast QC (311, 312). Trimming to remove low quality bases (those of <20base pairs (bp)) and adapter sequences was performed via Trim Galore (313). Any results of <20 bp post trimming were also removed.

This process was followed by alignment to the human reference genome, GRCh38, using STAR aligner (314). During this process the length of the overhang bases used when generating the splicing junction database from annotation files was set to 99. Finally, StringTie was used for transcript assembly and quantification of raw gene counts due to its ability to perform a reference guided assembly of transcriptomes and quantify transcripts' expression through read counts normalisation metrics and its capability to identify newly assembled transcripts in the genome (315).

Sample Analysis

Once again, just as described *3.2.6 Bulk RNA Sequencing Analysis*, R version 4.2.0 was used for sample analysis. The package DESeq2 was used to define DEGs (316). For this analysis count data was used with an associated RIN of ≥5.8 (as described above) and clinical data used was that collected at the time of the patients' study visit. Genes with <10 counts were excluded prior to the DESeq2 analyses to reduce false positive signals likely to arise from these. Covariates in the DESeq2 model included gender, RIN, batch number, BMI, age and T2D status, all as categorical variables with the same approach as highlighted in Chapter 3 *(3.2.6 Bulk RNA Sequencing Analysis)* to ensure compatibility. Prior to further analysis, the counts obtained from the samples were normalised and transformed to variance stabilised expression levels. The PCAtools package was used for the creation of scree and volcano plots, PCA loading plots and Eigencor graphs (318).

Evaluation of the PCA loading and Eigencor plots allowed for a further evaluation of possible CMR markers which could be investigated further. Further DESeq2 analysis was therefore performed with the same covariates described above and with the patient cohort being

subdivided into quartiles depending on their measurements of a specific CMR variable. Patients in top quartile were compared to those in the bottom quartile and a list of DEGs was extracted. Log fold-change shrinkage with Apeglm was applied to reduce false positive signals from weakly expressed genes (319). Genes with a false discovery rate (FDR)-adjusted P value of <0.05 and a log2 fold change (lfc) of >0.5 or <-0.5 were selected as hits to minimise false positives and focus on important biological differences, respectively.

GProfiler was used for functional enrichment analysis of DEGs (320). During the functional profiling of genes, a Benjamini-Hochberg FDR significance threshold of <0.05 was undertaken.

4.2.7 Statistical analysis

Statistical analysis of CMR data was performed using GraphPad Prism software (version 10.0.3). All data were checked for normality using the D'Agostino-Pearson Test. Data are presented as mean ±95% confidence intervals (when normally distributed) or medians with corresponding IQR (if nonparametric continuous variables). Categorical data are presented as numbers and percentages and compared with the Pearson χ^2 test. All comparisons between >2 groups were performed by 1-way ANOVA with *post hoc* Bonferroni corrections. Differences in nonparametric variables were assessed using a Kruskal-Wallis test. Student t-test was used for comparison of normally distributed datasets and Mann-Whitney U test was used for non-parametric tests where data were obtained for only two groups. Bivariate correlations were performed using Pearson's or Spearman's method, as appropriate. A 2-sided *P* value of <0.05 was applied as indicating threshold of significance.

4.3 RESULTS

Between 22nd March 2023 and 20th March 2024 a total of 73 patients were prospectively recruited. A total of 92 patients were approached, but the 19 patients that weren't included did not want to be included in research. Of this study cohort, 16 patients (22%) had a concomitant diagnosis of T2D and 57 were non-diabetic.

Table 12: Table of the Clinical Characteristics, Biochemistry and CMR of All Groups

Variable	DM n= 16	NODM n=57	P value
Age, y	69 (63, 75)	64 (62, 68)	0.1624
Female, n (%)	2 (13)	20 (36)	0.0693
BMI, kg/m²	29 (27, 31)	29 (27, 30)	0.6176
Heart rate, bpm	69 (61, 78)	65 (60, 70)	0.4319
Systolic BP, mmHg	124 (109, 139)	118 (112, 123)	0.2935
Diastolic BP, mmHg	75 69, 82)	69 (65, 73)	0.1485
Haemoglobin, g/L	152 (140,164)	146 (142, 150)	0.2198
HbA1c, mmol/mol	58 (48, 68)	38 (35, 40)	**<0.0001**
Cardiovascular Past Medical History			
Stroke / TIA, n (%)	2 (13)	3 (5)	0.3112
PAF, n (%)	7 (44)	12 (21)	0.0675
Hyperlipidemia, n (%)	13 (81)	17 (30)	**0.0003**
Hypertension, n (%)	9 (56)	29 (51)	0.7038
CMR Findings			
LV end-diastolic volume indexed to BSA, mL/m²	116 (98, 134)	128 (112, 144)	0.4270
LV end-systolic volume indexed to BSA, ml/m²	77 (61,92)	86 (70, 101)	0.5540
LV mass, g	153 (153, 171)	146 (134, 158)	0.5863
LV mass indexed to BSA, g/m²	74 (67, 81)	70 (62, 78)	0.6174
LV mass to LV end-diastolic volume, g/mL	0.69 (0.54, 0.83)	0.61 (0.57, 0.65)	0.1499
LV ejection fraction, %	34 (27, 42)	37 (34, 41)	0.4602
LA volume, ml	122 (76, 167)	102 (91, 113)	0.2004
Native T1, ms	1353 (1320, 1386)	1342 (1326, 1357)	0.5068
Extra cellular volume fraction, %	33 (30, 36)	31 (29, 33)	0.2800
Ischaemic LGE, n (%)	6 (38)	16 (28)	0.4676
Non-Ischaemic LGE, n (%)	10 (63)	6 (11)	**0.0070**
Stress MBF, ml/min/g	0.85 (0.67, 1.03)	1.56 (1.40, 1.71)	**<0.0001**
Rest MBF, ml/min/g	0.51 (0.42, 0.61)	0.58 (0.53, 0.64)	0.2093
Increase in RPP, %	7 [0, 25]	25 [11, 37]	**0.0228**

Normally distributed continuous variables are expressed as mean (±95% confidence intervals); nonparametric continuous variables are expressed as median [IQR]; and categorical variables are expressed as counts (percent). P signifies p value for comparisons across the groups with T-tests for normally distributed datasets and Mann-Whitney test for non-parametric values.

DM indicates T2 diabetes mellitus; NODM, no T2 diabetes; BMI, body mass index; HbA1c, glycemic hemoglobin; TIA, transient ischemic attack; PAF, paroxysmal atrial fibrillation; LV, left ventricle; BSA, body surface area; LA, left atrium; LGE, late gadolinium enhancement; MBF, myocardial blood flow; RPP, rate pressure product
y, indicates years; n, number; kg/m², kilograms per squared meter; bpm, beats per minute; mmHg, millimeters of mercury; g/L, grams per liter; mmol/mol, millimoles per mole; ml/m², indicates milliliters per square meter; grams per milliliter; ml, milliliters; ms, milliseconds; ml/min/g, milliliters per minute per gram.

4.3.1 Baseline characteristics

There were no significant differences in the sex or age distribution of the patients in the T2D and NODM groups. The two groups were also similar regarding BMI, resting heart rate, systolic and diastolic blood pressure. As expected, the patients with T2D exhibited higher HbA1c levels compared to the NODM group (58 [48, 68] vs 38 [35, 40] mmol/mol,

respectively; P <0.0001). The most prevalent comorbidity was hypercholesterolemia in the T2D group and hypertension in the NODM group (Table 12).

4.3.2 Cardiovascular magnetic resonance findings

There were no significant structural differences in the LV of the patients with and without T2D. Specifically, whilst there was a numerical difference in markers of left ventricular concentricity, this did not reach statistical significance; LV mass indexed: 74 (67, 81) in T2D vs 70 (62, 78) g/m2 in NODM, P = 0.6174 and LV mass to LV end-diastolic volume: 0.69 (0.54, 0.83) in T2D vs 0.61 (0.57, 0.65) g/mL in NODM, P = 0.1499 (Table 12). Native T1 and ECV, as markers of interstitial fibrosis, were numerically higher in the T2D cohort, but did not reach statistical significance when compared to the NODM group (Table 12).

There were significant differences in the myocardial scarring seen in late gadolinium enhancement (LGE) sequences. More specifically, patients with T2D were more likely exhibit non-ischaemic (i.e. within the myocardial mid-wall or in the sub-epicardium, but not including at the right ventricular insertion point) scar compared to their non-diabetic counterparts. Non-ischaemic LGE was present in 63% of the T2D group, compared to 11% of the non-diabetic group (P= 0.007; Table 12).

Under the influence of adenosine stress, patients with T2D had lower stress myocardial blood flow (MBF) than those without concomitant T2D, being 0.85 (0.67, 1.03) in T2D vs 1.56 (1.40, 1.71) ml/min/kg in the NODM group, P <0.0001. However, this was with a lower RPP

increment with adenosine stress in the T2D group compared to NODM. At rest, lower perfusion remained in the T2D group, but this was not statistically significant (Table 12).

4.3.3 RNA-Seq correlates of T2D and their corresponding CMR phenotypes

RNA sequencing was performed to understand myocardial molecular phenotypes associated with CMR phenotypes identified in people with HFrEF. RNA extraction was performed from the serum extracted from the blood samples of 73 patients presented above. Of these, 71 of the samples had a RIN ≥5.8 and so were included in these analyses.

Figure 11 shows the distribution of transcriptional variance accounted for the first 10 principal components, with the first 3 accounting for almost a quarter of the variance.

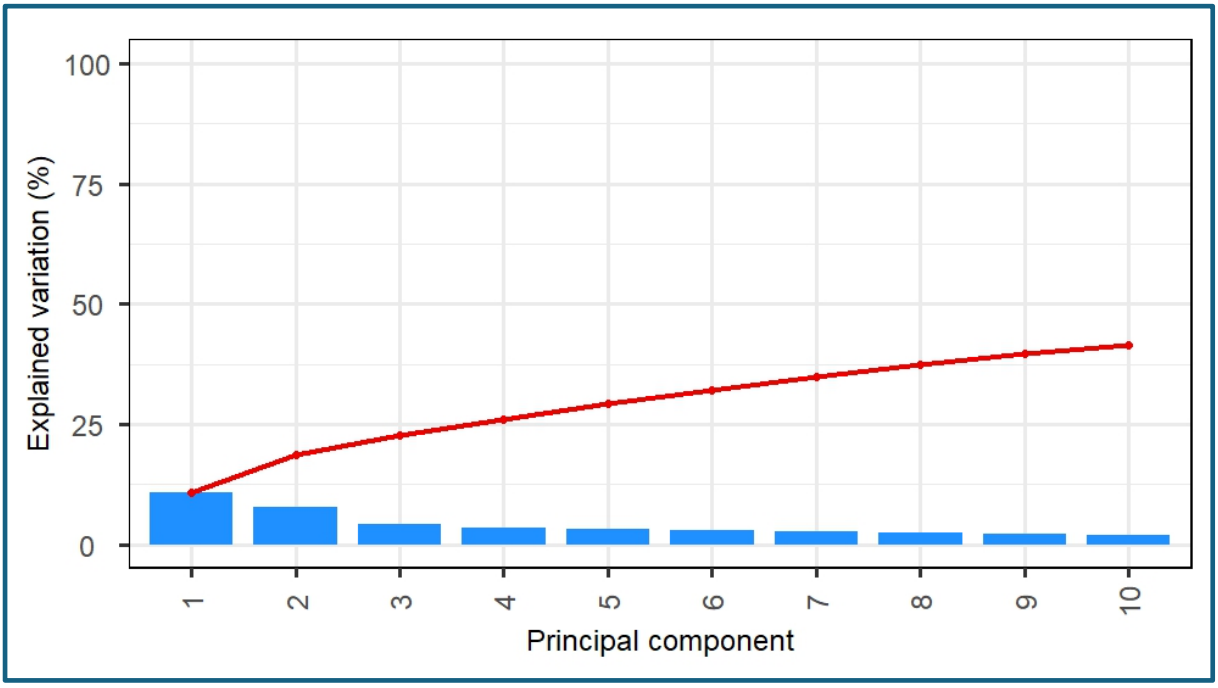

Figure 11: Scree plot of data highlighting variance of differentially expressed genes against principal components 1 to 10.

An initial analysis was undertaken to investigate DEGs in patients with diabetes. Out of 41,166 quantified genes, 467 were deemed 'significant' DEG based on the criteria: FDR adjusted p value <0.05 and LFC >0.5 or <-0.5. **Error! Reference source not found.** graphically depicts the associated up- and down-regulated genes.

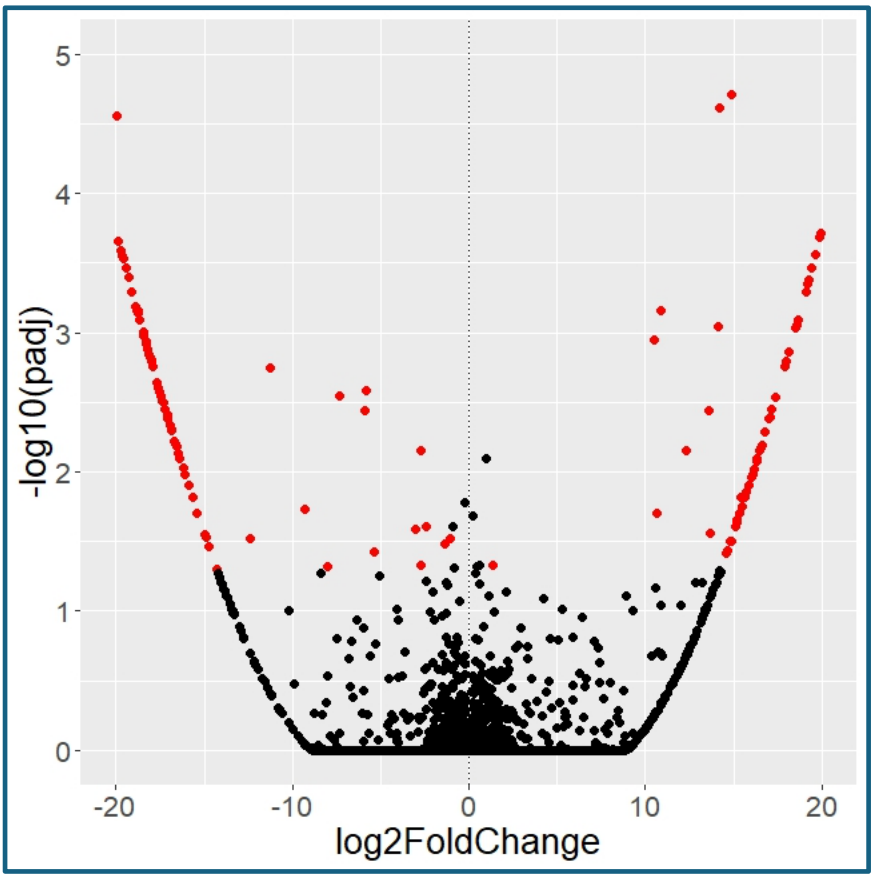

Figure 12.4: Volcano plot illustrating differential gene expression of DM vs NODM. Volcano plot illustrating differential gene expression. Each dot represents a gene, with red colour denoting those that achieve Benjamini–Hochberg FDR-adjusted P < 0.05 and log2 fold change <-0.5 or >0.5.

The 'significant' DEGs were then analysed using G:Profiler (320) for further functional enrichment characterisation and the resulting outputs can be found in Table 13.

Table 13: G Profiler output results of the significant DEGs associated with T2D in this cohort of HFrEF patients. P values presented to 3 decimal places. (GO:MF represents, molecular function and GO:BP represents biological process).

Source	Term name	Adjusted P value	Ensembl Gene ID (Gene Name) of contributory genes in DEGs
GO:MF	Olfactory receptor activity	0.003	ENSG00000172459 (non-coding), ENSG00000205329 (non-coding), ENSG00000254466 (non-coding), ENSG00000127529 (non-coding), ENSG00000177476 (non-coding), ENSG00000177174 (non-coding), ENSG00000176895 (non-coding), ENSG00000176299 (OR4M1 – Olfactory receptor family 4 subfamily M member 1)
GO:BP	Nervous system process	0.004	ENSG00000172155 (non-coding), ENSG00000172459 (non-coding), ENSG00000163377 (non-coding), ENSG00000205329 (non-coding), ENSG00000254466 (non-coding), ENSG00000127529 (non-coding), ENSG00000166828 (non-coding), ENSG00000177476 (non-coding), ENSG00000177174 (non-coding), ENSG00000171201 (non-coding), ENSG00000114200 (non-coding), ENSG00000176895 (non-coding), ENSG00000176299 (non-coding), ENSG00000105894 (non-coding), ENSG00000197584 (KCNMB2 – Potassium calcium activated channel subfamily M regulatory beta subunit)
GO:BP	G protein-coupled receptor signalling pathway	0.018	ENSG00000172459 (non-coding), ENSG00000205329 (non-coding), ENSG00000254466 (non-coding), ENSG00000127529 (non-coding), ENSG00000105954 (non-coding), ENSG00000146385 (non-coding), ENSG00000184502 (non-coding), ENSG00000177476 (non-coding), ENSG00000177174 (non-coding), ENSG00000204681 (non-coding), ENSG00000176895 (non-coding), ENSG00000176299 (OR4M1 – Olfactory receptor family 4 subfamily M member 1)

To understand associations between high-level global transcriptional variation (i.e. principal components) and clinical phenotype, PCA plots were performed to graphically depict any relationships between demographic parameters and T2D. Figure 13 highlights the distribution of samples between PC1 and 2 in relation to gender. The clear clustering suggests major blood transcriptomic differences between men and women HFrEF.

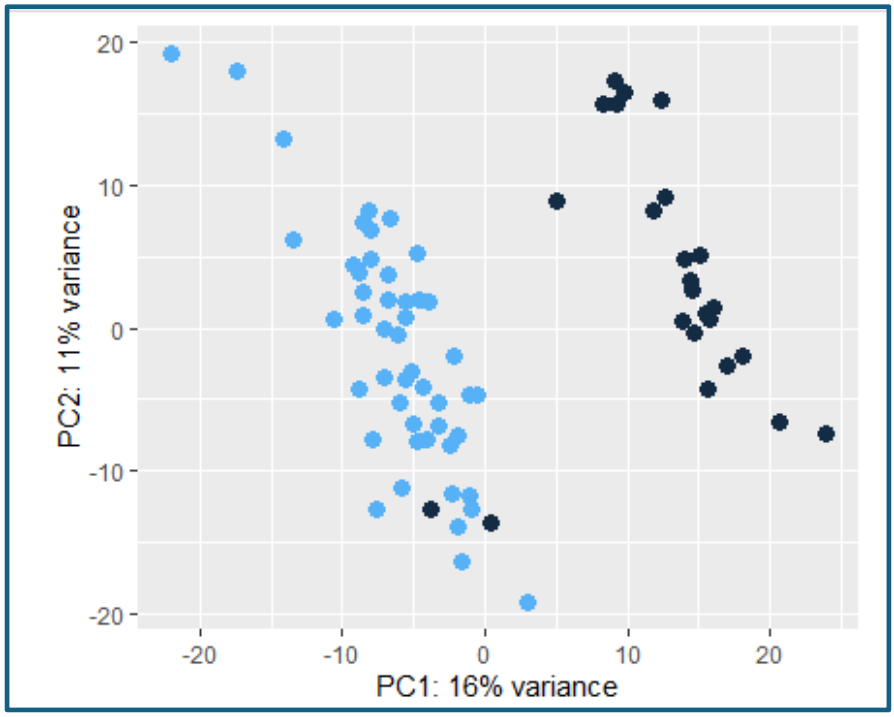

Figure 13: PCA plot showing the distribution of all patient samples along the first two principal components (PC1 and PC2), coloured by gender (pale blue denotes male and dark blue denotes female).

An Eigencor plot was then produced to illustrate correlation between demographic parameters and transcriptomic principal components (Figure 14). As expected from the PCA plot above (Figure 13), PC1 showed a strong statistically significant correlation with gender, and also a positive correlation with BSA. Whilst PC2 did not demonstrate any correlations with demographic parameters, PC3 showed a positive correlation with stress HR and a strong negative correlation with gender.

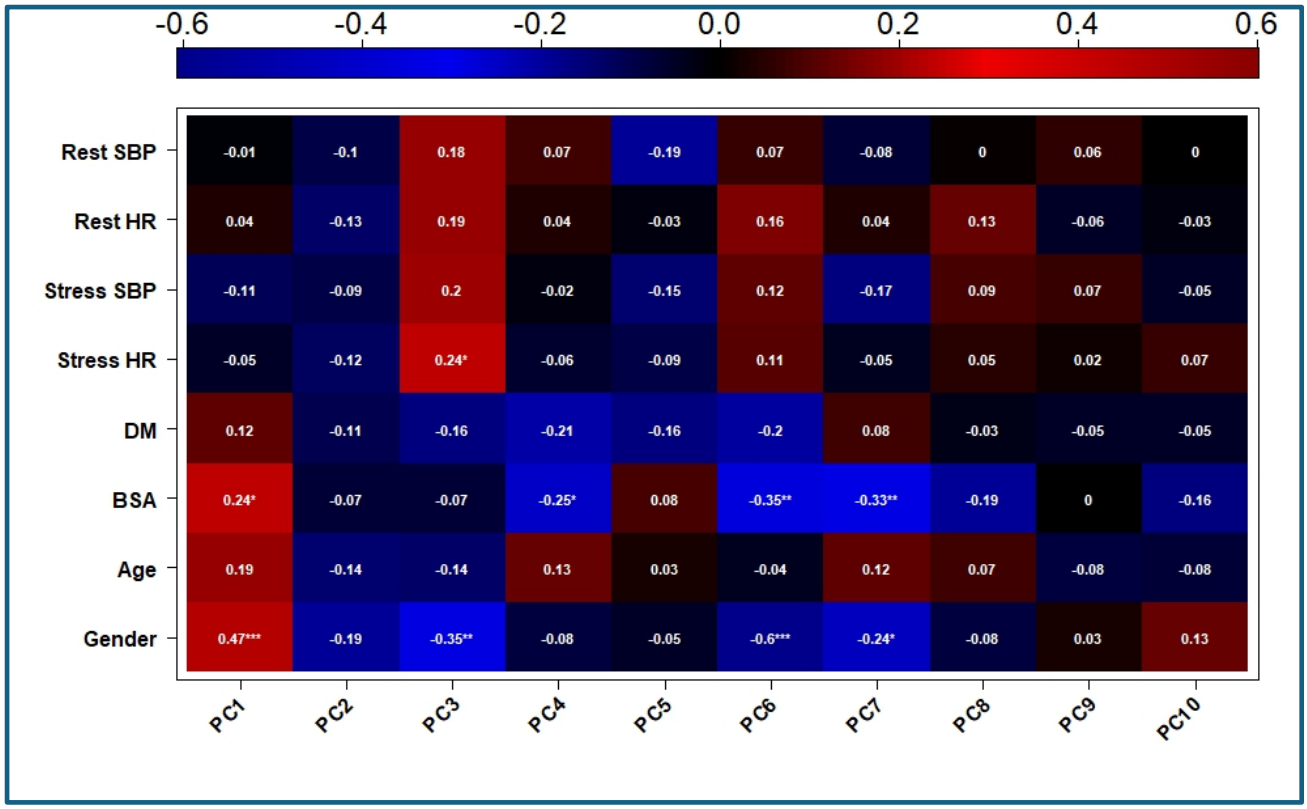

*Figure 14: Eigencor plot showing the correlation between principal components (1-10) on the x axis and baseline demographic traits on the y axis. Colours indicate the strength and direction of the correlation, with red representing positive correlations and blue representing negative correlations. The scaled bar on the right represents correlation coefficients, and significance levels are denoted by asterisks (*p < 0.05, **p < 0.01, ***p < 0.001). PC, principal component; BSA, body surface area; DM, Type 2 Diabetes; Stress HR, stress heart rate; Stress SBP, stress systolic blood pressure; Rest HR, rest heart rate; rest SBP, rest systolic blood pressure.*

An Eigencor plot was then generated to explore transcriptional correlates of CMR phenotypes (Figure 4.15). PC1 exhibited strong positive correlations with LV mass, milder positive correlations with indexed LVEDV and the presence of inducible ischaemia and a strong negative correlation with stress MBF. PC2, PC3, and PC5 on the other hand, showed no statistically significant correlations with any CMR parameters. PC4, however, had a mild positive correlation with rest MBF and a mild negative association with non-ischaemic LGE (i.e. any LGE seen in the sub-epicardium or midwall of the LV stack).

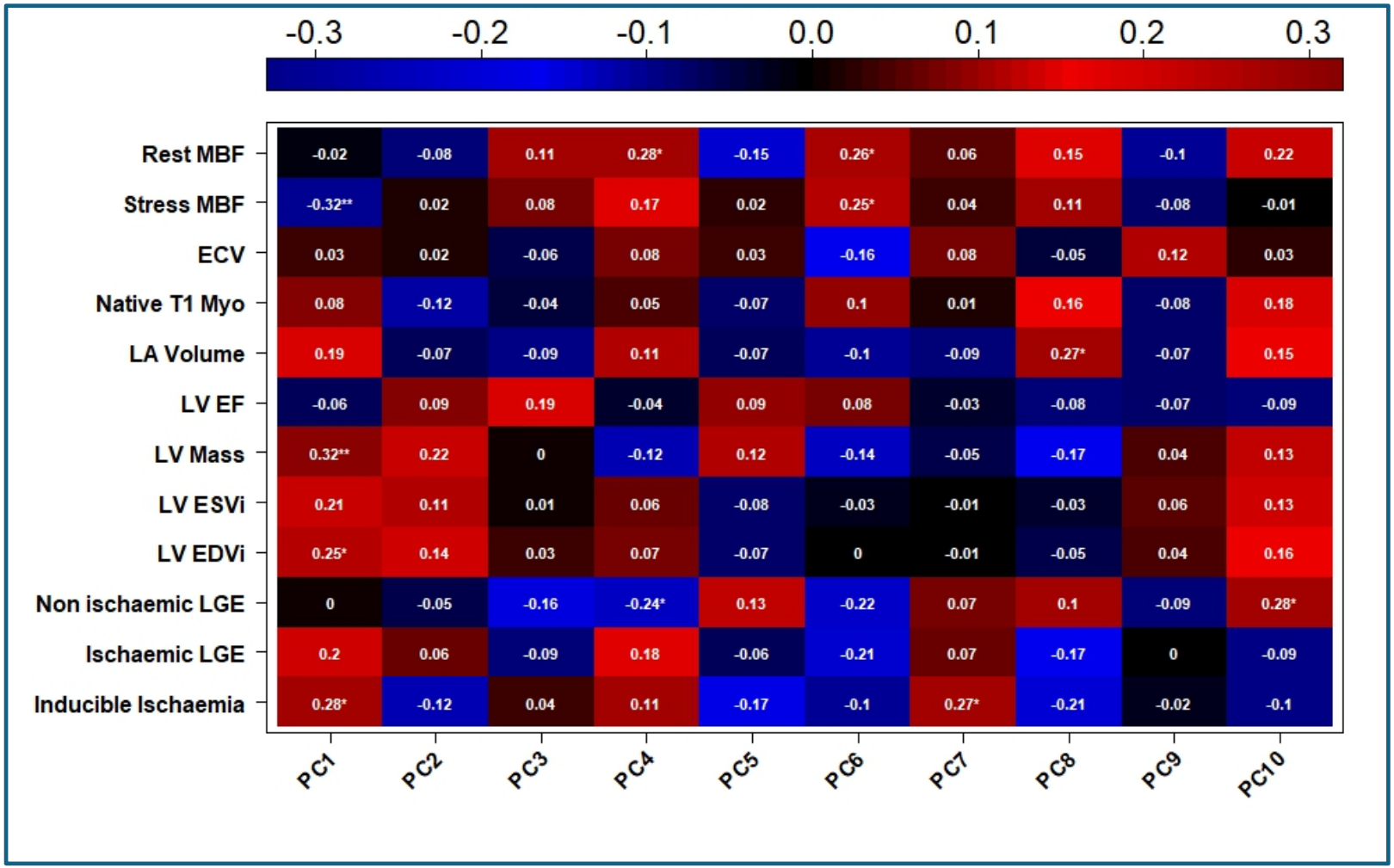

*Figure 4.15: Eigencor plot showing the correlation between principal components (1-10) on the x axis and cardiac MRI parameters from patients' study visit on the y axis. Colours indicate the strength and direction of the correlation, with red representing positive correlations and blue representing negative correlations. The scaled bar on the right represents correlation coefficients, and significance levels are denoted by asterisks (*p < 0.05, **p < 0.01, ***p < 0.001). PC, principal component; LGE, late gadolinium enhancement; LVEDVi, indexed left ventricular end diastolic volume; LVESVi, left ventricular end systolic volume indexed; LVEF, left ventricular ejection fraction; LA volume, left atrial volume; Native T1 Myo, myocardial native T1; Stress MBF, stress myocardial blood flow; Rest MBF, rest myocardial blood flow.*

A loading plot was generated to understand the genes that most strongly contributing to variance in PCs 1-5 and is displayed in Figure 16 (noting that PC1 was associated with most CMR phenotypes). Each of the identified genes are set out in Table 14.

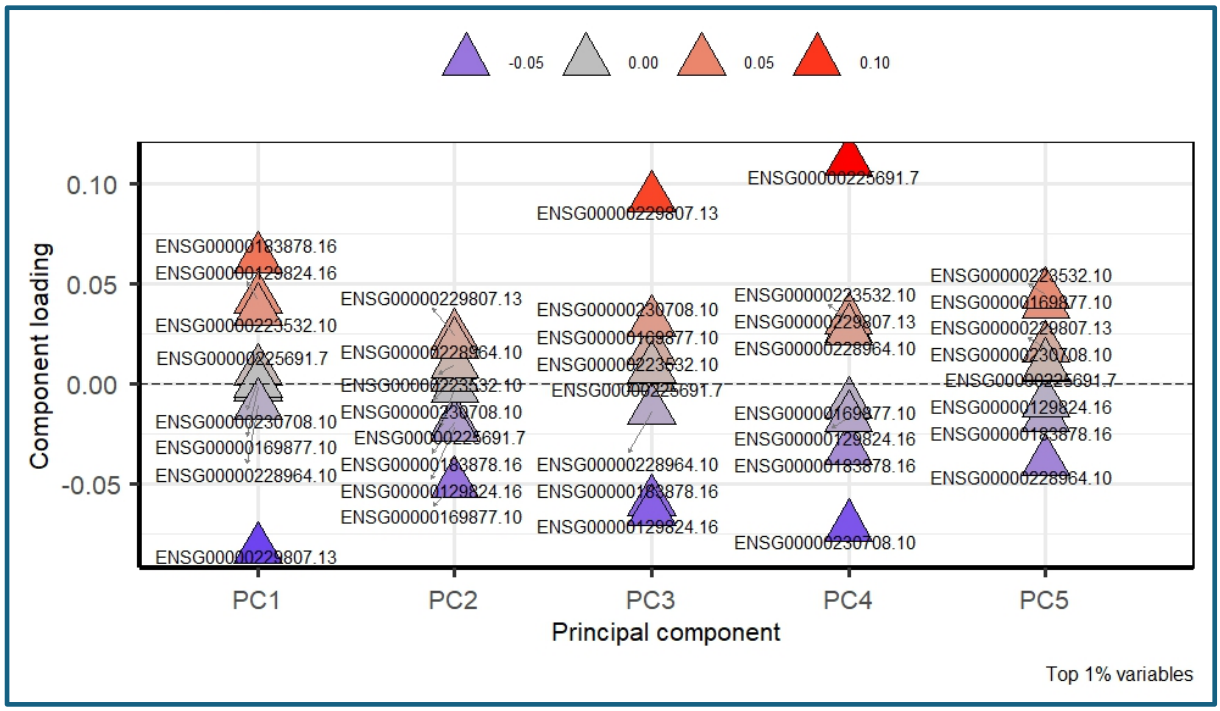

Figure 16: Loading plot depicting the DEGs associated with Principle components 1-5.

Table 14: Details of the differentially expressed genes extracted from all principal components of the loading plot displayed in ***Error! Reference source not found.****.*

PC	Ensembl ID	Gene Name	Gene Name Explained	Gene Type	Chromosome Location
1,2,3,4,5	ENSG00000183878	UTY	ubiquitously transcribed tetratricopeptide repeat containing, Y-linked	coding	Y
1,2,3,4,5	ENSG00000129824	RPS4Y1	ribosomal protein S4 Y-linked 1	coding	Y
1,2,3,4,5	ENSG00000223532	HLA-B	major histocompatibility complex, class I, B	coding	CHR_HSCHR6_MHC_COX_CTG1
1,3,5	ENG000000225691	-	-	Non-coding	-
1,2,3,4,5	ENSG00000230708	HLA-DPB1	major histocompatibility complex, class II, DP beta 1	coding	CHR_HSCHR6_MHC_COX_CTG1
1,2,3,4,5	ENSG00000169877	AHSP	alpha hemoglobin stabilizing protein	coding	16
1,2,3,4,5	ENSG00000228964	HLA-B	major histocompatibility complex, class I, B	coding	CHR_HSCHR6_MHC_SSTO_CTG1
1,2,3,4,5	ENSG00000229807	XIST	X inactive specific transcript	lncRNA	X

As shown in Table 14, the majority of the genes are coding and located on the sex chromosomes (321). Specifically, relating to cardiac function; UTY has been associated with accelerated heart failure in mouse studies (372, 373) and XIST has been associated with atherosclerosis, hypertrophy and cardiac fibrosis (374, 375).

As seen with the results generated in *3.3.5 RNA-Seq correlates of T2D and their corresponding CMR phenotypes* the small number of genes highlighted using this approach, along with their contribution to multiple PCs, makes it difficult to gain biological insights. Given the strong negative correlation of Stress MBF with the myocardial transcriptome (i.e. PC1), a further differential gene expression analysis was undertaken to attempt to identify DEGs that are

associated with quartile 4 (Q4 – lowest MBF) versus quartile 1 (Q1 – highest MBF) of Stress MBF, in order to dissect potential molecular pathways linked to myocardial perfusion. This was, once again, intended as a proof-of-principle, which could be extended in future to other CMR phenotypes associated with RNA-seq PCs.

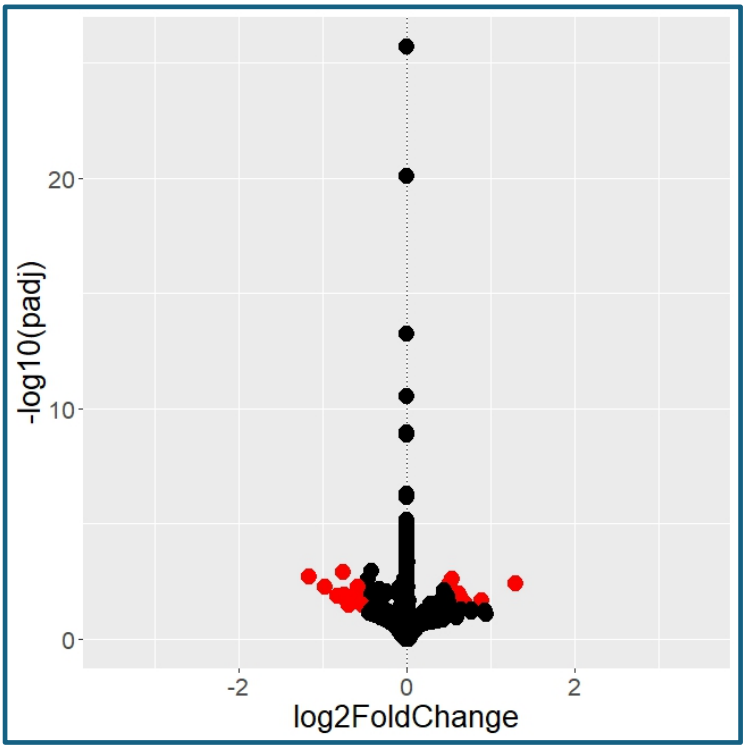

Figure 4.17: Volcano plot illustrating differential gene expression of upper vs lower quartiles of SMBF. Volcano plot illustrating differential gene expression. Each dot represents a gene, with red colour denoting those that achieve Benjamini–Hochberg FDR-adjusted P < 0.05 and log2 fold change <-0.5 or >0.5.

A total of 41,166 genes were quantified, with 1235 showing an FDR adjusted p-value <0.05 (Figure 4.17). DEGs were defined as those with log2 fold change greater than 0.5 or less than -0.5, in order to focus on larger biological effect sizes. These 30 DEGs are presented in Table 15.5.

Table 15: List of DEGs produced from undertaking differential gene expression analysis comparing Stress MBF quartile 1 to 4.

Ensemble Gene ID	Gene Name	Log2Fold Change	FDR P value	Description of function
ENSG00000235513	L3MBTL2-AS1	1.29104	0.00403	L3MBTL2 antisense RNA 1
ENSG00000134056	MRPS36	0.88576	0.02223	Mitochondrial ribosomal protein S36
ENSG00000273076	-	0.85271	0.04466	Novel transcript, antisense to SUN2
ENSG00000246705	H2AJ	0.69933	0.02938	H2AJ histone
ENSG00000206838	SNORA5A	0.66885	0.04317	Small nucleolar RNA, H/ACA box 5A
ENSG00000126453	BCL2L12	0.65041	0.03913	BCL2 like 12
ENSG00000176340	COX8A	0.64457	0.01652	Cytochrome c oxidase subunit 8A
ENSG00000101439	CST3	0.62679	0.04141	Cystatin C
ENSG00000099800	TIMM13	0.62464	0.01080	Translocase of inner mitochondrial membrane 13
ENSG00000065518	NDUFB4	0.55445	0.01756	NADH:ubiquinone oxidoreductase subunit B4
ENSG00000171421	MRPL36	0.54804	0.04033	Mitochondrial ribosomal protein L36
ENSG00000125877	ITPA	0.54366	0.00258	Inosine triphosphatase
ENSG00000179029	TMEM107	0.52623	0.03370	Transmembrane protein 107
ENSG00000143252	SDHC	0.50679	0.00381	Succinate dehydrogenase complex subunit C
ENSG00000130312	MRPL34	0.50484	0.0097	Mitochondrial ribosomal protein L34
ENSG00000147408	CSGALNACT1	-0.52928	0.03295	Chondroitin sulfate N-acetylgalactosaminyltransferase 1
ENSG00000236449	-	-0.58358	0.00568	Novel transcript, antisense to WIPF1 and CHRNA1
ENSG00000287555	-	-0.61094	0.01278	Novel transcript, antisense to FBXW7
ENSG00000271843	-	-0.62305	0.01392	Novel transcript
ENSG00000288881	-	-0.68966	0.01674	Novel transcript, sense intronic to NRF1
ENSG00000289727	-	-0.69106	0.03238	Novel transcript, antisense to NLRC4
ENSG00000172548	NIPAL4	-0.70297	0.02439	NIPA like domain containing 4
ENSG00000218313	-	-0.70522	0.01689	Novel TWIST neighbor (TWISTNB) pseudogene
ENSG00000286676	ACTBP4	-0.74678	0.01205	ACTB pseudogene 4

ENSG00000266598	-	-0.75813	0.01572	Novel transcript, antisense to GNA13
ENSG00000230482	ATP5MC2P3	-0.75921	0.00127	ATP5MC2 pseudogene 3
ENSG00000244203	FOXP1-AS1	-0.76949	0.01371	FOXP1 antisense RNA 1
ENSG00000244730	PHF5AP3	-0.82531	0.01367	PHF5A pseudogene 3
ENSG00000276809	-	-0.97222	0.00528	Novel transcript, sense intronic to DNAJC3
ENSG00000277715	-	-1.16810	0.00195	Novel transcript, antisense to CKAP4

The 'significant' DEGs were then analysed using G:Profiler (320) for further functional enrichment characterisation and the resulting outputs can be found in Table 16

Table 16: G Profiler output results of the significant DEGs associated with SMBF quartile 1 vs 4 in this cohort of HFrEF patients. (GO:MF represents, molecular function and GO:BP represents biological process).

Source	Term name	Adjusted P value	Ensembl Gene ID (Gene Name) of contributory genes in DEGs
GO:MF	Electron transfer activity	0.005	ENSG00000176340 (non-coding), ENSG00000065518 (non-coding), ENSG00000143252 (SDHC – Succinate Dehydrigenase Complex Subunit C)
GO:MF	XTP diphosphatase activity	0.014	ENSG00000125877 (ITPA – Inosine Triphosphate)
GO:MF	Peptidoglycan glycosyltransferase activity	0.014	ENSG00000147408 (CSGALNACT1 – Chondroitin sulfate N-acetylgalactosaminyltransferase 1)
GO:MF	Glucuronylgalactosylproteoglycan 4-beta-N-acetylgalactosaminyltransferase activity	0.021	ENSG00000147408 (CSGALNACT1 – Chondroitin sulfate N-acetylgalactosaminyltransferase 1)
GO:MF	Xoglutarate dehydrogenase (succinyl-transferring) activity	0.022	ENSG00000134056 (MRPS36 – Mitochondrial ribosomal protein S36)
GO:MF	Succinate dehydrogenase activity	0.022	ENSG00000143252 (SDHC – Succinate dehydrogenase complex subunit C)
GO:MF	Glucuronosyl-N-acetylgalactosaminyl-proteoglycan 4-beta-N-acetylgalactosaminyltransferase activity	0.031	ENSG00000147408 (CSGALNACT1 – Chondroitin sulfate N-acetylgalactosaminyltransferase 1)
GO:MF	Magnesium ion transmembrane transporter activity	0.047	ENSG00000172548 (NIPAL4 – NIPA like domain containing 4)
GO:BP	Aerobic respiration	0.003	ENSG00000134056 (non-coding), ENSG00000176340 (non-coding), ENSG00000065518 (non-coding), ENSG00000143252 (SDHC – Succinate dehydrogenase complex subunit C)
GO:BP	Negative regulation of elastin catabolic process	0.013	ENSG00000101439 (CST 3 – Cystatin C)
GO:BP	Negative regulation of collagen catabolic process	0.013	ENSG00000101439 (CST 3 – Cystatin C)
GO:BP	ITP catabolic process	0.013	ENSG00000125877 (ITPA – Inosine Triphosphate)
GO:BP	UDP-glucuronate metabolic process	0.018	ENSG00000147408 (CSGALNACT1 – Chondroitin sulfate N-acetylgalactosaminyltransferase 1)
GO:BP	Chondroitin sulfate proteoglycan biosynthetic process, polysaccharide chain biosynthetic process	0.018	ENSG00000147408 (CSGALNACT1 – Chondroitin sulfate N-acetylgalactosaminyltransferase 1)
GO:BP	Negative regulation of blood vessel remodeling	0.018	ENSG00000101439 (CST 3 – Cystatin C)

GO:BP	UDP-N-acetylgalactosamine metabolic process	0.023	ENSG00000147408 (CSGALNACT1 – Chondroitin sulfate N-acetylgalactosaminyltransferase 1)
GO:BP	Detection of nodal flow	0.023	ENSG00000179029 (TMEM107 – Transmembrane protein 107)
GO:BP	Bone morphogenesis	0.025	ENSG00000179029 (non-coding), ENSG00000147408 (CSGALNACT1 – Chondroitin sulfate N-acetylgalactosaminyltransferase 1)
GO:BP	Negative regulation of extracellular matrix disassembly	0.026	ENSG00000101439 (CST 3 – Cystatin C)
GO:BP	Mitochondrial translation	0.029	ENSG00000171421 (non-coding), ENSG00000130312 (MRPL34 – Mitochondrial ribosomal protein L34)
GO:BP	Dermatan sulfate proteoglycan biosynthetic process	0.038	ENSG00000147408 (CSGALNACT1 – Chondroitin sulfate N-acetylgalactosaminyltransferase 1)
GO:BP	Heparan sulfate proteoglycan biosynthetic process, polysaccharide chain biosynthetic process	0.038	ENSG00000147408 (CSGALNACT1 – Chondroitin sulfate N-acetylgalactosaminyltransferase 1)
GO:BP	Protein localization to ciliary transition zone	0.041	ENSG00000179029 (TMEM107 – Transmembrane protein 107)
GO:BP	Heparin biosynthetic process	0.047	ENSG00000147408 (CSGALNACT1 – Chondroitin sulfate N-acetylgalactosaminyltransferase 1)
GO:BP	Protein insertion into mitochondrial inner membrane	0.049	ENSG00000099800 (TIMM13 – Translocase of inner mitochondrial membrane 13)

4.4 DISCUSSION

This chapter has presented the phenotypic and blood transcriptomic characteristics of patients with newly diagnosed HFrEF, defining DEGs associated with T2D, followed by exploring the relationship between CMR phenotypes and blood transcriptome.

HFrEF and CMR characteristics in patients with T2D

In this group of patients with newly diagnosed HFrEF, age and sex profiles were similar in groups with and without T2D. Whilst, as expected, the HbA1c was significantly higher in the T2D group, BMI was not significantly different in those with T2D.

Participants with T2D had numerical differences in LV concentric remodeling parameters. Specifically, they exhibited higher LV mass and LV mass to LV end-diastolic volume. Such changes have been associated with diabetic heart disease (129), but the numbers of participants may be too small to elicit statistically significant differences. This phenotype may represent diabetic cardiomyopathy in some participants, given almost half did not have hypertension and ischaemic scar was present in around one third. Whilst LVEF was nominally lower in those with T2D, this did not achieve statistical significance.

With regards to markers of interstitial fibrosis, patients with T2D had numerically higher T1 and ECV metrics, compared to non-diabetic patients. This is in-keeping with published data, in which HFrEF patients with concomitant T2D had significantly higher T1 and ECV (376). That study included 4 times more participants than mine, suggesting my sample may be underpowered to define how T2D influences fibrosis in HFrEF.

Interestingly, although diabetes is one of the major risk factors for atherosclerosis and subsequent ischaemic heart disease, within my HFrEF patient cohort, those with concomitant T2D were more likely to exhibit non-ischaemic LGE. Non-ischaemic LGE in people with T2D is well-documented in the literature. For example, Bojer et al, reported that in 296 patients with T2D, almost 10% displayed non-ischaemic LGE (216). These lesions were usually situated in the midwall of the LV in the basal lateral or the basal inferolateral segments and were associated with normal to high wall thickness and normal contraction. Furthermore, study participants with non-ischemic LGE lesions, in comparison with patients without LGE lesions, had increased myocardial mass. Importantly, the authors suggested that such lesions were associated with the presence of wider diabetic complications and poorly controlled diabetes.

Despite a higher prevalence of non-ischaemic LGE, patients with T2D displayed significantly lower myocardial perfusion under adenosine stress than patients without diabetes. The RPP imbalance between the two groups may suggest a blunted response to adenosine in patients with T2D. This has certainly been shown before in the literature, as patients with T2D have shown a blunted response to both adenosine and regadenoson stress, even in the presence of normal perfusion imaging (377, 378). Similar responses have been shown in patients with HFrEF (379). Whilst specific studies focusing exclusively on patients with HFrEF and concomitant T2DM are limited, given the similar response of the two pathologies to adenosine stress, it could be speculated that this combination of pathologies could result in an additive effect to the blunted HR response. Despite this however, stress perfusion CMR is particularly valuable in this group of patients as it has been considered an effective method of evaluating prognosis in patients across the spectrum of diabetes. In a retrospective CMR study by Leungratanamart et al including over 400 pre-diabetic patients, those with inducible ischaemia had significantly greater rates of cardiovascular death, non-fatal MI, HF hospitalisation and ischaemic stroke, compared to patients without inducible ischaemia over a median follow up time of 8 years (211). In another study by Sharrack et al, where the team prospectively recruited patients across the spectrum of diabetes and performed stress CMR, the prevalence of silent IHD (defined as inducible ischemia or MI on LGE) was highest in patients with T2D (compared to pre-diabetes and non-diabetic controls). In keeping with this, stress MBF was lowest in patients with T2D than those without (380). Importantly, this cohort is very similar to that presented in this chapter as it consisted of patients with T2D and HFrEF, with a mean LVEF in the T2D group of 36%. Furthermore, within their cohort the prevalence of non-ischaemic LGE was higher than that of ischaemic LGE. Furthermore, the authors showed that as HbA1c increased, stress MBF and MPR declined. They found that T2D was

associated with higher rates of all cause death, HF admission, CV death, stroke and non-fatal MI than the pre-diabetic and the control group over a three year follow-up period (380). The presence of ischemic scar has been shown to be the strongest predictor of adverse outcome in patients with T2D (381).

Transcriptomic profile: T2D

Functional enrichment analysis of the DEGs associated with T2D revealed: G-protein coupled receptor activity, olfactory receptor activity and nervous system processes. As discussed in Chapter 3 (*3.4 DISCUSSION- Transcriptomic profile: T2D*), the literature has examples of studies linking the blood transcriptome in the context of T2D to the immune system. My findings appear to be novel, yet plausible. G protein coupled receptors are vital in the regulation of many biological phenomena, including the immune response (382, 383), and hence are a credible hit. However, most of the contributor genes are non-coding and so the value of this insight is unfortunately rather limited. Olfactory receptors are present, not only in the nose, but also in pancreatic islets, adipose tissue and in immune cells. As a result of this they have been associated with metabolic sensing, inflammation, insulin secretion, gluconeogenesis, glucose reabsorption and lipid metabolism. Fitting with the current data, they have been shown to activate multiple G protein pathways (384, 385). Finally, nervous system processes may reflect neurodegenerative signals, autonomic dysfunction or diabetic neuropathy. Interestingly in a study investigating the transcriptomic alterations of cortical units and neurovascular units in patients with T2D, Bury et al, the affected pathways included those of insulin signalling and oxidative phosphorylation and this affected both astrocytes and endothelial cells, highlighting that nervous system alterations in the setting of diabetes are not just limited to the central nervous system (386). This suggests that there may be possible

biomarkers for diabetic complications in the blood. More importantly these results highlight the complex interplay of processes that occur in patients with T2D between the immune, metabolic and neural systems.

Whilst interesting, these are rather generic terms and do not necessarily provide substantial insights. Moreover, the literature contains no other studies investigating the blood transcriptomic profile of T2D and concomitant HFrEF, meaning that validation of these gene sets or individual DEGs will require follow-on studies. Regarding what is known about the blood transcriptome of people with T2D, the work of Corbi et al studied its association of diabetes parameters in people without heart failure. In particular, when patients with well controlled T2D were compared to those with poorly controlled T2D, upregulated genes included CCND3, CEPBD, MAP2K5, ENO2 and VAMP2, whilst downregulated genes were LGALS12 and PPAP2B, both associated with lipid regulation (338). There is no overlap with the DEGs I identified, but this is not necessarily surprising, given the absence of heart failure in their cohort.

Transcriptomic profile: HFrEF

When considering published work assessing the blood transcriptome of heart failure versus control (i.e. not considering diabetes), Nath et al identified pathways including adaptive immune response, proteasome-mediated ubiquitin-dependent protein catabolic process, T-cell co-stimulation, positive regulation of T-cell proliferation, and erythrocyte development (387). In a similar study by Sweet et al, the most significant pathways were indeed the protein ubiquitination pathway, but also the pathways of mitochondrial dysfunction, oxidative phosphorylation and EIF2 signalling. It must be highlighted that the presence of diabetes was

not considered in these analyses, and so the lack of overlap with my findings is not unexpected (388).

Transcriptomic profile and CMR phenotype

The patterns observed in PC1 from the Eigencor plot in Figure 4.15—characterized by modest positive correlations in LV mass, modest positive associations with indexed LVEDV and the presence of inducible ischaemia, and a modest negative correlation with stress MBF—highlight key physiological markers that could inform future research. These relationships suggest that PC1 captures a composite profile relevant to cardiac stress response, which may be valuable for identifying at-risk individuals or evaluating treatment effects in subsequent studies.

Transcriptomic profile: Stress MBF

The Eigencor plot associating RNA-seq PCs with CMR parameters illustrated significant correlations of PC1 with LV mass, stress MBF, and the presence of inducible ischaemia. There were no significant correlations in PC2, 3 or 5, but PC4 significantly correlated with non-ischaemic LGE and rest MBF. These results highlight that differences in myocardial perfusion in people with HFrEF are associated with the biology of circulating cells, most likely leukocytes. In a study using LV myocardial RNA-seq to explore the basis of ischaemic versus non-ischaemic HFrEF (388), Sweet et al identified many immune system pathways including: including Antigen Presentation, CD28 in T Helper Cells, IL-6, CD40, JAK/Stat, fMLP in Neutrophils, and role of NFAT in Regulation of Immune Response. This is interesting as it provides support for the correlations I observed, but at the level of the myocardium rather than circulating blood.

To gain further insights regarding the basis of correlation between myocardial perfusion and the blood transcriptome, I defined DEGs between patients in the upper and lower quartiles of stress MBF. This identified numerous 'novel transcripts', emphasizing the gaps in our current understanding of the transcriptome. Of the identified genes, their main function is associated with electron transfer activity and aerobic respiration, suggesting a role of metabolism in circulating cells. Notably, there is a large literature showing that metabolism and mitochondrial function profoundly alters immune cell function (389, 390), and this may represent an avenue for future exploration.

Gender differences and CMR phenotype

The results presented here are novel in showing that biological sex is robustly associated with high-level variance in the blood transcriptome of people with HFrEF and that this correlates with CMR parameters. This is strikingly illustrated in the PCA plot showing near distinct clustering of males and females, but was also highlighted in the location of genes shown in loadings plots to contribute to PC1, nearly half of which reside on the sex chromosomes. In-keeping with this, one of the genes associated with high degrees of variance given its presence across all 5 PCs in the analysis of DEGs within this patient population was XIST. This gene, found on the X chromosome has been described as a scaffold for chromatin modification enzymes, modulating the expression of individual genes and whole chromosome regions (391). When dysregulated it has been associated with atherosclerosis, hypertrophy and cardiac fibrosis (375). XIST has also been implicated with the development of DM complications, including retinopathy, gestational diabetes and diabetic heart disease (392-394).

Published imaging studies have shown that in patients with T2D and HFrEF, men have significantly larger LV end-diastolic and systolic volumes and a higher incidence of LGE. Females on the other hand, exhibit more pronounced remodelling and have more significant LV hypertrophy (395, 396). Some groups have suggested that cardiovascular risk factors can influence cardiac remodelling differently according to sex, irrespective of underlying T2D status. In males, concentric remodelling has been associated with triglyceride values and self-reported alcohol intake, whereas in the same study strong association with LV remodelling in females was associated with the presence of T2D and self-reported sugar intake (397). In a cluster analysis of cardiovascular phenotypes of patients with T2D and established atherosclerotic cardiovascular disease, males with established coronary artery disease formed a different cluster to females with non-coronary atherosclerotic disease of the four main clusters that were discovered (398).

Limitations

The single centre and small sample size of my cohort reduce the generalisability of the results and increase the risk of false negative findings. Future studies with larger sample sizes are needed to rigorously examine the relationship between T2D, the blood transcriptome, and CMR phenotypes in patients HFrEF.

Another limitation arises from the challenge of defining the whole blood transcriptome using bulk RNA-seq. Whilst it is possible to isolate specific immune cell populations from the blood, this is logistically challenging in the wider context of my study, and so the decision was made to use whole blood. This contains large quantities of red blood cells that express a limited gene repertoire, which can bias results. To address this, globin mRNA depletion was

performed during library preparation, but this cannot account for other genes that are expressed in red blood cells. However, whilst a concern, this did not hinder my analysis from defining biologically plausible correlations between the blood transcriptome and CMR parameters, which offers some reassurance. Future studies could employ single cell RNA-seq methods to circumvent this limitation, although these would increase costs by more than 10-fold, which would need a large budget if adequate power was to be assured.

Finally, it is possible that some of my findings reflect differential abundance of leukocyte subsets (e.g. between males and females, T2D and NODM, or across quartiles of stress MBF). One crude way to address this is by including major subsets from the full blood count as covariates in the DESeq2 model, but this can only include categorical variables, limiting the capacity to account for this factor. I also hope to use validated deconvolution methods to infer the abundance of leukocyte subsets in each sample (399), which will allow me to correlate these with CMR phenotypes.

Future Directions

As mentioned in Chapter 3, I hope that some of the DEGs presented in this chapter will soon be explored at the plasma protein level using UK Biobank plasma proteomics data, potentially leading to circulating biomarkers corresponding to CMR phenotypes. Unfortunately, perfusion data is currently not available in UK Biobank, so analysis of the DEGs highlighted here for stress MBF will not be possible, but other CMR metrics can be pursued.

In future, I hope to conduct in-house validation studies, which are essential when performing RNA-seq studies. Using a larger cohort, this approach may also allow me to explore future

clinical outcomes. I also hope to validate DEGs using emerging publicly available RNA-seq data from people with HFrEF although, as noted above, the existing literature does not allow me to do this yet. Given my finding of altered metabolism and mitochondrial function being associated with stress MBF, I also hope to explore leukocyte metabolism (e.g. using SeaHorse respirometry) and correlate this with stress MBF as an orthogonal approach to validation.

4.5 CONCLUSIONS

This chapter highlights the many blood transcriptomic correlates of cardiac function and disease observed within patients with newly diagnosed HFrEF with and without T2D. My data also show robust biological sex-based differences in the blood transcriptome of people with HFrEF. Further exploration of these findings may help to define the biological phenomena underpinning CMR traits.

5. Defining sex-differences in CMR phenotypes and myocardial energetic measurements associated with T2D

5.1 INTRODUCTION

T2D is associated with substantially increased risk of incident HF with both reduced and preserved ejection fraction (400). The HF incidence is even higher for females with T2D (Female-T2D) compared to males with T2D (Male-T2D), being 5-fold vs 2.4-fold greater, respectively, even after adjustment for risk factors, such as age, coronary artery disease, and hypertension (401).

The phenotypic differences between the hearts of healthy males and females have been well described in the literature. The female heart is smaller with regards to cavity size, and arterial diameter and has a lighter mass when compared to a male heart of the same age and race (402, 403). Functionally, females have a higher heart rate than males, and also exhibit a longer time to relaxation from contraction (403). Furthermore, females are more likely to have higher LVEF compared to their age and BMI matched male counterparts (404, 405).

Whilst there is no consensus-based grading system for the effects of diabetes on the heart, a spectrum of disease has been described, somewhat akin to the American Heart Association heart failure stages**.** In the subclinical stage, cardiac energetic deficit, LV concentric remodeling, impaired cardiac contractility with reduced GLS even in the presence of normal LVEF, diastolic dysfunction and reduced myocardial perfusion reserve and vasodilator stress myocardial blood flow are among the first markers of heart disease in T2D. This may gradually progress to a smaller ventricular cavity, systolic dysfunction, and HF (19, 400).

Cardiac energetics, as measured by phosphorus spectroscopy, have been consistently shown to be higher in females compared to age matched male cohorts. This is particularly stark in the pre-menopausal age groups. This is likely due to the effects of high levels of circulatory oestrogen within this group (402, 406). The presence of T2D is known to reduce the PCr/ATP ratio (407, 408), but the effect of gender on this is yet to be described.

Chapter 3 described myocardial transcriptomic correlates of cardiac imaging phenotypes in people with severe aortic stenosis, with and without T2D. This revealed significant correlation between sex and high-level transcriptomic variance in principal component analyses. Chapter 4 also outlined the blood transcriptomic correlates of heart failure with reduced ejection fraction, with and without T2D. High-level transcriptomic variance (PC1) correlated with gender, showing important sex-differences in the immune system. These observations further underscore the important sex differences at a molecular level and support the need for sex-stratified analyses of heart disease associated with T2D. The aim of this study, therefore, was to determine the association of sex with the phenotypic expression and cardiac metabolism of diabetic heart disease in patients with T2D.

5.2 METHODS

5.2.1 Study design and ethics

This single-center, prospective cohort study complied with the Declaration of Helsinki and was approved by National Research Ethics Committees (ref: 19/WM/0365, ref: 22/SC/0335 ref: 23/EM/0074 for patients with T2DM and ref:18/YH/0168 for healthy volunteers). The

study was co-funded by the Wellcome Trust (Grant 207726/Z/17/Z) and Diabetes UK (18/0005908). All participants for all study cohorts provided written informed consent.

5.2.2 Inclusion criteria

Key inclusion criteria were adult (over 18 years of age) males or females and the ability and willingness to provide informed consent and comply with the requirements of the study. Patient inclusion criteria consisted of a T2D diagnosis at least 6 months before enrolment, and no known sequelae of the disease or other significant past medical history, in addition to 42 > HbA1c < 86mmol/mol and LVEF ≥50%. Participants were either on no T2D treatment, diet-control, oral anti-diabetes drugs or insulin. Healthy volunteers (HV) with no known T2D were recruited contemporaneously from primary care general practices in Yorkshire, United Kingdom.

5.2.3 Exclusion criteria

Participants were excluded if they had known coronary artery disease, severe valve disease, significant renal impairment (eGFR <30mL/min/1.73m^2), chronic obstructive lung disease, asthma, or known cardiomyopathy (including hypertrophic cardiomyopathy, infiltrative diseases [e.g., amyloidosis], accumulation diseases [e.g., haemochromatosis, Fabry disease], history of cardiac surgery, permanent atrial fibrillation, current tobacco smoking or any contraindications to CMR.

5.2.4 Past medical history

Participants' electronic notes were reviewed, and all past medical history documented in their GP and hospital records were documented.

5.2.5 Biochemical, anthropometric assessments

Height and weight were recorded, and BMI was calculated. A fasting blood sample was taken for assessments of NT-proBNP, fasting blood glucose, HbA1c and lipid profile.

5.2.6 ^{31}Phosphorus-magnetic resonance spectroscopy

^{31}Phosphorus (^{31}P)-MRS was performed on a 3.0 Tesla MR system (Prisma, Siemens, Erlangen, Germany) to obtain the PCr/ATP from a voxel placed in the mid-ventricular septum, with the participants lying supine in the iso-center of the magnet. ^{31}P-MRS data were acquired with a non-gated 3D acquisition-weighted CSI sequence (254). The acquisition matrix was 16 × 8 × 8 for the protocol. Field of view was 240 × 240 × 200 mm. The acquisition was run with a fixed repetition time of 720ms.

5.2.7 Cardiovascular magnetic resonance imaging

CMR imaging was also performed on a 3.0 Tesla MR system (Prisma, Siemens, Erlangen, Germany). The CMR protocol (Figure 5.1) consisted of cine imaging using a steady state free precession sequence, native pre- and post-contrast T1 mapping, dobutamine stress and rest perfusion, dobutamine stress and rest velocity-encoded mitral in-flow imaging, late gadolinium enhancement imaging, and it was performed on a 3.0 Tesla MR system (Prisma, Siemens, Erlangen, Germany).

The precise details of the protocol can be referred back to *2.2.4 Study Protocol, Cardiovascular magnetic resonance & ^{31Phosphorus} magnetic resonance spectroscopy. W*ith the exception being that in this protocol dobutamine was used as a stressor compared to adenosine. This change of pharmacological stressor of the protocol was performed to ensure a short and effective rest and stress ^{31Phosphorus} magnetic resonance spectroscopy protocol (as previously described, (221)).

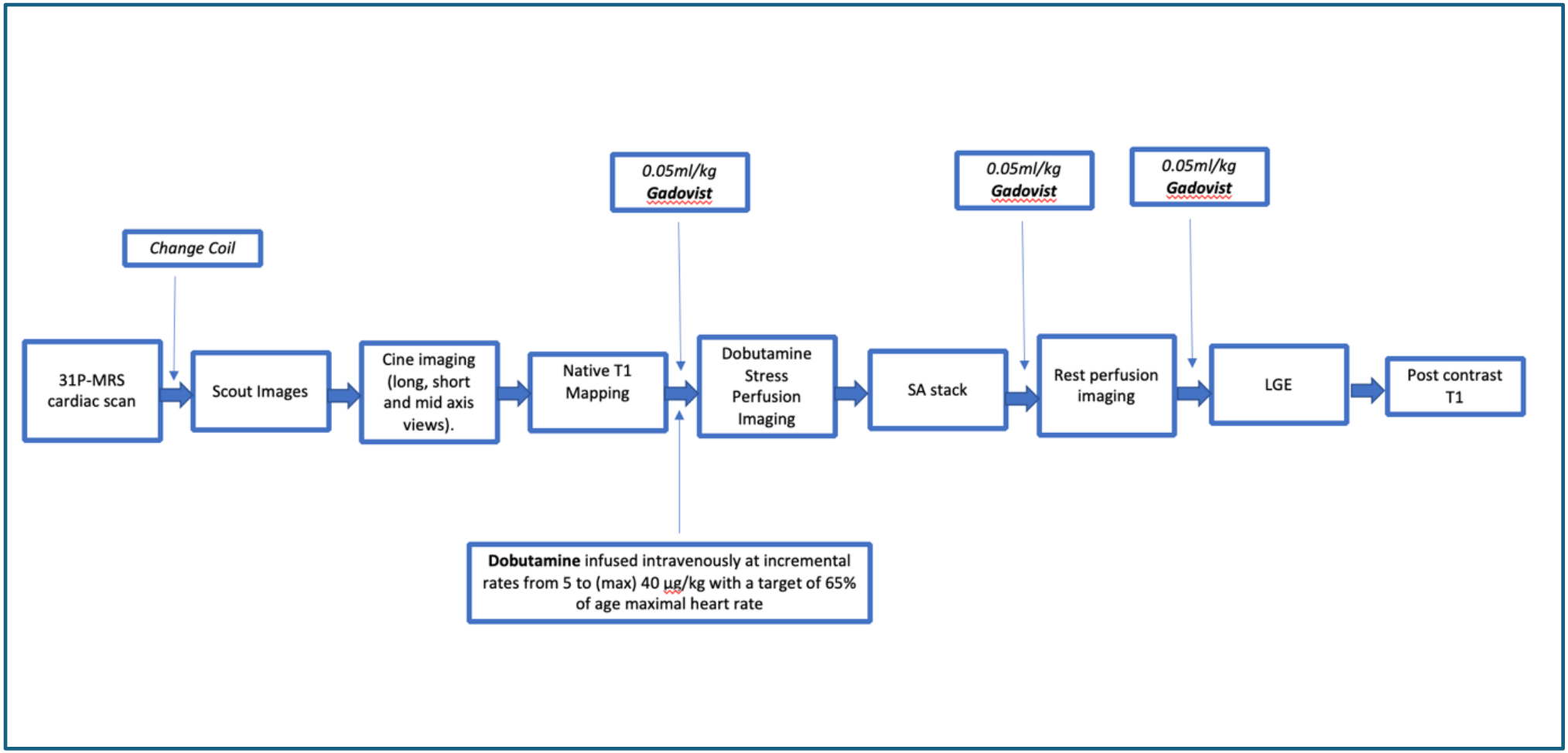

Figure 5.1: Multiparametric scan protocol. Cardiac phosphorus magnetic resonance (31P-MRS) scan was followed by cardiovascular magnetic resonance (CMR) imaging, which included cine imaging, native pre-contrast, and post-contrast T1 mapping, dobutamine stress perfusion imaging and late gadolinium enhancement (LGE) imaging.

Dobutamine stress perfusion

Perfusion imaging used free-breathing, FLASH magnetic resonance protocol with motion-corrected automated in-line perfusion mapping using the Gadgetron streaming software image reconstruction framework as previously described (236). Dobutamine was infused at a starting dose of 5μg/kg/min through a peripheral cannula. Dose was increased at 2 minute intervals up to a maximum of 40μg/kg/min to achieve each individual patient's target heart rate, which was calculated as: [(220-age) x 0.65]. Dobutamine stress was well tolerated by all study participants. A minimum 10-minute interval was kept between perfusion acquisitions to ensure equilibration of gadolinium kinetics and resolution of all hemodynamic effects of dobutamine. For each perfusion acquisition, an intravenous bolus of 0.05mmol/kg gadobutrol (Gadovist, Leverkusen, Germany) was administered at 5ml/s followed by a 20ml saline flush using an automated injection pump (Medrad MRXperion Injection System, Bayer).

Qualitative and quantitative analysis ^{31}P-MRS analysis and CMR data

All ^{31}P-MRS and MRI post-processing analysis (except for the GLS data) was performed offline and blinded to all participant details after completion of the study. CMR image analysis was performed using Cvi42© (Circle cardiovascular imaging, Calgary, Canada).

^{31}P-MRS data were analyzed using MATLAB version R2012a (MathWorks, Natick, Massachusetts) as previously described (253).

Perfusion Imaging

Myocardial perfusion image reconstruction and processing was implemented using the Gadgetron software framework as previously described (236). Rest/stress MBF were measured for each of the 16 segments using the American Heart Association (AHA) classification. MBF values for all remaining segments were averaged to provide a global value. MPR, was calculated as the ratio of stress to rest MBF. Both stress MBF and MPR were automatedly measured. Such use of artificial intelligence quantification of perfusion parameters has been shown to provide robust, independent predictors of adverse CVS outcomes (409). CMR rest/stress perfusion images were carefully reviewed for each of the 16 segments using the AHA classification to ensure quality control, a regional threshold of stress MBF >1.43ml/min/g was taken as evidence of maximal hyperaemia and adequate stress (410).

5.2.8 Statistical analysis

Statistical analysis was performed using GraphPad Prism software (version 9.5.1). All data were checked for normality using the Shapiro-Wilk test and presented as mean or median with 95% confidence intervals or interquartile range as appropriate. Categorical data are presented as numbers and percentages and compared with Pearson's chi-square test.

Multivariate linear regression is used to define statistically significant ($p<0.05$) DM-gender interaction, with participant characteristics (e.g. CMR metrics) as the dependent variable and DM, gender and a DM-gender interaction term as independent covariates. Differences in non-parametric variables were assessed using a Kruskal-Wallis test. The student t-test was used for comparison of normally distributed datasets and Mann-Whitney U test was used for non-

parametric tests where data were obtained for only two groups. A two-sided p-value of <0.05 was applied as indicating threshold of significance.

5.3 RESULTS

5.3.1 Comparison of demographic and biochemical parameters

Between 2020 and 2024, a total of 141 patients with T2D were recruited. The demographic, biochemical, and functional data are shown in **Error! Reference source not found.**. There were no significant differences in age or BMI between the two groups. In this asymptomatic cohort, females with T2D had numerically higher median NTproBNP levels than males with T2D (63 (35, 102) vs 44 (35, 82) ng/l, P=0.2), but both were clearly within the normal range

Among patients with T2D, females showed significantly lower fasting glucose (8.2 (6.2, 9.4) vs 10.2 (9.0, 11.4) mmol/l, P = 0.025) and HBA1c measurements compared to males. However, serum insulin concentrations were significantly higher in females with T2D compared to males (56 (20, 73) vs 21 (12, 49)pmol/L, P=0.12). There were no differences in the lipid profiles between the females and males with T2D. Females and males with T2D received broadly similar glucose lowering treatments, but sulphonylurea use was a more common choice for males with T2D (Table 5.1).

Table 5.1: Baseline characteristics between women and men with T2D and healthy volunteers.

VARIABLE	Males with T2D (n = 82)	Females with T2D (n = 54)	Male HV (n=17)	Female HV (n=17)	P Value for interaction (and pairwise tests)
Demographics					
Age, y	61 (59, 63)	61 (54, 65)	63 (57, 68)	65 (61, 68)	0.3700
BMI, kg/m²	29.6(28.5,30.6)	31.4(29.7,33.2)	26.2(24.4,27.8)	23.4(22.4,24.4)	**0.0166** †* ♂ ♀
Heart rate, bpm	69 (65, 72)	70 (62, 77)	56 (53, 60)	56 (53, 60)	0.3345 ♂ ♀
Systolic BP, mmHg	134 (129, 139)	124 (110, 137)	123 (116, 130)	133 (124, 140)	**0.0167** ♂
Creatinine, umol/l	74 [66, 87]	56 [52, 64]	71 [68, 81]	67 [55, 67]	0.2980 †*
Haemoglobin, g/l	149 (143, 154)	138 (133, 143)	155 (145, 165)	139 (133, 144)	0.4493 †*
Haematocrit, l/l	0.45(0.43,0.46)	0.42(0.41,0.43)	0.47(0.44,0.49)	0.42(0.41,0.44)	0.3964 †*
TG, mmol/l	1.8 [1.3, 3.3]	1.8 [1.2, 2.6]	1.1 [0.8, 1.6]	1.2 [0.9, 1.5]	0.4660 ♂ ♀
HbA1c, mmol/mol	61 [49, 72]	54 [49, 66]	38 [35, 39]	38 [34, 39]	0.3380 ♂ ♀
NT- proBNP, ng/l	44 [35, 82]	72 [48, 138]	44 [35,53]	72 [66, 77]	0.7271 †
Glucose, mmol/l	10.2 (9.0, 11.4)	8.2 (6.9, 9.4)	5.1 (4.8, 5.3)	4.7 (4.5, 4.8)	0.2520 †* ♂ ♀
Insulin, pmol/l	21.0[12.3,49.5]	56.0[20.0,73.3]	4.9 [3.2, 8.1]	5.8 [4.0, 7.6]	0.1213 ♂ ♀
HOMA-IR	4.6 [3.1, 10.0]	4.2 [2.5, 15.3]	1.5 [0.9, 2.0]	1.3 [0.8, 1.8]	0.4493 ♂ ♀
Co-morbidities					
HTN, n (%)	48 (59)	31 (57)	-	-	- ♂ ♀
Stroke/TIA, n (%)	2 (2)	-	-	-	-
Hyperlipidemia, n (%)	35 (43)	22 (41)	-	-	- ♂ ♀
Medications					
ACEi / ARB, n (%)	42 (51)	25 (46)	-	-	- ♂ ♀
Beta blocker, n (%)	16 (20)	7 (13)	-	-	- ♂
CCB, n (%)	19 (23)	10 (19)	-	-	- ♂
Diuretic, n (%)	8 (10)	11 (20)	-	-	- ♀
Statin, n (%)	59 (72)	38 (70)	1 (6)	2 (12)	- ♂ ♀
Antiplatelets, n (%)	10 (12)	9 (17)	-	-	-
DOAC/Warfarin, n (%)	5 (6)	1 (2)	-	-	-
Metformin, n (%)	61 (74)	35 (65)	-	-	- ♂ ♀
SGLT2, n (%)	26 (32)	12 (22)	-	-	- ♂
DPP-4, n (%)	7 (9)	-	-	-	-
GLP1RA, n (%)	3 (4)	1 (2)	-	-	-
Sulphonylurea, n (%)	16 (20)	4 (7)	-	-	- ♂
Insulin, n (%)	7 (9)	7 (13)	-		-

*A Shapiro-Wilk test is used to assess for normal distribution of variables. Normally distributed continuous variables are expressed as mean [95% confidence intervals]; nonparametric continuous variables are expressed as median (25th percentile, 75th percentile); and categorical variables are expressed as counts (percent). Normally distributed variables are compared using student t test and nonparametric variables are assessed using Mann-Whitney U test, † is used to represent statistical significance of <0.05 between DM groups, * is used to represent statistical significance of <0.05 between the HV volunteers, ♂ is used to represent statistical significance of <0.05 between the Male DM and Male HV, ♀ is used to represent statistical significance of <0.05 between the Female DM and Female HV. Chi-square and Fisher's Exact Test are used to assess categorical variables. Multiple Linear regression is used to quote the p-value investigating the DM/Gender interaction term, p<0.05 is considered significant. Dashes represent comparisons that are not possible.*

BMI, body mass index; BP, blood pressure; TG, triglycerides; HbA1c, glycated haemoglobin; NT-pro BNP, NT-pro B-type natriuretic peptide; HOMA-IR, Homeostatic Model Assessment of Insulin Resistance; HTN, hypertension; TIA, transient ischemic attack; ACEi, angiotensin-converting enzyme inhibitor; ARB, angiotensin receptor blocker; CCB, calcium channel blocker; DOAC, direct oral anti-coagulant; SGLT2, sodium glucose co-transporter-2 inhibitor; DPP-4, Dipeptidyl Peptidase-4 inhibitors; GLP1-RA, glucagon-like peptide-1 receptor agonists.

y, years; kg/m², kilograms per square meter; bpm, beats per minute; mmHg, millimeters of mercury; umol/L, micromoles per liter; g/l, grams per liter; L/L, litre of cells per litre of blood; mmol/l, millimoles per liter; mmol/mol, millimoles per mole; ng/l, nanograms per liter; pmol/l, picomoles pre litre; n, number.

5.3.2 The effect of T2D on HFrEF - Cardiovascular magnetic resonance and [31] Phosphorus-magnetic resonance spectroscopy findings

Left ventricular geometry and function

Significant differences were seen between the LV volume of men and women with T2DM, and versus sex matched healthy volunteers (LVEDVi - women with T2D; 65(62, 68), vs men with T2D; 72(68, 76) mL/m^2, P=0.0215; LVEDVi - women HV; 83(71, 94), P <0.0001 vs women with T2D; men HV 92(84, 101) mL/m^2, P <0.0001 vs men with T2D).

Concentric remodelling was present in both T2D groups compared to sex matched HVs, as defined by a higher LV mass-volume ratio, (LV mass: LVEDVi ratio – females with T2D: 0.57 (0.52, 0.62) vs females without T2D: 0.55 (0.52, 0.57), and males with T2D: 0.69 (0.65, 0.74), vs males without T2D: 0.61 (0.56, 0.66)), though this did not reach statistical significance (P= 0.06 and P = 0.18 for females and males respectively). Females with T2D also displayed less pronounced LV remodelling than males (LV mass: LVEDVi ratio – females with T2D; 0.57 (0.52, 0.62) vs males with T2D 69 (0.675, 0.74) g/mL, P =0.0002; and LV maximum wall thickness – females with T2D 9.8 (9.5,10.2) vs males with T2D; 11.6 (11.2, 11.9) mm, P <0.0001), although the same patterns was noted in HVs for LV mass: LVEDVi ratio (**Error! Reference source not found.**).

Overall cardiac function, as measured by LV ejection fraction and GLS at rest and stress were higher in females with T2D than males with T2D; (LVEF – females with T2D; 63 (62, 65), vs males with T2D; 60 (59, 62)%, P=0.009; rest GLS - females with T2D; 19.0 (18.01, 20.0), vs males with T2D; 17.1 (16.3, 17.8)%, P=0.0008; stress GLS – females with T2D; 21.4 (20.5, 22.3), vs males with T2D; 19.9 (19.1, 20.8)%, P=0.02).

While neither T2D group showed significant difference in E/A compared to sex-matched controls, this marker of diastolic function was also significantly higher in females than males with T2D (Female-T2D: 1.7[1.5-1.9], vs Male-T2D: 1.3[1.1-1.4]; *P*=0.0001), **Error! Reference source not found.**.

Left atrial function

As seen with the LV function, left atrial function was better in both females with and without T2D, compared to their male counterparts; (LAEF – Female-T2D: 56 (53,58) vs Male-T2D: 50 (47, 53)%, P= 0.005; Female-controls: 63 (58, 69) vs Male-controls: 54 (49, 58)%, P= 0.011). LAEF was lower in TD patients compared to healthy controls, with this difference being statistically significant in females (Female-T2D 56 (53,58), vs Female-controls 63 (58, 69), P= 0.01).

Cardiac perfusion

T2D was also associated with reductions in global stress-MBF and MPR in both sexes compared with sex-matched controls (**Error! Reference source not found.**). Between the T2D groups, there were no significant differences in global stress-MBF or MPR. However, rest-MBF (Female-T2D: 0.77 [0.64-0.890], vs Male-T2D: 0.66[0.59-0.74]ml/min/g; *P*=0.0004) and Endo/Epi stress-MBF ratio (Female-T2D: 1.05 [0.99-1.14], vs Male-T2D: 1.00 [0.96-1.07]; *P*=0.0019) were significantly higher in women than men with T2D (**Error! Reference source not found.**).

Cardiac energetics

There was significant cardiac energetic deficit (PCr/ATP ratio) in both sexes with T2D compared to their matched healthy controls (Female- T2D: 1.67 (1.38, 2.08) vs Female-control: 2.23 (1.74, 2.57), P=0.027; and Male- T2D: 1.75 (1.48, 2.08) vs Male-controls: 1.91 (1.72, 2.62), P<0.0001). Among patients with T2D the PCr/ATP ratio was almost identical between the two sexes, but amongst health controls this was numerically higher in females than males (P=0.14).

Other CMR findings

Healthy controls had numerically lower percentages of late gadolinium enhancement compared to their sex matched patients with T2D (LGE Female-controls 0.0 (0.0, 0.1) vs Female-T2D: 0.0 (0.0, 0.7)%, P=0.53; and Male-controls: 0.1 (0.0, 1.0) vs Mael-T2D: 0.6 (0.0, 1.9)%, P=0.55). The extent of LGE was similar in females and males with T2D.

Table 5.2: Comparisons of cardiovascular magnetic resonance findings between women and men with T2D.

Variable	Males with T2D (n = 82)	Females with T2D (n = 54)	Male HV (n=17)	Female HV (n=17)	P Value for interaction (and pairwise tests)
LV Anatomy					
LV EDVi, mL/m²	72 (68, 76)	65 (62, 68)	88 (77, 98)	75 (68, 81)	0.2809 †*♂♀
LV ESVi, ml/m²	29 (27, 31)	24 (22, 26)	35 (29, 40)	27 (24, 30)	0.4100 †*♂
LV SVi, ml/m²	43 (41, 46)	40 (38, 42)	53 (47, 59)	46 (41, 51)	**<0.0001** ♂♀
LV EF, %	60 (59, 62)	63 (62, 65)	61 (58, 63)	64 (62, 66)	0.8670 †*
LV mass, g	103 (96, 111)	70 (65, 76)	106 (90, 121)	69 (63, 76)	0.7644 †*
LV mass index, g/m²	46 (43, 50)	35 (33, 38)	53 (46, 59)	40 (37, 44)	0.9522 †*
LV mass to LV EDV ratio, g/mL	0.69 (0.65, 0.74)	0.57 (0.52, 0.62)	0.61 (0.56, 0.66)	0.55 (0.52, 0.57)	0.3780 †*
LV maximal wall thickness, mm	11.6 (11.2, 11.9)	9.8 (9.5, 10.2)	10.2 (9.5, 11.0)	9.2 (8.7, 9.7)	0.2614 †*♂♀
LA EDV	67 (62, 72)	63 (57, 69)	85 (75, 96)	68 (61, 74)	0.0929 *♂
LA ESV	33 (30, 37)	29 (26, 32)	44 (36, 53)	33 (27, 38)	0.2251 *♂
LA EF	50 (47, 53)	56 (53, 59)	49 (44, 54)	53 (47, 58)	0.3360 †
E/A	1.3 (1.1, 1.4)	1.7 (1.5, 1.9)	1.6 (1.3, 1.9)	1.8 (1.5, 2.2)	0.4645 †♂
Global longitudinal shortening rest, -%	17.1 (16.3, 17.8)	19.0 (18.1, 20.0)	17.1 (15.3, 19.0)	20.9 (18.9, 23.0)	0.1819 †*
Global longitudinal shortening stress, -%	19.9 (19.1, 20.8)	21.4 (20.5, 22.3)	22.1 (19.4, 24.7)	24.4 (22.1, 26.6)	0.6008 †♀
MAPSE rest, cm	12.5 (12.0, 13.1)	13.5 (12.9, 14.2)	14.3 (13.3, 15.3)	14.5 (13.7, 15.2)	0.7426 †♂
MAPSE stress, cm	12.5 (11.9, 13.1)	12.4 (11.7, 13.1)	14.2 (12.8, 16.0)	12.4 (10.8, 14.1)	0.4670
Mean native T1, ms	1237 (1210, 1264)	1258 (1231, 1285)	1268 (1250, 1285)	1285 (1274, 1296)	0.9160
ECV, %	25.2 (24.1, 26.3)	26.5 (24.7, 28.2)	24.0 (22.2, 25.8)	25.7 (24.1, 27.3)	0.6410
Scar percentage on LGE, %	0.6 [0.0, 1.9]	0.0 [0.0, 0.7]	0.1 [0.0, 1.0]	0.0 [0.0, 0.1]	0.8810 †
Perfusion Parameters & Cardiac Energetics					
Increase in RPP, %	94.0 (83.9, 104.2)	85.2 (74.5, 95.6)	42.4 (30.5, 54.3)	40.5 (30.4, 50.5)	0.7030 ♂♀
Rest RPP	8643 (8155, 9130)	8883 (8293, 9473)	7099 (6161, 8037)	8168 (7030, 9306)	0.3590 ♂
Stress RPP	17444 (16669, 18220)	16799 (15938, 17659)	7340 (6438, 8242)	8456 (7079, 9833)	0.1070 ♂♀
Stress MBF, ml/min/g	1.6 [1.22, 2.10]	1.47 [1.32, 2.23]	2.16 [1.96, 2.40]	2.19 [2.04, 2.68]	0.9475 ♀
Endo MBF Stress, ml/min/g	1.55 [1.23, 2.25]	1.63 [1.32, 2.30]	2.1 [1.96, 2.55]	2.13 [1.89, 2.60]	0.7127 ♂♀
Epi MBF Stress, ml/min/g	1.59 [1.28, 2.18]	1.40 [1.22, 2.06]	2.04 [1.94, 2.23]	2.05 [1.65, 2.29]	0.4430 ♀
Endo/Epi MBF Stress Ratio	1.00 [0.96, 1.07]	1.05 [0.99, 1.14]	0.99 [0.95, 1.25]	1.04 [0.99, 1.08]	0.2250 †
Rest-MBF, ml/min/g	0.66 [0.59, 0.74]	0.77 [0.64, 0.90]	0.57 [0.52, 0.66]	0.65 [0.60, 0.76]	0.8483 †*♀
Endo/Epi MBF Rest ratio	1.09 [1.03, 1.14]	1.08 [1.04, 1.12]	1.12 [1.09, 1.15]	1.12 [1.07, 1.16]	0.8284 ♀
MPR	2.27 [1.87, 2.79]	2.19 [1.73, 2.74]	3.39 [2.68, 3.53]	3.33 [2.84, 4.01]	0.3930 ♂♀
Endo MPR	2.28 [1.78, 3.10]	2.09 [1.65, 2.63]	3.33 [3.03, 4.00]	3.22 [2.87, 3.72]	0.8814 ♂♀
Epi MPR	2.51 [2.00, 3.12]	2.26 [1.71, 2.69]	3.67 [2.51, 3.92]	3.34 [2.96, 4.00]	0.9095 †♂♀
PCR/ATP rest	1.75 [1.48, 2.08]	1.67 [1.38, 2.08]	1.91 [1.72, 2.62]	2.23 [1.74, 2.57]	0.4358 ♂♀

*A Shapiro-Wilk test is used to assess for normal distribution of variables. Normally distributed continuous variables are expressed as mean [95% confidence intervals]; nonparametric continuous variables are expressed as median (25th percentile, 75th percentile); and categorical variables are expressed as counts (percent). Normally distributed variables are compared using student t test and nonparametric variables are assessed using Mann-Whitney U test, † is used to represent statistical significance of <0.05 between DM groups, *is used to represent statistical significance of <0.05 between the HV volunteers,♂ is used to represent statistical significance of <0.05 between the Male DM and Male HV,♀ is used to represent statistical significance of <0.05 between the Female DM and Female HV. Chi-square and Fisher's Exact Test are used to assess categorical variables. Multiple Linear regression is used to quote the p-value investigating the DM/Gender interaction term, p<0.05 is considered significant. Dashes represent comparisons that are not possible*

LV, Left ventricle; EDVi, indexed end-diastolic volume; ESVi, indexed end-systolic volume; Svi, stroke volume indexed; EF, ejection fraction; LA, left atrium; MAPSE, Mitral Annular Plane Systolic Excursion; ECV, extracellular volume; LGE, late gadolinium enhancement; RPP, rate pressure product; MBF, myocardial blood flow; Endo, endocardial; Epi, epicardial; MPR, myocardial perfusion reserve; PCr/ATP , phosphocreatine to adenosine triphosphate ratio. ml/m², milliliters per square meter; g, grams; g/m² , grams per square meters; g/ml, grams per milliliters; cm, centimeters; ms, milliseconds; ml/min/g, milliliters per minute per gram.

Linear Regression Analysis

Linear regression analysis was performed to investigate the whether the association between T2D and phenotypic or CMR parameters differed according to sex. Notably, the only CMR parameter showing interaction between sex and T2D was LVSVi, which was 6 ml/m^2 lower in females with T2D versus without T2D, yet 10 ml/m^2 in males with T2D versus without T2D (interaction P<0.0001; Table 2). Regarding baseline characteristics, interactions were also noted for BMI and SBP (P=0.0166 and P= 0.0167, respectively; Table 5.1). Female sex was linked to a larger increment in BMI in the presence of T2D, than in males. Blood pressure was lower in females with T2D versus without T2D, whereas the converse was seen in males. Whether these factors are linked to the observations on LVSVi is unclear.

5.3.3 Clinical Follow Up

As the cohort was not powered to provide outcome analysis, this cannot be formally considered. However, for completeness, electronic healthcare records were reviewed at an average follow up period of 24 months to document patient outcomes. There was one MACE event (a HF admission). In addition, there was one, non-cardiac related death (due to cancer). Both were within the male cohort. With regards to other adverse events, the female cohort only recorded two cases of new onset atrial fibrillation.

5.4 DISCUSSION

In my study of individuals with uncomplicated T2D, sex-related biological differences were evident, as reflected in certain demographic characteristics and cardiac function and myocardial remodeling assessed by CMR. Such phenotypic differences have previously been described as outlined in the discussion below, but mostly in the setting of complications associated with T2D, rather than in the presence of uncomplicated T2D.

Gender differences and demographic parameters in patients with uncomplicated T2D

According to the presented linear regression analysis, the association between BMI, systolic BP and T2D differs according to gender. I have shown that females are likely to have higher BMIs than males with T2D. This is in keeping with prior published data showing females with T2D are more likely to exhibit abdominal obesity (due to greater subcutaneous fat storage capacity), and clinically they may present with higher prevalence of hypertension, a worse lipid profile and a more marked endothelial dysfunction than males (411, 412). In a large cohort study using the UK Biobank database, Brown et al showed that females with T2D persistently had a worse phenotype than males, with higher BMI, waist and hip circumference, body fat percentage and whole body fat mass compared to men irrelevant of their weight classification is (normal vs overweight vs obese) (27). In keeping with the results presented in this chapter, the authors also showed that SBP increased with increasing BMI and was significantly higher in patients with T2D, than age and sex matched controls (27).

In the cohort presented in this chapter, females with T2D had better glycaemic control than their age matched male counterparts, with HbA1c concentrations only marginally higher than the threshold for T2D diagnosis.

The fasting glucose of the female T2D cohort was also significantly lower and within the borderline normal range (33). Interestingly, however, there were no major differences in the treatment of T2D, other than for higher rates of sulphonylurea use in males. The reasons for better glycaemic control in females in my study remains unclear, although it is possible that this contributed to their favourable CMR phenotype. In the future I plan to perform linear regression analysis to explore any associations between markers of diabetic control (HbA1C, glucose, insulin and HOMA-IR), with CMR parameters of cardiac remodelling adjusted to biological sex.

Gender differences, the myocardial phenotype and cardiac function in patients with uncomplicated T2D

The results presented in this study revealed that females with uncomplicated T2D have significantly better cardiac contractility, both in terms of ejection fraction and rest and stress than age, and sex matched men with uncomplicated T2D. Moreover, males with T2D exhibited greater LV concentric hypertrophy compared to the female cohort. My data are in keeping with the literature suggesting that the remodeling changes seen in the LV myocardium, in particular the increased concentricity, are more pronounced in women with T2D when compared to healthy female controls vs men with T2D compared with healthy male control healthy controls (413). Perhaps the most important interaction however, is between gender, T2D and LVSVi. Given that heart rate did not show the same interaction, it is likely

that indexed cardiac output shows a similar interaction. What remains unclear is how this aligns with the lack of interactions with LVEF and GLS. This highlights the need for future larger studies to understand the physiological basis of this finding and its relevance to informing gender-specific monitoring and potential therapies for diabetic heart disease.

Whilst neither my study, nor the wider literature, can explain the mechanisms linking sex to diabetic heart disease, it is likely that a complex interplay of factors contributes. For example, these have been proposed to include differences in cell signaling pathways, impaired excitation-contraction coupling, hormonal differences, fibrotic remodelling, inefficient energy production, metabolic differences, and reduced coronary flow reserve (87, 414-416).

Impaired excitation-contraction coupling

Sex differences at the cellular level affecting myofibril contraction have been described in various disease and non-disease states. Reiser et al have described sex differences in myosin heavy chain isoforms in patients with and without systolic dysfunction. In particular, they found a two-fold greater amount of MHC-β (the slower isoform of the myosin heavy chain) in the non-failing left atrium of women, compared to men (414, 417). McKee et al have also reported sex differences in myofilaments in hypertrophic cardiomyopathy, during their mouse model experiment, in which female hypertrophic cardiomyopathy (HCM) trabeculae were more sensitive to calcium than female wildtypes, male HCM and male wildtype. The authors postulated that this calcium-sensitive tension development was likely due to changes in calcium handling and sarcomeric proteins, including expression of Sarcoplasmic Reticulum Ca^{2+} ATPase (2a) (SERCA2a), β-myosin heavy chain (β-MyHC) and post-translational modifications of myofilament proteins (418).

Basal calcium handling and excitation–contraction coupling have also been found to differ between males and females, irrelevant of a concomitant disease state such as T2D. Parks et al have published work investigating the basis for reduced calcium concentrations in females and found altered sarcoplasmic reticulum calcium release due to sex differences in cyclic AMP and protein kinase A (419). Furthermore, Hoeker et al investigated gender differences in the duration of action potentials, calcium transient duration, and the calcium transient decay constant following administration of a non-selective β-agonist, isoproterenol, to adult rabbit hearts and found significantly smaller changes in action potential duration and calcium transient decay in females (420).

Hormonal differences

Another likely contributing factor to the differences seen in patients of different gender with T2D is sex hormones. Overall, oestrogen is considered cardioprotective and has been associated with changes in lipid metabolism, fat distribution, insulin sensitivity, and blood pressure control (421-423). Moreover, oestrogens have been shown to positively regulate vascular relaxation factors, including prostaglandin I2, especially those acting upon the endothelium (424-426). Oestrogen receptors, ERα and ERβ, are expressed in endothelial cells, vascular smooth muscle cells, and cardiomyocytes of both sexes (423, 427). However, increased expression of ERβ compared to ERα in females has been linked to increased oxidative stress, inflammation and atheromatous plaque formation, which ultimately can contribute to T2D and associated cardiovascular complications (428-430). Oestrogen has also been linked to increased oxidative stress in injured arteries (431). Such pathways can contribute to greater endothelial impairment seen in females compared to males with T2D

(424). Furthermore, greater impairment of LV function following cardiac ischemia-reperfusion has been noted in oophorectomised rodents, with greater apoptosis, pro-inflammatory cytokines, and ROS being present. Interestingly, exogenous estrogen treatment restored cardiac function, indicating the potentially 'cardioprotective' role of female sex hormones (432, 433). Importantly, as noted in a review by De Castro, women can spend as long as one third of their lives in the post-menopausal "oestrogen-free" state. This is associated with an abrupt increase in cardiac mortality after the menopause in women with diabetes (412).

Fibrotic remodelling

Collagen provides an essential structural framework for cardiomyocytes, imparting stiffness to the myocardial wall, hence aiding the transmission of forces that the heart generates (434). In the presence of hyperglycaemia, the formation of AGEs increase cross-linkage of collagen fibers. Other mechanisms which contribute to the dysfunction of the extracellular matrix are the pro-fibrotic signaling via the ERK/MAPK, TGF-β and NF-κB pathways and the activation of the RAAS pathway through lipotoxicity and ROS formation (435-438). Diabetic cardiomyopathy has been shown to promote fibrosis, with an increase in collagen type I and III deposition in the myocardium (414). Females with T2D have typically been described as developing concentric remodeling whereas males with T2D are more likely to develop eccentric remodeling. This has typically been associated with the development of HFpEF in females and HFrEF in males (439). The underlying physiological differences to explain the phenotypic differences in males and females however, remain unknown. Furthermore, in the results presented above, the marker of fibrosis ECV, was not significantly different both between the sexes in the T2D cohort but also when comparing each sex with their control

cohort. In a similar CMR study conducted by Shang et al exploring the cardiac phenotype of patients with T2D, they have shown that their cohort of diabetics has an increased ECV compared to healthy controls. The glucose control documented in their results is similar for both sexes to the cohort presented in this chapter. The cohorts however differ in that my cohort is older and has slightly worse BP control (440). This could suggest that the differences seen in the changes in ECV are more evident in the younger, fitter population, or this could simply be highlighting how diabetes affects the myocardium differently with age and duration of the disease and much of the disease process remains unknown.

Metabolic differences

Another consideration for the sex differences seen in patients with T2D may be that cardiac steatosis has a more deleterious effect on the myocardium of females compared to males with T2D. Using phosphorus magnetic resonance spectroscopy in a range of patients with altered glucose tolerance (lean normoglycaemic, overweight and obese normoglycaemic, impaired glucose tolerance and T2D), McGavock et al have shown that myocardial triglyceride content increases as glucose tolerance decreases (441). Using similar techniques, Levelt et al, have shown comparable results of an increase of myocardial triglycerides in patients with T2D, compared to healthy controls, and this correlated positively with concentric LV remodeling and negatively with cardiac energetics (measured by phosphorus spectroscopy)(129). Similarly, females with T2D have a more pronounced increase in intracardiac lipid content than males with T2D (442). Furthermore, sex differences have been reported in myocardial triglyceride metabolism in people without diabetes (443, 444). Metabolic inflexibility is commonly noticed in the diabetic heart, which mainly relies on fatty acid oxidation for energy production (445). Beyond the myocardium, females with T2D have

more severe atherogenic dyslipidemia with increased plasma triglycerides and lipoprotein cholesterol concentrations (446). Arterial accumulation of oxidized low-density lipoprotein contributes to atherogenesis, in part via its interactions with the low-density lipoprotein receptor-1 (LOX-1) (447). Notably, sex differences in arterial LOX-1 have been reported by Brinkley et al, with particularly high expression seen in diabetic and obese females (448).

When considering glucose metabolism, Peterson et al report greater myocardial glucose uptake in males than females without diabetes, and that the detrimental effects of obesity and diabetes on glucose metabolism are also more pronounced in males than in females (449). Hyperglycaemia is associated with increased incidence of HF in populations with insulin resistance and diabetes (401, 414, 450, 451). Some of this association is postulated to be via the effects of glycation, which increases with hyperglycaemia and is associated with myocardial hypertrophy and heart failure (452-454). Elevated levels of plasma glucose lead to glycation of lipids and proteins, the so called 'AGEs', which may contribute to the development of diabetic cardiomyopathy. AGE can crosslink the extracellular matrix and also contribute to micro- and macrovascular disease associated with diabetes. Furthermore, a receptor for AGE (RAGE), can be found on the vasculature. Soluble RAGE (sRAGE) is located in serum. Here it binds AGE and blocks it from activating RAGE hence is thought to be protective. Females exhibit lower levels of sRAGE, which may play a role in increased incidence of diabetic heart disease in comparison to males with T2D (414).

Despite the differences in myocardial metabolism described in the literature, PCr/ATP ratio (a marker of overall myocardial metabolic activity) was not significantly different between the

females and males with T2D in my study. However, it must be highlighted that that PCr/ATP was nominally higher in male than female healthy controls.

Reduced coronary flow reserve

Moreover, despite clear morphological and functional differences, I observed no sex differences in the degree of impairment in global stress perfusion in patients with T2D. However, differences in rest perfusion and Endo/Epi stress-MBF ratio were detected, with higher values observed in females than males with T2D.

Within my cohort, stress MBF was significantly impaired in each sex group with T2D compared to their corresponding healthy controls. Such results were also seen by Sorensen et al who performed CMR on patients with T2D and age and sex matched controls. In a cohort similar to mine (i.e. with no co-existing systolic dysfunction), they showed that patients with T2D had higher rest MBF and lower stress MBF than controls. The degree of stress MBF impairment was related to markers of glycaemic control and diabetes complications. Specifically, patients with micro- or macroalbuminuria had significantly lower stress MBF than normoalbuminuric patients and patients with macroalbuminuria had significantly lower stress MBF than those with microalbuminuria. Autonomic neuropathy and retinopathy were also associated with lower stress MBF. In a multivariable analysis, female sex was associated with significantly increased rest MBF, as noted in my T2D cohort. The authors postulated that these differences may reflect diffuse myocardial fibrosis, given positive correlation between stress MBF and ECV (P <0.001; R^2 = 0.37) (211).

MPR was also significantly impaired in each sex group with T2D when compared to their corresponding healthy controls. This is representative of already known data, that patients with T2D are more likely to exhibit microvascular dysfunction than age and sex matched controls (77). In a slightly larger cohort study than my own, Yeo et al found that such differences are more pronounced in the female sex, in contrast to my data (455). There is minimal other published data on sex differences in myocardial blood flow in people with T2D. These conflicting results highlight the need for ongoing investigation into this matter. However, Yeo et al suggested that higher rest MBF in females versus males with T2D was the driver of apparently lower MPR in females, and my own analysis corroborated the higher rest MBF in females with T2D, so our discrepancy in MPR may reflect the lower statistical power of my study.

Biological sex, T2D and clinical outcomes

The follow up data presented in the results of this chapter cannot be used to comment on potential associations with cardiovascular morbidity and mortality within this cohort, as they have not been powered to do so.

The literature however, has a plethora of studies describing the increased mortality and morbidity associated with the presence of T2D. The Framingham study and other epidemiological data have shown that diabetes mellitus confers an increased risk of both coronary heart disease and all-cause mortality (75). In particular, the relative risk of coronary heart disease and fatal ischaemic events are greater in women than men with diabetes. The risk of acute myocardial infarction (MI) has been reported as 150% higher in females with T2D than those without the condition, but only 50% greater in males with T2D compared to males

without T2D (75). This Framingham analysis was among the first studies to provide evidence of the higher relative risk of cardiovascular disease associated with diabetes in females versus males (412, 456).

The most common cause of heart failure in males and females is coronary artery disease. However, the progression of this phenotype to that of systolic dysfunction in females is different from that in males. Well recognised risk factors for the development of this heart failure include: the post-menopausal state, T2D, atrial fibrillation, myocardial infarction, chronic kidney disease, hypertension, obesity, current smoking, left bundle branch block, and left ventricular hypertrophy. T2D has been reported as the strongest predictor of HF, particularly in the setting of concomitant renal disease or morbid obesity (412, 457).

Kwak et al studied 4,180 patients admitted with heart failure, stratified by sex and diabetes status, with 1,765 deaths occurring during a median follow up time of 31.7 months. There was no difference in 5-year mortality rates between non-diabetic females and non-diabetic males, nor between males and females with diabetes, but both sex groups with diabetes had higher mortality than their non-diabetic counterparts. Cox regression analysis revealed that the mortality risk associated with diabetes was nominally greater in females than males, although not statistically significant (adjusted hazard ratio = 1.35 [95% confidence interval: 1.15–1.59] versus 1.24 [1.07–1.44], P interaction = 0.7) (413). Moreover, there was a stepwise increase in mortality of the female cohort with rising HbA1c concentrations, but this was not seen in males (413). However, it must be noted that the patients in this cohort had more advanced diabetic heart disease compared to the participants of my cohort, given that they

were admitted with heart failure, whereas the cohort presented here were all stable outpatients with newly diagnosed HF.

It is important to highlight that the clinical presenting complaints between the sexes also differ. In left ventricular systolic dysfunction associated with concomitant T2D, fatigue and dyspnoea are the most common symptoms in females, whereas males are more likely to present with dyspnoea and leg swelling. In ischaemic heart disease with concomitant T2D, women more commonly present with symptoms of atypical chest pain in the jaw, neck and shoulder, nausea, fatigue and dyspnoea (456). Such differences in clinical presentation may account for the differences in disease phenotypes and outcomes as diagnosis may be delayed.

In the EMPA-REG OUTCOME clinical trial, administration of the SGLT2i Empagliflozin to improve glycaemic control, was associated with reduced mortality attributed to heart failure (458, 459). Importantly, in a meta-analysis published by Rivera et al investigating the sex differences in cardiovascular outcomes of SGLT-2 inhibitors in heart failure which included 5 randomised control trials, did not report that the treatment effect of SGLT2i is influenced by sex upon completion of stratified analysis (460).

Other glucose lowering medications have also been trialled. The SELECT trial was a randomised control trial investigating the use of GLP1-RA Semaglutide in overweight patients with current diabetes or a history of diabetes. The primary outcome measure was defined as the use of GLP1-RA alongside standard of care medical management will reduce MACE (cardiovascular death, non-fatal MI and non-fatal stroke) from the time of randomisation until the study end-point which was event driven at 1225 events. This resulted in a mean duration

of exposure at 34 months and a mean duration of follow up at 40 months. The primary cardiovascular end point occurred in 6.5% of the treatment group compared to 8.0% of the placebo group, (HR 0.80, 95%CI 0.72-0.90, P <0.001). This suggests that Semaglutide can offer cardiovascular benefits in this population (though the cause of protection remains unclear). Unfortunately, no sex sub-group analysis was performed, and the authors did highlight that one of the disadvantages of the trial was that only 27.7% of participants were females (461). Further work is therefore required to investigate any sex differences to the positive results presented here.

The differences seen in the outcomes of the two sexes may not simply reflect biological factors, however. Differences in life course exposures, clinical presentation and sex-based health inequalities may also contribute. It must be noted however, that females have been persistently under-represented in clinical trials (460). Whilst the current study comprised of relatively even numbers of biological men and women with prospective targeted recruitment, numerically the females were fewer and this study alone is not enough to bridge the current knowledge gap. The factor of under-representation therefore must be addressed if answers to these questions are to be effectively sought.

Clinical Implications

The data presented in this chapter show that there is still much more to learn about the clinical effects of T2D on the myocardium. Whilst the functional and structural characteristics of the male and female heart are well documented (and corroborated in this chapter), the mechanisms underpinning the differential impact of T2D in men and women remain elusive.

Moving forward, the use of transcriptomic assessments, similar to those presented in Chapter 4, may be beneficial in exploring potential mechanisms of diabetic heart disease. By addressing this phenomenon, it may be possible to develop more effective specific treatments to prevent future cardiovascular disease for each sex in this high-risk patient group. This is particularly important given the conflicting data regarding outcomes of the two sexes within this patient cohort.

Limitations

Whilst this study builds on the existing body of literature by showing the phenotypic differences in men and women with T2D using advanced imaging techniques, there are some limitations that cannot be overlooked.

The single center nature of the cohort may be reflective of the patients with T2D in this region, hence limiting its 'real world' generalizability. Furthermore, the small sample size increases the risk of statistical type II errors. Moreover, the size of the cohort is not powered to be able to assess for future cardiovascular events, making it impossible to suggest any imaging markers which could be used to predict morbidity and mortality associated with uncomplicated T2D.

Additionally, the study design is unable to establish causation, nor can it lead to mechanistic hypotheses. RNA sequencing has previously been used to define DEGs from the myocardium of patients with diabetes which have been validated as plasma proteins (180). Such techniques can be adopted in future work to gather more evidence to explain the causation T2D-gender interactions in diabetic heart disease. Furthermore, analyses to see whether

these DEGs can be correlated with CMR markers can provide reproducible monitoring markers to assess for disease progression.

It is difficult to know whether the cohort can truly be described as 'uncomplicated T2D'. The results have highlighted that patients of both sexes with T2D were generally overweight or obese. There is emerging evidence that patients who are lean with T2D vs those that overweight have different underlying mechanisms of their disease and consequently respond differently to treatment. Lean T2D patients are more likely to have impaired insulin secretion vs the overweight patients who exhibit more prominent insulin resistance. Because of the aforementioned, lean diabetics tend to respond better to treatments targeting beta cell function vs overweight cohorts that require treatments to reduce insulin resistance (462, 463). The differences in adiposity between males and females with T2D have already been described (27) but the association of weight and its distribution between the two sexes and T2D cardiac phenotype and outcomes remains poorly understood.

Finally medical treatment options and their effects on patients with T2D must not be ignored. The diabetic cohort presented here had well controlled glucose levels whilst using a variety of agents. I have already discussed potential benefits in cardiovascular mortality using some diabetes medications above. It is therefore unclear how the advancement of these medications will affect the cardiac phenotype and outcomes in years to come. As a start, more work must be carried out on the differences of the cardiac phenotype across the spectrum of glycaemic control and duration of disease before considering how changes in medical management can affect this in the short and long term.

5.5 CONCLUSION

In conclusion, my findings support the notion that within a cohort of uncomplicated T2D there are phenotypic differences between male and female patients. Male sex is associated with a more adverse early subclinical cardiac disease phenotype in T2D, with more pronounced remodeling and worse cardiac function. However, the literature suggests that it is the females with T2D who have worse outcomes. Future larger studies are needed to assess the complex relationship between biological sex and T2D to better understand why the incidence of HF is even higher for the females with diabetes compared to males with diabetes. Particular attention must be paid to changes over time that precede the development of HFpEF and HFrEF, since understanding this process can help to inform better preventative therapies for both sexes with T2D.

6. General Discussion and Future Directions

This thesis has explored the implications of T2D for myocardial function and biology, both in people without heart disease and in those with AS or HFrEF, using imaging and transcriptomic approaches. While themes emerging from each chapter have been discussed in their respective chapter discussions, this section will briefly summarise the major findings, highlight common themes and point to potential future directions.

First, my work has added to the existing literature regarding the effects of T2D across the spectrum of AS using the advanced imaging techniques of CMR and ^{31}P-MRS. It also provides novel insights through the use of transcriptomics, eliciting DEGs associated with T2D, along with myocardial transcriptomic correlates of CMR phenotypes, the latter of which has never been described before. With further translational research, it is possible that these data could lead to novel biomarkers for the prediction of adverse myocardial remodelling in the people with AS, along with therapies targeted at preventing this in high-risk populations, such as people with T2D.

My data confirmed prior publications showing that concomitant T2D is associated with a more severe concentric LV remodelling phenotype in people with severe-AS (225). A novel observation in this thesis is that T2D is not associated with more exaggerated LV remodelling in the context of moderate AS. To my knowledge, this thesis also provides the first demonstration that the transition from moderate to symptomatic severe AS is preceded by myocardial perfusion alterations. These results suggest that impaired myocardial perfusion associated with moderate AS could be a useful indicator of likely disease progression. Notably, I have also corroborated prior findings that patients with T2D demonstrate persistent perfusion abnormalities even after SAVR, compared to their non-diabetic counterparts (225).

At the time of SAVR, RAA biopsies were collected to examine the myocardial transcriptomic profile of severe AS with versus without T2D, and to draw inferences about the biology of myocardial remodelling observed on CMR. RNA sequencing performed from the myocardial biopsy samples taken at the time of SAVR revealed just under 300 significant DEGs between the T2D and no-T2D cohorts. Enrichment analysis performed to identify biological themes amongst upregulated DEGs identified in immune response pathways indicating immune activation as a key underlying biological process. Notably, after finding correlations between high level transcriptional variation and many CMR parameters, I was also able to explore this in more detail for left atrial ejection fraction, eliciting DEGs that can be validated in future studies. If validated, these may lead to useful biomarkers and could inform therapeutic approaches to modulate myocardial remodelling.

In a separate cohort of people with HFrEF, in whom myocardial biopsy was not feasible, I also showed that the blood transcriptome is associated with CMR phenotypes. These molecular insights presumably arise from the immune system, potentially explaining the weaker correlations than seen for myocardial transcriptomics, but still provided interesting and unexpected insights. For example, the correlation of blood metabolic and mitochondrial gene sets with stress myocardial perfusion is novel and represents an interesting area for future exploration. Overall, these data suggest that blood transcriptomics provides a viable method of learning about the biology of heart disease in patients with and without T2D.

A common theme arising from my analyses is the important gender differences in the myocardial transcriptome, blood transcriptome, and in the CMR phenotype associated with uncomplicated T2D (this could not be assessed in AS or HFrEF due to inadequate sample size).

In uncomplicated T2D, male sex was associated with a more adverse subclinical cardiac disease, with more pronounced remodeling and worse cardiac function. In the presence of HFrEF, blood RNA-seq data showed pronounced gender clustering, and whilst less pronounced, this was also apparent in myocardial RNA-seq. This suggests that accounting for gender as a covariate and/or gender-stratified analyses are important when using such RNA-seq data. Such differences are not necessarily surprising, given the clinical use of gender-specific normal ranges in clinical CMR reports, but by showing the major contribution of gender to RNA-seq variance, my data emphasise the major biological differences between genders. These raise the question of whether gender specific biomarkers and therapies for heart disease may be warranted.

More generally, my work suggests that there is major potential to uncover the biology underpinning CMR phenotypes, which may permit more informed use of CMR data in clinical practice and lead to blood biomarkers that reduce the need for CMR. Much more work is needed to advance this hypothesis, and in the future I hope to expand on my myocardial and blood transcriptomic datasets paired with detailed CMR characterisation. As noted earlier, existing data from UK Biobank may also allow large scale validation of selected hits, but there remains a paucity of advanced CMR linked to omics data which will need more focussed prospective case-control and/or cohort studies.

Regarding the implications of diabetes for heart disease, my data suggest that even with contemporary therapy, T2D is associated with a different CMR and transcriptomic phenotype. This suggests that there remains scope for more personalised approaches to address the unique aspects of T2D. However, it is also notable that the implications of diabetes are

context specific, so a one size fits all approach is unlikely to be adequate. Further studies are needed to validate my specific findings in the various contexts I studied, but if corroborated, it is hoped that these can play a part in improving diagnostic and therapeutic approaches that improve outcomes for patients with T2D.

References

1. Banday MZ, Sameer AS, Nissar S. Pathophysiology of diabetes: An overview. Avicenna J Med. 2020;10(4):174-88.
2. Skyler JS, Bakris GL, Bonifacio E, Darsow T, Eckel RH, Groop L, et al. Differentiation of Diabetes by Pathophysiology, Natural History, and Prognosis. Diabetes. 2016;66(2):241-55.
3. Akil AA, Yassin E, Al-Maraghi A, Aliyev E, Al-Malki K, Fakhro KA. Diagnosis and treatment of type 1 diabetes at the dawn of the personalized medicine era. J Transl Med. 2021;19(1):137.
4. Gomez P, Sanchez J. Type 1 Diabetes Screening and Diagnosis. Endocrinol Metab Clin North Am. 2024;53(1):17-26.
5. Syed FZ. Type 1 Diabetes Mellitus. Ann Intern Med. 2022;175(3):Itc33-itc48.
6. UK D. How many people in the uk have diabetes? 2025 [Available from: https://www.diabetes.org.uk/about-us/about-the-charity/our-strategy/statistics.
7. UK D. Diagnostic criteria for diabetes 2025 [Available from: https://www.diabetes.org.uk/for-professionals/improving-care/clinical-recommendations-for-professionals/diagnosis-ongoing-management-monitoring/new_diagnostic_criteria_for_diabetes.
8. Association AD. Understanding Diabetes Diagnosis 2023 [Available from: https://diabetes.org/about-diabetes/diagnosis.
9. Organisation WH. Diabetes 2024 [Available from: https://www.who.int/news-room/fact-sheets/detail/diabetes.
10. Pernicova I, Korbonits M. Metformin--mode of action and clinical implications for diabetes and cancer. Nat Rev Endocrinol. 2014;10(3):143-56.
11. Ashcroft FM. Mechanisms of the glycaemic effects of sulfonylureas. Horm Metab Res. 1996;28(9):456-63.
12. Vella A. Mechanism of action of DPP-4 inhibitors--new insights. J Clin Endocrinol Metab. 2012;97(8):2626-8.
13. Fonseca-Correa JI, Correa-Rotter R. Sodium-Glucose Cotransporter 2 Inhibitors Mechanisms of Action: A Review. Front Med (Lausanne). 2021;8:777861.
14. Hauner H. The mode of action of thiazolidinediones. Diabetes Metab Res Rev. 2002;18 Suppl 2:S10-5.
15. Drucker DJ. Mechanisms of Action and Therapeutic Application of Glucagon-like Peptide-1. Cell Metab. 2018;27(4):740-56.
16. Ahlqvist E, Storm P, Käräjämäki A, Martinell M, Dorkhan M, Carlsson A, et al. Novel subgroups of adult-onset diabetes and their association with outcomes: a data-driven cluster analysis of six variables. The Lancet Diabetes & Endocrinology. 2018;6(5):361-9.
17. Ng SM, Soni A. Ten-year review of trends in children with type 1 diabetes in England and Wales. World J Diabetes. 2023;14(8):1194-201.
18. Lucier J, PM. M. Type 1 Diabetes StatPearls (Internet)2024 [Available from: https://www.ncbi.nlm.nih.gov/books/NBK507713/.
19. Zhao X, Liu S, Wang X, Chen Y, Pang P, Yang Q, et al. Diabetic cardiomyopathy: Clinical phenotype and practice. Front Endocrinol (Lausanne). 2022;13:1032268.

20. Wolfsdorf J, Glaser N, Sperling MA. Diabetic Ketoacidosis in Infants, Children, and Adolescents: A consensus statement from the American Diabetes Association. Diabetes Care. 2006;29(5):1150-9.
21. Lah Tomulić K, Matko L, Verbić A, Milardović A, Severinski S, Kolić I, et al. Epidemiologic Characteristics of Children with Diabetic Ketoacidosis Treated in a Pediatric Intensive Care Unit in a 10-Year-Period: Single Centre Experience in Croatia. Medicina (Kaunas). 2022;58(5).
22. Watts M. Type 2 Diabetes: Diabetes.co.uk; 2023 [Available from: https://www.diabetes.co.uk/type2-diabetes.html.
23. UK D. Type 2 Diabetes 2023 [Available from: https://www.diabetes.org.uk/about-diabetes/type-2-diabetes.
24. Galicia-Garcia U, Benito-Vicente A, Jebari S, Larrea-Sebal A, Siddiqi H, Uribe KB, et al. Pathophysiology of Type 2 Diabetes Mellitus. Int J Mol Sci. 2020;21(17).
25. Klein S, Gastaldelli A, Yki-Järvinen H, Scherer PE. Why does obesity cause diabetes? Cell Metab. 2022;34(1):11-20.
26. England PH. Adult obesity and type 2 diabetes. 2014.
27. Brown OI, Drozd M, McGowan H, Giannoudi M, Conning-Rowland M, Gierula J, et al. Relationship Among Diabetes, Obesity, and Cardiovascular Disease Phenotypes: A UK Biobank Cohort Study. Diabetes Care. 2023;46(8):1531-40.
28. Borse SP, Chhipa AS, Sharma V, Singh DP, Nivsarkar M. Management of Type 2 Diabetes: Current Strategies, Unfocussed Aspects, Challenges, and Alternatives. Med Princ Pract. 2021;30(2):109-21.
29. Davies MJ, Aroda VR, Collins BS, Gabbay RA, Green J, Maruthur NM, et al. Management of Hyperglycemia in Type 2 Diabetes, 2022. A Consensus Report by the American Diabetes Association (ADA) and the European Association for the Study of Diabetes (EASD). Diabetes Care. 2022;45(11):2753-86.
30. Plows JF, Stanley JL, Baker PN, Reynolds CM, Vickers MH. The Pathophysiology of Gestational Diabetes Mellitus. Int J Mol Sci. 2018;19(11).
31. UK D. Causes of gestational diabetes 2025 [Available from: https://www.diabetes.org.uk/about-diabetes/gestational-diabetes/causes.
32. UK D. gestational diabetes symptoms 2025 [Available from: https://www.diabetes.org.uk/about-diabetes/gestational-diabetes/symptoms.
33. UK D. diagnostic criteria for diabetes 2025 [cited 2025 01/03]. Available from: https://www.diabetes.org.uk/for-professionals/improving-care/clinical-recommendations-for-professionals/diagnosis-ongoing-management-monitoring/new_diagnostic_criteria_for_diabetes#:~:text=Haemoglobin%20A1c%20(HbA1c)%20testing%20to,diabetes%20diagnosed%20using%20glucose%20tests.
34. Ravikumar V, Ahmed A, Anjankar A. A Review on Latent Autoimmune Diabetes in Adults. Cureus. 2023;15(10):e47915.
35. UK D. Latent autoimmune diabetes in adults (lada) 2025 [Available from: https://www.diabetes.org.uk/about-diabetes/other-types-of-diabetes/latent-autoimmune-diabetes.
36. Hawa MI, Kolb H, Schloot N, Beyan H, Paschou SA, Buzzetti R, et al. Adult-Onset Autoimmune Diabetes in Europe Is Prevalent With a Broad Clinical Phenotype: Action LADA 7. Diabetes Care. 2013;36(4):908-13.
37. UK D. Maturity onset diabetes of the young (mody) 2025 [Available from: https://www.diabetes.org.uk/about-diabetes/other-types-of-diabetes/mody.

38. UK D. Secondary Diabtes 2023 [Available from: https://www.diabetes.co.uk/secondary-diabetes.html.
39. Rao SS, Disraeli P, McGregor T. Impaired glucose tolerance and impaired fasting glucose. Am Fam Physician. 2004;69(8):1961-8.
40. Statistics OFN. Risk factors for pre-diabetes and undiagnosed type 2 diabetes in England: 2013 to 2019 2024 [Available from: https://www.ons.gov.uk/peoplepopulationandcommunity/healthandsocialcare/healthinequalities/bulletins/riskfactorsforprediabetesandundiagnosedtype2diabetesinenglandd/2013to2019.
41. Abdul-Ghani MA, DeFronzo RA. Pathophysiology of prediabetes. Curr Diab Rep. 2009;9(3):193-9.
42. Organisation WH. Diabetes 2024 [Available from: https://www.who.int/news-room/fact-sheets/detail/diabetes.
43. Severino P, D'Amato A, Netti L, Pucci M, De Marchis M, Palmirotta R, et al. Diabetes Mellitus and Ischemic Heart Disease: The Role of Ion Channels. Int J Mol Sci. 2018;19(3).
44. Dal Canto E, Ceriello A, Rydén L, Ferrini M, Hansen TB, Schnell O, et al. Diabetes as a cardiovascular risk factor: An overview of global trends of macro and micro vascular complications. Eur J Prev Cardiol. 2019;26(2_suppl):25-32.
45. Tang H, Fang Z, Wang T, Cui W, Zhai S, Song Y. Meta-Analysis of Effects of Sodium-Glucose Cotransporter 2 Inhibitors on Cardiovascular Outcomes and All-Cause Mortality Among Patients With Type 2 Diabetes Mellitus. Am J Cardiol. 2016;118(11):1774-80.
46. Romon I, Fosse S, Eschwège E, Simon D, Weill A, Varroud-Vial M, et al. Prevalence of macrovascular complications and cardiovascular risk factors in people treated for diabetes and living in France: the ENTRED study 2001. Diabetes Metab. 2008;34(2):140-7.
47. Lee CH, Wu YL, Kuo JF, Chen JF, Chin MC, Hung YJ. Prevalence of diabetic macrovascular complications and related factors from 2005 to 2014 in Taiwan: A nationwide survey. J Formos Med Assoc. 2019;118 Suppl 2:S96-s102.
48. Lu Y, Wang W, Liu J, Xie M, Liu Q, Li S. Vascular complications of diabetes: A narrative review. Medicine (Baltimore). 2023;102(40):e35285.
49. Fowler MJ. Microvascular and Macrovascular Complications of Diabetes. Clinical Diabetes. 2008;26(2):77-82.
50. Boyle PJ. Diabetes mellitus and macrovascular disease: mechanisms and mediators. Am J Med. 2007;120(9 Suppl 2):S12-7.
51. Negussie YM, Sento M, Fati NM. Diabetic microvascular complications among adults with type 2 diabetes in Adama, central Ethiopia. Scientific Reports. 2024;14(1):24910.
52. Bitla A, N H, Vs K. Molecular mechanisms underlying diabetic microvascular complications. Journal of Clinical and Scientific Research. 2016;5:112-23.
53. Nguyen DV, Shaw L, Grant M. Inflammation in the pathogenesis of microvascular complications in diabetes. Frontiers in Endocrinology. 2012;3.
54. Nguyen C, Luthra R, Kuti E, Willey VJ. Assessing risk of future cardiovascular events, healthcare resource utilization and costs in patients with type 2 diabetes, prior cardiovascular disease and both. Curr Med Res Opin. 2020;36(12):1927-38.

55. Flyvbjerg A. Pathogenesis of Microvascular Complications. Textbook of Diabetes2017. p. 541-53.
56. Ford ES. Body mass index, diabetes, and C-reactive protein among U.S. adults. Diabetes Care. 1999;22(12):1971-7.
57. Festa A, D'Agostino R, Jr., Howard G, Mykkänen L, Tracy RP, Haffner SM. Chronic subclinical inflammation as part of the insulin resistance syndrome: the Insulin Resistance Atherosclerosis Study (IRAS). Circulation. 2000;102(1):42-7.
58. Müller S, Martin S, Koenig W, Hanifi-Moghaddam P, Rathmann W, Haastert B, et al. Impaired glucose tolerance is associated with increased serum concentrations of interleukin 6 and co-regulated acute-phase proteins but not TNF-alpha or its receptors. Diabetologia. 2002;45(6):805-12.
59. Temelkova-Kurktschiev T, Henkel E, Koehler C, Karrei K, Hanefeld M. Subclinical inflammation in newly detected Type II diabetes and impaired glucose tolerance. Diabetologia. 2002;45(1):151.
60. Vithian K, Hurel S. Microvascular complications: pathophysiology and management. Clin Med (Lond). 2010;10(5):505-9.
61. Forbes JM, Cooper ME. Mechanisms of Diabetic Complications. Physiological Reviews. 2013;93(1):137-88.
62. Cole JB, Florez JC. Genetics of diabetes mellitus and diabetes complications. Nat Rev Nephrol. 2020;16(7):377-90.
63. Pop-Busui R, Boulton AJ, Feldman EL, Bril V, Freeman R, Malik RA, et al. Diabetic Neuropathy: A Position Statement by the American Diabetes Association. Diabetes Care. 2017;40(1):136-54.
64. Koch KL. Diabetic gastropathy: gastric neuromuscular dysfunction in diabetes mellitus: a review of symptoms, pathophysiology, and treatment. Dig Dis Sci. 1999;44(6):1061-75.
65. Young CF, Moussa M, Shubrook JH. Diabetic Gastroparesis: A Review. Diabetes Spectrum. 2020;33(3):290-7.
66. Packer CF, Syed AA, Biagio M. Diabetic Foot Ulcer. StasPearls [Internet]. 2023.
67. Reardon R, Simring D, Kim B, Mortensen J, Williams D, Leslie A. The diabetic foot ulcer. Australian Journal for General Practitioners. 2020;49:250-5.
68. Khaw K. T., Wareham N. J., Bingham S., Luben R, Welch A, N D. Association of Hemoglobin A1c with Cardiovascular Disease and Mortality in Adults: The European Prospective Investigation into Cancer in Norfolk. Annals of Internal Medicine. 2004;141(6):413-20.
69. Stamler J, Vaccaro O, Neaton JD, Wentworth D. Diabetes, other risk factors, and 12-yr cardiovascular mortality for men screened in the Multiple Risk Factor Intervention Trial. Diabetes Care. 1993;16(2):434-44.
70. An Y, Zhang P, Wang J, Gong Q, Gregg EW, Yang W, et al. Cardiovascular and All-Cause Mortality Over a 23-Year Period Among Chinese With Newly Diagnosed Diabetes in the Da Qing IGT and Diabetes Study. Diabetes Care. 2015;38(7):1365-71.
71. Haffner SM, Lehto S, Rönnemaa T, Pyörälä K, Laakso M. Mortality from coronary heart disease in subjects with type 2 diabetes and in nondiabetic subjects with and without prior myocardial infarction. N Engl J Med. 1998;339(4):229-34.
72. Rajbhandari J, Fernandez CJ, Agarwal M, Yeap BXY, Pappachan JM. Diabetic heart disease: A clinical update. World J Diabetes. 2021;12(4):383-406.

73. Serhiyenko VA, Serhiyenko AA. Cardiac autonomic neuropathy: Risk factors, diagnosis and treatment. World J Diabetes. 2018;9(1):1-24.
74. Shah AD, Langenberg C, Rapsomaniki E, Denaxas S, Pujades-Rodriguez M, Gale CP, et al. Type 2 diabetes and incidence of cardiovascular diseases: a cohort study in 1·9 million people. Lancet Diabetes Endocrinol. 2015;3(2):105-13.
75. Kannel WB, McGee DL. Diabetes and cardiovascular disease. The Framingham study. Jama. 1979;241(19):2035-8.
76. Garcia MJ, McNamara PM, Gordon T, Kannel WB. Morbidity and mortality in diabetics in the Framingham population. Sixteen year follow-up study. Diabetes. 1974;23(2):105-11.
77. Jia G, Hill MA, Sowers JR. Diabetic Cardiomyopathy: An Update of Mechanisms Contributing to This Clinical Entity. Circ Res. 2018;122(4):624-38.
78. Levy D, Garrison RJ, Savage DD, Kannel WB, Castelli WP. Prognostic implications of echocardiographically determined left ventricular mass in the Framingham Heart Study. N Engl J Med. 1990;322(22):1561-6.
79. Bluemke DA, Kronmal RA, Lima JA, Liu K, Olson J, Burke GL, et al. The relationship of left ventricular mass and geometry to incident cardiovascular events: the MESA (Multi-Ethnic Study of Atherosclerosis) study. J Am Coll Cardiol. 2008;52(25):2148-55.
80. Devereux RB, Roman MJ, Paranicas M, O'Grady MJ, Lee ET, Welty TK, et al. Impact of diabetes on cardiac structure and function: the strong heart study. Circulation. 2000;101(19):2271-6.
81. Gulsin GS, Henson J, Brady EM, Sargeant JA, Wilmot EG, Athithan L, et al. Cardiovascular Determinants of Aerobic Exercise Capacity in Adults With Type 2 Diabetes. Diabetes Care. 2020;43(9):2248-56.
82. Taegtmeyer H, McNulty P, Young ME. Adaptation and maladaptation of the heart in diabetes: Part I: general concepts. Circulation. 2002;105(14):1727-33.
83. Dhalla NS, Liu X, Panagia V, Takeda N. Subcellular remodeling and heart dysfunction in chronic diabetes. Cardiovasc Res. 1998;40(2):239-47.
84. Hardin NJ. The myocardial and vascular pathology of diabetic cardiomyopathy. Coron Artery Dis. 1996;7(2):99-108.
85. Rijzewijk LJ, van der Meer RW, Smit JW, Diamant M, Bax JJ, Hammer S, et al. Myocardial steatosis is an independent predictor of diastolic dysfunction in type 2 diabetes mellitus. J Am Coll Cardiol. 2008;52(22):1793-9.
86. Neubauer S. The failing heart--an engine out of fuel. N Engl J Med. 2007;356(11):1140-51.
87. Boudina S, Abel ED. Diabetic cardiomyopathy, causes and effects. Rev Endocr Metab Disord. 2010;11(1):31-9.
88. Sharma U, Chakraborty M, Chutia D, Bhuyan NR. Cellular and molecular mechanisms, genetic predisposition and treatment of diabetes-induced cardiomyopathy. Curr Res Pharmacol Drug Discov. 2022;3:100126.
89. Peterson LR, Gropler RJ. Metabolic and Molecular Imaging of the Diabetic Cardiomyopathy. Circ Res. 2020;126(11):1628-45.
90. Mereweather LJ, Montes Aparicio CN, Heather LC. Positioning Metabolism as a Central Player in the Diabetic Heart. J Lipid Atheroscler. 2020;9(1):92-109.
91. Hegab Z, Mohamed TMA, Stafford N, Mamas M, Cartwright EJ, Oceandy D. Advanced glycation end products reduce the calcium transient in cardiomyocytes by

increasing production of reactive oxygen species and nitric oxide. FEBS Open Bio. 2017;7(11):1672-85.
92. Shuvo SD, Hossen MT, Riazuddin M, Hossain MS, Mazumdar S, Parvin R, et al. Prevalence of comorbidities and its associated factors among type-2 diabetes patients: a hospital-based study in Jashore District, Bangladesh. BMJ Open. 2023;13(9):e076261.
93. Cicek M, Buckley J, Pearson-Stuttard J, Gregg EW. Characterizing Multimorbidity from Type 2 Diabetes: Insights from Clustering Approaches. Endocrinol Metab Clin North Am. 2021;50(3):531-58.
94. Iglay K, Hannachi H, Joseph Howie P, Xu J, Li X, Engel SS, et al. Prevalence and co-prevalence of comorbidities among patients with type 2 diabetes mellitus. Curr Med Res Opin. 2016;32(7):1243-52.
95. Pati S, Schellevis FG. Prevalence and pattern of co morbidity among type2 diabetics attending urban primary healthcare centers at Bhubaneswar (India). PLoS One. 2017;12(8):e0181661.
96. Muhamad N, Mutalip H, Mustapha N, Mohd Dali NS, Aris T, Ismail F, et al. Association between Comorbidities and Selected Sociodemographic Factors with Complications of Diabetes: Results from the National Diabetic Registry Malaysia. Journal of Diabetes Mellitus. 2018;08:84-97.
97. Mamas MA, Sperrin M, Watson MC, Coutts A, Wilde K, Burton C, et al. Do patients have worse outcomes in heart failure than in cancer? A primary care-based cohort study with 10-year follow-up in Scotland. Eur J Heart Fail. 2017;19(9):1095-104.
98. Stewart S, Ekman I, Ekman T, Odén A, Rosengren A. Population impact of heart failure and the most common forms of cancer: a study of 1 162 309 hospital cases in Sweden (1988 to 2004). Circ Cardiovasc Qual Outcomes. 2010;3(6):573-80.
99. Raghavan S, Vassy JL, Ho YL, Song RJ, Gagnon DR, Cho K, et al. Diabetes Mellitus–Related All-Cause and Cardiovascular Mortality in a National Cohort of Adults. Journal of the American Heart Association. 2019;8(4):e011295.
100. Rao Kondapally Seshasai S, Kaptoge S, Thompson A, Di Angelantonio E, Gao P, Sarwar N, et al. Diabetes mellitus, fasting glucose, and risk of cause-specific death. N Engl J Med. 2011;364(9):829-41.
101. Patsouras A, Farmaki P, Garmpi A, Damaskos C, Garmpis N, Mantas D, et al. Screening and Risk Assessment of Coronary Artery Disease in Patients With Type 2 Diabetes: An Updated Review. In Vivo. 2019;33(4):1039-49.
102. Naito R, Kasai T. Coronary artery disease in type 2 diabetes mellitus: Recent treatment strategies and future perspectives. World J Cardiol. 2015;7(3):119-24.
103. Norhammar A, Malmberg K, Diderholm E, Lagerqvist B, Lindahl B, Rydén L, et al. Diabetes mellitus: the major risk factor in unstable coronary artery disease even after consideration of the extent of coronary artery disease and benefits of revascularization. J Am Coll Cardiol. 2004;43(4):585-91.
104. Creager MA, Lüscher TF, Cosentino F, Beckman JA. Diabetes and vascular disease: pathophysiology, clinical consequences, and medical therapy: Part I. Circulation. 2003;108(12):1527-32.
105. Maron DJ, Hochman JS, Reynolds HR, Bangalore S, O'Brien SM, Boden WE, et al. Initial Invasive or Conservative Strategy for Stable Coronary Disease. New England Journal of Medicine. 2020;382(15):1395-407.

106. Newman JD, Anthopolos R, Mancini GBJ, Bangalore S, Reynolds HR, Kunichoff DF, et al. Outcomes of Participants With Diabetes in the ISCHEMIA Trials. Circulation. 2021;144(17):1380-95.
107. Donahoe SM, Stewart GC, McCabe CH, Mohanavelu S, Murphy SA, Cannon CP, et al. Diabetes and mortality following acute coronary syndromes. Jama. 2007;298(7):765-75.
108. Babes EE, Bustea C, Behl T, Abdel-Daim MM, Nechifor AC, Stoicescu M, et al. Acute coronary syndromes in diabetic patients, outcome, revascularization, and antithrombotic therapy. Biomedicine & Pharmacotherapy. 2022;148:112772.
109. Stampouloglou PK, Anastasiou A, Bletsa E, Lygkoni S, Chouzouri F, Xenou M, et al. Diabetes Mellitus in Acute Coronary Syndrome. Life (Basel). 2023;13(11).
110. Sugiyama T, Yamamoto E, Bryniarski K, Xing L, Fracassi F, Lee H, et al. Coronary Plaque Characteristics in Patients With Diabetes Mellitus Who Presented With Acute Coronary Syndromes. J Am Heart Assoc. 2018;7(14).
111. Milzi A, Burgmaier M, Burgmaier K, Hellmich M, Marx N, Reith S. Type 2 diabetes mellitus is associated with a lower fibrous cap thickness but has no impact on calcification morphology: an intracoronary optical coherence tomography study. Cardiovasc Diabetol. 2017;16(1):152.
112. Jex N, Chowdhary A, Thirunavukarasu S, Procter H, Sengupta A, Natarajan P, et al. Coexistent Diabetes Is Associated With the Presence of Adverse Phenotypic Features in Patients With Hypertrophic Cardiomyopathy. Diabetes Care. 2022;45(8):1852-62.
113. Han K, Shi D, Yang L, Xie M, Zhong R, Wang Z, et al. Diabetes Is Associated With Rapid Progression of Aortic Stenosis: A Single-Center Retrospective Cohort Study. Front Cardiovasc Med. 2021;8:812692.
114. Banovic M, Athithan L, McCann GP. Aortic stenosis and diabetes mellitus: An ominous combination. Diabetes & Vascular Disease Research. 2019;16(4):310-23.
115. Yan AT, Koh M, Chan KK, Guo H, Alter DA, Austin PC, et al. Association Between Cardiovascular Risk Factors and Aortic Stenosis: The CANHEART Aortic Stenosis Study. J Am Coll Cardiol. 2017;69(12):1523-32.
116. Larsson SC, Wallin A, Håkansson N, Stackelberg O, Bäck M, Wolk A. Type 1 and type 2 diabetes mellitus and incidence of seven cardiovascular diseases. Int J Cardiol. 2018;262:66-70.
117. Ljungberg J, Johansson B, Engström KG, Albertsson E, Holmer P, Norberg M, et al. Traditional Cardiovascular Risk Factors and Their Relation to Future Surgery for Valvular Heart Disease or Ascending Aortic Disease: A Case-Referent Study. J Am Heart Assoc. 2017;6(5).
118. Lu Q, Lv J, Ye Y, Li Z, Wang W, Zhang B, et al. Prevalence and impact of diabetes in patients with valvular heart disease. iScience. 2024;27(3):109084.
119. Rawshani A, Sattar N, McGuire DK, Wallström O, Smith U, Borén J, et al. Left-Sided Degenerative Valvular Heart Disease in Type 1 and Type 2 Diabetes. Circulation. 2022;146(5):398-411.
120. Manduteanu I, Simionescu D, Simionescu A, Simionescu M. Aortic valve disease in diabetes: Molecular mechanisms and novel therapies. J Cell Mol Med. 2021;25(20):9483-95.
121. Elliott PM, Anastasakis A, Borger MA, Borggrefe M, Cecchi F, Charron P, et al. 2014 ESC Guidelines on diagnosis and management of hypertrophic cardiomyopathy:

the Task Force for the Diagnosis and Management of Hypertrophic Cardiomyopathy of the European Society of Cardiology (ESC). Eur Heart J. 2014;35(39):2733-79.
122. Maron BJ, Gardin JM, Flack JM, Gidding SS, Kurosaki TT, Bild DE. Prevalence of hypertrophic cardiomyopathy in a general population of young adults. Echocardiographic analysis of 4111 subjects in the CARDIA Study. Coronary Artery Risk Development in (Young) Adults. Circulation. 1995;92(4):785-9.
123. Wasserstrum Y, Barriales-Villa R, Fernández-Fernández X, Adler Y, Lotan D, Peled Y, et al. The impact of diabetes mellitus on the clinical phenotype of hypertrophic cardiomyopathy. Eur Heart J. 2019;40(21):1671-7.
124. Liu Q, Li D, Berger AE, Johns RA, Gao L. Survival and prognostic factors in hypertrophic cardiomyopathy: a meta-analysis. Sci Rep. 2017;7(1):11957.
125. Yu SQ, Shi K, Li Y, Wang J, Gao Y, Shi R, et al. The impact of diabetes mellitus on cardiac function assessed by magnetic resonance imaging in patients with hypertrophic cardiomyopathy. Cardiovasc Diabetol. 2024;23(1):293.
126. Lee H-J, Kim H-K, Kim B-S, Han K-D, Rhee T-M, Park J-B, et al. Impact of diabetes mellitus on the outcomes of subjects with hypertrophic cardiomyopathy: A nationwide cohort study. Diabetes Research and Clinical Practice. 2022;186:109838.
127. Thirunavukarasu S, Ansari F, Cubbon R, Forbes K, Bucciarelli-Ducci C, Newby DE, et al. Maternal Cardiac Changes in Women With Obesity and Gestational Diabetes Mellitus. Diabetes Care. 2022;45(12):3007-15.
128. Kramer CK, Campbell S, Retnakaran R. Gestational diabetes and the risk of cardiovascular disease in women: a systematic review and meta-analysis. Diabetologia. 2019;62(6):905-14.
129. Levelt E, Mahmod M, Piechnik SK, Ariga R, Francis JM, Rodgers CT, et al. Relationship Between Left Ventricular Structural and Metabolic Remodeling in Type 2 Diabetes. Diabetes. 2016;65(1):44-52.
130. Musa TA, Treibel TA, Vassiliou VS, Captur G, Singh A, Chin C, et al. Myocardial Scar and Mortality in Severe Aortic Stenosis. Circulation. 2018;138(18):1935-47.
131. Engblom H, Xue H, Akil S, Carlsson M, Hindorf C, Oddstig J, et al. Fully quantitative cardiovascular magnetic resonance myocardial perfusion ready for clinical use: a comparison between cardiovascular magnetic resonance imaging and positron emission tomography. J Cardiovasc Magn Reson. 2017;19(1):78.
132. Kellman P, Hansen MS, Nielles-Vallespin S, Nickander J, Themudo R, Ugander M, et al. Myocardial perfusion cardiovascular magnetic resonance: optimized dual sequence and reconstruction for quantification. J Cardiovasc Magn Reson. 2017;19(1):43.
133. Levelt E, Rodgers CT, Clarke WT, Mahmod M, Ariga R, Francis JM, et al. Cardiac energetics, oxygenation, and perfusion during increased workload in patients with type 2 diabetes mellitus. Eur Heart J. 2016;37(46):3461-9.
134. White SK, Sado DM, Flett AS, Moon JC. Characterising the myocardial interstitial space: the clinical relevance of non-invasive imaging. Heart. 2012;98(10):773-9.
135. Moon JC, Messroghli DR, Kellman P, Piechnik SK, Robson MD, Ugander M, et al. Myocardial T1 mapping and extracellular volume quantification: a Society for Cardiovascular Magnetic Resonance (SCMR) and CMR Working Group of the European Society of Cardiology consensus statement. J Cardiovasc Magn Reson. 2013;15(1):92.

136. Liu S, Han J, Nacif MS, Jones J, Kawel N, Kellman P, et al. Diffuse myocardial fibrosis evaluation using cardiac magnetic resonance T1 mapping: sample size considerations for clinical trials. J Cardiovasc Magn Reson. 2012;14(1):90.
137. Skali H, Shah A, Gupta DK, Cheng S, Claggett B, Liu J, et al. Cardiac structure and function across the glycemic spectrum in elderly men and women free of prevalent heart disease: the Atherosclerosis Risk In the Community study. Circ Heart Fail. 2015;8(3):448-54.
138. De Marco M, de Simone G, Roman MJ, Chinali M, Lee ET, Calhoun D, et al. Cardiac geometry and function in diabetic or prediabetic adolescents and young adults: the Strong Heart Study. Diabetes Care. 2011;34(10):2300-5.
139. Heizer J, Carbone S, Billingsley HE, BW VANT, Arena R, Abbate A, et al. Left ventricular concentric remodeling and impaired cardiorespiratory fitness in patients with heart failure and preserved ejection fraction. Minerva Cardiol Angiol. 2021;69(4):438-45.
140. Association AH. Ejection Fraction Heart Failure Measurement 2023 [Available from: https://www.heart.org/en/health-topics/heart-failure/diagnosing-heart-failure/ejection-fraction-heart-failure-measurement.
141. Rosano GM, Vitale C, Seferovic P. Heart Failure in Patients with Diabetes Mellitus. Card Fail Rev. 2017;3(1):52-5.
142. Rubler S, Dlugash J, Yuceoglu YZ, Kumral T, Branwood AW, Grishman A. New type of cardiomyopathy associated with diabetic glomerulosclerosis. Am J Cardiol. 1972;30(6):595-602.
143. van Heerebeek L, Hamdani N, Handoko ML, Falcao-Pires I, Musters RJ, Kupreishvili K, et al. Diastolic stiffness of the failing diabetic heart: importance of fibrosis, advanced glycation end products, and myocyte resting tension. Circulation. 2008;117(1):43-51.
144. Wong TC, Piehler KM, Kang IA, Kadakkal A, Kellman P, Schwartzman DS, et al. Myocardial extracellular volume fraction quantified by cardiovascular magnetic resonance is increased in diabetes and associated with mortality and incident heart failure admission. Eur Heart J. 2014;35(10):657-64.
145. Swoboda PP, McDiarmid AK, Erhayiem B, Ripley DP, Dobson LE, Garg P, et al. Diabetes Mellitus, Microalbuminuria, and Subclinical Cardiac Disease: Identification and Monitoring of Individuals at Risk of Heart Failure. J Am Heart Assoc. 2017;6(7).
146. Boyer JK, Thanigaraj S, Schechtman KB, Pérez JE. Prevalence of ventricular diastolic dysfunction in asymptomatic, normotensive patients with diabetes mellitus. Am J Cardiol. 2004;93(7):870-5.
147. From AM, Scott CG, Chen HH. The development of heart failure in patients with diabetes mellitus and pre-clinical diastolic dysfunction a population-based study. J Am Coll Cardiol. 2010;55(4):300-5.
148. Di Bonito P, Moio N, Cavuto L, Covino G, Murena E, Scilla C, et al. Early detection of diabetic cardiomyopathy: usefulness of tissue Doppler imaging. Diabet Med. 2005;22(12):1720-5.
149. Taegtmeyer H, Lam T, Davogustto G. Cardiac Metabolism in Perspective. Compr Physiol. 2016;6(4):1675-99.
150. Murashige D, Jang C, Neinast M, Edwards JJ, Cowan A, Hyman MC, et al. Comprehensive quantification of fuel use by the failing and nonfailing human heart. Science. 2020;370(6514):364-8.

151. Facts.net S. Oxidative Phosphorylation 2023 [Available from: https://www.sciencefacts.net/oxidative-phosphorylation.html.
152. Heather LC, Clarke K. Metabolism, hypoxia and the diabetic heart. J Mol Cell Cardiol. 2011;50(4):598-605.
153. Kodde IF, van der Stok J, Smolenski RT, de Jong JW. Metabolic and genetic regulation of cardiac energy substrate preference. Comp Biochem Physiol A Mol Integr Physiol. 2007;146(1):26-39.
154. Taegtmeyer H. Metabolism--the lost child of cardiology. J Am Coll Cardiol. 2000;36(4):1386-8.
155. Obrzut S, Jamshidi N, Karimi A, Birgersdotter-Green U, Hoh C. Imaging and modeling of myocardial metabolism. J Cardiovasc Transl Res. 2010;3(4):384-96.
156. Scheuermann-Freestone M, Madsen PL, Manners D, Blamire AM, Buckingham RE, Styles P, et al. Abnormal cardiac and skeletal muscle energy metabolism in patients with type 2 diabetes. Circulation. 2003;107(24):3040-6.
157. Shivu GN, Phan TT, Abozguia K, Ahmed I, Wagenmakers A, Henning A, et al. Relationship between coronary microvascular dysfunction and cardiac energetics impairment in type 1 diabetes mellitus. Circulation. 2010;121(10):1209-15.
158. Ingwall JS, Weiss RG. Is the failing heart energy starved? On using chemical energy to support cardiac function. Circ Res. 2004;95(2):135-45.
159. Shah RV, Abbasi SA, Kwong RY. Role of cardiac MRI in diabetes. Curr Cardiol Rep. 2014;16(2):449.
160. Levelt E, Pavlides M, Banerjee R, Mahmod M, Kelly C, Sellwood J, et al. Ectopic and Visceral Fat Deposition in Lean and Obese Patients With Type 2 Diabetes. J Am Coll Cardiol. 2016;68(1):53-63.
161. Nagel E. Cardiovascular Magnetic Resonance in Diabetic Patients: The Method of Choice? Circ Cardiovasc Imaging. 2016;9(4):e004699.
162. Einarson TR, Acs A, Ludwig C, Panton UH. Prevalence of cardiovascular disease in type 2 diabetes: a systematic literature review of scientific evidence from across the world in 2007-2017. Cardiovasc Diabetol. 2018;17(1):83.
163. Hajar R. Diabetes as "Coronary Artery Disease Risk Equivalent": A Historical Perspective. Heart Views. 2017;18(1):34-7.
164. Wackers FJ, Young LH, Inzucchi SE, Chyun DA, Davey JA, Barrett EJ, et al. Detection of silent myocardial ischemia in asymptomatic diabetic subjects: the DIAD study. Diabetes Care. 2004;27(8):1954-61.
165. Elhendy A, Arruda AM, Mahoney DW, Pellikka PA. Prognostic stratification of diabetic patients by exercise echocardiography. J Am Coll Cardiol. 2001;37(6):1551-7.
166. D'Andrea A, Severino S, Caso P, De Simone L, Liccardo B, Forni A, et al. Prognostic value of pharmacological stress echocardiography in diabetic patients. Eur J Echocardiogr. 2003;4(3):202-8.
167. Marwick TH, Case C, Sawada S, Vasey C, Short L, Lauer M. Use of stress echocardiography to predict mortality in patients with diabetes and known or suspected coronary artery disease. Diabetes Care. 2002;25(6):1042-8.
168. Heydari B, Juan YH, Liu H, Abbasi S, Shah R, Blankstein R, et al. Stress Perfusion Cardiac Magnetic Resonance Imaging Effectively Risk Stratifies Diabetic Patients With Suspected Myocardial Ischemia. Circ Cardiovasc Imaging. 2016;9(4):e004136.
169. Korosoglou G, Humpert PM, Ahrens J, Oikonomou D, Osman NF, Gitsioudis G, et al. Left ventricular diastolic function in type 2 diabetes mellitus is associated with

myocardial triglyceride content but not with impaired myocardial perfusion reserve. J Magn Reson Imaging. 2012;35(4):804-11.
170. Larghat AM, Swoboda PP, Biglands JD, Kearney MT, Greenwood JP, Plein S. The microvascular effects of insulin resistance and diabetes on cardiac structure, function, and perfusion: a cardiovascular magnetic resonance study. Eur Heart J Cardiovasc Imaging. 2014;15(12):1368-76.
171. Patel AR, Salerno M, Kwong RY, Singh A, Heydari B, Kramer CM. Stress Cardiac Magnetic Resonance Myocardial Perfusion Imaging. JACC. 2021;78(16):1655-68.
172. Herzog B, Greenwood J, Plein S, Garg P, P. H, S. O. Cardiovascular Magnetic Resonance Pocket Guide. Herzog B, Greenwood J, Plein S, editors: European Society of Cardiovascular Imaging
European Society of Cardiology; 2017.
173. Karamitsos TD, Ntusi NA, Francis JM, Holloway CJ, Myerson SG, Neubauer S. Feasibility and safety of high-dose adenosine perfusion cardiovascular magnetic resonance. J Cardiovasc Magn Reson. 2010;12(1):66.
174. Paetsch I, Jahnke C, Wahl A, Gebker R, Neuss M, Fleck E, et al. Comparison of dobutamine stress magnetic resonance, adenosine stress magnetic resonance, and adenosine stress magnetic resonance perfusion. Circulation. 2004;110(7):835-42.
175. Abdelaty A. Diagnostic accuracy of adenosine versus dobutamine stress perfusion cardiovascular magnetic resonance to detect severe coronary artery disease in patients with reduced left ventricular ejection fraction. Viva2022 [Available from: https://doi.org/10.25392/leicester.data.19354862.v1.
176. Craven TP, Tsao CW, La Gerche A, Simonetti OP, Greenwood JP. Exercise cardiovascular magnetic resonance: development, current utility and future applications. Journal of Cardiovascular Magnetic Resonance. 2020;22(1):65.
177. Adams J. Transcriptome: Connecting the Genome to Gene Function. Nature Education. 2008;1(1):195.
178. Liu Y, Morley M, Brandimarto J, Hannenhalli S, Hu Y, Ashley EA, et al. RNA-Seq identifies novel myocardial gene expression signatures of heart failure. Genomics. 2015;105(2):83-9.
179. Hong M, Tao S, Zhang L, Diao LT, Huang X, Huang S, et al. RNA sequencing: new technologies and applications in cancer research. J Hematol Oncol. 2020;13(1):166.
180. Conning-Rowland MS, Giannoudi M, Drozd M, Brown OI, Yuldasheva NY, Cheng CW, et al. The diabetic myocardial transcriptome reveals Erbb3 and Hspa2 as a novel biomarkers of incident heart failure. Cardiovasc Res. 2024;120(15):1898-906.
181. Occhi G, Rampazzo A, Beffagna G, Antonio Danieli G. Identification and characterization of heart-specific splicing of human neurexin 3 mRNA (NRXN3). Biochem Biophys Res Commun. 2002;298(1):151-5.
182. Cherpaz M, Meugnier E, Seillier G, Pozzi M, Pierrard R, Leboube S, et al. Myocardial transcriptomic analysis of diabetic patients with aortic stenosis: key role for mitochondrial calcium signaling. Cardiovasc Diabetol. 2024;23(1):239.
183. Liu H, Han X, Li Y. Identifying disrupted pathways by tracking altered modules in type 2 DM-related heart failure. Herz. 2017;42(1):98-106.
184. Aiello LP, Wong J-S. Role of vascular endothelial growth factor in diabetic vascular complications. Kidney International. 2000;58:S113-S9.

185. Sidarala V, Kowluru A. The Regulatory Roles of Mitogen-Activated Protein Kinase (MAPK) Pathways in Health and Diabetes: Lessons Learned from the Pancreatic β-Cell. Recent Pat Endocr Metab Immune Drug Discov. 2017;10(2):76-84.
186. Jubaidi FF, Zainalabidin S, Taib IS, Abdul Hamid Z, Mohamad Anuar NN, Jalil J, et al. The Role of PKC-MAPK Signalling Pathways in the Development of Hyperglycemia-Induced Cardiovascular Complications. Int J Mol Sci. 2022;23(15).
187. Nishimura RA, Otto CM, Bonow RO, Carabello BA, Erwin JP, 3rd, Fleisher LA, et al. 2017 AHA/ACC Focused Update of the 2014 AHA/ACC Guideline for the Management of Patients With Valvular Heart Disease: A Report of the American College of Cardiology/American Heart Association Task Force on Clinical Practice Guidelines. Circulation. 2017;135(25):e1159-e95.
188. Antony I, Mehari Abraha H, Hameed A, Conway C. A European update on transcatheter aortic valve implantation (TAVI) in the COVID era. J Anat. 2023;242(1):50-63.
189. Eggebrecht H, Mehta RH. Transcatheter aortic valve implantation (TAVI) in Germany: more than 100,000 procedures and now the standard of care for the elderly. EuroIntervention. 2019;14(15):e1549-e52.
190. Gao H, Feng XJ, Li ZM, Li M, Gao S, He YH, et al. Downregulation of adipose triglyceride lipase promotes cardiomyocyte hypertrophy by triggering the accumulation of ceramides. Arch Biochem Biophys. 2015;565:76-88.
191. Rizzello V. Moderate gradient severe aortic stenosis: diagnosis, prognosis and therapy. Eur Heart J Suppl. 2021;23(Suppl E):E133-e7.
192. Treibel TA, Kozor R, Schofield R, Benedetti G, Fontana M, Bhuva AN, et al. Reverse Myocardial Remodeling Following Valve Replacement in Patients With Aortic Stenosis. J Am Coll Cardiol. 2018;71(8):860-71.
193. Chambers J. The left ventricle in aortic stenosis: evidence for the use of ACE inhibitors. Heart. 2006;92(3):420-3.
194. Bennett J, Thornton GD, Nitsche C, Gama FF, Aziminia N, Gul U, et al. Left Ventricular Hypertrophy in Aortic Stenosis: Early Cell and Matrix Regression 2 Months Post-Aortic Valve Replacement. Circulation: Cardiovascular Imaging. 2024;17(12):e017425.
195. Julián MT, Alonso N, Lupón J, Gavidia-Bovadilla G, Ferrer E, de Antonio M, et al. Long-term LVEF trajectories in patients with type 2 diabetes and heart failure: diabetic cardiomyopathy may underlie functional decline. Cardiovasc Diabetol. 2020;19(1):38.
196. Ito S, Miranda WR, Nkomo VT, Connolly HM, Pislaru SV, Greason KL, et al. Reduced Left Ventricular Ejection Fraction in Patients With Aortic Stenosis. J Am Coll Cardiol. 2018;71(12):1313-21.
197. Perry AS, Li S. Optimal Threshold of Left Ventricular Ejection Fraction for Aortic Valve Replacement in Asymptomatic Severe Aortic Stenosis: A Systematic Review and Meta-Analysis. Journal of the American Heart Association. 2021;10(7):e020252.
198. Gulmez O, Parildar H, Cigerli O, Demirağ N. Assessment of left atrial function in patients with type 2 diabetes mellitus with a disease duration of six months. Cardiovasc J Afr. 2018;29(2):82-7.
199. Tadic M, Cuspidi C. Left atrial function in diabetes: does it help? Acta Diabetol. 2021;58(2):131-7.

200. Lisi M, Pastore MC, Fiorio A, Cameli M, Mandoli GE, Righini FM, et al. Left Atrial Remodeling in Response to Aortic Valve Replacement: Pathophysiology and Myocardial Strain Analysis. Life (Basel). 2022;12(12).
201. O'Connor K, Magne J, Rosca M, Piérard LA, Lancellotti P. Left atrial function and remodelling in aortic stenosis. European Journal of Echocardiography. 2011;12(4):299-305.
202. Lam B, Stromp TA, Hui Z, Vandsburger M. Myocardial native-T1 times are elevated as a function of hypertrophy, HbA1c, and heart rate in diabetic adults without diffuse fibrosis. Magn Reson Imaging. 2019;61:83-9.
203. Shu H, Xu H, Pan Z, Liu Y, Deng W, Zhao R, et al. Early detection of myocardial involvement by non-contrast T1ρ mapping of cardiac magnetic resonance in type 2 diabetes mellitus. Front Endocrinol (Lausanne). 2024;15:1335899.
204. Mahmod M, Piechnik SK, Levelt E, Ferreira VM, Francis JM, Lewis A, et al. Severe aortic stenosis has blunted myocardial T1 relaxation response to vasodilator stress: a cardiac magnetic resonance adenosine stress test study. Journal of Cardiovascular Magnetic Resonance. 2015;17(1):O28.
205. Lee H, Park JB, Yoon YE, Park EA, Kim HK, Lee W, et al. Noncontrast Myocardial T1 Mapping by Cardiac Magnetic Resonance Predicts Outcome in Patients With Aortic Stenosis. JACC Cardiovasc Imaging. 2018;11(7):974-83.
206. Fehrmann A, Treutlein M, Rudolph T, Rudolph V, Weiss K, Giese D, et al. Myocardial T1 and T2 mapping in severe aortic stenosis: Potential novel insights into the pathophysiology of myocardial remodelling. Eur J Radiol. 2018;107:76-83.
207. Cao Y, Zeng W, Cui Y, Kong X, Wang M, Yu J, et al. Increased myocardial extracellular volume assessed by cardiovascular magnetic resonance T1 mapping and its determinants in type 2 diabetes mellitus patients with normal myocardial systolic strain. Cardiovasc Diabetol. 2018;17(1):7.
208. Everett RJ, Treibel TA, Fukui M, Lee H, Rigolli M, Singh A, et al. Extracellular Myocardial Volume in Patients With Aortic Stenosis. J Am Coll Cardiol. 2020;75(3):304-16.
209. Suzuki M, Toba T, Izawa Y, Fujita H, Miwa K, Takahashi Y, et al. Prognostic Impact of Myocardial Extracellular Volume Fraction Assessment Using Dual-Energy Computed Tomography in Patients Treated With Aortic Valve Replacement for Severe Aortic Stenosis. Journal of the American Heart Association. 2021;10(18):e020655.
210. Vignale D, Palmisano A, Gnasso C, Margonato D, Romagnolo D, Barbieri S, et al. Extracellular volume fraction (ECV) derived from pre-operative computed tomography predicts prognosis in patients undergoing transcatheter aortic valve implantation (TAVI). European Heart Journal - Cardiovascular Imaging. 2023;24(7):887-96.
211. Sørensen MH, Bojer AS, Pontoppidan JRN, Broadbent DA, Plein S, Madsen PL, et al. Reduced Myocardial Perfusion Reserve in Type 2 Diabetes Is Caused by Increased Perfusion at Rest and Decreased Maximal Perfusion During Stress. Diabetes Care. 2020;43(6):1285-92.
212. Kibel A, Selthofer-Relatic K, Drenjancevic I, Bacun T, Bosnjak I, Kibel D, et al. Coronary microvascular dysfunction in diabetes mellitus. Journal of International Medical Research. 2017;45(6):1901-29.
213. McConkey HZR, Marber M, Chiribiri A, Pibarot P, Redwood SR, Prendergast BD. Coronary Microcirculation in Aortic Stenosis. Circulation: Cardiovascular Interventions. 2019;12(8):e007547.

214. Aslam S, Dattani A, Alfuhied A, Gulsin GS, Arnold JR, Steadman CD, et al. Effect of aortic valve replacement on myocardial perfusion and exercise capacity in patients with severe aortic stenosis. Scientific Reports. 2024;14(1):21522.
215. Rajappan K, Rimoldi OE, Camici PG, Bellenger NG, Pennell DJ, Sheridan DJ. Functional Changes in Coronary Microcirculation After Valve Replacement in Patients With Aortic Stenosis. Circulation. 2003;107(25):3170-5.
216. Bojer AS, Sørensen MH, Vejlstrup N, Goetze JP, Gæde P, Madsen PL. Distinct non-ischemic myocardial late gadolinium enhancement lesions in patients with type 2 diabetes. Cardiovasc Diabetol. 2020;19(1):184.
217. Tao M, Moussa S, Sheng S, Dhaliwal S, Tam E, Goldschmidt M, et al. Association of late-gadolinium enhancement on cardiac magnetic resonance with cardiovascular outcomes and mortality in patients with aortic stenosis. European Heart Journal. 2023;44(Supplement_2).
218. Barone-Rochette G, Piérard S, De Meester de Ravenstein C, Seldrum S, Melchior J, Maes F, et al. Prognostic Significance of LGE by CMR in Aortic Stenosis Patients Undergoing Valve Replacement. Journal of the American College of Cardiology. 2014;64(2):144-54.
219. Maltês S, Abecasis J, Santos RR, Lopes P, Oliveira L, Guerreiro S, et al. LGE prevalence and patterns in severe aortic stenosis: When "junctional" means the same. Int J Cardiol. 2023;378:159-63.
220. Ripley EM, Clarke GD, Hamidi V, Martinez RA, Settles FD, Solis C, et al. Reduced skeletal muscle phosphocreatine concentration in type 2 diabetic patients: a quantitative image-based phosphorus-31 MR spectroscopy study. Am J Physiol Endocrinol Metab. 2018;315(2):E229-e39.
221. Valkovič L, Apps A, Ellis J, Neubauer S, Tyler DJ, Schmid AI, et al. Increased cardiac Pi/PCr in the diabetic heart observed using phosphorus magnetic resonance spectroscopy at 7T. PLOS ONE. 2022;17(6):e0269957.
222. Tsampasian V, Cameron D, Sobhan R, Bazoukis G, Vassiliou VS. Phosphorus Magnetic Resonance Spectroscopy ((31)P MRS) and Cardiovascular Disease: The Importance of Energy. Medicina (Kaunas). 2023;59(1).
223. Monga S, Valkovič L, Myerson SG, Neubauer S, Mahmod M, Rider OJ. Role of Cardiac Energetics in Aortic Stenosis Disease Progression: Identifying the High-risk Metabolic Phenotype. Circulation: Cardiovascular Imaging. 2023;16(10):e014863.
224. Monga S, Valkovič L, Tyler D, Lygate CA, Rider O, Myerson SG, et al. Insights Into the Metabolic Aspects of Aortic Stenosis With the Use of Magnetic Resonance Imaging. JACC: Cardiovascular Imaging. 2022;15(12):2112-26.
225. Jex N, Greenwood JP, Cubbon RM, Rider OJ, Chowdhary A, Thirunavukarasu S, et al. Association Between Type 2 Diabetes and Changes in Myocardial Structure, Contractile Function, Energetics, and Blood Flow Before and After Aortic Valve Replacement in Patients With Severe Aortic Stenosis. Circulation. 2023;148(15):1138-53.
226. Badiani S, Bhattacharyya S, Aziminia N, Treibel TA, Lloyd G. Moderate Aortic Stenosis: What is it and When Should We Intervene? Interv Cardiol. 2021;16:e09.
227. Pankayatselvan V, Raber I, Playford D, Stewart S, Strange G, Strom JB. Moderate aortic stenosis: culprit or bystander? Open Heart. 2022;9(1).

228. Strange G, Stewart S, Celermajer D, Prior D, Scalia GM, Marwick T, et al. Poor Long-Term Survival in Patients With Moderate Aortic Stenosis. Journal of the American College of Cardiology. 2019;74(15):1851-63.
229. Delesalle G, Bohbot Y, Rusinaru D, Delpierre Q, Maréchaux S, Tribouilloy C. Characteristics and Prognosis of Patients With Moderate Aortic Stenosis and Preserved Left Ventricular Ejection Fraction. Journal of the American Heart Association. 2019;8(6):e011036.
230. Stewart S, Chan Y-K, Playford D, Strange GA. Incident aortic stenosis in 49 449 men and 42 229 women investigated with routine echocardiography. Heart. 2022;108(11):875.
231. Thornton GD, Musa TA, Rigolli M, Loudon M, Chin C, Pica S, et al. Association of Myocardial Fibrosis and Stroke Volume by Cardiovascular Magnetic Resonance in Patients With Severe Aortic Stenosis With Outcome After Valve Replacement: The British Society of Cardiovascular Magnetic Resonance AS700 Study. JAMA Cardiol. 2022;7(5):513-20.
232. Rosenhek R, Klaar U, Schemper M, Scholten C, Heger M, Gabriel H, et al. Mild and moderate aortic stenosis. Natural history and risk stratification by echocardiography. Eur Heart J. 2004;25(3):199-205.
233. Iung B, Delgado V, Rosenhek R, Price S, Prendergast B, Wendler O, et al. Contemporary Presentation and Management of Valvular Heart Disease: The EURObservational Research Programme Valvular Heart Disease II Survey. Circulation. 2019;140(14):1156-69.
234. Thornton George D, Bennett Jonathan B, Nitsche C, Gama F, Aziminia N, Knott K, et al. Myocardial Hypoperfusion in Severe Aortic Stenosis Is Reversed Early After Aortic Valve Replacement. JACC: Cardiovascular Imaging. 2024;17(8):1006-8.
235. Chin Calvin WL, Everett Russell J, Kwiecinski J, Vesey Alex T, Yeung E, Esson G, et al. Myocardial Fibrosis and Cardiac Decompensation in Aortic Stenosis. JACC: Cardiovascular Imaging. 2017;10(11):1320-33.
236. Kellman P, Hansen MS, Nielles-Vallespin S, Nickander J, Themudo R, Ugander M, et al. Myocardial perfusion cardiovascular magnetic resonance: optimized dual sequence and reconstruction for quantification. Journal of Cardiovascular Magnetic Resonance. 2017;19(1):43.
237. McConkey HZR, Marber M, Chiribiri A, Pibarot P, Redwood SR, Prendergast BD. Coronary Microcirculation in Aortic Stenosis. Circulation: Cardiovascular Interventions.12(8):e007547.
238. Markley R, Del Buono MG, Mihalick V, Pandelidis A, Trankle C, Jordan JH, et al. Abnormal left ventricular subendocardial perfusion and diastolic function in women with obesity and heart failure and preserved ejection fraction. Int J Cardiovasc Imaging. 2023;39(4):811-9.
239. Neubauer S. The Failing Heart — An Engine Out of Fuel. New England Journal of Medicine. 2007;356(11):1140-51.
240. Wal P, Rathore S, Aziz N, Singh YK, Gupta A. Aortic stenosis: a review on acquired pathogenesis and ominous combination with diabetes mellitus. The Egyptian Heart Journal. 2023;75(1):26.
241. D'Arcy J, Myerson SG. Investigations in valvular heart disease. Clin Med (Lond). 2010;10(2):172-6.

242. Grodecki K, Warniello M, Spiewak M, Kwiecinski J. Advanced Cardiac Imaging in the Assessment of Aortic Stenosis. J Cardiovasc Dev Dis. 2023;10(5).
243. Kontogeorgos SM, Rosengren A, Zverkova Sandstrom T, Lindgren M. Progression of aortic stenosis in patients with diabetes mellitus type 2 compared with matched controls. European Heart Journal. 2024;45(Supplement_1).
244. Mourino-Alvarez L, Corbacho-Alonso N, Sastre-Oliva T, Corros-Vicente C, Solis J, Tejerina T, et al. Diabetes Mellitus and Its Implications in Aortic Stenosis Patients. Int J Mol Sci. 2021;22(12).
245. Peterzan Mark A, Clarke William T, Lygate Craig A, Lake Hannah A, Lau Justin YC, Miller Jack J, et al. Cardiac Energetics in Patients With Aortic Stenosis and Preserved Versus Reduced Ejection Fraction. Circulation. 2020;141(24):1971-85.
246. Bois JP, Crowson CS, Khullar T, Achenbach SJ, Krause ML, Mankad R. Progression rate of severity of aortic stenosis in patients with rheumatoid arthritis. Echocardiography. 2017;34(10):1410-6.
247. Amanullah MR, Pio SM, Sin KYK, Marsan NA, Ding ZP, Stassen J, et al. Factors Affecting Rate of Progression of Aortic Stenosis and Its Impact on Outcomes. Am J Cardiol. 2022;185:53-62.
248. Raghunathan D, Bhardwaj A. Moderate Aortic Stenosis Progression. JACC: Advances. 2024;3(4):100882.
249. Delesalle G, Bohbot Y, Rusinaru D, Delpierre Q, Marechaux S, Tribouilloy C. Characteristics and Prognosis of Patients With Moderate Aortic Stenosis and Preserved Left Ventricular Ejection Fraction. Journal of the American Heart Association. 2019;8(6) (no pagination).
250. Howard T, Majmundar M, Sarin S, Kumar A, Ajay A, Krishnaswamy A, et al. Predictors of Major Adverse Cardiovascular Events in Patients with Moderate Aortic Stenosis: Implications for Aortic Valve Replacement. Circulation: Cardiovascular Imaging. 2023;16(7):557-65.
251. Manzo R, Ilardi F, Nappa D, Mariani A, Angellotti D, Immobile Molaro M, et al. Echocardiographic Evaluation of Aortic Stenosis: A Comprehensive Review. Diagnostics (Basel). 2023;13(15).
252. Casanova C, Celli BR, Barria P, Casas A, Cote C, Torres JPd, et al. The 6-min walk distance in healthy subjects: reference standards from seven countries. European Respiratory Journal. 2011;37(1):150.
253. Thirunavukarasu S, Jex N, Chowdhary A, Hassan IU, Straw S, Craven TP, et al. Empagliflozin Treatment Is Associated With Improvements in Cardiac Energetics and Function and Reductions in Myocardial Cellular Volume in Patients With Type 2 Diabetes. Diabetes. 2021;70(12):2810-22.
254. Dass S, Cochlin LE, Holloway CJ, Suttie JJ, Johnson AW, Tyler DJ, et al. Development and validation of a short 31P cardiac magnetic resonance spectroscopy protocol. Journal of Cardiovascular Magnetic Resonance. 2010;12(1):P123.
255. Pennell DJ, Sechtem UP, Higgins CB, Manning WJ, Pohost GM, Rademakers FE, et al. Clinical indications for cardiovascular magnetic resonance (CMR): Consensus Panel report. J Cardiovasc Magn Reson. 2004;6(4):727-65.
256. Xue H, Artico J, Davies RH, Adam R, Shetye A, Augusto JB, et al. Automated In-Line Artificial Intelligence Measured Global Longitudinal Shortening and Mitral Annular Plane Systolic Excursion: Reproducibility and Prognostic Significance. J Am Heart Assoc. 2022;11(4):e023849.

257. Porcari A, Merlo M, Baggio C, Gagno G, Cittar M, Barbati G, et al. Global longitudinal strain by CMR improves prognostic stratification in acute myocarditis presenting with normal LVEF. Eur J Clin Invest. 2022;52(10):e13815.
258. Romano S, Judd RM, Kim RJ, Heitner JF, Shah DJ, Shenoy C, et al. Feature-Tracking Global Longitudinal Strain Predicts Mortality in Patients With Preserved Ejection Fraction: A Multicenter Study. JACC Cardiovasc Imaging. 2020;13(4):940-7.
259. Janwetchasil P, Yindeengam A, Krittayaphong R. Prognostic value of global longitudinal strain in patients with preserved left ventricular systolic function: A cardiac magnetic resonance real-world study. Journal of Cardiovascular Magnetic Resonance. 2024;26(2).
260. Xue H, Inati S, Sørensen TS, Kellman P, Hansen MS. Distributed MRI reconstruction using Gadgetron-based cloud computing. Magn Reson Med. 2015;73(3):1015-25.
261. Kramer CM, Barkhausen J, Flamm SD, Kim RJ, Nagel E, Society for Cardiovascular Magnetic Resonance Board of Trustees Task Force on Standardized P. Standardized cardiovascular magnetic resonance (CMR) protocols 2013 update. Journal of cardiovascular magnetic resonance : official journal of the Society for Cardiovascular Magnetic Resonance. 2013;15(1):91-.
262. Cerqueira MD, Weissman NJ, Dilsizian V, Jacobs AK, Kaul S, Laskey WK, et al. Standardized myocardial segmentation and nomenclature for tomographic imaging of the heart. A statement for healthcare professionals from the Cardiac Imaging Committee of the Council on Clinical Cardiology of the American Heart Association. Circulation. 2002;105(4):539-42.
263. LLC. C. [Available from: https://clincalc.com.
264. de Frutos F, Ochoa JP, Fernández AI, Gallego-Delgado M, Navarro-Peñalver M, Casas G, et al. Late gadolinium enhancement distribution patterns in non-ischaemic dilated cardiomyopathy: genotype–phenotype correlation. European Heart Journal - Cardiovascular Imaging. 2023;25(1):75-85.
265. Grigoratos C, Pantano A, Meschisi M, Gaeta R, Ait-Ali L, Barison A, et al. Clinical importance of late gadolinium enhancement at right ventricular insertion points in otherwise normal hearts. Int J Cardiovasc Imaging. 2020;36(5):913-20.
266. Yi JE, Park J, Lee HJ, Shin DG, Kim Y, Kim M, et al. Prognostic implications of late gadolinium enhancement at the right ventricular insertion point in patients with non-ischemic dilated cardiomyopathy: A multicenter retrospective cohort study. PLoS One. 2018;13(11):e0208100.
267. Richardson C, Gilbert T, Aslam S, Brookes CL, Singh A, Newby DE, et al. Rationale and design of the early valve replacement in severe asymptomatic aortic stenosis trial. Am Heart J. 2024;275:119-27.
268. Bluemke DA, Kronmal RA, Lima JAC, Liu K, Olson J, Burke GL, et al. The Relationship of Left Ventricular Mass and Geometry to Incident Cardiovascular Events: The MESA (Multi-Ethnic Study of Atherosclerosis) Study. Journal of the American College of Cardiology. 2008;52(25):2148-55.
269. Gonzales H, Douglas PS, Pibarot P, Hahn RT, Khalique OK, Jaber WA, et al. Left Ventricular Hypertrophy and Clinical Outcomes Over 5 Years After TAVR: An Analysis of the PARTNER Trials and Registries. JACC: Cardiovascular Interventions. 2020;13(11):1329-39.

270. Treibel TA, López B, González A, Menacho K, Schofield RS, Ravassa S, et al. Reappraising myocardial fibrosis in severe aortic stenosis: an invasive and non-invasive study in 133 patients. Eur Heart J. 2018;39(8):699-709.
271. Mahmod M, Piechnik SK, Levelt E, Ferreira VM, Francis JM, Lewis A, et al. Adenosine stress native T1 mapping in severe aortic stenosis: evidence for a role of the intravascular compartment on myocardial T1 values. J Cardiovasc Magn Reson. 2014;16(1):92.
272. Ferreira VM, Piechnik SK. CMR Parametric Mapping as a Tool for Myocardial Tissue Characterization. Korean Circ J. 2020;50(8):658-76.
273. Dweck MR, Joshi S, Murigu T, Alpendurada F, Jabbour A, Melina G, et al. Midwall Fibrosis Is an Independent Predictor of Mortality in Patients With Aortic Stenosis. Journal of the American College of Cardiology. 2011;58(12):1271-9.
274. Thornton GD, Vassiliou VS, Musa TA, Aziminia N, Craig N, Dattani A, et al. Myocardial Scar and Remodelling Predict Long-Term Mortality in Severe Aortic Stenosis Beyond 10 Years. European Heart Journal. 2024:ehae067.
275. Bottomley PA, Wu KC, Gerstenblith G, Schulman SP, Steinberg A, Weiss RG. Reduced myocardial creatine kinase flux in human myocardial infarction: an in vivo phosphorus magnetic resonance spectroscopy study. Circulation. 2009;119(14):1918-24.
276. Nemes A, Forster T, Csanády M. Patients with aortic valve stenosis and Type 2 diabetes have similar coronary flow reserve and aortic distensibility compared with non-diabetic patients with aortic valve stenosis. Diabetes Res Clin Pract. 2007;77(1):159-60.
277. Alahdab F, Ahmed AI, Nayfeh M, Han Y, Abdelkarim O, Alfawara MS, et al. Myocardial Blood Flow Reserve, Microvascular Coronary Health, and Myocardial Remodeling in Patients With Aortic Stenosis. J Am Heart Assoc. 2024;13(11):e033447.
278. Liga R, Giorgetti A, Bertasi M, Filidei E, Gimelli A. Myocardial ischemia in patients with mild-to-moderate aortic stenosis: Interaction with cardiac remodeling and adverse events. J Nucl Cardiol. 2024;40:102017.
279. Paolisso P, Gallinoro E, Vanderheyden M, Esposito G, Bertolone DT, Belmonte M, et al. Absolute coronary flow and microvascular resistance reserve in patients with severe aortic stenosis. Heart. 2022;109(1):47-54.
280. Johnson NP, Gould KL, De Bruyne B. Autoregulation of Coronary Blood Supply in Response to Demand: JACC Review Topic of the Week. J Am Coll Cardiol. 2021;77(18):2335-45.
281. Beyerbacht HP, Lamb HJ, van der Laarse A, Vliegen HW, Leujes F, Hazekamp MG, et al. Aortic Valve Replacement in Patients with Aortic Valve Stenosis Improves Myocardial Metabolism and Diastolic Function. Radiology. 2001;219(3):637-43.
282. Mahmod M, Francis JM, Pal N, Lewis A, Dass S, De Silva R, et al. Myocardial perfusion and oxygenation are impaired during stress in severe aortic stenosis and correlate with impaired energetics and subclinical left ventricular dysfunction. J Cardiovasc Magn Reson. 2014;16(1):29.
283. Kamalesh M, Matorin R, Sawada S. Prognostic value of a negative stress echocardiographic study in diabetic patients. Am Heart J. 2002;143(1):163-8.
284. Dattani A, Brady EM, Alfuhied A, Gulsin GS, Steadman CD, Yeo JL, et al. Impact of diabetes on remodelling, microvascular function and exercise capacity in aortic stenosis. Open Heart. 2023;10(2).

285. Hwang IC, Kim S, Boo D, Park C, Yoo S, Yoon YE, et al. Impact of glycemic control on the progression of aortic stenosis: a single-center cohort study using a common data model. BMC Endocr Disord. 2023;23(1):143.
286. Kang D-H, Park S-J, Lee S-A, Lee S, Kim D-H, Kim H-K, et al. Early Surgery or Conservative Care for Asymptomatic Aortic Stenosis. New England Journal of Medicine. 2020;382(2):111-9.
287. Généreux P, Schwartz A, Oldemeyer JB, Pibarot P, Cohen DJ, Blanke P, et al. Transcatheter Aortic-Valve Replacement for Asymptomatic Severe Aortic Stenosis. New England Journal of Medicine. 2025;392(3):217-27.
288. Loganath K, Craig NJ, Everett RJ, Bing R, Tsampasian V, Molek P, et al. Early Intervention in Patients With Asymptomatic Severe Aortic Stenosis and Myocardial Fibrosis: The EVOLVED Randomized Clinical Trial. JAMA. 2025;333(3):213-21.
289. Kang SH, Ahn JM, Lee CH, Lee PH, Kang SJ, Lee SW, et al. Differential Event Rates and Independent Predictors of Long-Term Major Cardiovascular Events and Death in 5795 Patients With Unprotected Left Main Coronary Artery Disease Treated With Stents, Bypass Surgery, or Medication: Insights From a Large International Multicenter Registry. Circ Cardiovasc Interv. 2017;10(7).
290. Sen J, Wahi S, Vollbon W, Prior M, de Sá AGC, Ascher DB, et al. Definition and Validation of Prognostic Phenotypes in Moderate Aortic Stenosis. JACC Cardiovasc Imaging. 2025;18(2):133-49.
291. Jacquemyn X, Strom JB, Strange G, Playford D, Stewart S, Kutty S, et al. Moderate Aortic Valve Stenosis Is Associated With Increased Mortality Rate and Lifetime Loss: Systematic Review and Meta-Analysis of Reconstructed Time-to-Event Data of 409 680 Patients. J Am Heart Assoc. 2024;13(9):e033872.
292. Yechoor P, Blaustein AS, Bakaeen FG, Cornwell LD, Coselli JS, LeMaire SA, et al. The natural history of moderate aortic stenosis in a veteran population. J Thorac Cardiovasc Surg. 2013;145(6):1550-3.
293. Howard T, Majmundar M, Sarin S, Kumar A, Ajay A, Krishnaswamy A, et al. Predictors of Major Adverse Cardiovascular Events in Patients With Moderate Aortic Stenosis: Implications for Aortic Valve Replacement. Circ Cardiovasc Imaging. 2023;16(7):557-65.
294. Bae HJ, Hwang J, Han S, Hur SH, Chung JW, Kim H. Long Term Clinical Outcomes in Patients with Moderate Aortic Stenosis. Heart Surg Forum. 2020;23(3):E358-e65.
295. Coisne A, Montaigne D, Ninni S, Lamblin N, Lemesle G, Delsart P, et al. Diabetes mellitus and cardiovascular mortality across the spectrum of aortic stenosis. Heart. 2022;108(22):1815-21.
296. Moon I, Kim M, Choi JW, Park JB, Hwang HY, Kim HK, et al. Early Surgery versus Watchful Waiting in Patients with Moderate Aortic Stenosis and Left Ventricular Systolic Dysfunction. Korean Circ J. 2020;50(9):791-800.
297. Vahanian A, Beyersdorf F, Praz F, Milojevic M, Baldus S, Bauersachs J, et al. 2021 ESC/EACTS Guidelines for the management of valvular heart disease: Developed by the Task Force for the management of valvular heart disease of the European Society of Cardiology (ESC) and the European Association for Cardio-Thoracic Surgery (EACTS). European Heart Journal. 2021;43(7):561-632.
298. Banovic M, Iung B, Wojakowski W, Van Mieghem N, Bartunek J. Asymptomatic Severe and Moderate Aortic Stenosis: Time for Appraisal of Treatment Indications. Struct Heart. 2023;7(5):100201.

299. Chimenti C, Frustaci A. Contribution and Risks of Left Ventricular Endomyocardial Biopsy in Patients With Cardiomyopathies. Circulation. 2013;128(14):1531-41.
300. Bermpeis K, Esposito G, Gallinoro E, Paolisso P, Bertolone DT, Fabbricatore D, et al. Safety of Right and Left Ventricular Endomyocardial Biopsy in Heart Transplantation and Cardiomyopathy Patients. JACC: Heart Failure. 2022;10(12):963-73.
301. Frey N, Meder B, Katus HA. Left Ventricular Biopsy in the Diagnosis of Myocardial Diseases. Circulation. 2018;137(10):993-5.
302. Mulari S, Eskin A, Lampinen M, Nummi A, Nieminen T, Teittinen K, et al. Ischemic Heart Disease Selectively Modifies the Right Atrial Appendage Transcriptome. Front Cardiovasc Med. 2021;8:728198.
303. Cunningham KS, Veinot JP, Butany J. An approach to endomyocardial biopsy interpretation. J Clin Pathol. 2006;59(2):121-9.
304. Ancona Roberta PSC. Epidemiology of aortic valve stenosis (AS) and of aortic valve incompetence (AI): is the prevalence of AS/AI similar in different parts of the world? e-Journal of Cardiology Practice. 2020;18(10).
305. Lim MS, Strange G, Playford D, Stewart S, Celermajer DS. Characteristics of Bicuspid Aortic Valve Disease and Stenosis: The National Echo Database of Australia. Journal of the American Heart Association. 2021;10(17):e020785.
306. Talanas G, Laconi A, Kereiakes DJ, Merella P, Reardon MJ, Spano A, et al. Long-Term Outcomes of Transcatheter vs Surgical Aortic Valve Replacement: Meta-analysis of Randomized Trials. Journal of the Society for Cardiovascular Angiography & Interventions. 2024;3(7).
307. Alabbadi S, Malas J, Chen Q, Cheng W, Tam DY, Cohen RG, et al. Guidelines vs Practice: Surgical Versus Transcatheter Aortic Valve Replacement in Adults ≤60 Years. Ann Thorac Surg. 2024.
308. Handa K, Maeda K, Pak K, Shimamura K, Yamashita K, Kawamura A, et al. Midterm Clinical Outcomes after Isolated Surgical and Transcatheter Aortic Valve Replacement in Low-Risk Patients with Aortic Stenosis. Ann Thorac Cardiovasc Surg. 2024;30(1).
309. Conning-Rowland M, Cubbon RM. Molecular mechanisms of diabetic heart disease: Insights from transcriptomic technologies. Diab Vasc Dis Res. 2023;20(6):14791641231205428.
310. Harvard BIoMa. GTEX Portal 2025 [Available from: https://gtexportal.org/home/.
311. Wingett SW, Andrews S. FastQ Screen: A tool for multi-genome mapping and quality control. F1000Res. 2018;7:1338.
312. Bioinformatics B. FastQC 2025 [Available from: http://www.bioinformatics.babraham.ac.uk/projects/fastqc/.
313. Bioinformatics B. Trim Galore 2025 [Available from: https://www.bioinformatics.babraham.ac.uk/projects/trim_galore/.
314. Dobin A, Davis CA, Schlesinger F, Drenkow J, Zaleski C, Jha S, et al. STAR: ultrafast universal RNA-seq aligner. Bioinformatics. 2013;29(1):15-21.
315. Kovaka S, Zimin AV, Pertea GM, Razaghi R, Salzberg SL, Pertea M. Transcriptome assembly from long-read RNA-seq alignments with StringTie2. Genome Biol. 2019;20(1):278.

316. Love MI, Huber W, Anders S. Moderated estimation of fold change and dispersion for RNA-seq data with DESeq2. Genome Biol. 2014;15(12):550.
317. Organisation WH. Obesity and overweight: 2025; 2025 [Available from: https://www.who.int/news-room/fact-sheets/detail/obesity-and-overweight.
318. Blighe K, Lun A. PCAtools: everything Principal Components Analysis 2019 [Available from: https://github.com/kevinblighe/PCAtools.
319. Zhu A, Ibrahim JG, Love MI. Heavy-tailed prior distributions for sequence count data: removing the noise and preserving large differences. Bioinformatics. 2018;35(12):2084-92.
320. Reimand J, Kull M, Peterson H, Hansen J, Vilo J. g:Profiler--a web-based toolset for functional profiling of gene lists from large-scale experiments. Nucleic Acids Res. 2007;35(Web Server issue):W193-200.
321. Ge SX, Jung D, Yao R. ShinyGO: a graphical gene-set enrichment tool for animals and plants. Bioinformatics. 2019;36(8):2628-9.
322. Medicine NLo. SLC25A6 solute carrier family 25 member 6 [Homo sapiens (human)]. 2025.
323. Jeon J, Tian JB, Zhu MX. TRPC4 as a coincident detector of G(i/o) and G(q/11) signaling: mechanisms and pathophysiological implications. Curr Opin Physiol. 2020;17:34-41.
324. Boss O, Hagen T, Lowell BB. Uncoupling proteins 2 and 3: potential regulators of mitochondrial energy metabolism. Diabetes. 2000;49(2):143-56.
325. Yun J, Zuscik MJ, Gonzalez-Cabrera P, McCune DF, Ross SA, Gaivin R, et al. Gene expression profiling of alpha(1b)-adrenergic receptor-induced cardiac hypertrophy by oligonucleotide arrays. Cardiovasc Res. 2003;57(2):443-55.
326. Busnadiego O, González-Santamaría J, Lagares D, Guinea-Viniegra J, Pichol-Thievend C, Muller L, et al. LOXL4 is induced by transforming growth factor β1 through Smad and JunB/Fra2 and contributes to vascular matrix remodeling. Mol Cell Biol. 2013;33(12):2388-401.
327. Gulsin GS, Swarbrick DJ, Hunt WH, Levelt E, Graham-Brown MPM, Parke KS, et al. Relation of Aortic Stiffness to Left Ventricular Remodeling in Younger Adults With Type 2 Diabetes. Diabetes. 2018;67(7):1395-400.
328. Thornton GD, Bennett JB, Nitsche C, Gama F, Aziminia N, Knott K, et al. Myocardial Hypoperfusion in Severe Aortic Stenosis Is Reversed Early After Aortic Valve Replacement. JACC Cardiovasc Imaging. 2024;17(8):1006-8.
329. Vollema EM, Singh GK, Prihadi EA, Regeer MV, Ewe SH, Ng ACT, et al. Time course of left ventricular remodelling and mechanics after aortic valve surgery: aortic stenosis vs. aortic regurgitation. European Heart Journal - Cardiovascular Imaging. 2019;20(10):1105-11.
330. Sousa Nunes F, Amaral Marques C, Isabel Pinho A, Sousa-Pinto B, Beco A, Ricardo Silva J, et al. Reverse left ventricular remodeling after aortic valve replacement for aortic stenosis: a systematic review and meta-analysis. Frontiers in Cardiovascular Medicine. 2024;11.
331. Fairbairn TA, Steadman CD, Mather AN, Motwani M, Blackman DJ, Plein S, et al. Assessment of valve haemodynamics, reverse ventricular remodelling and myocardial fibrosis following transcatheter aortic valve implantation compared to surgical aortic valve replacement: a cardiovascular magnetic resonance study. Heart. 2013;99(16):1185-91.

332. Chin CWL, Everett RJ, Kwiecinski J, Vesey AT, Yeung E, Esson G, et al. Myocardial Fibrosis and Cardiac Decompensation in Aortic Stenosis. JACC: Cardiovascular Imaging. 2017;10(11):1320-33.
333. Westermann D, Rutschow S, Jäger S, Linderer A, Anker S, Riad A, et al. Contributions of Inflammation and Cardiac Matrix Metalloproteinase Activity to Cardiac Failure in Diabetic Cardiomyopathy: The Role of Angiotensin Type 1 Receptor Antagonism. Diabetes. 2007;56(3):641-6.
334. Krayenbuehl HP, Hess OM, Monrad ES, Schneider J, Mall G, Turina M. Left ventricular myocardial structure in aortic valve disease before, intermediate, and late after aortic valve replacement. Circulation. 1989;79(4):744-55.
335. Delgado V, Kong WKF, Bax JJ. Myocardial fibrosis in severe aortic stenosis: how and when should we measure it? EuroIntervention. 2020;15(16):1390-2.
336. Gallinoro E, Paolisso P, Bertolone DT, Esposito G, Belmonte M, Leone A, et al. Absolute coronary flow and microvascular resistance before and after transcatheter aortic valve implantation. EuroIntervention. 2024;20(19):e1248-e528.
337. Villa E, Troise G, Cirillo M, Brunelli F, Tomba MD, Mhagna Z, et al. Factors affecting left ventricular remodeling after valve replacement for aortic stenosis. An overview. Cardiovasc Ultrasound. 2006;4:25.
338. Rajappan K, Rimoldi OE, Camici PG, Bellenger NG, Pennell DJ, Sheridan DJ. Functional changes in coronary microcirculation after valve replacement in patients with aortic stenosis. Circulation. 2003;107(25):3170-5.
339. Lodo V, Italiano EG, Zingarelli E, Pietropaolo C, Pidello S, Buono G, et al. Transcatheter aortic valve implantation versus surgery: 4-year survival according to life expectancy. J Geriatr Cardiol. 2024;21(9):846-54.
340. Gupta T, DeVries JT, Gilani F, Hassan A, Ross CS, Dauerman HL. Temporal Trends in Transcatheter Aortic Valve Replacement for Isolated Severe Aortic Stenosis. J Soc Cardiovasc Angiogr Interv. 2024;3(7):101861.
341. Mas-Peiro S, Fichtlscherer S, Walther C, Vasa-Nicotera M. Current issues in transcatheter aortic valve replacement. J Thorac Dis. 2020;12(4):1665-80.
342. Khan S, Dargham S, Al Suwaidi J, Jneid H, Abi Khalil C. Trends and Outcomes of Aortic Valve Replacement in Patients With Diabetes in the US. Front Cardiovasc Med. 2022;9:844068.
343. Abu Khadija H, Alnees M, Gandelman G, Awwad M, Schiller T, Hamdan Y, et al. Clinical Impact of Glucose Levels on Patient Outcome after Transcatheter Aortic Valve Replacement. Rev Cardiovasc Med. 2025;26(2):25336.
344. Lindman BR, Pibarot P, Arnold SV, Suri RM, McAndrew TC, Maniar HS, et al. Transcatheter versus surgical aortic valve replacement in patients with diabetes and severe aortic stenosis at high risk for surgery: an analysis of the PARTNER Trial (Placement of Aortic Transcatheter Valve). J Am Coll Cardiol. 2014;63(11):1090-9.
345. Conning-Rowland M, Cubbon RM. Molecular mechanisms of diabetic heart disease: Insights from transcriptomic technologies. Diabetes & Vascular Disease Research. 2023;20(6):14791641231205428.
346. Lv B, Bao X, Li P, Lian J, Wu Y, An T, et al. Transcriptome Sequencing Analysis of Peripheral Blood of Type 2 Diabetes Mellitus Patients With Thirst and Fatigue. Front Endocrinol (Lausanne). 2020;11:558344.

347. Lin Q, Zhou W, Wang Y, Huang J, Hui X, Zhou Z, et al. Abnormal Peripheral Neutrophil Transcriptome in Newly Diagnosed Type 2 Diabetes Patients. J Diabetes Res. 2020;2020:9519072.
348. Sárközy M, Szűcs G, Fekete V, Pipicz M, Éder K, Gáspár R, et al. Transcriptomic alterations in the heart of non-obese type 2 diabetic Goto-Kakizaki rats. Cardiovascular Diabetology. 2016;15(1):110.
349. Corbi SCT, Bastos AS, Nepomuceno R, Cirelli T, Dos Santos RA, Takahashi CS, et al. Expression Profile of Genes Potentially Associated with Adequate Glycemic Control in Patients with Type 2 Diabetes Mellitus. J Diabetes Res. 2017;2017:2180819.
350. Hardy OT, Czech MP, Corvera S. What causes the insulin resistance underlying obesity? Curr Opin Endocrinol Diabetes Obes. 2012;19(2):81-7.
351. Gastaldelli A, Gaggini M, DeFronzo RA. Role of Adipose Tissue Insulin Resistance in the Natural History of Type 2 Diabetes: Results From the San Antonio Metabolism Study. Diabetes. 2017;66(4):815-22.
352. Ahmed B, Sultana R, Greene MW. Adipose tissue and insulin resistance in obese. Biomed Pharmacother. 2021;137:111315.
353. Saxena A, Mathur N, Tiwari P, Mathur SK. Whole transcriptome RNA-seq reveals key regulatory factors involved in type 2 diabetes pathology in peripheral fat of Asian Indians. Scientific Reports. 2021;11(1):10632.
354. Zhou H, Gao J, Lu ZY, Lu L, Dai W, Xu M. Role of c-Fos/JunD in protecting stress-induced cell death. Cell Prolif. 2007;40(3):431-44.
355. Le Nezet E, Marqueze-Pouey C, Guisle I, Clavel M-A. Molecular Features of Calcific Aortic Stenosis in Female and Male Patients. CJC Open. 2024;6(9):1125-37.
356. Myasoedova VA, Massaiu I, Moschetta D, Chiesa M, Songia P, Valerio V, et al. Sex-Specific Cell Types and Molecular Pathways Indicate Fibro-Calcific Aortic Valve Stenosis. Front Immunol. 2022;13:747714.
357. Croteau D, Luptak I, Chambers JM, Hobai I, Panagia M, Pimentel DR, et al. Effects of Sodium-Glucose Linked Transporter 2 Inhibition With Ertugliflozin on Mitochondrial Function, Energetics, and Metabolic Gene Expression in the Presence and Absence of Diabetes Mellitus in Mice. Journal of the American Heart Association. 2021;10(13):e019995.
358. Bhullar SK, Dhalla NS. Status of Mitochondrial Oxidative Phosphorylation during the Development of Heart Failure. Antioxidants (Basel). 2023;12(11).
359. Blaser MC, Bäck M, Lüscher TF, Aikawa E. Calcific aortic stenosis: omics-based target discovery and therapy development. European Heart Journal. 2024;46(7):620-34.
360. Le Nezet E, Voisine M, Tam R, LI Z, Gaudreault N, Cote N, et al. Abstract 11668: Transcriptomic Analysis Reveals Sex Differences in Gene Expression Profiling of Stenotic Aortic Valves. Circulation. 2023;148(Suppl_1):A11668-A.
361. Jolanda S, Salvatore De R, Isabella L, Antonio S, Sabrina La B, Sabato S, et al. Early reduction of left atrial function predicts adverse clinical outcomes in patients with severe aortic stenosis undergoing transcatheter aortic valve replacement. Open Heart. 2021;8(2):e001685.
362. Ferreira J, Gonçalves V, Marques-Alves P, Martins R, Monteiro S, Teixeira R, et al. Left atrial functional assessment and mortality in patients with severe aortic stenosis with sinus rhythm. Cardiovasc Ultrasound. 2021;19(1):1.

363. Nicin L, Schroeter SM, Glaser SF, Schulze-Brüning R, Pham MD, Hille SS, et al. A human cell atlas of the pressure-induced hypertrophic heart. Nat Cardiovasc Res. 2022;1(2):174-85.
364. Conning-Rowland M, Cheng CW, Brown O, Giannoudi M, Levelt E, Roberts LD, et al. Application of CIBERSORTx and BayesPrism to deconvolution of bulk RNA-seq data from human myocardium and skeletal muscle. Heliyon. 2025;11(4):e42499.
365. NICE NIfHaCE. Heart Failure - Chronic: How common is it? 2025 [cited 2025 28/02]. Available from: https://cks.nice.org.uk/topics/heart-failure-chronic/background-information/prevalence/.
366. Conrad N, Judge A, Tran J, Mohseni H, Hedgecott D, Crespillo AP, et al. Temporal trends and patterns in heart failure incidence: a population-based study of 4 million individuals. Lancet. 2018;391(10120):572-80.
367. Peterzan MA, Rider OJ, Anderson LJ. The Role of Cardiovascular Magnetic Resonance Imaging in Heart Failure. Card Fail Rev. 2016;2(2):115-22.
368. Organisation WH. Data 2024 [Available from: https://data.who.int/countries/826.
369. Chowdhary A, Thirunavukarasu S, Jex N, Coles L, Bowers C, Sengupta A, et al. Coronary microvascular function and visceral adiposity in patients with normal body weight and type 2 diabetes. Obesity. 2022;30(5):1079-90.
370. Qiagen. PAXgene Blood RNA Tubes (IVD) 2025 [Available from: https://www.qiagen.com/us/products/discovery-and-translational-research/sample-collection-stabilization/rna/paxgene-blood-rna-tubes.
371. PreAnalytiX. PAXgene Blood RNA Kit Instructions for Use (Handbook). 2023.
372. Horitani K, Chavkin NW, Arai Y, Wang Y, Ogawa H, Yura Y, et al. Disruption of the Uty epigenetic regulator locus in hematopoietic cells phenocopies the profibrotic attributes of Y chromosome loss in heart failure. Nature Cardiovascular Research. 2024;3(3):343-55.
373. Sano S, Horitani K, Ogawa H, Halvardson J, Chavkin NW, Wang Y, et al. Hematopoietic loss of Y chromosome leads to cardiac fibrosis and heart failure mortality. Science. 2022;377(6603):292-7.
374. Xiao L, Gu Y, Sun Y, Chen J, Wang X, Zhang Y, et al. The long noncoding RNA XIST regulates cardiac hypertrophy by targeting miR-101. J Cell Physiol. 2019;234(8):13680-92.
375. Almalki WH. Unraveling the role of Xist RNA in cardiovascular pathogenesis. Pathol Res Pract. 2024;253:154944.
376. Iyer NR, Chan SP, Liew OW, Chong JPC, Bryant JA, Le TT, et al. Global longitudinal strain and plasma biomarkers for prognosis in heart failure complicated by diabetes: a prospective observational study. BMC Cardiovasc Disord. 2024;24(1):141.
377. Hage FG, Heo J, Franks B, Belardinelli L, Blackburn B, Wang W, et al. Differences in heart rate response to adenosine and regadenoson in patients with and without diabetes mellitus. Am Heart J. 2009;157(4):771-6.
378. Bravo PE, Hage FG, Woodham RM, Heo J, Iskandrian AE. Heart rate response to adenosine in patients with diabetes mellitus and normal myocardial perfusion imaging. Am J Cardiol. 2008;102(8):1103-6.
379. Gulsin GS, Abdelaty A, Shetye A, Lai FY, Bajaj A, Das I, et al. Haemodynamic effects of pharmacologic stress with adenosine in patients with left ventricular systolic dysfunction. Int J Cardiol. 2019;278:157-61.

380. Sharrack N, Brown LAE, Farley J, Wahab A, Jex N, Thirunavukarasu S, et al. Occult coronary microvascular dysfunction and ischemic heart disease in patients with diabetes and heart failure. J Cardiovasc Magn Reson. 2024;26(2):101073.
381. Kwong RY, Sattar H, Wu H, Vorobiof G, Gandla V, Steel K, et al. Incidence and prognostic implication of unrecognized myocardial scar characterized by cardiac magnetic resonance in diabetic patients without clinical evidence of myocardial infarction. Circulation. 2008;118(10):1011-20.
382. Varney MJ, Benovic JL. The Role of G Protein-Coupled Receptors and Receptor Kinases in Pancreatic β-Cell Function and Diabetes. Pharmacol Rev. 2024;76(2):267-99.
383. Langenhan T, Aust G, Hamann J. Sticky signaling--adhesion class G protein-coupled receptors take the stage. Sci Signal. 2013;6(276):re3.
384. Faour M, Magnan C, Gurden H, Martin C. Olfaction in the context of obesity and diabetes: Insights from animal models to humans. Neuropharmacology. 2022;206:108923.
385. Yang Z, Cheng J, Shang P, Sun J-P, Yu X. Emerging roles of olfactory receptors in glucose metabolism. Trends in Cell Biology. 2023;33(6):463-76.
386. Bury JJ, Chambers A, Heath PR, Ince PG, Shaw PJ, Matthews FE, et al. Type 2 diabetes mellitus-associated transcriptome alterations in cortical neurones and associated neurovascular unit cells in the ageing brain. Acta Neuropathol Commun. 2021;9(1):5.
387. Nath M, Romaine SP, Koekemoer A, Hamby S, Webb TR, Nelson CP, et al. Whole blood transcriptomic profiling identifies molecular pathways related to cardiovascular mortality in heart failure. European Journal of Heart Failure. 2022;24(6):1009-19.
388. Sweet ME, Cocciolo A, Slavov D, Jones KL, Sweet JR, Graw SL, et al. Transcriptome analysis of human heart failure reveals dysregulated cell adhesion in dilated cardiomyopathy and activated immune pathways in ischemic heart failure. BMC Genomics. 2018;19(1):812.
389. Mills EL, Kelly B, O'Neill LAJ. Mitochondria are the powerhouses of immunity. Nat Immunol. 2017;18(5):488-98.
390. Hotamisligil GS. Foundations of Immunometabolism and Implications for Metabolic Health and Disease. Immunity. 2017;47(3):406-20.
391. Gomes CPdC, Schroen B, Kuster GM, Robinson EL, Ford K, Squire IB, et al. Regulatory RNAs in Heart Failure. Circulation. 2020;141(4):313-28.
392. Li Y, Yuan X, Shi Z, Wang H, Ren D, Zhang Y, et al. LncRNA XIST serves as a diagnostic biomarker in gestational diabetes mellitus and its regulatory effect on trophoblast cell via miR-497-5p/FOXO1 axis. Cardiovasc Diagn Ther. 2021;11(3):716-25.
393. Chen X, Tong C, Li H, Peng W, Li R, Luo X, et al. Dysregulated Expression of RPS4Y1 (Ribosomal Protein S4, Y-Linked 1) Impairs STAT3 (Signal Transducer and Activator of Transcription 3) Signaling to Suppress Trophoblast Cell Migration and Invasion in Preeclampsia. Hypertension. 2018;71(3):481-90.
394. Zarubin T, Han J. Activation and signaling of the p38 MAP kinase pathway. Cell Research. 2005;15(1):11-8.
395. Shi K, Zhang G, Fu H, Li XM, Jiang L, Gao Y, et al. Sex differences in clinical profile, left ventricular remodeling and cardiovascular outcomes among diabetic

patients with heart failure and reduced ejection fraction: a cardiac-MRI-based study. Cardiovasc Diabetol. 2024;23(1):266.
396. Chandramouli C, Teng TK, Tay WT, Yap J, MacDonald MR, Tromp J, et al. Impact of diabetes and sex in heart failure with reduced ejection fraction patients from the ASIAN-HF registry. Eur J Heart Fail. 2019;21(3):297-307.
397. Verma MS, Lindsay K, Ni J, Friedrich MG, Luu JM. Sex-Specific Associations of Cardiovascular Risk Factors with Subclinical Cardiac Remodeling: A Magnetic Resonance Imaging Study. Can J Cardiol. 2025.
398. Sharma A, Zheng Y, Ezekowitz JA, Westerhout CM, Udell JA, Goodman SG, et al. Cluster Analysis of Cardiovascular Phenotypes in Patients With Type 2 Diabetes and Established Atherosclerotic Cardiovascular Disease: A Potential Approach to Precision Medicine. Diabetes Care. 2021;45(1):204-12.
399. Newman AM, Liu CL, Green MR, Gentles AJ, Feng W, Xu Y, et al. Robust enumeration of cell subsets from tissue expression profiles. Nat Methods. 2015;12(5):453-7.
400. Allen LA, Magid DJ, Gurwitz JH, Smith DH, Goldberg RJ, Saczynski J, et al. Risk factors for adverse outcomes by left ventricular ejection fraction in a contemporary heart failure population. Circ Heart Fail. 2013;6(4):635-46.
401. Kannel WB, Hjortland M, Castelli WP. Role of diabetes in congestive heart failure: the Framingham study. Am J Cardiol. 1974;34(1):29-34.
402. Zaid M, Sala L, Despins L, Heise D, Popescu M, Skubic M, et al. Cardiovascular sex-differences: insights via physiology-based modeling and potential for noninvasive sensing via ballistocardiography. Front Cardiovasc Med. 2023;10:1215958.
403. St Pierre SR, Peirlinck M, Kuhl E. Sex Matters: A Comprehensive Comparison of Female and Male Hearts. Front Physiol. 2022;13:831179.
404. Prajapati C, Koivumäki J, Pekkanen-Mattila M, Aalto-Setälä K. Sex differences in heart: from basics to clinics. European Journal of Medical Research. 2022;27(1):241.
405. Hayward CS, Kalnins WV, Kelly RP. Gender-related differences in left ventricular chamber function. Cardiovascular Research. 2001;49(2):340-50.
406. Köstler H, Landschütz W, Koeppe S, Seyfarth T, Lipke C, Sandstede J, et al. Age and gender dependence of human cardiac phosphorus metabolites determined by SLOOP 31P MR spectroscopy. Magn Reson Med. 2006;56(4):907-11.
407. de Wit-Verheggen VHW, Schrauwen-Hinderling VB, Brouwers K, Jörgensen JA, Schaart G, Gemmink A, et al. PCr/ATP ratios and mitochondrial function in the heart. A comparative study in humans. Scientific Reports. 2023;13(1):8346.
408. Scheuermann-Freestone M, Madsen PL, Manners D, Blamire AM, Buckingham RE, Styles P, et al. Abnormal Cardiac and Skeletal Muscle Energy Metabolism in Patients With Type 2 Diabetes. Circulation. 2003;107(24):3040-6.
409. Knott KD, Seraphim A, Augusto JB, Xue H, Chacko L, Aung N, et al. The Prognostic Significance of Quantitative Myocardial Perfusion. Circulation. 2020;141(16):1282-91.
410. Kotecha T, Monteagudo JM, Martinez-Naharro A, Chacko L, Brown J, Knight D, et al. Quantitative cardiovascular magnetic resonance myocardial perfusion mapping to assess hyperaemic response to adenosine stress. Eur Heart J Cardiovasc Imaging. 2021;22(3):273-81.

411. Ballotari P, Ranieri SC, Luberto F, Caroli S, Greci M, Giorgi Rossi P, et al. Sex differences in cardiovascular mortality in diabetics and nondiabetic subjects: a population-based study (Italy). Int J Endocrinol. 2015;2015:914057.
412. Castro MLd. Third in a series on diabetes and the heart. Diabetic heart disease in women: prevalence as compared to men? Implications for treatment? E-Journal of Cardiology Practice - Volume 14. 2016;14(16).
413. Kwak S, Hwang I-C, Park JJ, Park J-H, Park J-B, Cho G-Y. Sex-specific impact of diabetes mellitus on left ventricular systolic function and prognosis in heart failure. Scientific Reports. 2021;11(1):11664.
414. Murphy E, Amanakis G, Fillmore N, Parks RJ, Sun J. Sex Differences in Metabolic Cardiomyopathy. Cardiovasc Res. 2017;113(4):370-7.
415. Toedebusch R, Belenchia A, Pulakat L. Diabetic Cardiomyopathy: Impact of Biological Sex on Disease Development and Molecular Signatures. Front Physiol. 2018;9:453.
416. Miki T, Yuda S, Kouzu H, Miura T. Diabetic cardiomyopathy: pathophysiology and clinical features. Heart Fail Rev. 2013;18(2):149-66.
417. Reiser PJ, Moravec CS. Sex differences in myosin heavy chain isoforms of human failing and nonfailing atria. Am J Physiol Heart Circ Physiol. 2014;307(3):H265-72.
418. McKee LA, Chen H, Regan JA, Behunin SM, Walker JW, Walker JS, et al. Sexually dimorphic myofilament function and cardiac troponin I phosphospecies distribution in hypertrophic cardiomyopathy mice. Arch Biochem Biophys. 2013;535(1):39-48.
419. Parks RJ, Ray G, Bienvenu LA, Rose RA, Howlett SE. Sex differences in SR Ca(2+) release in murine ventricular myocytes are regulated by the cAMP/PKA pathway. J Mol Cell Cardiol. 2014;75:162-73.
420. Hoeker GS, Hood AR, Katra RP, Poelzing S, Pogwizd SM. Sex differences in β-adrenergic responsiveness of action potentials and intracellular calcium handling in isolated rabbit hearts. PLoS One. 2014;9(10):e111411.
421. Dantas AP, Fortes ZB, de Carvalho MH. Vascular disease in diabetic women: Why do they miss the female protection? Exp Diabetes Res. 2012;2012:570598.
422. Kander MC, Cui Y, Liu Z. Gender difference in oxidative stress: a new look at the mechanisms for cardiovascular diseases. J Cell Mol Med. 2017;21(5):1024-32.
423. Cid MC, Schnaper HW, Kleinman HK. Estrogens and the vascular endothelium. Ann N Y Acad Sci. 2002;966:143-57.
424. Fourny N, Beauloye C, Bernard M, Horman S, Desrois M, Bertrand L. Sex Differences of the Diabetic Heart. Front Physiol. 2021;12:661297.
425. Ranucci M, Aloisio T, Di Dedda U, Menicanti L, de Vincentiis C, Baryshnikova E. Gender-based differences in platelet function and platelet reactivity to P2Y12 inhibitors. PLoS One. 2019;14(11):e0225771.
426. Alameddine A, Fajloun Z, Bourreau J, Gauquelin-Koch G, Yuan M, Gauguier D, et al. The cardiovascular effects of salidroside in the Goto-Kakizaki diabetic rat model. J Physiol Pharmacol. 2015;66(2):249-57.
427. Iorga A, Cunningham CM, Moazeni S, Ruffenach G, Umar S, Eghbali M. The protective role of estrogen and estrogen receptors in cardiovascular disease and the controversial use of estrogen therapy. Biol Sex Differ. 2017;8(1):33.
428. Donahue RP, Rejman K, Rafalson LB, Dmochowski J, Stranges S, Trevisan M. Sex differences in endothelial function markers before conversion to pre-diabetes: does the

clock start ticking earlier among women? The Western New York Study. Diabetes Care. 2007;30(2):354-9.
429. Hunter I, Soler A, Joseph G, Hutcheson B, Bradford C, Zhang FF, et al. Cardiovascular function in male and female JCR:LA-cp rats: effect of high-fat/high-sucrose diet. Am J Physiol Heart Circ Physiol. 2017;312(4):H742-h51.
430. Wannamethee SG, Papacosta O, Lawlor DA, Whincup PH, Lowe GD, Ebrahim S, et al. Do women exhibit greater differences in established and novel risk factors between diabetes and non-diabetes than men? The British Regional Heart Study and British Women's Heart Health Study. Diabetologia. 2012;55(1):80-7.
431. Xing D, Nozell S, Chen YF, Hage F, Oparil S. Estrogen and mechanisms of vascular protection. Arterioscler Thromb Vasc Biol. 2009;29(3):289-95.
432. Lagranha CJ, Deschamps A, Aponte A, Steenbergen C, Murphy E. Sex differences in the phosphorylation of mitochondrial proteins result in reduced production of reactive oxygen species and cardioprotection in females. Circ Res. 2010;106(11):1681-91.
433. Yang Y, Wang IW, Turrentine M, Wang M. Postischemic application of estrogen ameliorates myocardial damage in an in vivo mouse model. J Surg Res. 2018;231:366-72.
434. Horn MA, Trafford AW. Aging and the cardiac collagen matrix: Novel mediators of fibrotic remodelling. J Mol Cell Cardiol. 2016;93:175-85.
435. Sharma A, De Blasio M, Ritchie RH. Current challenges in the treatment of cardiac fibrosis: Recent
insights into the sex-specific differences of glucose-lowering
therapies on the diabetic heart: IUPHAR Review 33. British Journal of Pharmacology. 2022(Translational Advances in Fibrosis as a Therapeutic Agent).
436. Li JH, Huang XR, Zhu H-J, Oldfield M, Cooper M, Truong LD, et al. Advanced glycation end products activate Smad signaling via TGF-β-dependent and -independent mechanisms: implications for diabetic renal and vascular disease. The FASEB Journal. 2004;18(1):176-8.
437. Peng Y, Kim J-M, Park H-S, Yang A, Islam C, Lakatta EG, et al. AGE-RAGE signal generates a specific NF-κB RelA “barcode” that directs collagen I expression. Scientific Reports. 2016;6(1):18822.
438. Tuleta I, Frangogiannis NG. Fibrosis of the diabetic heart: Clinical significance, molecular mechanisms, and therapeutic opportunities. Adv Drug Deliv Rev. 2021;176:113904.
439. Kessler EL, Rivaud MR, Vos MA, van Veen TAB. Sex-specific influence on cardiac structural remodeling and therapy in cardiovascular disease. Biology of Sex Differences. 2019;10(1):7.
440. Shang Y, Zhang Y, Leng W, Lei X, Chen L, Zhou X, et al. Sex Differences in Type 2 Diabetes Mellitus-Related Left Ventricular Remodeling: A Cardiovascular Magnetic Resonance Study. J Diabetes Res. 2022;2022:1427864.
441. McGavock JM, Lingvay I, Zib I, Tillery T, Salas N, Unger R, et al. Cardiac Steatosis in Diabetes Mellitus. Circulation. 2007;116(10):1170-5.
442. Iozzo P, Lautamaki R, Borra R, Lehto HR, Bucci M, Viljanen A, et al. Contribution of glucose tolerance and gender to cardiac adiposity. J Clin Endocrinol Metab. 2009;94(11):4472-82.

443. Banke NH, Yan L, Pound KM, Dhar S, Reinhardt H, De Lorenzo MS, et al. Sexual dimorphism in cardiac triacylglyceride dynamics in mice on long term caloric restriction. J Mol Cell Cardiol. 2012;52(3):733-40.
444. Devanathan S, Whitehead TD, Fettig N, Gropler RJ, Nemanich S, Shoghi KI. Sexual dimorphism in myocardial acylcarnitine and triglyceride metabolism. Biol Sex Differ. 2016;7:25.
445. Vallerie SN, Bornfeldt KE. Metabolic Flexibility and Dysfunction in Cardiovascular Cells. Arteriosclerosis, Thrombosis, and Vascular Biology. 2015;35(9):e37-e42.
446. Walden CE, Knopp RH, Wahl PW, Beach KW, Strandness E, Jr. Sex differences in the effect of diabetes mellitus on lipoprotein triglyceride and cholesterol concentrations. N Engl J Med. 1984;311(15):953-9.
447. Chen M, Masaki T, Sawamura T. LOX-1, the receptor for oxidized low-density lipoprotein identified from endothelial cells: implications in endothelial dysfunction and atherosclerosis. Pharmacol Ther. 2002;95(1):89-100.
448. Brinkley TE, Kume N, Mitsuoka H, Phares DA, Hagberg JM. Elevated soluble lectin-like oxidized LDL receptor-1 (sLOX-1) levels in obese postmenopausal women. Obesity (Silver Spring). 2008;16(6):1454-6.
449. Peterson LR, Herrero P, Coggan AR, Kisrieva-Ware Z, Saeed I, Dence C, et al. Type 2 diabetes, obesity, and sex difference affect the fate of glucose in the human heart. Am J Physiol Heart Circ Physiol. 2015;308(12):H1510-6.
450. Kenchaiah S, Evans JC, Levy D, Wilson PW, Benjamin EJ, Larson MG, et al. Obesity and the risk of heart failure. N Engl J Med. 2002;347(5):305-13.
451. Iribarren C, Karter AJ, Go AS, Ferrara A, Liu JY, Sidney S, et al. Glycemic control and heart failure among adult patients with diabetes. Circulation. 2001;103(22):2668-73.
452. Núñez J, Bonanad C, Navarro JP, Bondanza L, Artero A, Ventura S, et al. Differential Effect of Glycosylated Hemoglobin Value and Antidiabetic Treatment on the Risk of 30-day Readmission Following a Hospitalization for Acute Heart Failure. Rev Esp Cardiol (Engl Ed). 2015;68(10):852-60.
453. Lunde IG, Aronsen JM, Kvaløy H, Qvigstad E, Sjaastad I, Tønnessen T, et al. Cardiac O-GlcNAc signaling is increased in hypertrophy and heart failure. Physiol Genomics. 2012;44(2):162-72.
454. Erickson JR, Pereira L, Wang L, Han G, Ferguson A, Dao K, et al. Diabetic hyperglycaemia activates CaMKII and arrhythmias by O-linked glycosylation. Nature. 2013;502(7471):372-6.
455. Yeo JL, Gulsin GS, Brady EM, Athithan L, Arnold JR, Singh A, et al. Abstract 11702: Sex Differences in Diabetic Cardiomyopathy: Greater Reduction in Myocardial Perfusion Reserve in Women Than Men Driven by Increased Resting Perfusion. Circulation. 2021;144(Suppl_1):A11702-A.
456. Barrett-Connor E, Giardina EG, Gitt AK, Gudat U, Steinberg HO, Tschoepe D. Women and heart disease: the role of diabetes and hyperglycemia. Arch Intern Med. 2004;164(9):934-42.
457. Bibbins-Domingo K, Lin F, Vittinghoff E, Barrett-Connor E, Hulley SB, Grady D, et al. Predictors of heart failure among women with coronary disease. Circulation. 2004;110(11):1424-30.

458. Zinman B, Wanner C, Lachin JM, Fitchett D, Bluhmki E, Hantel S, et al. Empagliflozin, Cardiovascular Outcomes, and Mortality in Type 2 Diabetes. N Engl J Med. 2015;373(22):2117-28.
459. Fitchett D, Inzucchi SE, Cannon CP, McGuire DK, Scirica BM, Johansen OE, et al. Empagliflozin Reduced Mortality and Hospitalization for Heart Failure Across the Spectrum of Cardiovascular Risk in the EMPA-REG OUTCOME Trial. Circulation. 2019;139(11):1384-95.
460. Rivera FB, Tang VAS, De Luna DV, Lerma EV, Vijayaraghavan K, Kazory A, et al. Sex differences in cardiovascular outcomes of SGLT-2 inhibitors in heart failure randomized controlled trials: A systematic review and meta-analysis. Am Heart J Plus. 2023;26.
461. Lincoff AM, Brown-Frandsen K, Colhoun HM, Deanfield J, Emerson SS, Esbjerg S, et al. Semaglutide and Cardiovascular Outcomes in Obesity without Diabetes. New England Journal of Medicine. 2023;389(24):2221-32.
462. George AM, Jacob AG, Fogelfeld L. Lean diabetes mellitus: An emerging entity in the era of obesity. World J Diabetes. 2015;6(4):613-20.
463. Coleman NJ, Miernik J, Philipson L, Fogelfeld L. Lean versus obese diabetes mellitus patients in the United States minority population. J Diabetes Complications. 2014;28(4):500-5.